A Theoretical and Experimental Investigation of an Absorption Refrigeration System for Application with Solar Energy Units

by

Mahieddine Dalichaouch

A Thesis submitted for the degree of Doctor of Philosophy

July 1989

Department of Mechanical Engineering

The University of Newcastle Upon Tyne

ABSTRACT

Application of the second law of thermodynamics to refrigeration systems is useful in identifying the thermodynamic losses and in finding out where improvements might be made.

Theoretical absorption refrigeration cycles are analysed using the first law-based equations of energy balances and the second law-based concept of lost work.

A thermodynamic efficiency, defined and formulated from the lost work approach, is used to examine a lithium bromide -water absorption cooling cycle with hot water as the heat source and cooling water as the heat sink. The cycle parameters are varied over applicable operating ranges in order to find their effect on the cycle thermodynamic efficiency. To accomplish this objective and to make a parameteric analysis for the L_iB_r-water absorption cycle under steady-state conditions, two computer programmes are written. The results indicate the system might be improved by better design. The efficiency variation is compared to variations of coefficient of performance found in the literature.

A L_iB_r-water absorption refrigeration system for low hot water temperature applications has been proposed and detailed design aspects have been considered. Fabrication and testing of a laboratory model of the absorption refrigeration system have been described.

As new design methodologies of solar energy applications have been developed recently, a study of solar thermal systems for absorption refrigeration has been presented. This includes the classification, description and modelling of solar systems.

Types of design procedures of solar systems for absorption refrigeration are discussed and a computer programme has been implemented which prints out the yearly solar fraction of a solar thermal system with daily storage for supplying heat to an absorption cooling cycle. Numerical performance tests are carried out and the results show that the phibar-f chart design method is a simple and convenient mean of predicting the thermal performance of solar systems.

ACKNOWLEDGEMENTS

I wish to thank my supervisor Dr B. Agnew for his invaluable guidance and support throughout the period of this research.

I would also like to thank all the persons who have contributed directly or indirectly in completing the experimental project.
My stay and my research activities at Newcastle university have been financed by the Algerian ministry of higher studies to whom I am obliged.

Last but not least, this work is dedicated to the memory of my parents, to my wife and son and to all members of my family.

TABLE OF CONTENTS

LIST OF FIGURES

LIST OF TABLES

LIST OF MAIN SYMBOLS

A	Heat exchanger surface area. Parameter given by eqn 8.17 (a)
A_C	solar collector area
A_c	Cross sectional area
A_i	Inside surface area
A_m	Mean surface area
A_o	Outside surface area
b	Availability function. Constant in eqns 4.11 and 8.13
COP	Coefficient of performance
C_P	Specific heat at constant pressure
$decl$	Solar declination
D	Diameter
D_e	Equivalent diameter given by eqn 5.17
D_i	Inside diameter
D_o	Outside diameter
f	Friction factor
f_M	Monthly solar fraction
f_Y	Yearly solar fraction
F	Heat exchanger correction factor
F_R	Solar collector heat removal factor
g	Gravitational acceleration
G	Mass flowrate per unit cross sectiona area
h	Enthalpy per unit of mass
h_b	Nucleate boiling heat transfer coefficient
h_c	Convective heat transfer coefficient
h_d	Average heat transfer coefficient given by eqn 5.2
h_i	Inside heat transfer coefficient
h_o	Outside heat transfer coefficient
HX	Solution heat exchanger effectiveness
I	Irreversibility
k	Thermal conductivity
$\bar{K}$	Monthly average clearness index of the atmosphere

L	Latitude. Length
LW	Lost work
$\dot{m}$	Mass flowrate
M	Mass
n	Day of year. Number of tubes
N_u	Nusselt number
P	Pressure
P_r	Prandtl number
Q	Heat
$\dot{Q}$	Time rate of heat
Q_A	Heat transfer in absorber
Q_C	Heat transfer in condenser. Useful heat transfer in solar collector
Q_E	Heat transfer in evaporator
Q_{HX}	Heat transfer in solution heat exchanger
Q_{LM}	Monthly total heat load in eqns 8.14, 8.15, 8.19
Q_o	Heat rejected to the environment
Q_U	Useful heat transfer to the load in eqns 8.4 and 8.8
Q_{UM}	Monthly heat transfer to the load in eqns 8.6 and 8.7
Q_W	Heat losses from the storage tank in eqns 8.3 and 8.4
$\bar{r}_T$	Ratio of radiation at noon on a tilted collector to that on a horizontal surface for the average day of the month
r_{fW}	Fouling factor
R_e	Reynolds number
$\bar{R}_T$	Ratio of the monthly average radiation on a tilted surface to that on a horizontal surface
s	Specific entropy
S	Entropy
t	Temperature (°C)
T	Temperature (°K)
U_o	Overall heat transfer coefficient
U_L	Overall heat loss coefficient of solar collector

V	Velocity. Volume
W	Work
X	Concentration of L_iB_r in solution. Dimensionless variable defined by eqns 8.13 and 8.14.
$\overline{X}_{CK}$	Dimensionless critical radiation ratio in eqns 8.16 and B1.22
Y	Dimensionless variable defined by eqn 8.15
Z	Elevation in eqn 3.2. Dimensionless Parameter in eqns 8.18 and 8.19
α	Thermal diffusivity
β	Slope of collector
Γ	Mass flowrate of falling film per unit perimeter
δ	Thickness
η	Efficiency
τ	Time
μ	Dynamic viscosity
ν	Kinematic viscosity
π	$\pi = 3.14159$
ρ	Density. Ground albedo
$\overline{\tau_r \alpha}$	Solar collector optical efficiency
$\overline{\Phi}_K$	Daily utilizability fraction

Subscripts

A	Absorber
Aux	Auxiliary
cf,1	Cooling fluid in condenser
cf,2	Cooling fluid in absorber
C	Condenser
CHW	Chilled water
CW	Cooling water
CW,1	Cooling water in condenser
CW,2	Cooling water in absorberr

e	Exit. Equivalent
E	Evaporator
G	Generator
H	Hot
i	Inlet. Inside
L	Load
p	Pump
r	refrigerated fluid
rev	Reversible
o	Surroundings. Outside
S	Storage
SS	Strong solution
W	Water
WS	Weak solution

Superscripts

$\bar{X}$	denotes average value of the quantity X

CHAPTER ONE
INTRODUCTION

Absorption refrigeration is of considerable interest for several reasons, in the preservation of food and medical supplies, air conditioning and industrial process requirements.

An absorption refrigeration system is a heat operated device based on two factors which produce a refrigeration effect; these are

(i) A primary fluid will boil at low temperatures.

(ii) A secondary fluid will absorb the primary fluid which has been vaporized in the evaporator.

When the system utilizes a mechanical pump to circulate the absorbent-refrigerant solution, a small amount of work input will be required.

The heat source may be steam or an another hot fluid. There are two main types of absorption systems: the aqueous lithium bromide system and the aqua-ammonia system. Other absorbent-refrigerant combinations have recently been considered [1-5].

The majority of modern absorption refrigeration units currently in use are operated by solar energy. A large number of successful and reliable cycles have been produced commercially.

Improvement in cooling by absorption and changes in operation have been reported in the literature [6-9]. Investigators have examined many aspects of research such as the thermodynamic analysis of the basic cycle, the effect of variations in cooling water temperature, the improvement of mechanical design, the evaluation of performance under conditions of reduced capacity or transient start-up, and the full scale testing.

However, in recent years the increasing interest in energy conservation and the efficient use of energy has led to a new methodology and a powerful approach to analyse all processes and installations.

Concepts based on the second law of thermodynamics have been developed and new efficiencies of processes have been defined. Today, analysis and design of engineering systems, based on the first law only, are not entirely adequate; Application of material balances, energy balances and equilibrium relationships does not indicate how effectively a system utilizes a particular energy resource. The investigations described in this thesis are concerned with the aqueous lithium bromide absorption refrigeration cycles using hot water as the heat source. Nevertheless, the theoretical analysis, presented in chapter 3, is general being applicable to all absorption cycles.
The objectives of this thesis are :

(i) The analysis and optimization of absorption refrigeration cycles.

(ii) The design, construction and testing of an improved laboratory refrigeration model.

(iii) The study and design of a solar thermal system for supplying heat to an absorption refrigeration process.

Formulations of the second law, thermodynamic principles using irreversibility and lost work concepts, cycle analyses and efficiency definitions are critically reviewed and reported in chapter 3. Chapter 4 consists of three sections. The first describes an aqueous lithium bromide absorption refrigeration model and the second describes computer programmes that have been developed to examine the effects of variations of internal and external parameters on the second law efficiency of a lithium bromide-water cooling cycle. The third section deals with a discussion of those effects on cycle optimisation, The results being compared to the computer simulation results of the coefficient of performance variation of aqueous lithium bromide systems [5, 10].
Given the general methods of typical system analysis [10-15] and the conclusions of the study on cycle optimisation, a thermodynamic model of the cooling machine was designed as described in chapter 5.

The experimental rig needed to investigate the relevance of the thermodynamic model is described in chapter 6. The generator, condenser, evaporator and absorber components of the laboratory model were arranged in two shells. A 1 kW-capacity unit was equipped with drip headers in the absorber, evaporator and also in the generator so as to provide liquid-film boiling instead of the pool boiling of the lithium bromide-water solution.

Measurements obtained from experiments have been presented in chapter 7; although the system was not typical in its operation and performance, the experience derived from the tests will be useful for further development of aqueous lithium bromide cooling units.

In chapter 8, solar thermal systems for absorption refrigeration are described and classified. The design procedures published in the literature have been introduced. A computer programme based on the phibar-f chart method has been prepared to estimate the size of a solar thermal system.

Conclusions and recommendations are presented in chapters 9 and 10.

CHAPTER TWO

LITERATURE REVIEW

2.1 Introduction

Theoretical and experimental studies of aqueous lithium bromide absorption refrigeration systems involve the thermodynamic analysis and design of cycles, the design and layout of the heat-exchanging apparatuses as well as the performance prediction and evaluation of the process.

It is usual for lithium bromide cooling units to be designed for low grade thermal energy applications. Therefore, the study and design of solar thermal systems is of importance to absorption cooling.

The second law analysis of energy systems has drawn considerable attention over the past two decades; its application to absorption refrigeration is of particular interest.

2.2 Design and Performance of Absorption Refrigeration Systems

The operating principles of absorption refrigeration have been described in numerous publications [10-17].

Mc Neely [18] reviewed the published thermodynamic properties of aqueous solutions of lithium bromide and the data supplied by the major manufacturers of lithium bromide absorption equipment. The data have been reduced to equations for use in computer programmes; New equilibrium chart, diagrams and tables were presented.

Rozenfel'd and Shmuilov [19] examined the design refinements of the principal components of large capacity absorption chillers.

The available literature does not give mass transfer coefficients under conditions prevailing in the absorber and generator of the absorption refrigeration system. Little information is given on diffusivities of concentrated solutions. Most of the data are related to very dilute solutions at about atmospheric pressures.

The effect of pressure on liquid diffusivity has received little attention. If low pressure diffusion coefficient data can be used in conjunction with a correction factor to estimate high pressure coefficients, no method has been proposed to connect diffusion coefficients to vacuum pressures. The conditions prevailing in the aqueous lithium bromide absorption refrigeration system are such that the solution concentration is between 50% and 60%, the operating pressures are relatively high vacuum pressures and the effect of latent heat is important.

Mass transfer in the absorption of water vapour by the aqueous lithium bromide solution is accompanied by a significant release of heat, therefore all known analytical models are not suitable. Mass transfer coefficients are determined experimentally [20]. However, more recently Nakotyakov et al. [21, 22] obtained approximate solutions of the problem of the nonisothermal absorption of water vapour by films of aqueous lithium bromide. Dimensionless correlations are provided for heat and mass transfer coefficients in simple models.

The pioneer work on the operation of the aqueous lithium bromide cycles with solar energy [23, 24] was performed using commercial machines without modifications for the solar experiments.

Currently, refrigeration units are specially designed and optimized for low temperature applications such as solar systems. A great amount of work on research and development of solar-operated chillers has been carried out. Discussion on this subject is available in a number of publications [6, 7, 25].

The most common systems used for absorption refrigeration are the solar-supplemented systems in which solar energy supplies part of the required thermal load, the rest being furnished by an auxiliary source. However, an aqueous lithium bromide absorption refrigeration system working with solar energy alone has been analysed and designed [20]. The thermodynamic analysis of this system has been made using the first law based-mass and energy balance equations.

Simulation methods of solar absorption cooling have been used extensively in the study of performance and the design of the components of the physical system.

Several sophisticated programmes were published [26-29]. The TRNSYS and SIMSHAC programmes are more useful as analysis tools than design tools be-

cause they are expensive to use and require expertise in programming. The transient system simulation programme or TRNSYS and the simulation programme for solar heating and cooling of buildings or SIMSHAC both consist of a number of subroutines for modelling system components. The user can simulate the performance of a particular system by means of an executive programme that calls the subroutines according to the description of the system. User written subroutines can be added to the programmes.

The main objective in the development of the TRNSYS and SIMSHAC programmes was to develop a dynamic point design performance analysis of simple models as well as of more complex models.

Winn [7] discussed and compared several computer simulation programmes. The f-chart programme [30], based on correlations to the TRNSYS results, was developed and served as a design tool that is easy and inexpensive to use. It consists basically of a set of three algebraic correlations that can be used to predict the monthly solar fraction of standard system configurations for space and domestic hot water heating with daily storage. The f-chart correlation for domestic hot-water systems is applicable only when the inlet water temperature is between 5 and 20°C and the upper hot water temperature is between 50 and 70°C.

The phibar-f chart method, a generalised version of the f-chart procedure, presented by Duffie and Beckman [31] is typically applicable to solar absorption systems. No restrictions are imposed on the temperature limits of the heated fluid in the solar thermal system. The phibar-f chart method was developed for solar systems with auxiliary heater in parallel.

A modified empirical correlation similar to that of the original phibar-f chart method was proposed for systems with auxiliary heater in series.

Both methods assume a constant and uniform thermal load over each day and for at least a month. The phibar-f chart method also requires that the thermal energy supplied to the load must be above a minimum temperature. It yields values of monthly solar fractions for one set of variable parameters specifying the size of the system components. The calculation should be repeated for each of the twelve months and also for different sets of parameters .

Comparisons with TRNSYS programme [30] have shown that the prediction accuracy of the phibar-f chart method is excellent on an annual basis and is satisfactory for most months.
The phibar-f chart procedure requires little climatic data, is simple and convenient to use but its application is limited to closed-loop system configuration and to the range of parameters for which it has been constructed.
El sayed et al. [32] proposed a simple technique to develop a simulation programme for a solar-operated lithium bromide-water cooling unit.
Anand et al. [33] investigated the modelling of the dynamic performance and the transient behaviour during start-up and shut down of a water-cooled aqueous lithium bromide chiller. New absorption machines with higher performance are being developed [34].

2.3 Application of The Second Law of Thermodynamics to Absorption Refrigeration Systems

The second law of thermodynamics provides a scientific basis of assessing and improving the efficiency of real processes and systems. Its application to engineering has led to significant developments within only the past thirty years. Various ways of applying it have been proposed with resulting confusing in terminology. Haywood [35] reviewed the different concepts and terms and included a critical historical survey; other authors also summarized the different methods and approaches [36, 37, 38].
An early application of the second law to absorption refrigeration was made by Bosnyakovic [39] who analysed in detail the irreversibility and heat losses in absorption cooling machines.
The maximum attainable coefficient of performance has been derived for an ideal or completely reversible absorption system [13, 14, 40].
De Never and Seader [41] used the concept of lost work to define and compute a second law thermodynamic efficiency for processes that exchange work with the surroundings and for those that do not; application to an absorption refrigeration cycle of negligible work exchange was considered.

An aqua-ammonia absorption cycle was analysed to determine where improvements might be made [42].

In the last few years, many researchers have been active in the second law analysis of solar systems in general and absorption solar cooling in particular [43-46]. The second law of thermodynamics has been used to analyse the principal components of two existing solar-operated aqueous lithium bromide absorption systems [46]. A computer programme was used to calculate the irreversibility of each of the system component; first and second law losses were clearly identified.

CHAPTER THREE

THEORETICAL ANALYSIS

3.1 Introduction

In order to design a thermodynamic system it is necessary to investigate in detail its theoretical basis, identify and then minimize the losses if possible. The analysis and synthesis of absorption refrigeration systems require the application of principles of engineering thermodynamics and heat transfer. This chapter describes the thermodynamic analysis of absorption refrigeration cycles. It is based on the conventional heat balance method derived from the first law and on the lost work approach developed from the second law.
The formulation of the second law efficiency of the process is obtained in a convenient form to allow easy computations.

3.2 Thermodynamic Principles

Conversion between work and heat in energy systems must be done within the limitations imposed by the laws of thermodynamics. The first law is a statement of conservation of energy: the net change of the energy of a system is equal to the net transfer of energy across the system boundary as heat and work [47]. It is the basis of the heat balance method of design and performance analysis that is commonly applied in engineering practice.
The state of the working fluid throughout a system is determined by the equations of heat balance, principle of conservation of mass and by the thermodynamic properties of the fluid.
A well known measure of energy use efficiency in absorption refrigeration is the coefficient of performance, also called the heat ratio, which is defined as the ratio of the useful effect produced to the energy input for the system.
However, the conventional first law-based heat balance method of evaluating losses and efficiency of systems is not a true representation of effectiveness. This

procedure gives a very poor indication of how well a system uses a particular energy to perform a given task.
Since the coefficient of performance can be greater than unity, its value alone as an index of possible performance improvement is limited.

The location, magnitude and type of inefficient use of energy should be a primary factor in the design and performance analysis of systems.
The second law of thermodynamics provides a means of assigning a quality index to energy. The general statement of the second law [47] from the macroscopic point of view is the principle of increase of entropy : the total change in the entropy of a system and its surroundings, when the system undergoes a change of state, is always greater than or equal to zero. In other words, the only processes that can occur are those in which the net total change of entropy increases.
Real processes are irreversible and the transfer of heat and work from one form to another always results in some loss of available work. Each time the working fluid in a system goes through a process, some of the initial available work in the fluid is lost.
An increase in entropy production indicates that the process is irreversible. For efficient energy conservation, the second law of thermodynamics gives a right measure of the losses in the system processes through an evaluation of the lost available work, the entropy production or the irreversibility.
Other ways of applying the second law to engineering systems have been proposed; one of the most known methods is the use of availability or exergy analysis.
Using these second law-based concepts, it is possible to define a thermodynamic efficiency whose value points out the effectiveness of energy utilization. The second law efficiency is defined [48] as the ratio of the required minimum energy input for an ideal system to the actual input of a real system when achieving any task.
In general, the second law efficiencies are much lower than those based on the first law since they take into account not only the energy lost in waste streams but also the degradation of the energy quality of the product streams.

Results of calculations of availability-based second law efficiencies for many common energy conversion processes [49] show that for a typical absorption air conditioner extracting heat from a reservoir at a temperature below the ambient temperature of 308°K, the second law efficiency is approximately 2% .
However, the efficiency index of energy quality utilization, provided by the second law, does not contain economic factors which may be equally important in the analysis of absorption cooling systems [50]. The various concepts are not mutually exclusive and must give the same answer if used properly.
There are basically two classes of approaches to the problem of analysing real processes:

(i) The exergy or availability formulation

(ii) The lost work or entropy production or irreversibility concept.

The criteria for selecting the best method to calculate thermodynamic efficiencies should be based on convenience of use, facility and best correspondence with the background of users.

3.3 The Absorption Cycle

The absorption refrigeration cycle shown in figure 3.1 is a closed cycle where the working fluid remains within the closed system and the interface with the surroundings is at boundaries through which heat and work are transferred.

The working fluid for the absorption system is a solution of refrigerant and absorbent which have a strong chemical affinity for each other.
Heat from a high-temperature source is added to the solution in the generator; as a result, a part of the refrigerant evaporates from the boiling solution which becomes stronger in absorbent concentration. Heat is removed from the refriger-

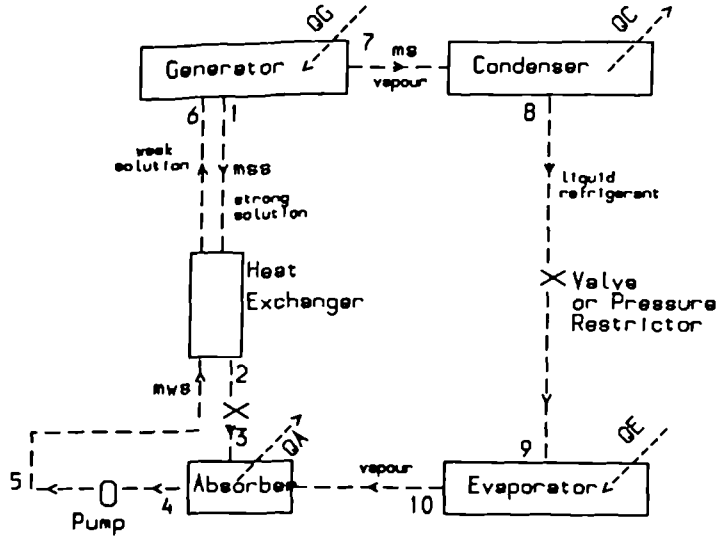

Fig.3.1 Schematic of an absorption refrigeration process

ant vapour as it is condensed in the condenser. The liquid refrigerant goes then to the evaporator via an expansion valve or a pressure restrictor in the feeding pipes.

For systems using lithium bromide and water, a U-tube may be used in which the small pressure difference between the high pressure side of the system (generator and condenser) and the low pressure side (evaporator and absorber) is maintained by a column of liquid.

Evaporation of the refrigerant liquid takes place in the evaporator because the vapour pressure of the solution in the absorber, at the absorber temperature, is lower than that of the refrigerant at the evaporator temperature. The solution draws vapour away from the refrigerant surface and causes the refrigerant temperature to fall until it can perform some useful refrigeration.

The vapour leaving the evaporator is mixed with a strong solution in the absorber. Since this reaction is exothermic, heat must be removed from the absorber to maintain its temperature at a sufficiently low value to assure a high chemical affinity between the refrigerant and the solution.

The liquid solution, weak in its affinity for refrigerant, is now pumped to the generator so that the cycle can be continuous. The solution returns to the absorber through an expansion valve (or a pressure restrictor or a U-tube). A heat exchanger is placed in the solution circuit between the generator and absorber to minimize the sensible heat losses.

3.4 First Law Analysis

Figure 3.2 shows the energy transfers to and from the fluids of an aborption system.

The rate of heat transfer to the refrigerant in the evaporator, denoted by $\dot{Q}_E$, is the refrigerating capacity. The system rejects heat Q_o to the environment (cooling water or atmospheric air) in the absorber and condenser. Heat Q_G is added in the generator and work W_P in the pump.

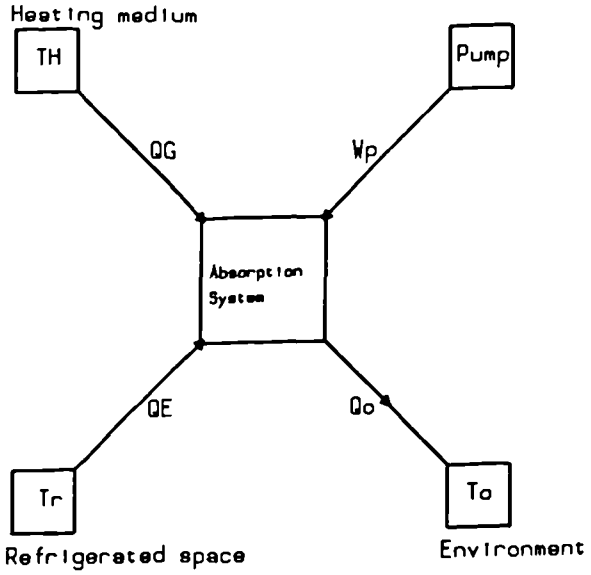

Fig.3.2 External energy transfers for an absorption refrigeration system

The heat rejected to the environment is equal to the heat transfer Q_A from the absorber plus the heat Q_C from the condenser.
Under steady conditions, the rate equation form of the first law for the whole system is:

$$\dot{Q}_A + \dot{Q}_C = \dot{Q}_G + \dot{Q}_E + \dot{W}_P \tag{3.1}$$

The closed system is formed of a series of individual processes. Each process can be analysed separately from the system by applying the first law to the component involved in the process.
The steady state, steady flow energy equation is

$$\dot{Q} + \dot{W} = \dot{m}(h_e + \frac{V_e^2}{2} + gZ_e) - \dot{m}(h_i + \frac{V_i^2}{2} + gZ_i) \tag{3.2}$$

Where
$\dot{Q}$ and $\dot{W}$ are the rates of heat and work transfer across a closed surface surrounding the component,
m is the steady flow of mass in and out of the control volume,
h is the specific enthalpy,
V the velocity
Z elevation
g the acceleration due to gravity.
The subscripts i and e denote the states of inlet and exit of the component.
In refrigeration, the terms representing the kinetic and gravitational energy changes are usually neglected when considering a particular component.
Equation (3.2) reduces to

$$\dot{Q} + \dot{W} = \dot{m}(h_e - h_i) \tag{3.3}$$

Energy losses of real absorption cooling cycles are observed in:

(i) Heat transfer through a finite temperature difference.

(ii) Mixing in the absorption process and throttling through the valves.

(iii) Boiling in the evaporator and generator.

(iv) Heat losses to the environment.

Neglecting the small work input to the solution pump, the coefficient of performance of absorption cycles is

$$COP = \frac{\dot{Q}_E}{\dot{Q}_G} \tag{3.4}$$

Computer simulation results [10, 51, 52] of the performance of absorption cooling cycles systems show that the parameters of refrigerant flow rates, solution heat echanger effectiveness and operating temperatures of the generator, condenser, absorber and evaporator have strong effects on system COP when they are varied over applicable working ranges. When expressed as a function of the temperatures of the external fluids (heating, cooling and refrigerated), the results are more useful in developing reliable performance predictions.
From figures 3.3 and 3.4 [10], it can be seen that the COP is strongly affected by the cooling fluid temperature; the system performance improves if the absorber and condenser are cooled in parallel streams instead of cooled in series.

3.5 Second Law Analysis

The approach of lost work (or entropy production or irreversibility) is selected to analyse absorption refrigeration cycles mainly because it focuses more on thermodynamic systems and seems simpler to apply.
Consider a closed system performing a thermodynamic cycle and in thermal contact with n heat reservoirs as shown in figure 3.5.

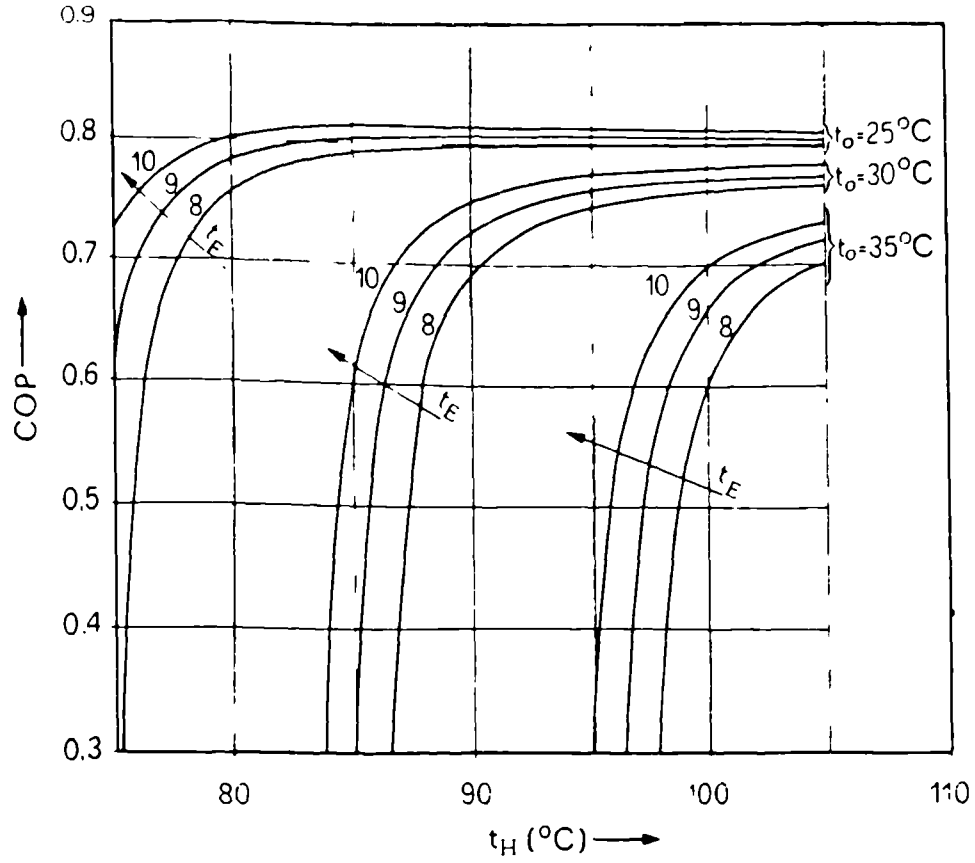

Fig.3.3 Coefficient of performance for different values of the external parameters.Cooling in series

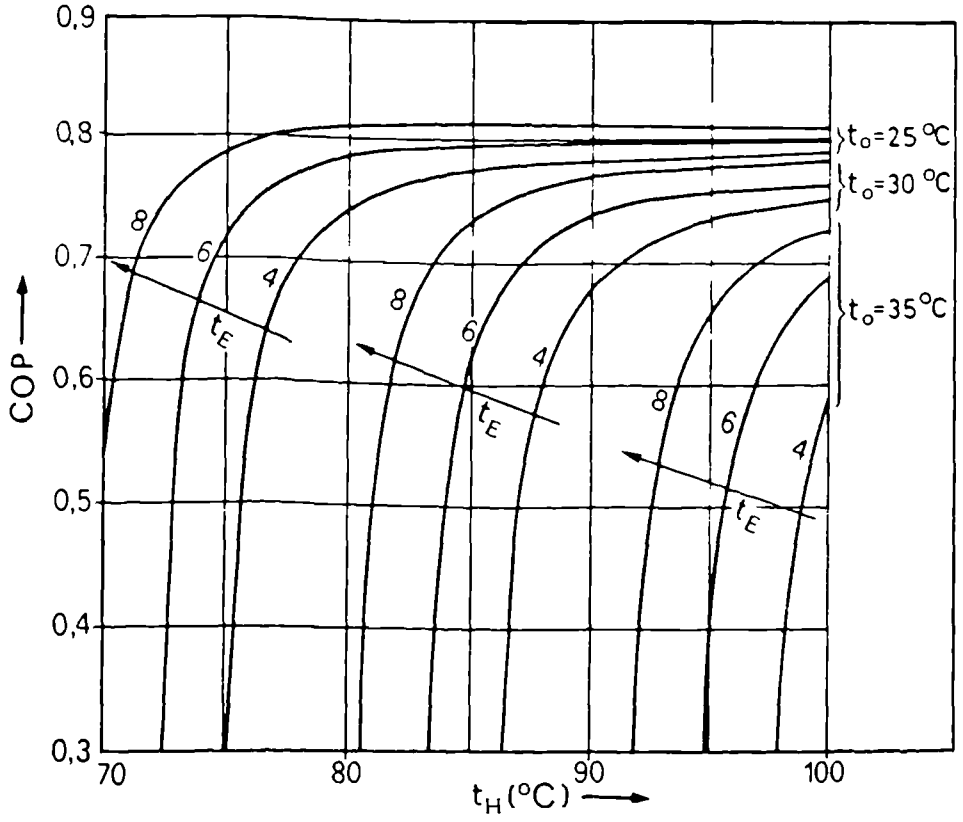

Fig.3.4 Coefficient of performance for different values of the external parameters.Cooling in parallel

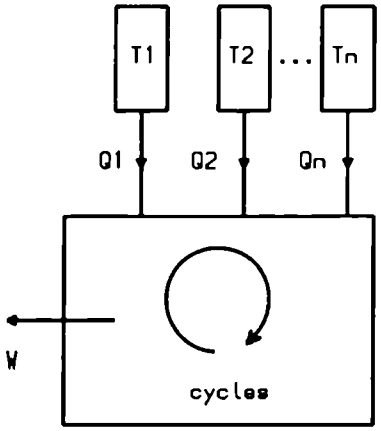

Fig.3.5 Closed system in contact with n heat reservoirs

W is the work done by the system, Q_i the heat transfer across a portion i of the system boundary and T_i is the corresponding temperature of that part of the boundary.

By the first law,

$$W = \sum_{i=1}^{n} Q_i \tag{3.5}$$

By the second law,

$$\Delta S_{system} + \Delta S_{\substack{heat \\ reservoirs}} \geq 0 \tag{3.6}$$

For steady state operation of the closed system executing a cycle,

$$\Delta S_{system} = 0$$

For the surroundings

$$\Delta S_{\substack{heat \\ reservoirs}} = \sum_{i=1}^{n} (-\frac{Q_i}{T_i})$$

If equation (3.6) is written as an equality by introducing the term S_{prod} for the irreversible entropy increase (or entropy production), then

$$\Delta S_{system} = \sum_{i=1}^{n} (\frac{Q_i}{T_i}) + S_{prod}$$

or

$$S_{prod} = -\sum_{i=1}^{n} (\frac{Q_i}{T_i}) \geq 0 \tag{3.7}$$

Lost work LW is related to entropy production S_{prod} by the expression

$$LW = T_o S_{prod}$$

Where T_o is the absolute temperature of the infinite surroundings.

The lost work of the considered closed system is

$$LW = -T_o \sum_{i=1}^{n} (\frac{Q_i}{T_i}) \tag{3.8}$$

Adding equations (3.5) and (3.8) produces

$$LW + W = \sum_{i=1}^{n} Q_i(1 - \frac{T_o}{T_i}) \tag{3.9}$$

The sum of the lost work and the useful work done by the system is the work of a totally reversible system with heat exchange at the same temperature levels other than T_o.

$$W_{rev} = LW + W$$

Equation (3.9) may be obtained directly by using the general expression of the reversible work for open systems [41],

$$LW + W = \sum_{j} (mb)_j + \sum_{i} (1 - \frac{T_o}{T_i}) Q_i - \Delta[m(b - Pv)]_{syst}$$

Where m is the mass flow across portions of the system boundary and b the availability function, $b = h - T_o s$.

Application to a steady-state cycle exchanging heat with more than one reservoir gives the same result as by equation (3.9).

The irreversibility concept has also been used [46] to develop the second law for the uniform state, uniform flow process. Appropriate simplifications yield the equation for the thermodynamic cycle exchanging heat with n reservoirs,

$$I = \sum_{i=1}^{n} Q_i(1 - \frac{T_o}{T_i}) - W$$

Where I, the irreversibility of the process, is defined as the difference between the reversible work that could theoretically be produced and the work that is actually produced.

For the absorption refrigeration process shown in figure 3.6, the cycle exchanges heat with four reservoirs as well as the surroundings.

From equation (3.9),

$$(LW)_{cycle} = \sum_{i=1}^{5} Q_i(1 - \frac{T_o}{T_i}) - W_p$$

or

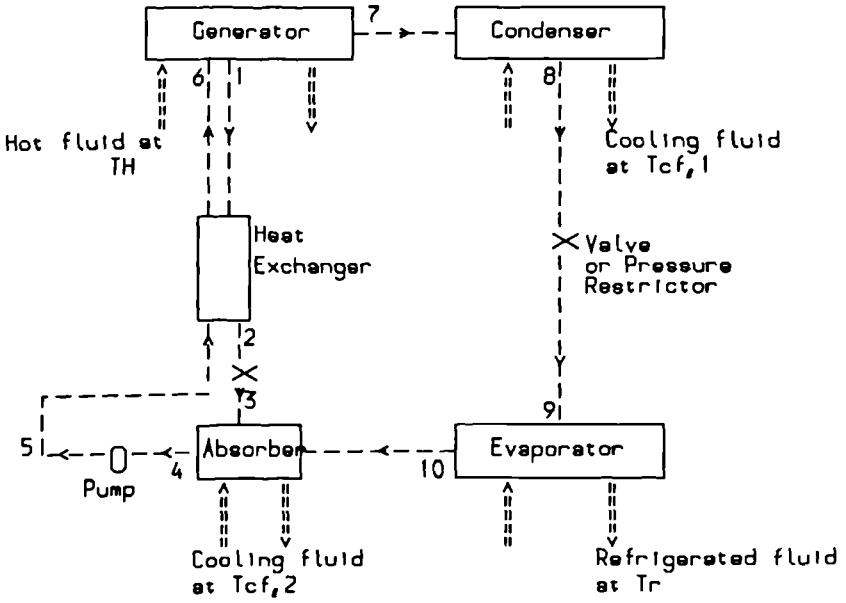

Fig.3.6 Schematic of an absorption refrigeration process

$$(LW)_{cycle} = Q_G(1 - \frac{T_o}{T_H}) + Q_C(1 - \frac{T_o}{T_{cf,1}}) + Q_A(1 - \frac{T_o}{T_{cf,2}}) + Q_E(1 - \frac{T_o}{T_r}) - W_p \quad (3.10)$$

Where Q_G, Q_E are positive and Q_C, Q_A, W_p are negative.

The term for the heat transfer to the surroundings does not appear in equation (3.10) because T_i=T_o. Similarly, if the temperatures of the cooling mediums are equal to T_o (case of absorber and condenser cooled by atmospheric air), then

$$LW = Q_G(1 - \frac{T_o}{T_H}) + Q_E(1 - \frac{T_o}{T_r}) - W_p \quad (3.11)$$

Small capacity absorption refrigeration systems can operate without mechanical pumps when the solution is circulated by use of vapour-lift pump.
For such systems there is no work input or output (W=0). When a mechanical liquid pump is used, the work input is usually small.
There is however lost work in each individual component of the absorption cooling cycle which must be taken into consideration. The overall cycle lost work is equal to the sum of the lost work of the individual processes.
Consider the steady-state operation of the open system of figure 3.7.

From the first law,

$$W = \sum_j Q_j + Q_o + \sum m_i h_i - \sum m_e h_e$$

From the second law,

$$S_{prod} = -\sum_j \frac{Q_j}{T_j} - \frac{Q_o}{T_o} + \sum m_e s_e - \sum m_i s_i$$

and

$$LW = -Q_o - \sum_j Q_j \frac{T_o}{T_j} + \sum m_e T_o s_e - \sum m_i T_o s_i \quad (3.12)$$

Applying equation (3.12) to each component of the absorption refrigeration system gives the expression of the lost work in each individual segment of the

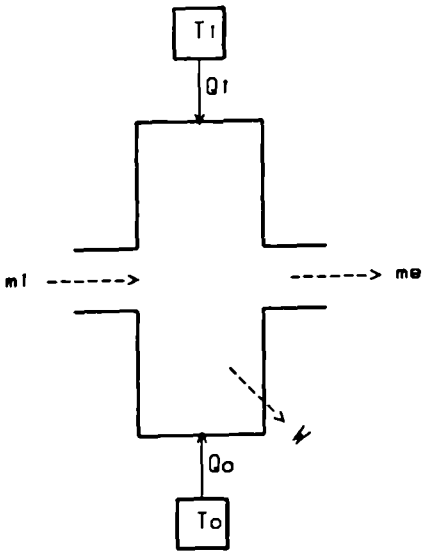

Fig.3.7 Open system in thermal contact with n heat reservoirs

process.

Reffering to figures 3.1 and 3.6 and taking the external fluids at the boundary of, but outside of, the system,

$$LW_{in\ generator} = -Q_G\frac{T_o}{T_H} + m_7T_os_7 + m_1T_os_1 - m_6T_os_6 - Q_{losses,gen}$$

$$LW_{in\ condenser} = -Q_C\frac{T_o}{T_{cf,1}} + m_2T_o(s_2 - s_1) - Q_{losses,cond}$$

$$LW_{in\ evaporator} = -Q_E\frac{T_o}{T_r} + m_{10}T_o(s_{10} - s_9) - Q_{losses,evap}$$

$$LW_{in\ absorber} = -Q_A\frac{T_o}{T_{cf,2}} + m_4T_os_4 - m_{10}T_os_{10} - m_3T_os_3 - Q_{losses,abs}$$

$$LW_{in\ pump} = m_5T_o(s_5 - s_4) - Q_{losses,pump}$$

$$LW_{in\ heat\ exchanger} = m_2T_os_2 + m_6T_os_6 - m_1T_os_1 - m_5T_os_5 - Q_{losses,h.exch}$$

$$LW_{in\ valves} = m_9T_o(s_9 - s_8) \text{ and } m_3T_o(s_3 - s_2)$$

The sum of the lost work for each individual segment should be equal to the overall cycle lost work as given by equation (3.10).

The principal sources of lost work or irreversibility for the absorption refrigeration cycle are:

(i) Heat transfer through a finite temperature difference in the heat exchanging components.

(ii) Mixing in the absorber. The refrigerant vapour and the solution, that are mixed, differ with regard to temperature and to concentration.

(iii) Free expansion during the throttling process in the valves.

3.6 Thermodynamic Efficiency

One procedure of defining a second law-based thermodynamic efficiency of

absorption refrigeration processes is to devise an ideal system that performs the same task as the actual system but in a reversible way and to form the ratio of the coefficient of performance of the two systems.

Consider an ideal absorption system (figure 3.8) operating among a heat source temperature of T_H, a heat sink temperature of T_o for heat rejection and a refrigerated medium temperature of T_r.

The ideal cycle operating with thermodynamically reversible processes between two temperatures is the carnot cycle. From figure 3.8 the ideal absorption cycle is a combination of a carnot engine working between T_H and T_o and a carnot refrigeration cycle operating between T_r and T_o.

For the carnot engine,

$$\frac{Q_G}{W} = \frac{T_H}{T_H - T_o}$$

For the refrigeration cycle,

$$\frac{Q_E}{W} = \frac{T_r}{T_o - T_r}$$

The COP of the ideal cycle is

$$(COP)_{ideal} = \frac{Q_E}{Q_G} = \frac{T_r(T_H - T_o)}{T_H(T_o - T_r)} \tag{3.13}$$

The maximum coefficient of performance for an absorption system is equal to the coefficient for a carnot refrigeration cycle working between T_r and T_o multiplied by the thermal efficiency of a carnot engine working between T_H and T_o.

In figure 3.9 the COP of this ideal system is varied over ranges of operating parameters [5]. It can be seen that a higher COP can be obtained at lower heat source temperatures if the refrigerated medium is maintained at higher temperatures and the heat sink is maintained at lower temperatures.

The same result of equation (3.13) can also be obtained [14] by applying the first and second law to the system shown in figure 3.2.

$$Q_o = Q_G + Q_E + W_p$$

For the closed system performing cycles in steady state,

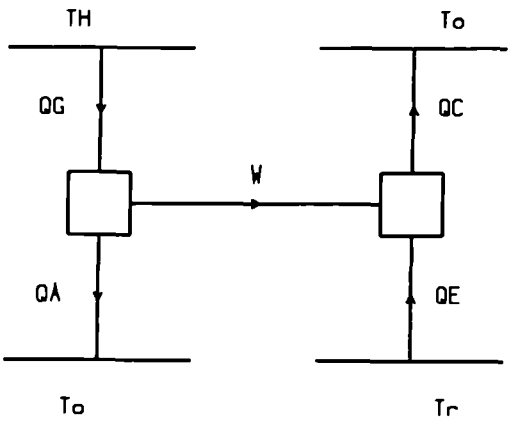

Fig.3.8 Ideal absorption cycle

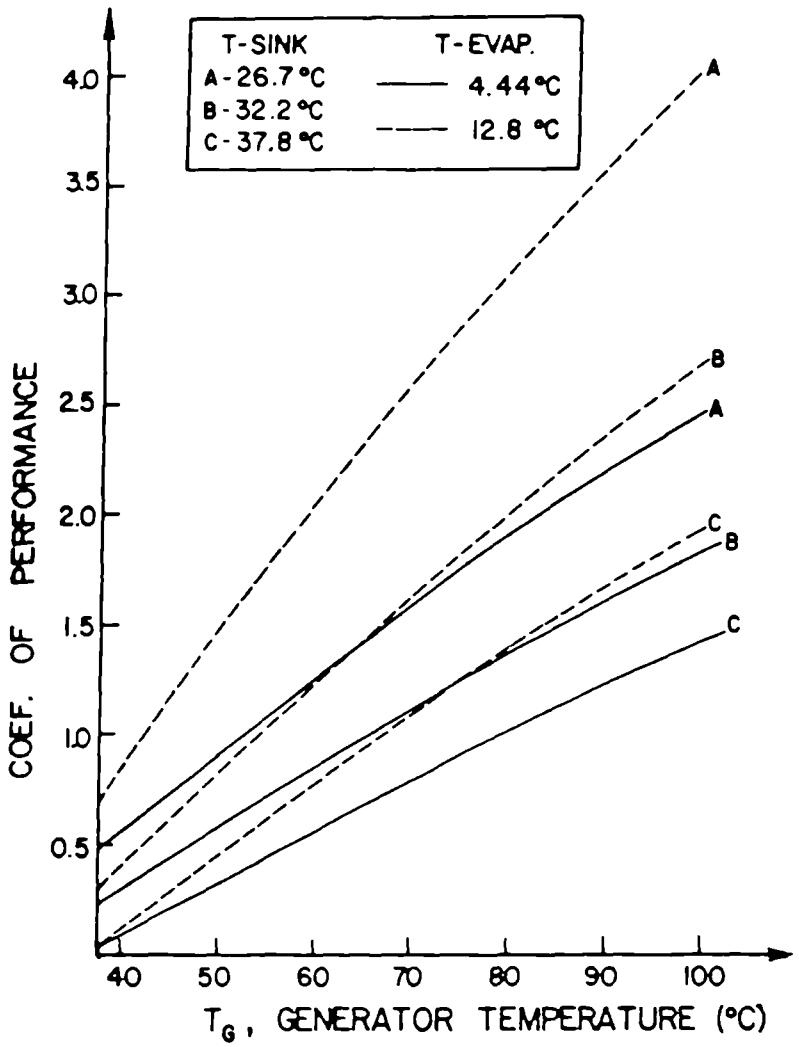

Fig.3.9 System COP of an ideal absorption cycle

$$(\Delta S)_{system} = 0$$

$$(\Delta S)_{\substack{heat \\ reservoirs}} = \sum_i (-\frac{Q_i}{T_i})$$

$$(\Delta S)_{surroundings} = +\frac{Q_o}{T_o}$$

by the second law,

$$(\Delta S)_{total} = -\frac{Q_G}{T_H} - \frac{Q_E}{T_r} + \frac{Q_o}{T_o} \geq 0$$

rearranging the last equation,

$$\frac{Q_G(T_H - T_o)}{T_H} \geq \frac{Q_E(T_o - T_r)}{T_r} - W_p$$

or if we assume that W_p is negligible,

$$COP = \frac{Q_E}{Q_G} \leq \frac{T_r(T_H - T_o)}{T_H(T_o - T_r)}$$

and for an ideal system,

$$COP_{ideal} = \frac{T_r(T_H - T_o)}{T_H(T_o - T_r)}$$

The second law efficiency definition has been given in section 3.2 of this chapter. The main task of an absorption cooling cycle is the removal of heat from the refrigerated medium. If the work input is small, the second law efficiency is

$$\eta = \frac{(Q_G)_{ideal\ cycle}}{(Q_G)_{actual\ cycle}}$$

$$\eta = \frac{\frac{(Q_E)}{(COP)_{ideal}}}{\frac{(Q_E)}{(COP)_{actual}}} = \frac{COP}{(COP)_{ideal}} \tag{3.14}$$

and

$$\eta = \frac{Q_E(\frac{T_o - T_r}{T_r})}{Q_G(\frac{T_H - T_o}{T_H})}$$

$$= \frac{-Q_E(1 - \frac{T_o}{T_r})}{Q_G(1 - \frac{T_o}{T_H})} \tag{3.15}$$

Consider now the absorption cycle shown in figure (3.6) where the system rejects heat to two reservoirs at $T_{cf,1}$ and $T_{cf,2}$.

By equation (3.10),

$$W_{rev} = Q_G(1 - \frac{T_o}{T_H}) + Q_C(1 - \frac{T_o}{T_{cf,1}}) + Q_A(1 - \frac{T_o}{T_{cf,2}}) + Q_E(1 - \frac{T_o}{T_r}) \quad (3.16)$$

For the absorption cycle whose task is neither to produce work nor to consume work, it can be observed that the terms on the right side of equation (3.16) represent the possible accomplishements of the process plus the inputs necessary to perform them. A general definition of second law efficiency has been formulated as the ratio of the desired result to the inputs necessary to accomplish that result [41].

Then,

$$\eta = \frac{-Q_E(1 - \frac{T_o}{T_r})}{Q_G(1 - \frac{T_o}{T_H}) + Q_C(1 - \frac{T_o}{T_{cf,1}}) + Q_A(1 - \frac{T_o}{T_{cf,2}})} \quad (3.17)$$

The minus sign appears because the two terms in the efficiency definition will have opposite algebraic signs due to thermodynamic conventions. If the temperatures $T_{cf,1}$ and $T_{cf,2}$ of the cooling mediums are equal to the ambient temperature T_o then the efficiency expression reduces to the efficiency formulation of equation (3.15).

3.7 Conclusion

In this chapter, the absorption refrigeration cycle has been analysed using the first and second law of thermodynamics.

The principles and concepts necessary for the analysis were critically discussed. The steady state, steady flow energy equation for closed and open systems has been used for the first law analysis. For real systems, the heat losses and their locations have been identified, the variation of the coefficient of performance was reported.

Application of the second law of thermodynamics for closed systems in thermal contact with reservoirs gives expressions of the lost work and reversible work;

consequently, the lost work of the absorption cycle was expressed.

The second law efficiency was defined and two different methods of obtaining the COP of an ideal system have been used. As a result, the second law efficiency of the absorption refrigeration cycle has been given in a form that it is readily computed.

CHAPTER FOUR

CYCLE OPTIMISATION

4.1 Introduction

In this chapter a model is described of the aqueous L_iB_r absorption cooling cycle. A parametric study of the second law efficiency of the cycle is undertaken for which two computer programmes are implemented. As a result, considerable insight may be gained into the cycle performance.
Changes made to optimize the entire absorption refrigeration cycle are discussed and a comparison is given with results from the classical analysis of such cycles using the coefficient of performance.

4.2 Aqueous Lithium Bromide Cooling Cycle

Consider the basic system of aqueous lithium bromide absorption cooling in figure 4.1.

The cycle uses water as the refrigerant and a solution of lithium bromide, L_iB_r , in water as the absorbent. When a solid salt such as lithium bromide is dissolved in water it becomes a solution. If aqueous solutions of lithium bromide are boiled the vapour produced will be pure water vapour because lithium bromide is virtually involatile.
The liquid solution exerts a water vapour pressure that is a function of the temperature and the concentration of the solution. The presentation of vapour pressure of solutions is usually an equilibrium diagram of pressure against temperature for different concentrations.
Hot water is the heat source in the generator and water is the cooling fluid in the absorber and condenser. The aqueous L_iB_r cooling system is principally utilized to produced chilled water in the evaporator. The operating principles

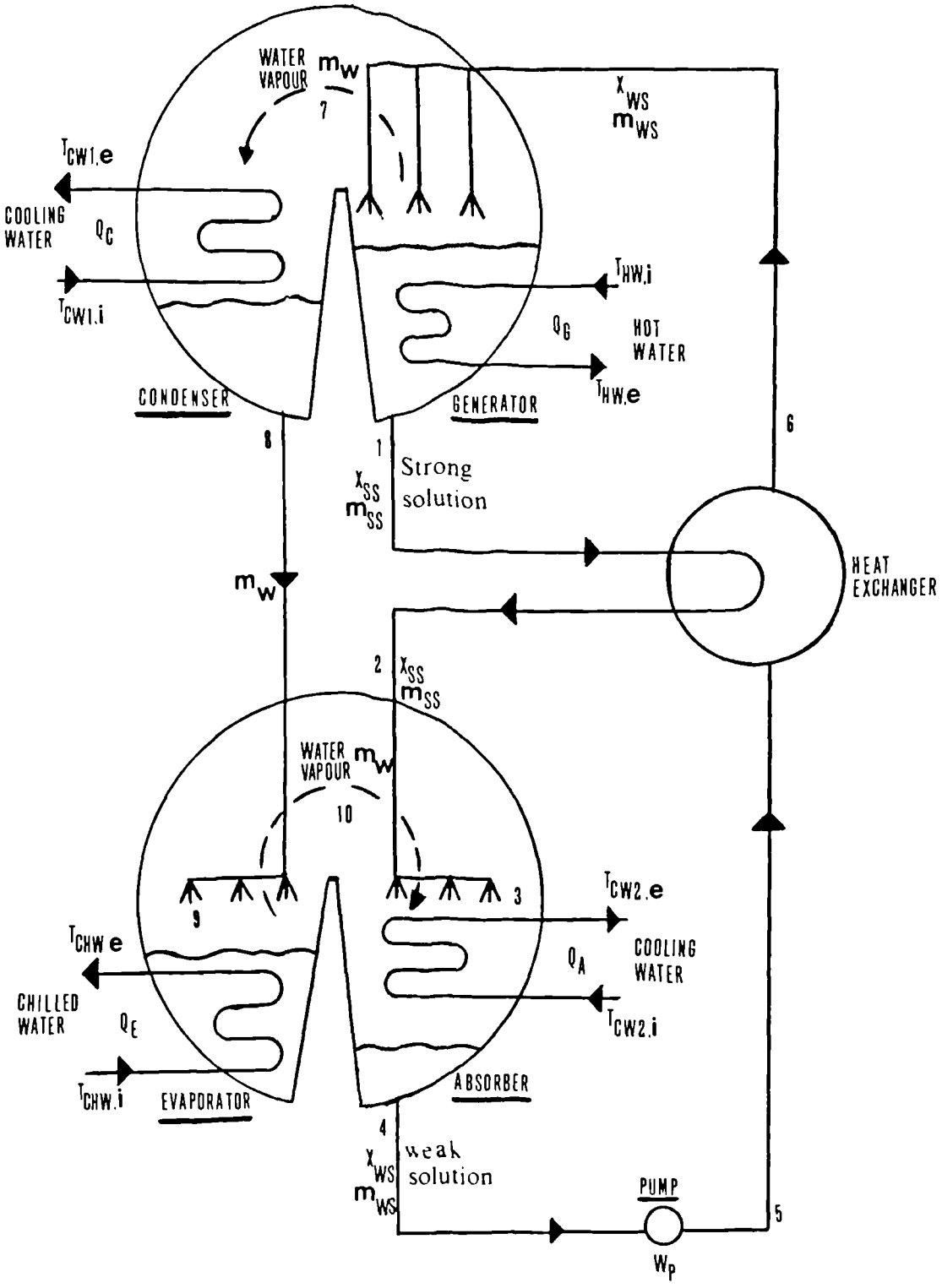

Fig.4.1 Basic system of aqueous LiBr cooling cycle

are similar to those described in chapter 3.

There are two pressure levels in the cycle. The pressure in the generator and condenser is the high pressure. The other is the low pressure in the evaporator and absorber. Since both pressures are well below atmospheric pressure (5 to 100 mm Hg), the specific volume of water vapour is large and big pipes are needed to prevent vapour pressure drops. To minimize these losses the generator and condenser are combined in one vessel and so are the evaporator and absorber. The four components may also be arranged in a single shell with pressure sides separated by a diaphragm.

The pressure differences between the high and low pressure sides of aqueous L_iB_r systems are small; therefore instead of valves, U-tubes are used in small units and spray nozzle restrictors in large units.

Small capacity lithium bromide-water machines (10 to 90 kw) can operate without a mechanical pump as the solution is circulated thermally by vapour-lift action. The use of pump however avoids crystallization and reduces submergence in pool boiling generators. Crystallization is the solidification of L_iB_r from the solution, which can block the flow of fluid within the unit.

The crystallization lines (figure 4.2) differ appreciably according to various authors[10]. The theoretical $L_iB_r - H_2O$ cycle is represented on the P-T-X equilibrium diagram shown in figure 4.3.

The process of a continuously operating absorption system is characterized by the points 1 to 6.

Point 1 to 3: The strong solution leaves the generator and enters the absorber via the heat exchanger. The position of point 3 is determined by the evaporator pressure (or the evaporator temperature T_E).

Point 3 to 4: The solution absorbs the water vapour coming from the

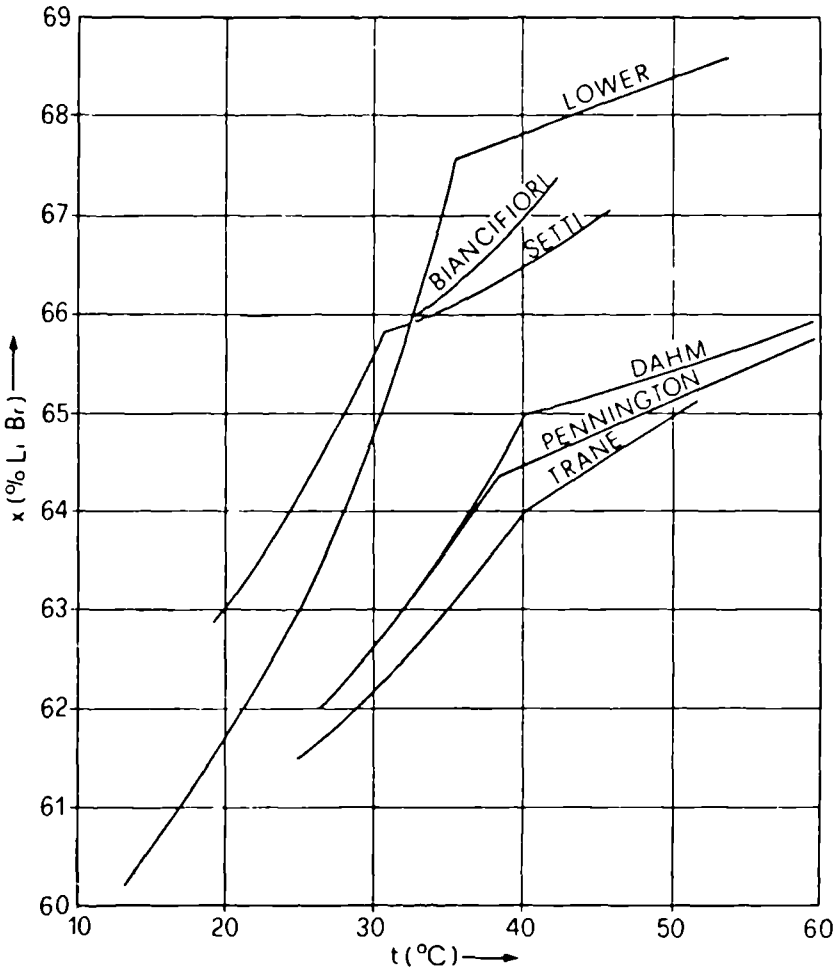

Fig.4.2 Crystallization lines for LiBr

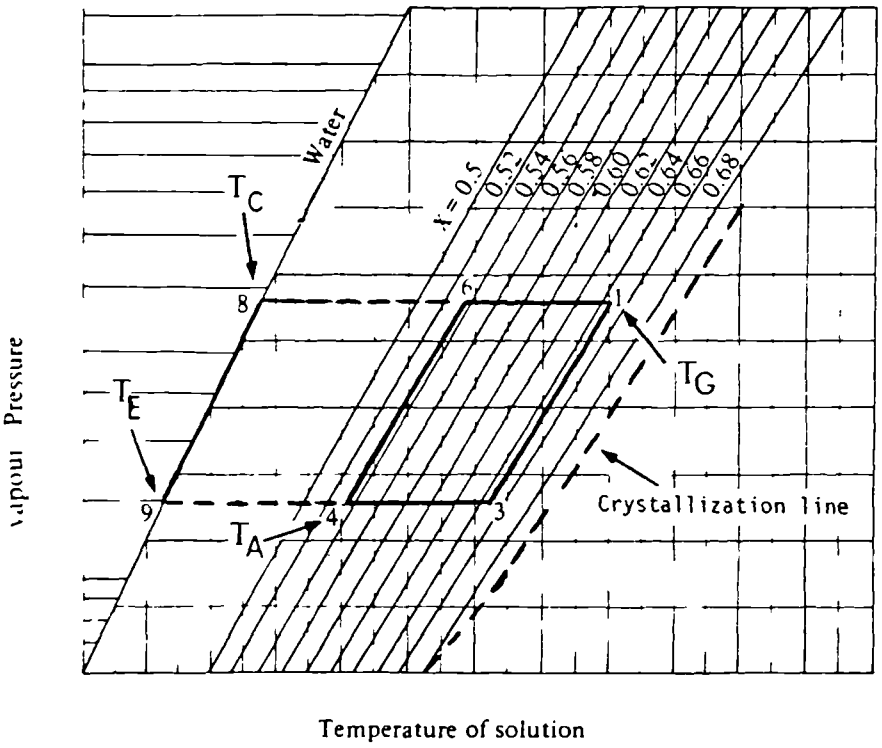

Fig.4.3 Pressure-temperature-concentration diagram for aqueous solutions of LiBr

evaporator. The absorber temperature T_A defines point 4 and gives the concentration of the weak solution, X_{WS}.

Point 4 to 6 : The weak solution is transported from the absorber to the generator via the heat exchanger. The location of point 6 depends on the given temperature T_C and thus on the condenser pressure.

Point 6 to 1 : Boiling of the solution in the generator. The generator temperature T_G defines point 1 and determines the concentration of the strong solution, X_{SS}.

Point 6 to 8 : Water vapour goes from generator to condenser and is condensed.

Point 8 to 9 : Water liquid flows from condenser to evaporator.

Point 9 to 4 : Evaporation and absorption of water vapour by the solution.

In actual absorption processes there are some deviations from the theoretical ones, the main reasons include the following.

(1) Pressure drops. The generator pressure is greater than the condenser pressure. The absorber pressure is slightly less than the evaporator pressure.

(2) Departures from equilibrium. The strong solution leaving the generator and the weak solution leaving the absorber are not completely saturated.

(3) A pressure difference is necessary between the vapour and the absorption solution (1 to 1.5 mm Hg) for mass transfer.

(4) Hydrostatic pressure in pool boiling generators. This results in incom-

plete vaporization of the solution which is measured by a difference in concentration.

(5) Heat transfer to the evaporator and heat losses to the surroundings.

Referring to figure 4.1, two mass flow balances over the generator give the following equations.

Total mass flow balance

$$m_{WS} = m_{SS} + m_W \tag{4.1}$$

L_iB_r balance

$$m_{WS}X_{WS} = m_{SS}X_{SS} \tag{4.2}$$

where m_{SS}, m_{WS}, m_W are the mass flow of the strong solution, weak solution, and water refrigerant, and X_{SS}, X_{WS} are the concentrations of L_iB_r in the strong and weak solutions.
The concentration is defined as the ratio of the mass fraction of L_iB_r in a solution to the total mass of L_iB_r and water contained in the solution.

$$X = \frac{mass\ L_iB_r}{mass\ L_iB_r + mass\ H_2O}$$

From equations (4.1) and (4.2)

$$\frac{m_{WS}}{m_W} = \frac{X_{SS}}{X_{SS} - X_{WS}} \tag{4.3}$$

$$\frac{m_{SS}}{m_W} = \frac{X_{WS}}{X_{SS} - X_{WS}} \tag{4.4}$$

To perform thermal calculations on the absorption refrigeration cycle, enthalpy data for the aqueous L_iB_r solution are needed. Enthalpy values are dependent upon the choice of standard state of the constituents. The enthalpy data that

will be used for calculations in these investigations are based on a reference state of zero enthalpy at 0°C for each of the two constituents, water and lithium bromide.

The conventional steam tables can be used in conjunction with the enthalpy data of solutions since the reference state is also 0°C.

Using the notation of figure 4.1, the steady state steady flow energy equation (3.3) will be applied to each component assuming equilibrium states and uniform temperatures.

(1) Generator: The rate of heat transfer to the solution is

$$\dot{Q}_G = \dot{m}_7 h_7 + \dot{m}_1 h_1 - \dot{m}_6 h_6$$

but

$$\dot{m}_1 = \dot{m}_2 = \dot{m}_3 = \dot{m}_{SS}$$

$$\dot{m}_4 = \dot{m}_5 = \dot{m}_6 = \dot{m}_{WS}$$

$$\dot{m}_7 = \dot{m}_8 = \dot{m}_9 = \dot{m}_{10} = \dot{m}_W$$

or

$$\dot{Q}_G = \dot{m}_W h_7 + \dot{m}_{SS} h_1 - \dot{m}_{WS} h_6 \tag{4.5}$$

where

h_1=enthalpy of saturated strong solution at T_1 and X_{SS}

h_6=enthalpy of weak solution at T_6 and X_{WS}

h_7=enthalpy of saturated water vapour at T_7

Generator temperature= $T_1 = T_7 = T_G$

(2) Condenser: The rate of heat transfer from the condenser is

$$\dot{Q}_C = \dot{m}_W (h_7 - h_8) \tag{4.6}$$

h_8=enthalpy of saturated water liquid at T_8

Condenser temperature=T_8=T_C

(3) Water pressure restrictor:

$$h_9 = h_8$$

h_9 = enthalpy of water liquid at T_9

(4) Evaporator: The rate of heat transfer to the evaporator i. e. the refrigerating capacity is

$$\begin{aligned} \dot{Q}_E &= \dot{m}_W(h_{10} - h_9) \\ &= \dot{m}_W(h_{10} - h_8) \end{aligned} \tag{4.7}$$

h_{10}=enthalpy of water vapour at T_{10}

Evaporator temperature=T_{10}=T_E

(5) Solution pressure restrictor:

$$h_3 = h_2$$

h_2=enthalpy of solution at T_2 and X_{SS}

h_3=enthalpy of solution at T_3 and X_{SS}

(6) Absorber: The rate of heat transfer from the absorber is

$$\begin{aligned} \dot{Q}_A &= \dot{m}_3 h_3 + \dot{m}_{10} h_{10} - \dot{m}_4 h_4 \\ &= \dot{m}_{SS} h_2 + \dot{m}_W h_{10} - \dot{m}_{WS} h_4 \end{aligned} \tag{4.8}$$

h_4=enthalpy of saturated weak solution at T_4 and X_{WS}

h_{10}=enthalpy of saturated water vapour at T_E

Absorber temperature=T_4=T_A

(7) Heat exchanger: Assuming that heat losses to the surroundings are negligible, the rate of heat transfer between the strong and weak solutions is

$$\dot{Q}_{HX} = \dot{m}_{SS}(h_1 - h_2) = \dot{m}_{WS}(h_6 - h_5) \tag{4.9}$$

(8) Solution pump: The power input to the pump is

$$\dot{W}_P = \dot{m}_{WS}(h_5 - h_4) \tag{4.10}$$

h_5=enthalpy of weak solution at T_5 and X_{WS}.

The difference between h_4 and h_5 is not distinguished on the charts of specific enthalpy of L_iB_r-water solutions as the temperature is approximately the same.

The coefficient of performance of the cycle is

$$COP = \frac{\dot{Q}_E}{\dot{Q}_G} = \frac{\dot{m}_W(h_{10} - h_8)}{\dot{m}_W h_7 + \dot{m}_{SS} h_1 - \dot{m}_{WS} h_6}$$

The second law efficiency of the cycle, given by equation 3. 17, is

$$\eta = \frac{-\dot{Q}_E(1 - \frac{T_o}{T_r})}{\dot{Q}_G(1 - \frac{T_o}{T_H}) + \dot{Q}_C(1 - \frac{T_o}{T_{cf,1}}) + \dot{Q}_A(1 - \frac{T_o}{T_{cf,2}})}$$

where

T_r=average temperature of chilled water=$\frac{(T_{CHW,i}+T_{CHW,e})}{2}$

T_H=average temperature of hot water=$\frac{(T_{HW,i}+T_{HW,e})}{2}$

$T_{cf,1}$=average temperature of cooling water=$\frac{(T_{CW1,i}+T_{CW1,e})}{2}$

$T_{cf,2}$=average temperature of cooling water=$\frac{(T_{CW2,i}+T_{CW2,e})}{2}$

T_o=ambient temperature

4.3 Optimisation Through Lost Work

A lost work analysis could be applied to improve the efficiency of energy usage in a refrigeration cycle.

The efficiency of existing processes and facilities is generally increased by modifying equipments or changing the operational conditions. The data developed in first law analysis are used as the basis for making a lost work balance of the system.

As the principal sources of lost work are isolated and the losses in each process evaluated, practical ideas for improvements should be found.

Certain causes of lost work can be acceptable as inevitable with present technology so the search focuses on areas most likely to be improved with conventional technology.

For the design of new systems, the losses can be calculated for different configurations, different types of equipment and procedures of operation.

Their effects on the system efficiency can be known before selecting the final design and operating conditions which minimize the lost work.

Reducing the lost work in a component of the absorption refrigeration process will not necessarily lead to a reduced system lost work because a change in one parameter that results in a decrease in lost work of one component can result in an increase in lost work of another component. The effect on the complete cycle must be considered.

Aqueous L_iB_r cooling cycles have been examined and optimized in relation to the first law of thermodynamics by studying the results of computer simulation of system COP. To study and optimize the cycle in respect of the

lost work, it is necessary to analyse the results of computer calculations of the second law efficiency with regard to the parameters of generator, condenser, absorber, evaporator temperatures , solution heat echanger effectiveness, ambient temperature, temperature differences between the internal working fluids (aqueous solution of lithium bromide, water refrigerant) and the external fluids (hot, cooling and chilled water).

Computer programmes to be prepared will examine the performance of L_iB_r absorption cycles through the model described in section 4.2 of this chapter.

Suitable analytical expressions for the enthalpy of lithium bromide solutions and water refrigerant are needed.

The enthalpy of the binary solution is given [18] as a function of the solution temperature and concentration.

$$h = 2.326(a + b(1.8t + 32) + c(1.8t + 32)^2) \tag{4.11}$$

where

h is in kJ/kg, t in °C,

a=-1015.07+(79.5387)X-(2.358016)X^2+(0.03031583)X^3-(1.400261E-4)X^4

b=4.68108-(3.037676E-1)X+(8.44845E-3)X^2-(1.047721E-4)X^3+(4.80097E-7)X^4

c=-4.9107E-3+(3.83184E-4)X-(1.078963E-5)X^2+(1.3152E-7)X^3-(5.897E-10)X^4

The equilibrium solution temperature is [18]

$$t = (a_o + a_1X + a_2X^2 + a_3X^3)t' + (b_o + b_1X + b_2X^2 + b_3X^3) \tag{4.12}$$

where

t' is the saturation temperature of water (°C)

a_o=-2.00755 b_o= 124.937

a_1= 0.16976 b_1=-7.7165

a_2=-3.13336E-5 b_2= 0.152286

a_3= 1.97668E-5 b_3=-7.9509E-4

Range: $-20 \leq t' \leq 110°C$

$5 \leq t \leq 180°C$

$45\% \leq X \leq 70\%$

The enthalpy of water refrigerant is given [12] in simplified form.

For water liquid

$$h_W = 4.19\,(t - t_o) \qquad kJ/kg \tag{4.13}$$

t is the temperature and t_o the datum temperature, 0°C.

For water vapour at low pressure

$$h_v = 2501 + 1.88\,(t - t_o) \qquad kJ/kg \tag{4.14}$$

The absorber and evaporator are assumed at the same pressure at equilibrium though in actual processes a small pressure is necessary. Therefore, the evaporator pressure or temperature and the absorber temperature define the concentration, X_{WS}, of the weak solution in the absorber.

Concentrations X_{WS} at the absorber and evaporator temperatures of interest are taken from the available charts [18] and used as input for running performance tests.

The condenser and generator are assumed at the same pressure at equilibrium. The condenser temperature and concentration of the strong solution in the generator, X_{SS}, can determine the generator temperature using equation (4.12).

The generator temperature may vary from a minimum to a maximum. The minimum is due to the fact that the solution starts to boil and vapour is produced only above the saturation temperature of the solution.

The maximum value is due to crystallization of the solution. Different crystallization lines are given in the literature (fig. 4.2). For the purpose of this study the exact value of the strong solution concentration, X_{SS}, at which the maximum generator temperature is calculated, is not critical. A maximum concentration of 64.9% was taken using charts of equilibrium vapour pressure of aqueous solutions of lithium bromide [18].

The evaporator temperature varies from the theoretical value of 0°C (water solidifies at this temperature) to the highest practical limit of 10°C for a useful refrigeration effect.

The absorber and condenser temperatures depend on the cooling water conditions and are within the reasonable range of 20°C to 40°C.

While the ambient temperature is taken as 25°C or 30°C, the heat exchanger is included in the study through its effectiveness. The heat exchanger effectiveness, HX, is defined as the ratio of the temperature drop of strong solution to the temperature difference of the strong and weak solutions entering the heat exchanger.

$$HX = \frac{t_G - t_2}{t_G - t_5}$$

but

$$t_5 = t_4 = t_A$$

so that

$$t_2 = (HX.t_A) + (1 - HX)t_G \tag{4.15}$$

For a set of external fluids , the cycle parameters are varied over the range of interest. The inlet and exit temperatures of the external fluids are chosen to be representative of existing absorption units [10] :

1. $t_{HW,e}$=t_G + 5°C

2. $t_{HW,i}=t_{HW,e} + 5°C$
3. $t_{CW1,e}=t_C - 2°C$
4. $t_{CW1,i}=t_{CW1,e} - 3°C$
5. $t_{CW2,e}=t_A - 2°C$
6. $t_{CW2,i}=t_{CW2,e} - 5°C$
7. $t_{CHW,e}=t_E + 6°C$
8. $t_{CHW,i}=t_{CHW,e} + 4°C$

The average temperature of external fluids (in °K) are then expressed as

$$\bar{T}_{HW} = t_G + 280.66°K \tag{4.16}$$

$$\bar{T}_{CW,1} = t_C + 269.66°K \tag{4.17}$$

$$\bar{T}_{CW,2} = t_A + 268.66°K \tag{4.18}$$

$$\bar{T}_{CHW} = t_E + 281.16°K \tag{4.19}$$

The influence of the temperature of all external fluids on the cycle efficiency is investigated by varying the temperature differences $\bar{t}_{HW} - t_G$, $\bar{t}_{CW,1} - t_C$, $\bar{t}_{CW,2} - t_A$ and and $\bar{t}_{CHW} - t_E$.

Two computer programmes are prepared. The first calculates the efficiency of the cycle for a set of constant temperature differences (equations 4.16 to 4.19) but with varying internal parameters.

In the second programme, the efficiency is computed as a function of the temperature differences for several sets of constant internal parameters.

The following procedure for preparing the first programme has been constructed.

0. Input data.

(i) Refrigerating capacity $\dot{Q}_E$ of the system

(ii) Average temperatures of external fluids

(iii) Equilibrium concentrations of weak solutions for calculation of minimum generator temperatures (from charts)

(iv) Maximum permissible concentration of strong solutions for calculations of maximum generator temperatures

1. Assume ambient temperature t_o
2. Assume evaporator temperature t_E
3. Calculate h_{10} from equ. (4.14) with $t=t_E$
4. Assume absorber temperature t_A
5. Calculate h_4 from equ. (4.11) with $t=t_A$ and X=X_{WS}
6. Assume condenser temperature t_C
7. Calculate h_8 from equ. (4.13) with $t=t_C$
8. Calculate minimum generator temperature t_{Gmin} from equ. (4.12) with $t'=t_C$ and X=X_{SS}=X_{WS}
9. Set new value of X_{SS} as $X_{SS}=X_{SS}+\Delta X$
10. Calculate refrigerant massflow rate $\dot{m}_W$ from equ. (4.7)
11. Calculate strong solution massflow rate $\dot{m}_{SS}$ from equ. (4.4)
12. Calculate weak solution massflow rate $\dot{m}_{WS}$ from equ. (4.3)
13. Calculate t_G from equ. (4.12) with t'=t_C and X=X_{SS}
14. Calculate h_1 from equ. (4.11) with t=t_G and X=X_{SS}
15. Calculate t_2 from equ. (4.15)
16. Calculate h_2 from equ. (4.11) with t=t_2 and X=X_{SS}
17. Calculate h_7 from equ. (4.14) with t=t_G
18. Calculate h_6 from equ. (4.9) with $h_4=h_5$

19. Calculate rate of heat input to generator $\dot{Q}_G$ from equ. (4.5)
20. Calculate rate of heat output from absorber $\dot{Q}_A$ from equ. (4.8)
21. Calculate rate of heat output from condenser $\dot{Q}_C$ from equ. (4.6)
22. Calculate second law efficiency from equ. (3. 17)
23. Repeat steps 9 to 22 until X_{SS} equal to maximum permissible concentration
24. Repeat steps 6 to 23 for different condenser temperatures
25. Repeat steps 4 to 24 for different absorber temperatures
26. Repeat steps 2 to 25 for different evaporator temperatures
27. Repeat steps 1 to 26 for different ambient temperatures

The numerical results were obtained for the following conditions

(i) Evaporator temperature of 4°C, 7°C, 10°C

(ii) Absorber temperature of 20°C, 30°C, 40°C

(iii) Condenser temperature of 20°C, 30°C, 40°C

(iv) Ambient temperature of 25°C and 30°C

(v) Constant temperature differences between the internal and external fluids as indicated from equations 4.14 to 4.17

(vi) Heat exchanger effectiveness is 0.0, 0.75, 0.95

(vii) The calculations of massflow rates, enthalpy and heat transfer rates have been made per unit refrigerating capacity of 1 kWatt

The second law efficiency is plotted versus the generator temperature in figures 4.4 to 4.9.

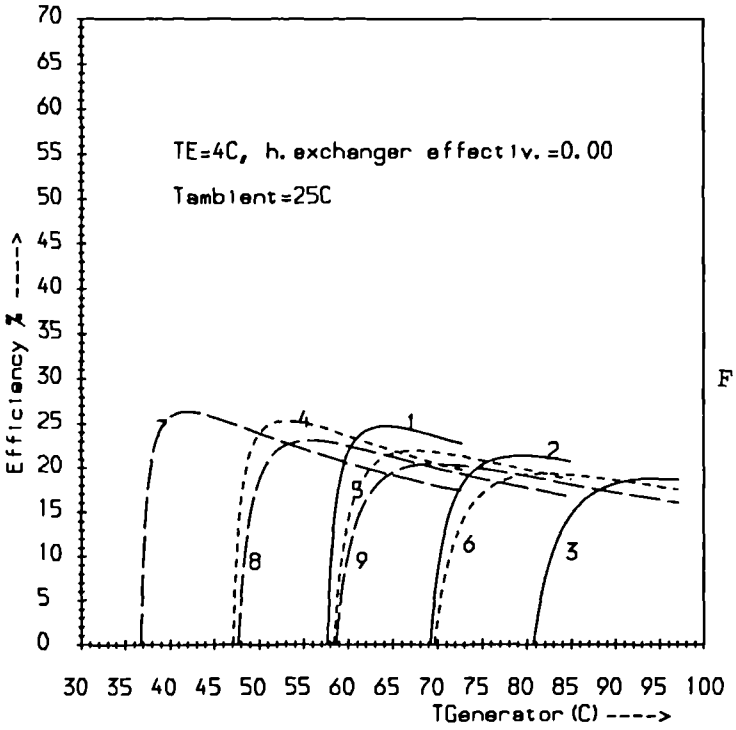

Fig.4.4 (a)

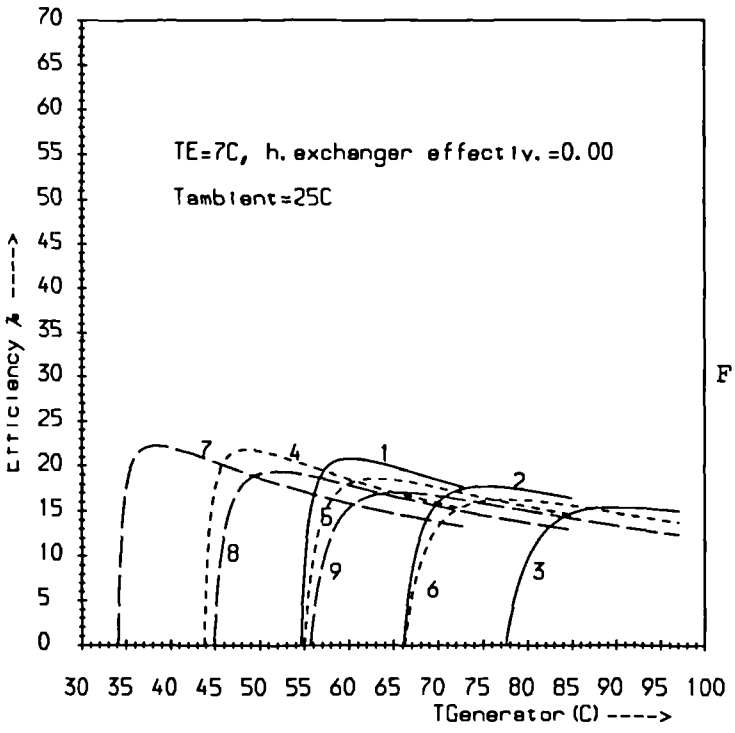

Fig.4.4 (b)

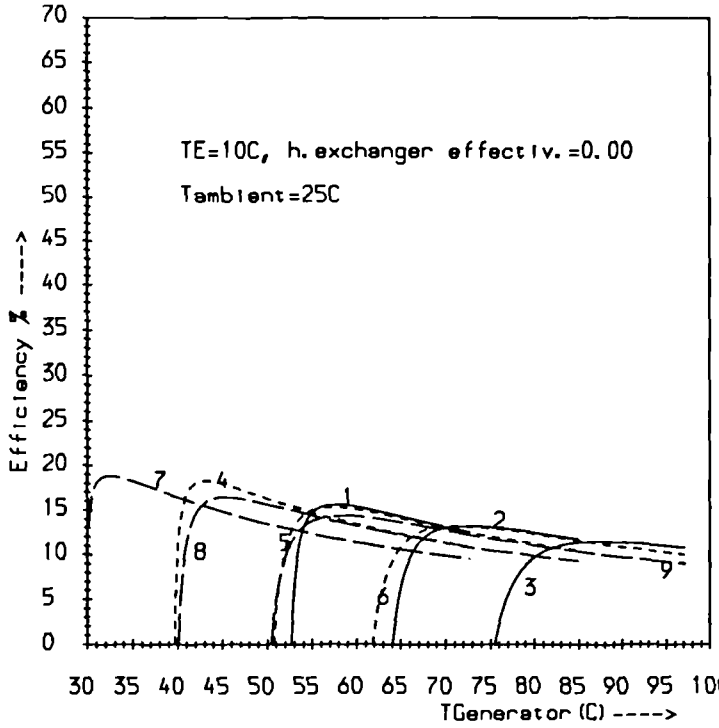

Fig.4.4 (c)

Legend: (TA, TC)

1: (40C, 20C), 2: (40C, 30C), 3: (40C, 40C)

4: (30C, 20C), 5: (30C, 30C), 6: (30C, 40C)

7: (20C, 20C), 8: (20C, 30C), 9: (20C, 40C)

Fig.4.4 (a),(b),(c) Cycle efficiency for a first set of operating parameters

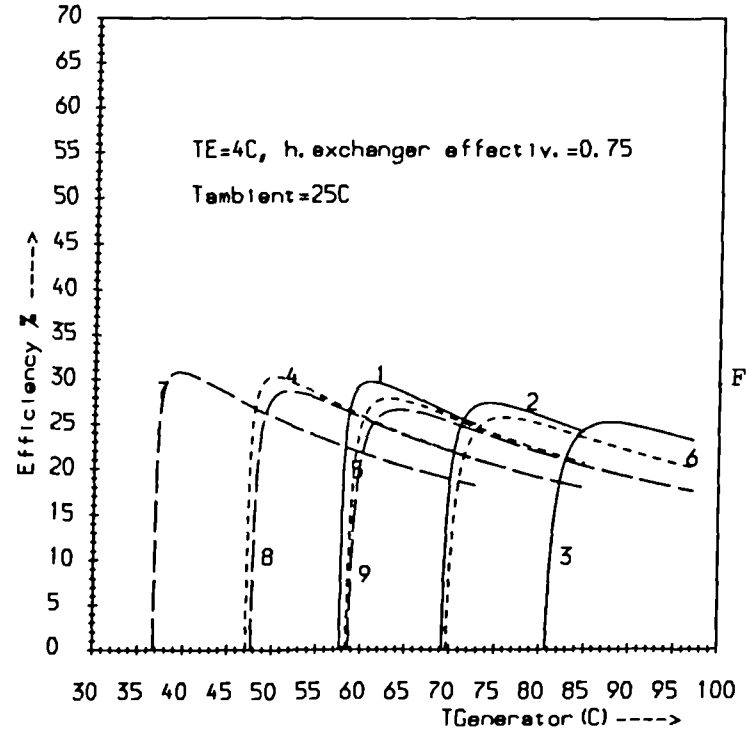

Fig.4.5 (a)

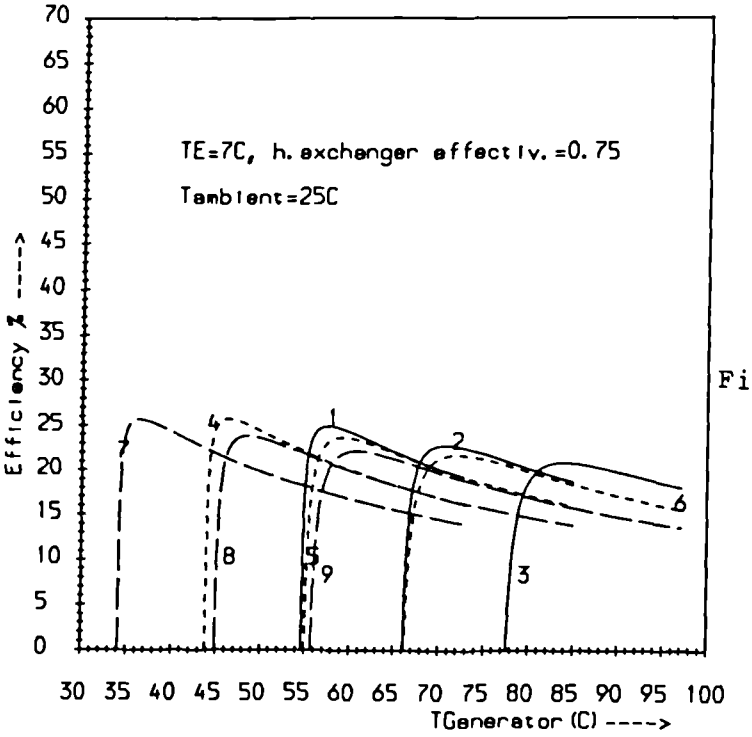

Fig.4.5 (b)

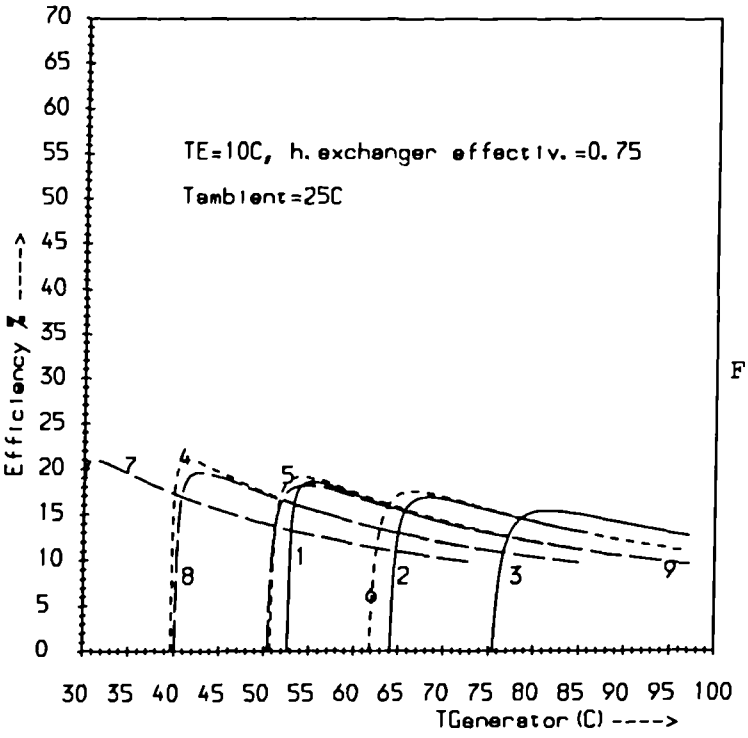

Fig.4.5 (c)

Legend: (TA, TC)

1: (40C, 20C), 2: (40C, 30C), 3: (40C, 40C)

4: (30C, 20C), 5: (30C, 30C), 6: (30C, 40C)

7: (20C, 20C), 8: (20C, 30C), 9: (20C, 40C)

Fig.4.5 (a),(b),(c) Cycle efficiency for a second set of operating parameters

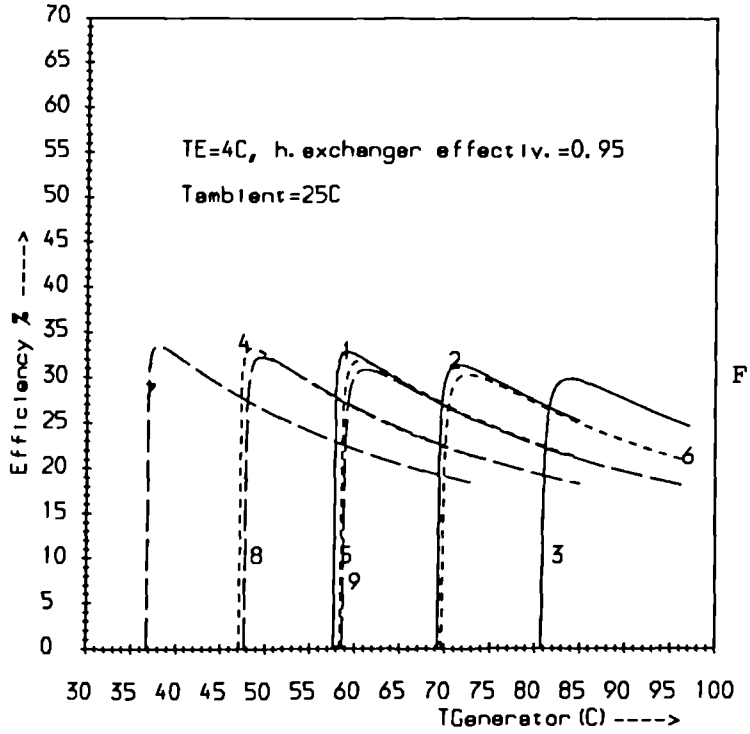

Fig.4.6 (a)

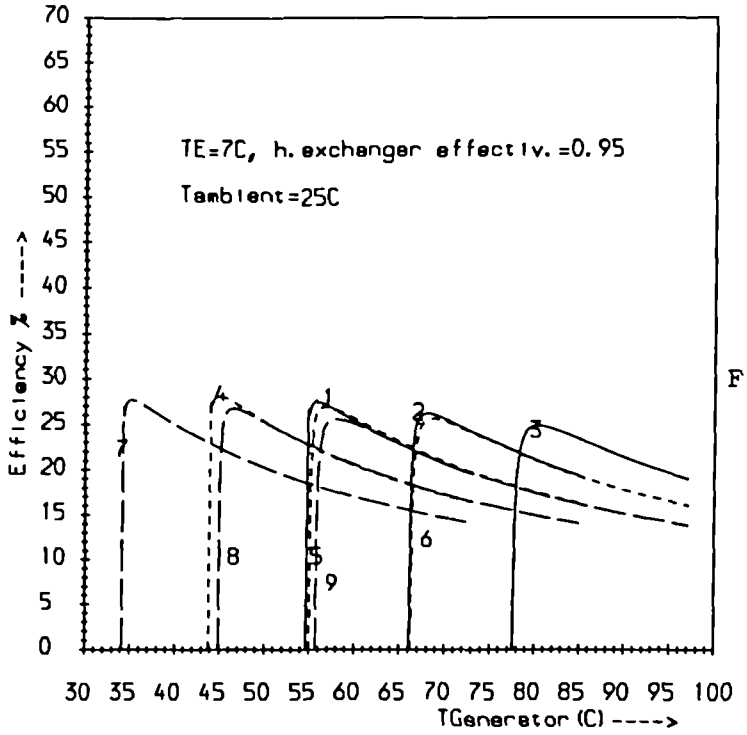

Fig.4.6 (b)

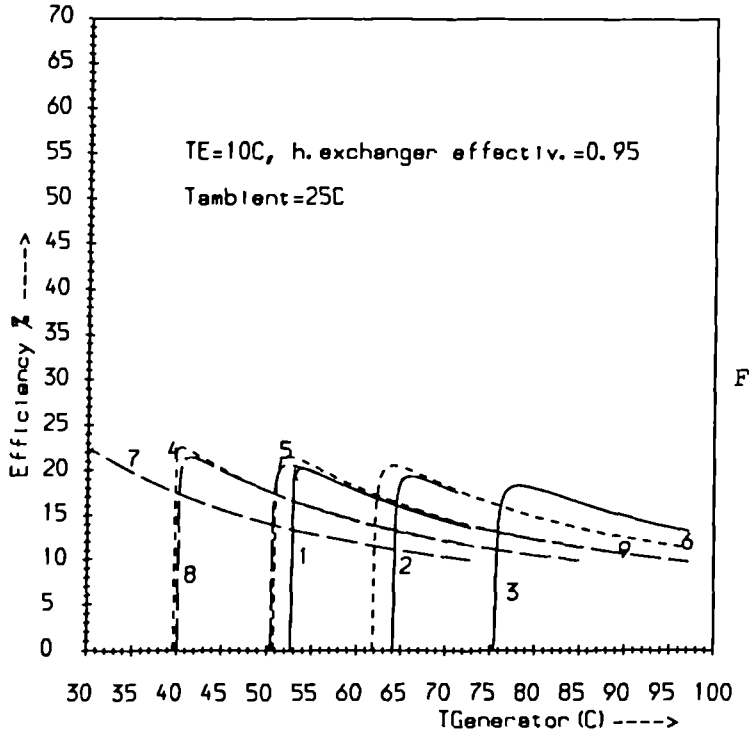

Fig.4.6 (c)

Legend: (TA, TC)

1: (40C, 20C), 2: (40C, 30C), 3: (40C, 40C)

4: (30C, 20C), 5: (30C, 30C), 6: (30C, 40C)

7: (20C, 20C), 8: (20C, 30C), 9: (20C, 40C)

Fig.4.6 (a),(b),(c) Cycle efficiency for a third set of operating parameters

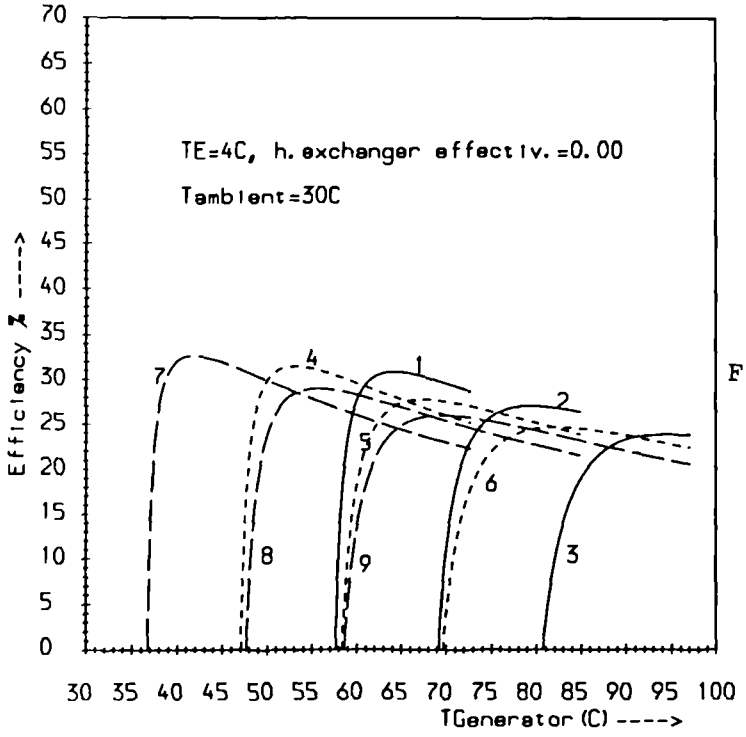

Fig.4.7 (a)

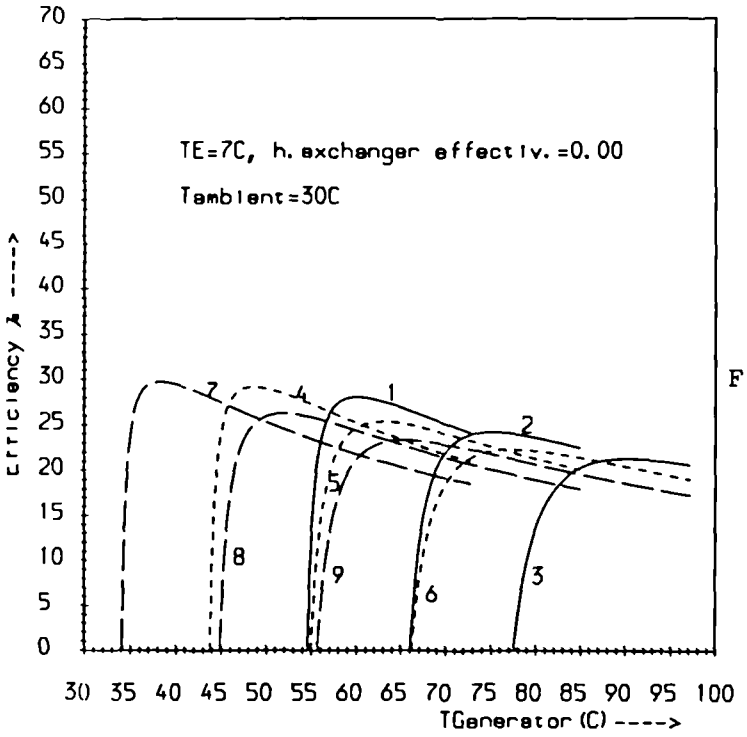

Fig.4.7 (b)

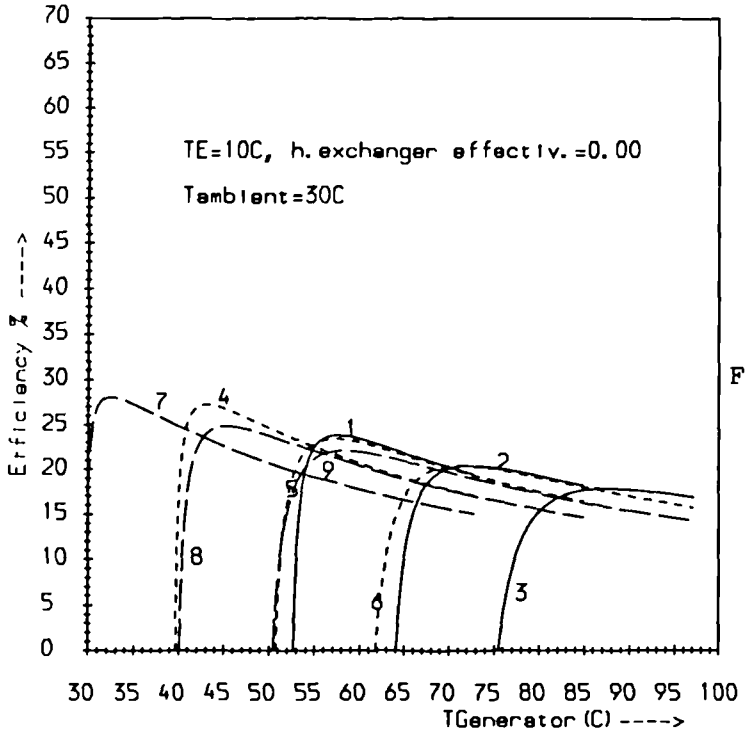

Fig.4.7 (c)

Legend: (TA, TC)

1: (40C, 20C), 2: (40C, 30C), 3: (40C, 40C)

4: (30C, 20C), 5: (30C, 30C), 6: (30C, 40C)

7: (20C, 20C), 8: (20C, 30C), 9: (20C, 40C)

Fig.4.7 (a),(b),(c) Cycle efficiency for a fourth set of operating parameters

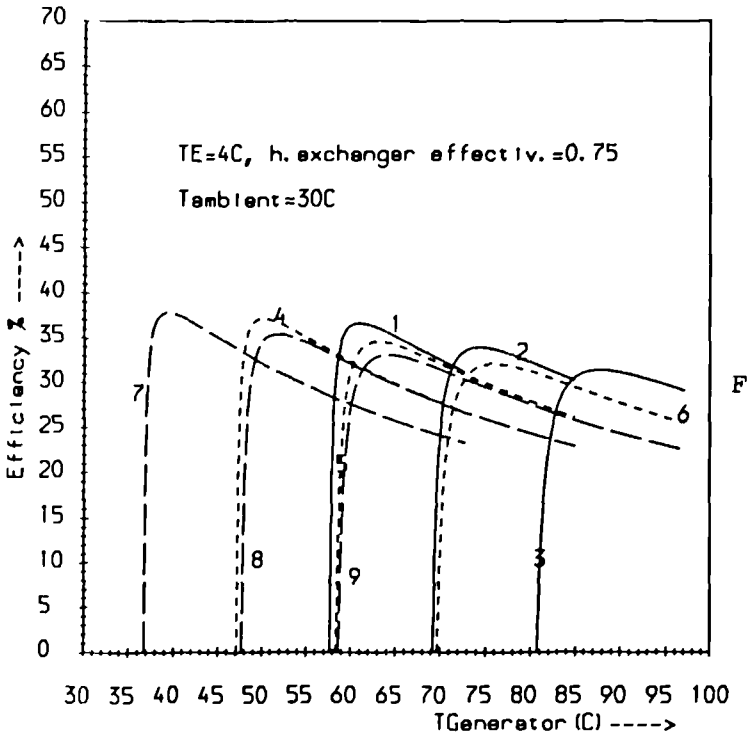

Fig.4.8 (a)

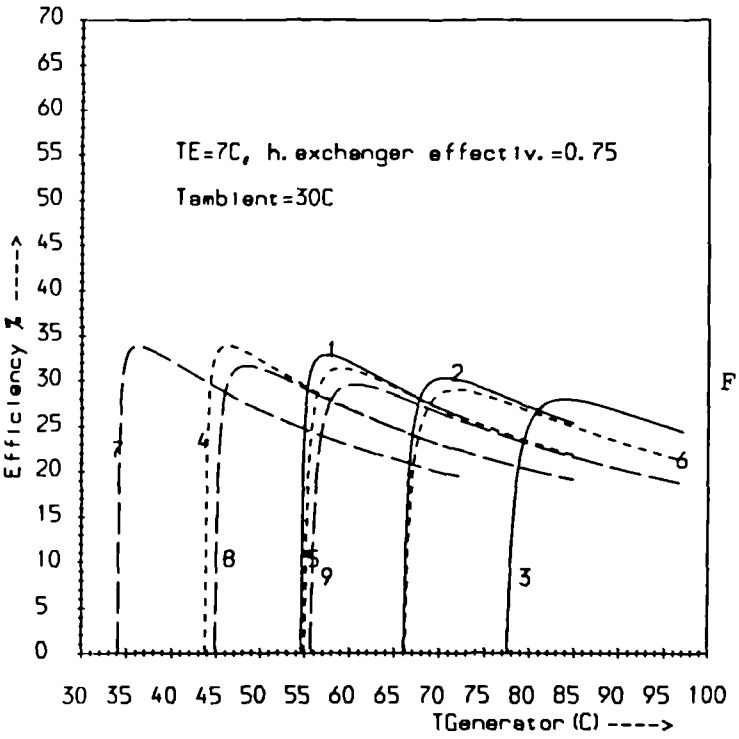

Fig.4.8 (b)

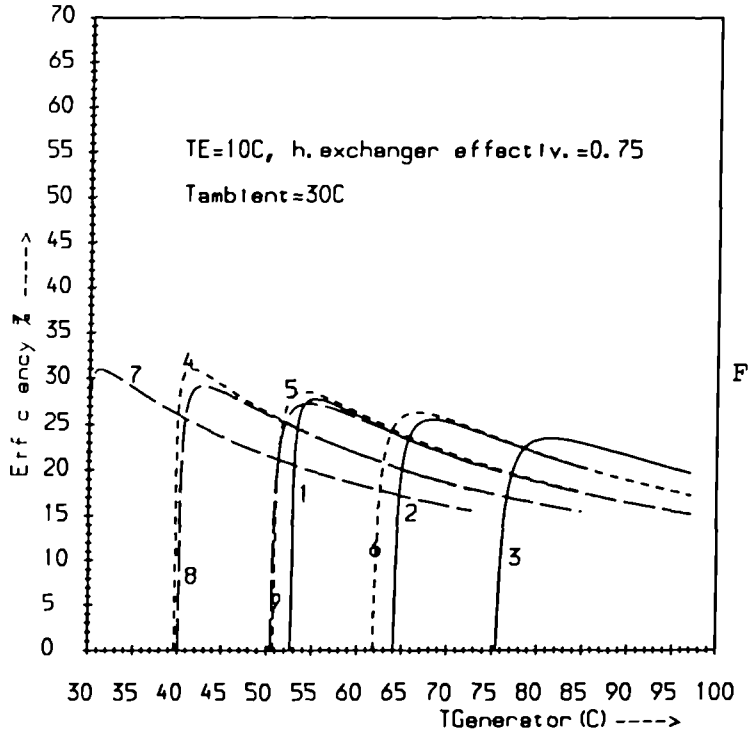

Fig.4.8 (c)

Legend: (TA, TC)

1: (40C, 20C), 2: (40C, 30C), 3: (40C, 40C)

4: (30C, 20C), 5: (30C, 30C), 6: (30C, 40C)

7: (20C, 20C), 8: (20C, 30C), 9: (20C, 40C)

Fig.4.8 (a),(b),(c) Cycle efficiency for a fifth set of operating parameters

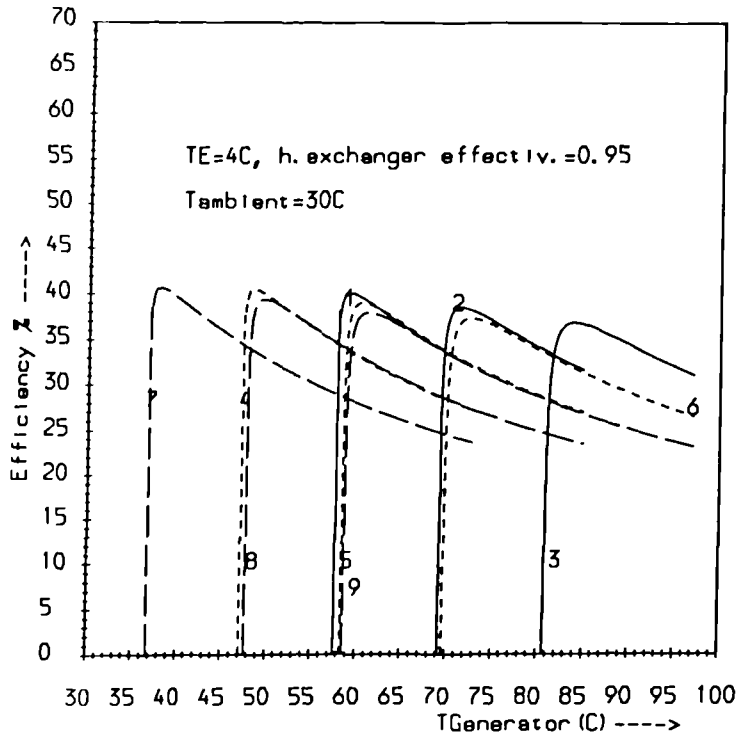

Fig.4.9 (a)

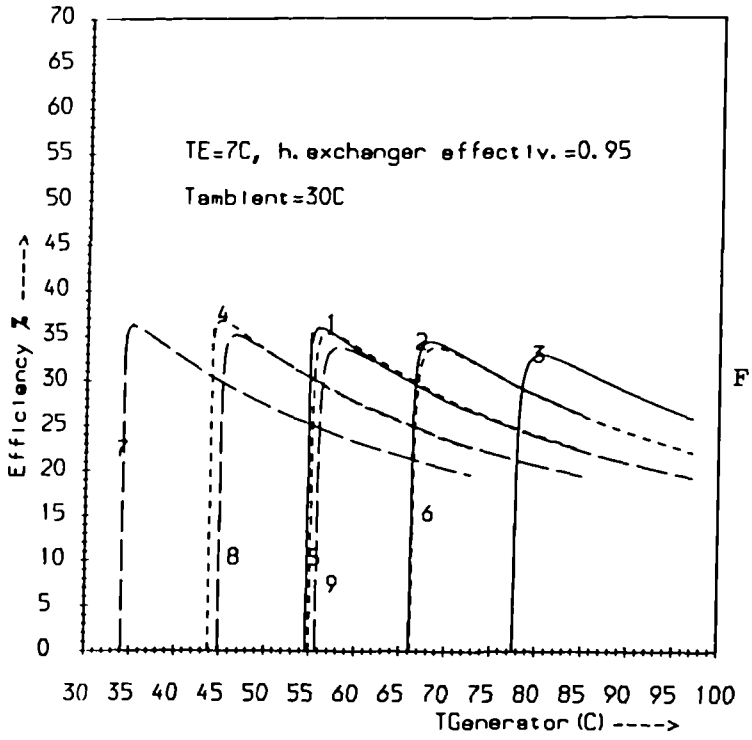

Fig.4.9 (b)

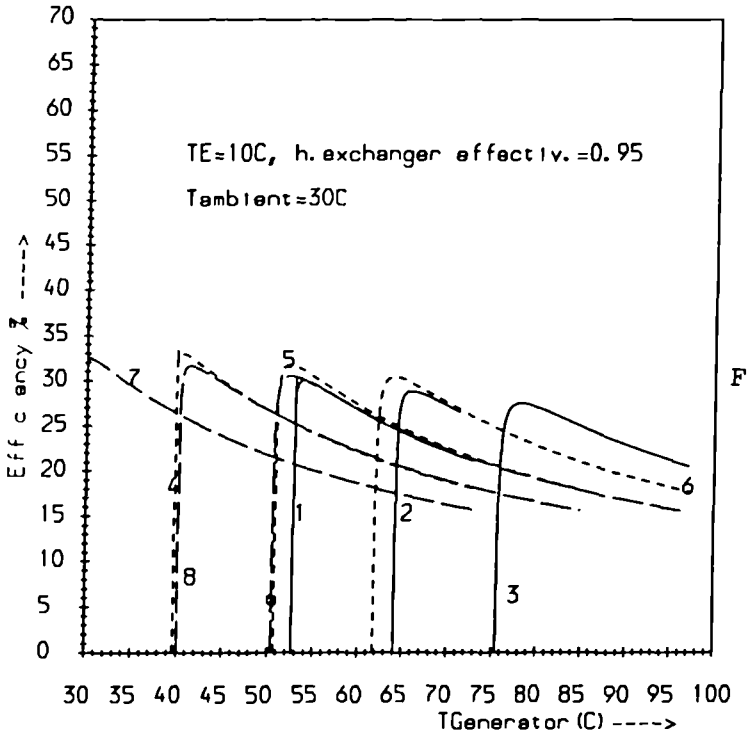

Fig.4.9 (c)

Legend: (TA, TC)

1. (40C, 20C), 2. (40C, 30C), 3. (40C, 40C)

4. (30C, 20C), 5. (30C, 30C), 6. (30C, 40C)

7. (20C, 20C), 8. (20C, 30C), 9. (20C, 40C)

Fig.4.9 (a),(b),(c) Cycle efficiency for a sixth set of operating parameters

The programmes of second law efficiency computation and plotting are listed in appendices A1 and A2.

The variation of cycle efficiency with the difference between the average temperature of external fluids and the temperature of internal fluids is considered by developing a second computer programme based on the following procedure.

0. Input data

   (i) $\dot{Q}_E$

   (ii) X_{WS} from charts of equilibrium vapour pressure for the evaporator and absorber temperatures of interest

1. Assume t_o
2. Assume t_G
3. Assume t_A
4. Assume t_C
5. Assume t_E
6. Calculate h_{10}
7. Calculate h_4
8. Calculate h_8
9. Calculate $\dot{m}_W$, $\dot{m}_{WS}$, $\dot{m}_{SS}$
10. Calculate t_2
11. Calculate h_2, h_6, h_7
12. Calculate $\dot{Q}_G$
13. Calculate $\dot{Q}_A$
14. Calculate $\dot{Q}_C$
15. Calculate efficiency for variant $\bar{t}_{CHW}$-t_E
16. Calculate efficiency for variant $\bar{t}_{HW}$-t_G
17. Calculate efficiency for variant $\bar{t}_{CW1}$-t_C

18. Calculate efficiency for variant $\bar{t}_{CW2}$-t_A
19. Repeat steps 5 to 18 for different t_E
20. Repeat steps 4 to 19 for different t_C
21. Repeat steps 3 to 20 for different t_A
22. Repeat steps 2 to 21 for different t_G
23. Repeat steps 1 to 22 for different t_o

Results of the programme have been obtained for temperature differences increasing from 0 to 20°C, ambient temperatures of 25°C and 30°C, evaporator temperatures of 4°C and 7°C, heat exchanger effectiveness equal to 0.75, generator temperature of 65°C, absorber temperature of 40°C and condenser temperature of 20°C. The calculations have also been based on a unit refrigerating capacity of 1 kWatt.
The second law efficiency is plotted versus the temperature differences in figures 4.10 and 4.11.
The programmes used to calculate and plot the efficiency are listed in appendices A3 and A4.

4.4 Discussion of results

Figures 4.4, 4.5, 4.6 show the efficiency of the aqueous L_iB_r cooling cycle for an ambient temperature of 30°C and different values of the operating parameters.
Figures 4.7, 4.8, 4.9 represent the variation of efficiency for an ambient temperature of 25°C.
The figures show a maximum and then a decrease for increasing generator temperatures t_G. When there is no heat exchanger in the cycle (effectiveness=0) and the cooling water in the absorber and condenser is at a higher temperature (40°C), the efficiency increases to a maximum then becomes insensitive to generator temperature (curves 3 in figures 4.4 and 4.7).
It is evident from the figures that a higher heat exchanger effectiveness decreases the generator temperature corresponding to maximum efficiency.

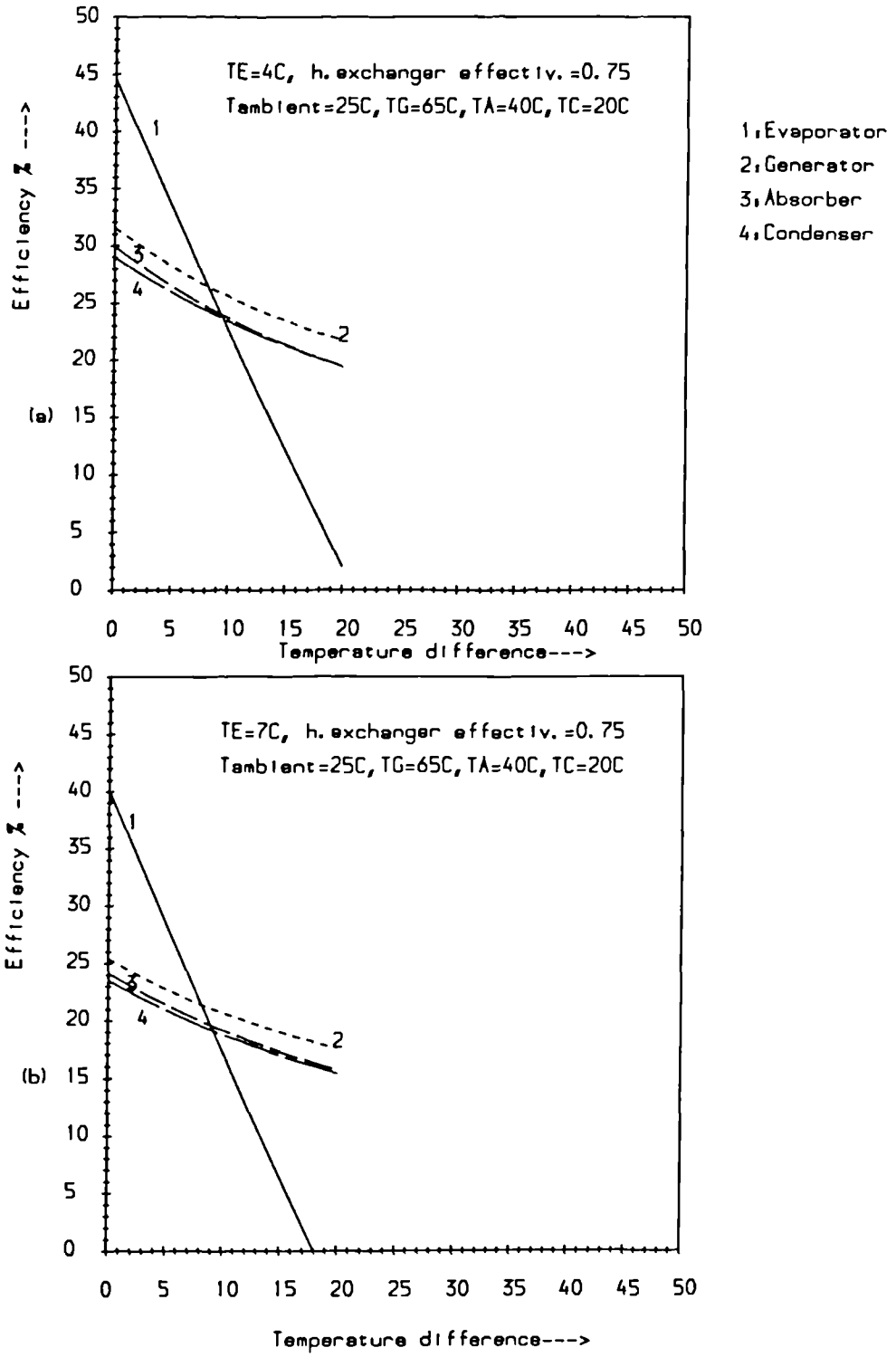

Fig.4.10 (a),(b) Variation of cycle efficiency with temperature differences for a first set of operating parameters

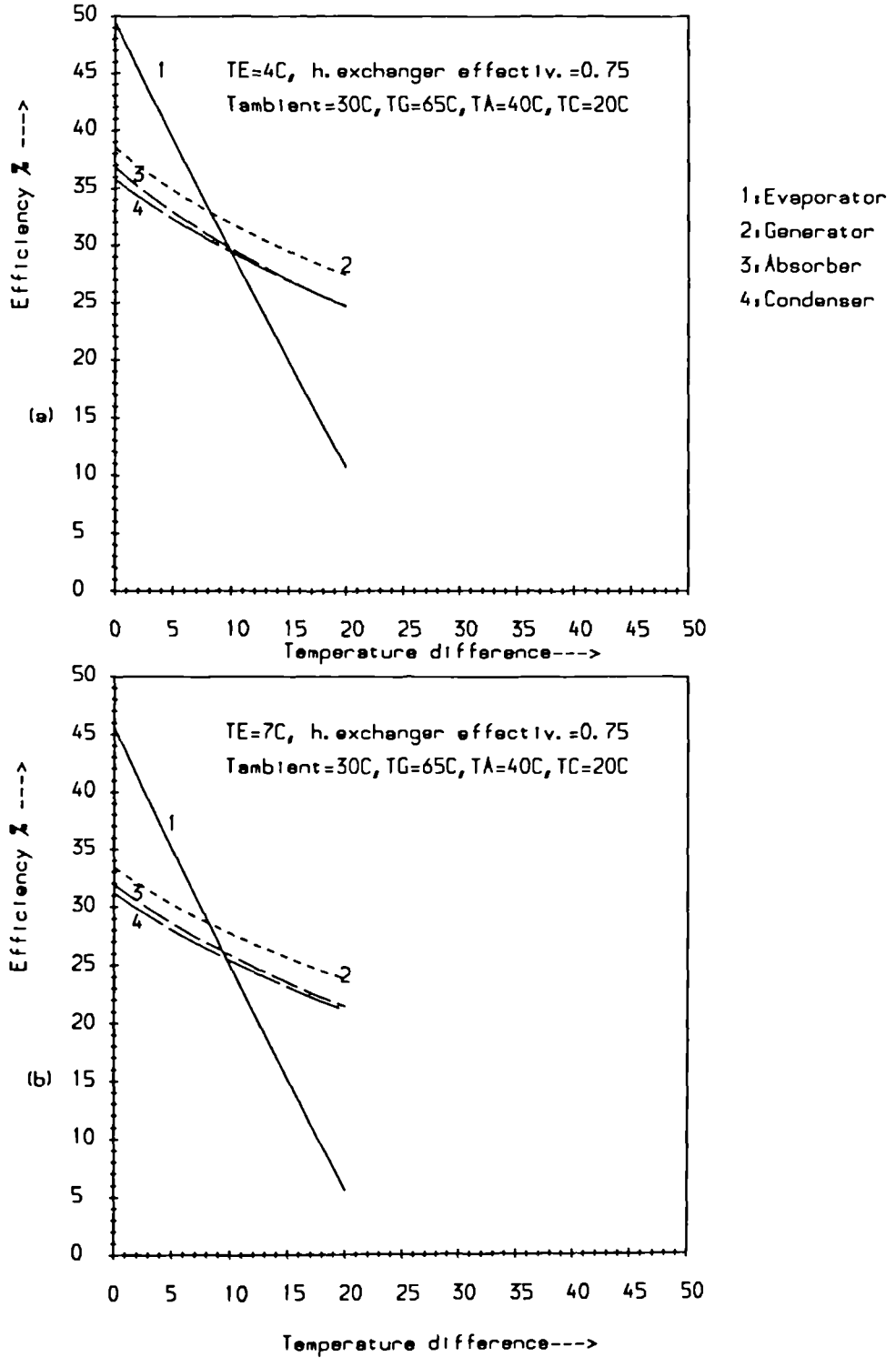

Fig.4.11 (a),(b) Variation of cycle efficiency with temperature differences for a second set of operating parameters

Raising generator temperature beyond the value that gives maximum efficiency can result in a 16% decrease of the efficiency.

It can also be seen that the second law efficiency decreases with :

1. increasing evaporator temperature t_E
2. increasing condenser temperature t_C
3. increasing absorber temperature t_A
4. decreasing heat exchanger effectiveness HX
5. decreasing ambient temperature t_o

} All other conditions remaining constan

A change in t_C from 20°C to 40°C at lower HX resulted in a 6.5% reduction of efficiency while at higher heat exchanger effectiveness, the decrease is smaller. Similarly an increase in t_A from 20°C to 40°C resulted in a 3.5% decrease in efficiency.

Lowering t_E from 10°C to 4°C can lead to an improvement of efficiency up to 8.5% and 11.5% for ambient temperatures of 30°C and 25°C respectively.

Figures 4.10 and 4.11 show the cycle efficiency variation with temperature differences.

When the temperature difference in the evaporator decreases from 20°C to a hypothetical 0°C, the efficiency is greatly improved (39%). A decrease of 1°C improves the efficiency by approximately 2%.

Smaller variations take place across the temperature differences in the generator (7 to 11%), in the absorber (8 to 11.5%) and in the condenser (8 to 11.5%).

In the study of performance of aqueous L_iB_r cooling cycles using the coefficient of performance COP [10, 46], it has been shown that the COP increases to a maximum for higher generator temperatures and then either decreases slightly or becomes insensitive to generator temperature. This behaviour of COP is similar to the variation of second law efficiency which however decreases more rapidly after it reaches a maximum value.

Comparing the curves of variation of second law efficiency and those of COP (figures 4.12 to 4.15) for similar sets of operating parameters, it can be seen that the generator temperature corresponding to maximum efficiency is always much lower than the generator temperature corresponding to maximum COP.

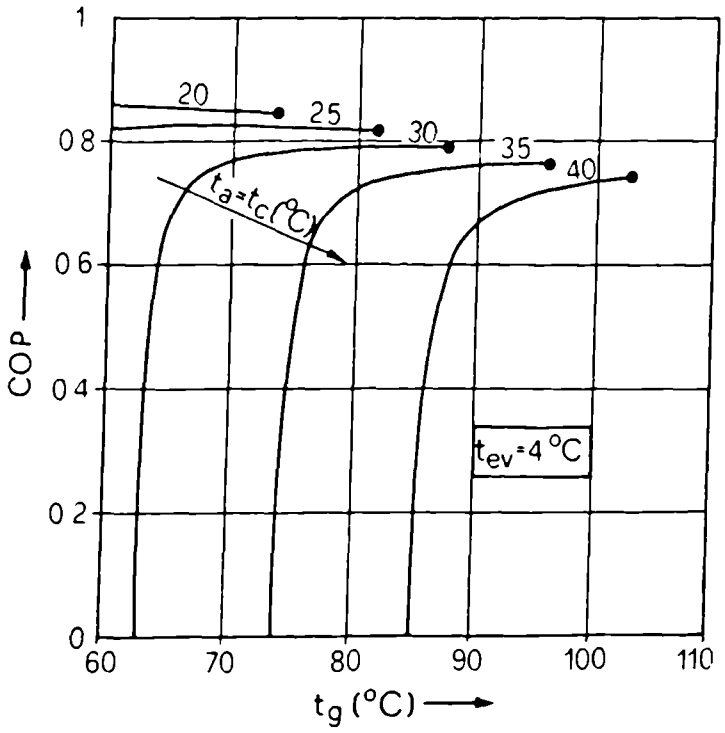

Fig.4.12 COP of aqueous LiBr cooling cycles for a first set of parameters

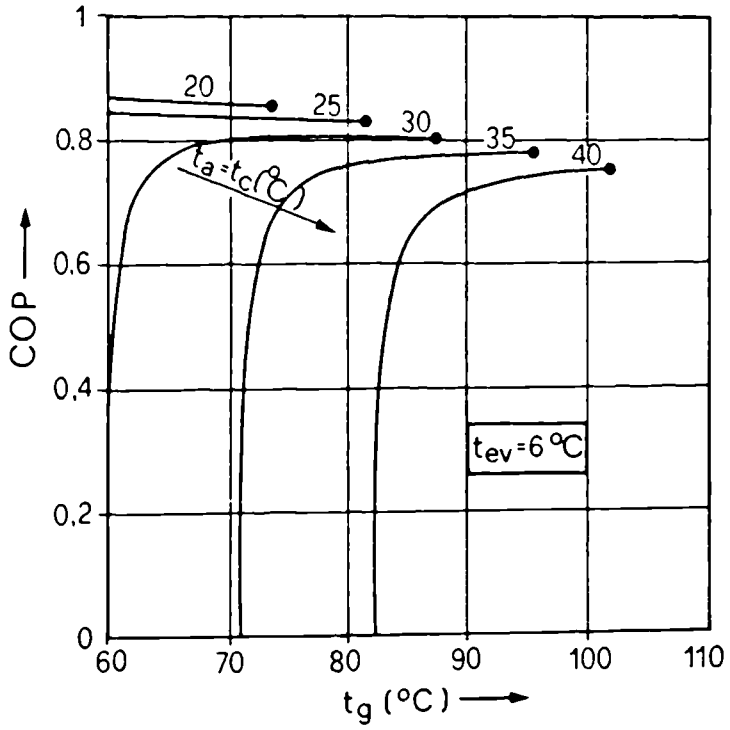

Fig.4.13 COP of aqueous LiBr cooling cycles for a second set of parameters

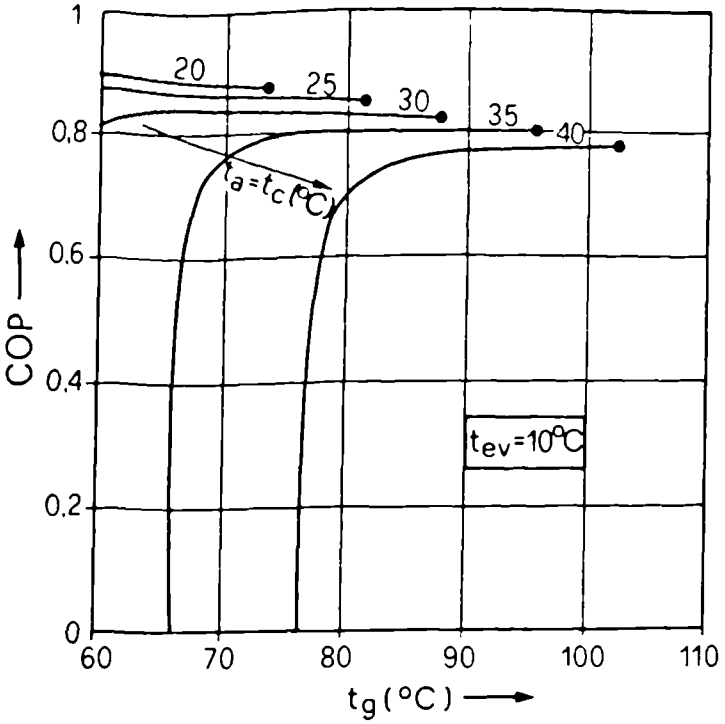

Fig.4.14 COP of aqueous LiBr cooling cycles for a third set of parameters

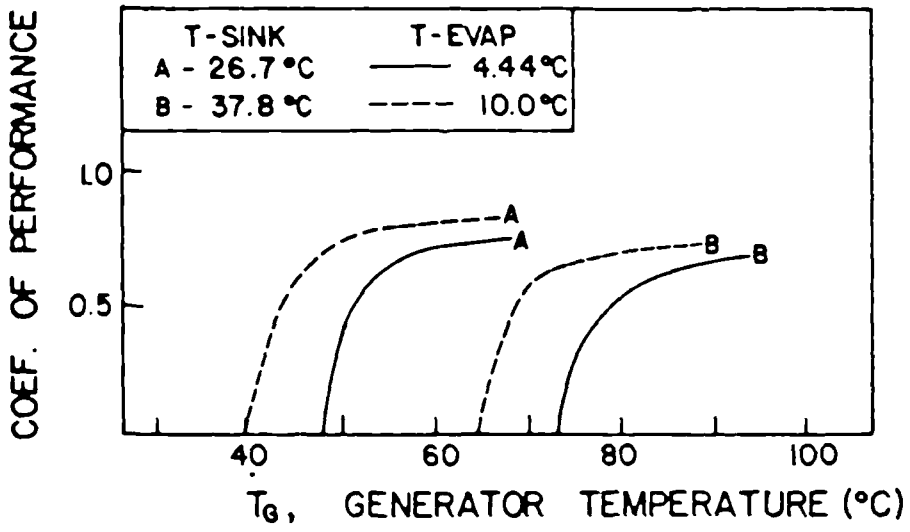

Fig.4.15 COP of aqueous LiBr cooling cycles with solution heat exchanger effectiveness of 0.75

Since the efficiency decreases rapidly after its maximum value, it is clear that generator temperatures giving maximum COP are, in fact, corresponding to reduced cycle efficiency.
The system COP increases with increasing evaporator temperature while on the contrary the second law cycle efficiency decreases. COP and efficiency are similarly affected by absorber and condenser temperatures.

In general, it can be concluded that many ways are at hand for improving the second law efficiency of the L_iB_r-water absorption cycle.
Design generator temperature should be selected to maximize efficiency.
Higher generator temperatures are to be avoided whereas lower evaporator temperatures should be chosen.
Decreasing the absorber and condenser temperatures is recommended.
Improvement of the solution heat exchanger effectiveness leads to an increase of cycle efficiency. Efforts in reducing the temperature differences between the cycle fluids and the external fluids in the components, are highly advisable particularly in the evaporator component.

4.5 Conclusion

In this chapter, aqueous lithium bromide absorption refrigeration cycles have been modelled and optimized.
To study the system performance two computer programmes were developed producing a second law efficiency as a function of all operating parameters. Efficiency variation was plotted versus the generator temperature for several sets of parameters and versus the temperature differences between the internal and external fluids in the various components.
The influence of temperatures of generator, evaporator, absorber, condenser, environment and of the heat exchanger effectiveness was examined as well as the influence of the temperature of the heating, cooling and refrigerated mediums.

Improvement in cycle efficiency can be obtained by proper design.

A comparison was made of variations of cycle efficiency and cycle COP with working parameters. Design recommendations were given.

CHAPTER FIVE

THERMODYNAMIC DESIGN

5.1 Introduction

Following the results of the cycle optimization of chapter 4 a thermodynamic L_iB_r-water absorption refrigeration system has been designed and is discussed in this chapter.

The continuous cycle operates with hot water in the generator, chilled water in the evaporator and cooling water in the absorber and condenser. Rates of heat transfer in the components have been calculated for the selected set of cycle operating parameters.

The process operating data are presented in figure 5.2.

Required areas for heat transfer in the heat exchangers have been evaluated from appropriate correlations of heat transfer coefficients available in the literature.

Generator,absorber and evaporator components are shell and coil heat exchangers of the falling-film or spray-type. The condenser is a shell and coil heat exchanger with refrigerant vapour condensing in the shell. The solution heat exchanger is formed of closely spaced plates.

Figures 5.5 to 5.8 show the coils of designed generator, condenser, evaporator and absorber.

The cross sectional arrangement of the solution heat exchanger is illustrated in figure 5.9.

5.2 Design of System

The thermodynamic design of L_iB_r-water absorption refrigeration systems by the first law only is usually based on given or assumed steady-state operating conditions. Absorber, condenser and evaporator temperatures are fixed as well as the temperature approach in the solution heat exchanger. System refrigerating capacity is also known.

The lowest generator temperature below which the cycle will not operate is determined; then generator temperature is designed for operation at a value sufficiently above the lowest generator temperature for better performance. Rates of heat added to or substracted from the system are found from equations of mass and energy balances; system COP is calculated. Heat transfer areas are determined from appropriate correlations of heat transfer coefficients.

In this study, both first and second laws are used to design a thermodynamic sytem of aqueous L_iB_r absorption refrigeration .
From considerations given in chapter 4, it is possible to fix a practical thermodynamic cycle of operation.
The operating conditions are selected using the design recommendations provided in chapter 4.
The design procedure can be summarized as follows.
(i) Assume refrigerating capacity of system $\dot{Q}_E$
(ii) Select cycle operating conditions

1 Absorber temperature t_A

2 Condenser temperature t_C

3 Evaporator temperature t_E

4 External fluids temperatures t_{CHW}, t_{HW}, t_{CW1}, $t_{CW,2}$

5 Temperature difference approach for the solution in the heat exchanger $t_2 - t_A$

6 Generator temperature t_G

(iii) Calculate rates of heat transfer, system COP and second law efficiency
(iv) Determine required heat transfer areas

Consider the design of a L_iB_r-water absorption cooling cycle having a refrigerating capacity of 1 kWatt.

As lower condenser and absorber temperatures increase cycle efficiency, they should be chosen as low as possible. However in practice they are more or less fixed by the cooling water available.

In this study, a condenser temperature of 28°C and an absorber temperature of 37°C are selected.

The evaporator temperature is normally between 4 and 12°C for air conditioning of space maintained between 24 and 27°C. An evaporator temperature of 12°C is sufficient to cool the air; however, the evaporator temperature of an actual absorption cycle has to be designed at 4 or 5°C to absorb the excess humidity in the air. Reduced evaporator temperatures give higher second law efficiency of aqueous L_iB_r absorption refrigeration cycles.

Refrigerant temperature in the evaporator should be therefore designed at or below 4°C to satisfy both practical requirements and needs of higher second law efficiency. Nevertheless, in this design of a laboratory model, an evaporator temperature of 10°C is selected.

This is due to two reasons. The first is that operation at very low evaporator temperatures implies relatively high vacuum working pressures that need rigid standards of vacuum integrity to be maintained. The second reason is that for an evaporator temperature of 10°C and for an absorber temperature of 37°C, the weak solution concentration in the absorber will be typical of concentrations used in small L_iB_r-water refrigeration units.

From steam tables, the saturation pressure of refrigerant water vapour at 10°C is equal to 9.21 mm Hg. Assuming a small pressure difference of 1 mm Hg between evaporator and absorber, the pressure in the absorber will be 8.21 mm Hg.

From charts of equilibrium vapour pressure of aqueous solutions of L_iB_r [18] based on equation 4.12, the concentration of the weak solution at 37°C and 8.21 mm Hg is 54%.

From steam tables, the saturation pressure of water vapour at 28°C in the con-

denser is 28.37 mm Hg. Assuming a small pressure difference of 3% between condenser and generator the pressure in the generator becomes equal to 29.22 mm Hg.

The temperature of all external fluids is to be fixed for closer temperature approaches as shown by the results of variation of efficiency with temperatures differences (figures 4.10,4.11). Differences between the average temperature of heating, cooling, refrigerated fluids and the temperature of cycle working fluids should be reduced to values that might be attained with practical equipment. The following temperature differences are assigned for the thermodynamic cycle in consideration.

1. Evaporator: Chilled water enters at a temperature 5°C higher than evaporating refrigerant temperature. A drop of 3°C in its temperature is assumed so that the exit temperature is 2°C higher than evaporating water temperature. Then

$$t_{CHW,i} = t_E + 5^oC = 15^oC,$$

$$t_{CHW,e} = 12^oC,$$

$$\bar{t}_{CHW} = 13.5^oC$$

2. Generator: Hot water enters at a temperature 6°C higher than temperature of boiling aqueous solutions of L_iB_r and leaves the generator after a drop of 2°C in its temperature.

$$t_{HW,i} = t_G + 6^oC,$$

$$t_{HW,e} = t_G + 4^oC,$$

$$\bar{t}_{HW} = t_G + 5^oC$$

3. Absorber and Condenser: Cooling water inlet temperature is 4°C lower than absorber solution temperature and condenser refrigerant vapour temperature.

Temperature of cooling streams rise by 2°C in absorber and condenser.

So,

$$t_{CW1,i} = t_C - 4 = 24^oC,$$
$$t_{CW1,e} = 26^oC,$$
$$\bar{t}_{CW1} = 25^oC$$

and

$$t_{CW2,i} = t_A - 4 = 33^oC,$$
$$t_{CW2,e} = 35^oC,$$
$$\bar{t}_{CW2} = 34^oC$$

The temperature drops are due to heat exchanges and flow rates; reducing them would of course increase the required heat transfer areas and/or increase the flowrates of external fluids.

Finally, before a generator temperature is selected, a value of the solution heat exchanger effectiveness HX is necessary.

By definition of HX, higher values mean lower exit temperatures of cooled strong solution in the heat exchanger. However, under some conditions of operation the solution is so strong leaving the generator that it would crystallize if cooled below a certain temperature.

Besides, assumed values of heat exchanger effectiveness should result in acceptable temperature approaches for the cold-end of the solution heat exchanger. A minimum temperature approach of 25°F (13.8°C) is usually allowed in heat exchangers of absorption refrigeration cycles. Assume a heat exchanger effectiveness of 36% in this design.

Generator temperature will be found using the second law efficiency variation curves, then temperature approach in heat exchanger is checked. If it is unsatisfactory, a new HX will be assumed and new t_G determined.

The efficiency variation was plotted in figure 5.1 for the selected set of cycle

parameters and for an ambient temperature of 30°C.

A generator temperature of 69°C can be selected so as to give higher values of efficiency and to be sufficiently higher than minimum generator temperature of 60°C for better operation.

From equation 4.15, the exit temperature of the strong solution in the heat exchanger is

$$t_2 = (HX.t_A) + (1 - HX).t_G$$

For HX 0.36, t_A=37°C, t_G=69°C : t_2=57.5°C.
Thus the temperature approach in the cold end of the heat exchanger , being equal to $t_2 - t_A$, is 20.5°C. Although it can be reduced further, this temperature approach is acceptable for the purpose of this design.
From figure 5.1, the maximum generator temperature is 83°C.
The strong solution concentration in the generator is thus found from charts of equilibrium vapour pressure of L_iB_r-water solutions [18] for a temperature of 69°C and a pressure of 29.22 mm Hg,

$$X_{SS} = 58.5\%$$

The rates of heat transfer have been evaluated as

$$\dot{Q}_G = 1.3493\ kW$$

$$\dot{Q}_A = 1.3033\ kW$$

$$\dot{Q}_C = 1.0462\ kW$$

With massflow rate of refrigerant $\dot{m}_W$=1.499 kg/h, massflow rate of strong solution $\dot{m}_{SS}$=17.99 kg/h and massflow rate of weak solution $\dot{m}_{WS}$=19.49 kg/h.

Using a heat balance equation around the heat exchanger, the exit temperature of the weak solution is found equal to 50.5°C. The heat transfer rate

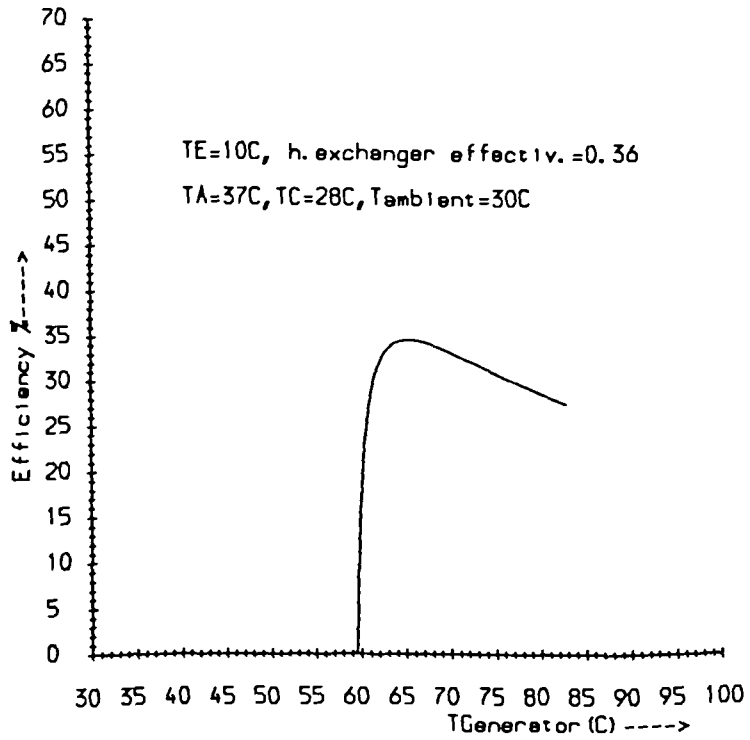

Fig.5.1 Cycle efficiency variation for one set of parameters

in the heat exchanger given by equation (4.9) is 0.114 kWatt.
The work input to the system in the pump is small and neglected in the calculation of COP and efficiency. However in practice it is usually estimated in order to size the driving motor.

$$\dot{W}_p = \frac{\dot{v}\Delta P}{\eta_p} \qquad (in\ Watt)$$

Where
$\dot{v}$ is the volume rate of flow in m^3/s,
ΔP the difference between inlet and exit pressures in pascals,
η_p the pump efficiency.

The density of the weak solution leaving the absorber and entering the pump at 37°C and 54% is [11] ρ_{sol}=1575 kg/m^3.
Assuming a pump efficiency of 70%,

$$\dot{W}_p = \frac{\dot{m}_{WS}}{\rho_{sol}}(\frac{\Delta P}{0.7}) = 0.014W$$

A summary of the operating conditions of the designed thermodynamic cycle is illustrated in figure 5.2.

The COP of this cycle is equal to 74.1% and its second law efficiency to 33.5%.

5.3 Design of Generator

Generators of absorption refrigeration machines are usually of the flooded type where the tubes carrying the hot fluid are totally immersed in the cycle working solution.
Commercial machines are also available with generators of the spray type so

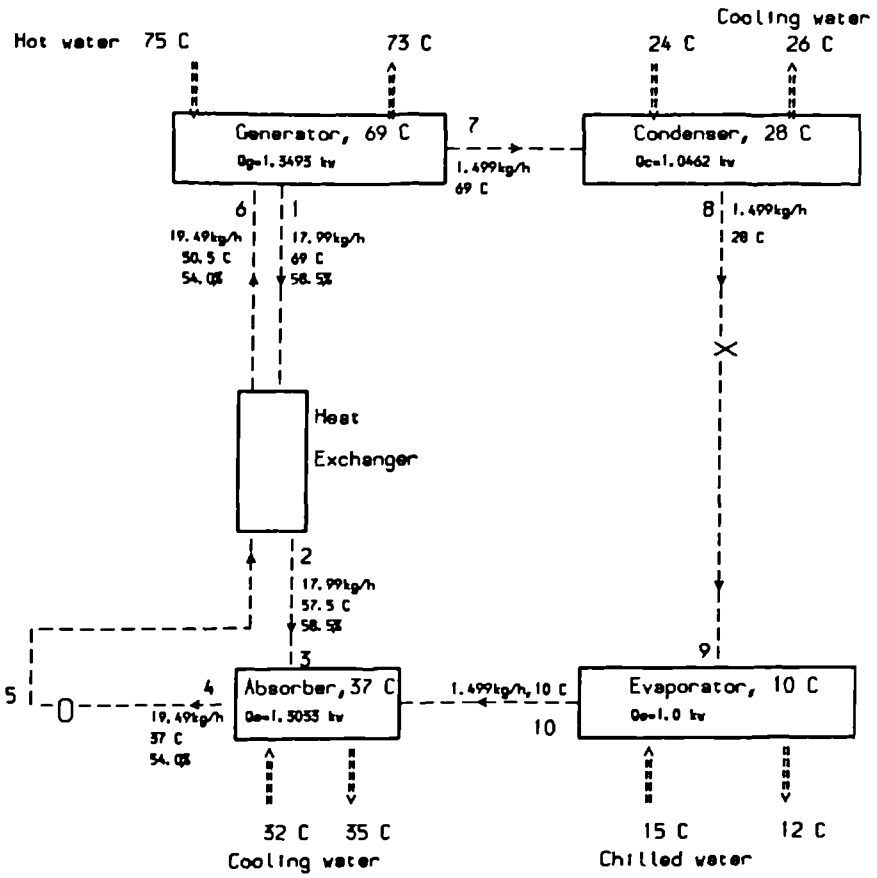

Fig.5.2 Shematic of absorption refrigeration process with operating conditions data

that falling films of solutions are boiled on horizontal tubes [9,33]. Flooded type generators require a heat source at a high temperature while spray type generators can operate at low and moderate temperatures.

It has been shown in chapter 4 that higher efficiencies of L_iB_r-water absorption cooling cycles can be obtained with lower generator temperatures and closer temperature approaches between hot water and solution in the generator.

Relatively high heat fluxes can be attained with small temperature differences by boiling of films on horizontal tubes. Spray type generators are therefore preferred to flooded type generators.

For L_iB_r-water absorption cycles using spray type generators, the incorporation of a pregenerator in the cycle between the solution heat exchanger and the generator has been examined [9] and results show that it reduces the generator area considerably.

No improvement in cycle COP has been obtained at full capacity but with a pregenerator in the cycle, the solution is superheated which improves its distribution over the generator tubes.

If new calculations are carried out for the designed thermodynamic cycle with a pregenerator (figure 5.3) then, the following applies :

Rate of heat added in the pregenerator $\dot{Q}_{PG}$=0.1446 kW

Rate of heat added in the generator $\dot{Q}_G$=1.20 kW.

Including the term of lost work in the pregenerator, the cycle efficiency becomes equal to 33.7%.

Cycle COP is

$$COP \quad \frac{\dot{Q}_E}{\dot{Q}_{PG} + \dot{Q}_G} = 74.4\%$$

An improvement of cycle efficiency of only 0.2% is obtained by addition of a pregenerator to the basic cycle. Therefore, no incorporation of a pregenerator

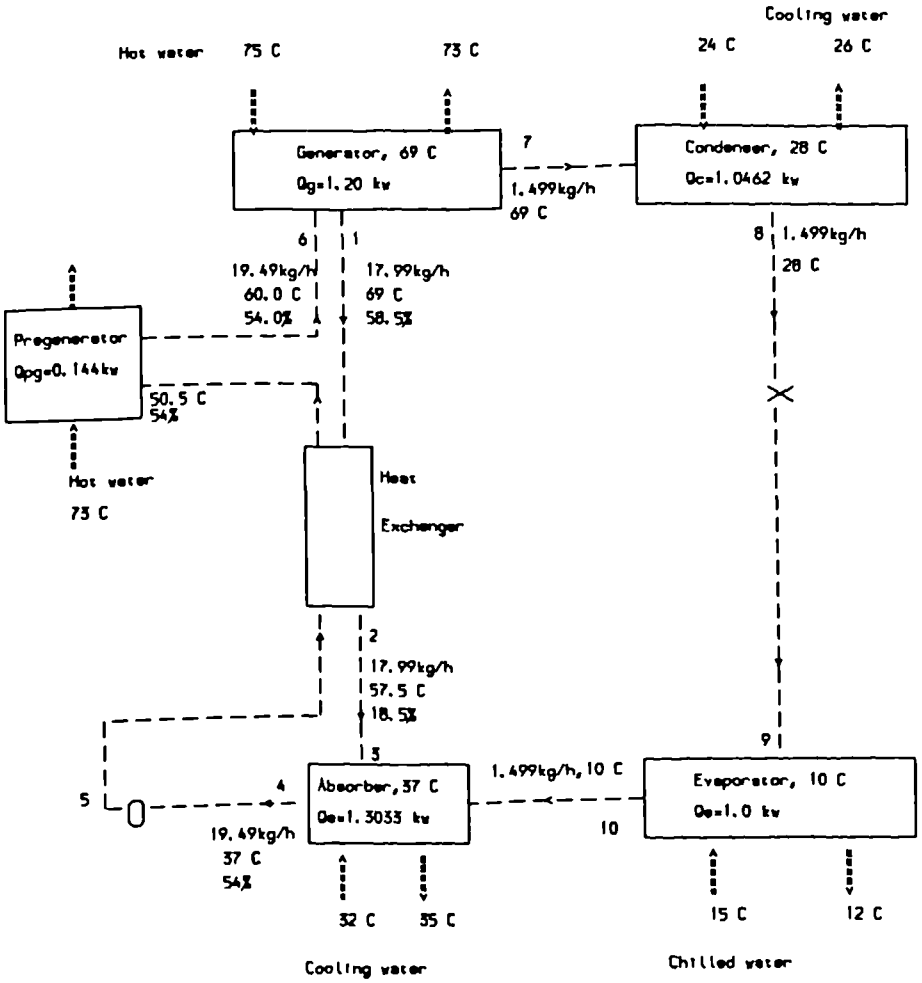

Fig.5.3 Shematic of absorption refrigeration process with a pregenerator

has been considered in this design.

A shell and coil generator of the spray type is designed in which hot water flows inside the tubes and solution is distributed over the tubes.

The design data are :

1. $\dot{Q}_G$=1.35 kW, t_G=69°C
2. $\dot{m}_{SS}$=17.99 kg/h, t_{SS}=69°C, X_{SS}=58.5%
3. $\dot{m}_{WS}$=19.49 kg/h, t_{WS}=50.5°C, X_{WS}= 54.0%
4. $t_{HW,i}$=75°C, $t_{HW,e}$=73°C, $\bar{t}_{HW}$=74°C
5. The properties of hot water at 74°C are [53]

   ρ_W −975.32 kg/m^3, μ_W=0.369 10^{-3} kg/m-s

   k_W −0.665 W/m-°C, $C_{P,W}$=4.193 kJ/kg-°C

   $P_{r,W}$=2.33

6. The properties of L_iB_r-water solution at 69°C and 58.5% are from [11]

   ρ_{SS} −1670 kg/m^3, μ_{SS}=2.95 10^{-3} kg/m-s

   $C_{P,SS}$=1.905 kJ/kg-°C

   By extrapolation of data from [54] k_{SS}=0.419 W/m-°C.

The heat transfer coefficient h_i for the hot water flow on the inside of the tubes is evaluated first.

The massflow rate of hot water inside tubes is

$$\dot{m}_W = \frac{\dot{Q}_G}{C_{P,W}\Delta t_W} = \frac{1350}{4193\text{x}2} = 0.161\ kg/s$$

The Reynolds number is

$$R_e = \frac{\dot{m}_W D_i}{A\mu_W}$$

Where A is the cross sectional area of the tubes

D_i the inside diameter of tubes.

15 mm nominal diameter tubes are used with following dimensions :

inside diameter D_i=13.565 mm

outside diameter D_o=14.965 mm

thickness 0.7 mm

Thus R_e 40953.4

Since the flow is turbulent, the Nusselt number for fluids flowing inside tubes is [55]

$$N_u = 0.023\ R_e^{0.8} P_r^n$$

Where n 0.4 for heating and n=0.3 for cooling.

thus

$$N_u = 0.023(40953.4)^{0.8}(2.33)^{0.3} = 145.13$$

and

$$h_i = N_u \frac{k}{D_i} = 7114.84$$

The outside heat transfer coefficient h_o is calculated from a correlation [56] developed for predicting heat transfer by combined boiling and evaporation of falling liquid films on horizontal tubes.

The average heat transfer coefficient over the tube circumferential length L is

$$h_o = h_b + h_d\frac{L_d}{L} + h_c(1 - \frac{L_d}{L}) \qquad (5.1)$$

Where

h_b is the nucleate boiling heat transfer,

h_d the average heat transfer coefficient in the thermal developing region where the fluid is being superheated,

h_c the convective heat transfer coefficient due to evaporation of liquid films at the vapour-liquid interface,

L_d the thermal developing length.

h_d is given by

$$h_d = \frac{3}{8} C_P \frac{\Gamma}{L_d} \tag{5.2}$$

Where

$$\Gamma = \frac{\dot{m}}{2L_{tube}}$$

$$L_d = \frac{\Gamma^{\frac{4}{3}}}{4\pi\rho\alpha}\left(\frac{3\mu}{g\rho^2}\right)^{\frac{1}{2}} \tag{5.3}$$

α is the thermal diffusivity.

h_c is found from

$$h_c = 0.821\left(\frac{\nu^2}{k^3 g}\right)^{0.33}\left(\frac{4\Gamma}{\mu}\right)^{-0.22} \quad for\ laminar\ flow \tag{5.4}$$

$$-\ 3.8\ 10^{-3}\left(\frac{\mu^2}{k^3 g}\right)^{0.33}\left(\frac{4\Gamma}{\mu}\right)^{0.4}\left(\frac{\nu}{\alpha}\right)^{0.65} \quad for\ turbulent\ flow \tag{5.5}$$

ν is the kinematic viscosity. No nuclear boiling occurs if the temperature difference is small between the saturated liquid film and the hot water in the tubes. Therefore, equation (5.1) is rewritten as

$$h_o = h_d \frac{L_d}{L} + h_c\left(1 - \frac{L_d}{L}\right) \tag{5.6}$$

Assume a tube length of 0.30 m.

$$\Gamma = \frac{\dot{m}_{SS}}{2L_{tube}} = \frac{19.49}{3600\text{x}2\text{x}0.3} = 9.023\text{x}10^{-3}\ kg/m-s$$

$$\alpha_{SS} = \frac{k_{SS}}{\rho_{SS} C_{P,SS}} = \frac{0.419}{1670\text{x}1905} = 1.32\text{x}10^{-7}\ m^2/s$$

$$L_d = \frac{(9.023\text{x}10^{-3})^{\frac{4}{3}}}{4\pi\text{x}1670\text{x}1.32\text{x}10^{-7}} \left(\frac{3\text{x}2.95\text{x}10^{-3}}{9.81\text{x}(1670)^2}\right)^{\frac{1}{2}} = 1.22\text{x}10^{-5}\ m$$

and

$$h_d = 528344.72\ W/m^2 - s$$

The point of transition from equation (5.4) to (5.5) in calculating h_c is [56]

$$\left(\frac{4\Gamma}{\mu}\right)_{tr} = 5800\left(\frac{\nu}{\alpha}\right)^{-1.06} \tag{5.7}$$

$$= 5800\left(\frac{2.95\text{x}10^{-3}}{1670\text{x}1.32\text{x}10^{-7}}\right)^{-1.06} = 370.94$$

In this design,

$$\left(\frac{4\Gamma}{\mu}\right) \quad \frac{4\text{x}9.023\text{x}10^{-3}}{2.95\text{x}10^{-3}} = 12.23$$

So the correlation for the laminar case in equation (5.4) may be used to give h_c 2902.44 $W/m^2 - ^o C$.

The outside heat transfer coefficient can now be computed from equation (5.6).

$$h_o = 3175.14\ W/m^2 - ^o C$$

The overall heat transfer coefficient U_o based on the outside area of the tubes is [11]

$$U_o = \left(\frac{D_o}{D_i h_i} + \frac{D_o}{D_i} r_{fw} + \frac{1}{h_o} + \frac{D_o}{2k_t} \ln \frac{D_o}{D_i}\right)^{-1} \tag{5.8}$$

Where

r_{fw} is the fouling factor for the hot water side,

k_t the thermal conductivity of copper tubes.

For city water r_{fw}=0.176x10^{-3}

For copper tubes k_t=390 $W/m -^o C$

Substituting numerical values into equation (5.7), U_o becomes

$$U_o = 1501.4\ W/m^2 -^o C$$

The logarithmic mean temperature difference $LMTD$ is

$$LMTD = \frac{(t_G - t_{HW,e}) - (t_G - t_{HW,i})}{\ln \frac{t_G - t_{HW,e}}{t_G - t_{HW,i}}} = \frac{(69 - 73) - (69 - 75)}{\ln \frac{6}{4}} \qquad (5.9)$$

$$- 4.93\ ^oC$$

Because the solution entering the generator is usually subcooled, the temperature difference is higher and there is a small error in using the solution saturation temperature T_G in the $LMTD$ expression. However, the convection coefficient in the subcooling section is normally lower than the evaporating heat transfer coefficient.

The two errors compensate for each other and the application of equation (5.8) is common practice.

Therefore,the required wetted area can be calculated.

$$A = \frac{\dot{Q}_G}{F\ U_o\ LMTD} = \frac{1350}{1501.4\text{x}4.93} = 0.1824\ m^2$$

With the correction factor F–1.0 for a phase change.

The total length of tubes is

$$L_{total} - \frac{A}{\pi D_o} = 3.88\ m$$

The number of tubes is

$$n = \frac{L_{total}}{L_{tube}} = \frac{3.88}{0.30} = 12.93 \quad or \quad n = 13.$$

In the design of falling film evaporators and generators with working fluid of

relatively low viscosity, tube spacing effects might be important as well as entrainment and deflection of droplets by the vapour crossflow [57].
Aqueous solutions of L_iB_r have relatively high viscosities so such effects are assumed negligible. Nevertheless, to ensure good thermal performance a space of 12 mm between horizontal tubes has been chosen so that the solution droplets falling from one tube impige upon the next lower tube.
Figure 5.4 shows the generator coil.

The pressure drop of the hot water side is calculated from

$$\Delta P = f\frac{L}{D_i}\frac{V^2}{2}\rho \tag{5.10}$$

Where
f is the friction factor,
V is the water velocity,
L is the length of straight tubes plus the equivalent length of the return bends. If each return bend consists of two 90° elbows then its equivalent length of straight tube is twice the equivalent length of one 90° elbow.
For a 90° elbow of a tube of 15 mm diameter, the equivalent length is 0.6 m [13]. In the generator coil there are 13 tubes of 0.30 m length each and 12 return bends of 1.2 m equivalent length each.
The hot water velocity in the tubes is

$$V - \frac{\dot{m}}{\rho\frac{\pi}{4}D_i^2} = 1.142\ m/s$$

For Reynolds number of 40953.4, f is obtained from Moody charts [13] as 0.0218. Then $\Delta P - 14.7\ kpa$ which is less than the allowable pressure drop of 70 kpa [13].
For liquid films falling on the outside of horizontal tubes the Reynolds number rarely exceeds 2100 [16]. The solution side pressure drop is negligible as the gravity flow is laminar and its rate very small.

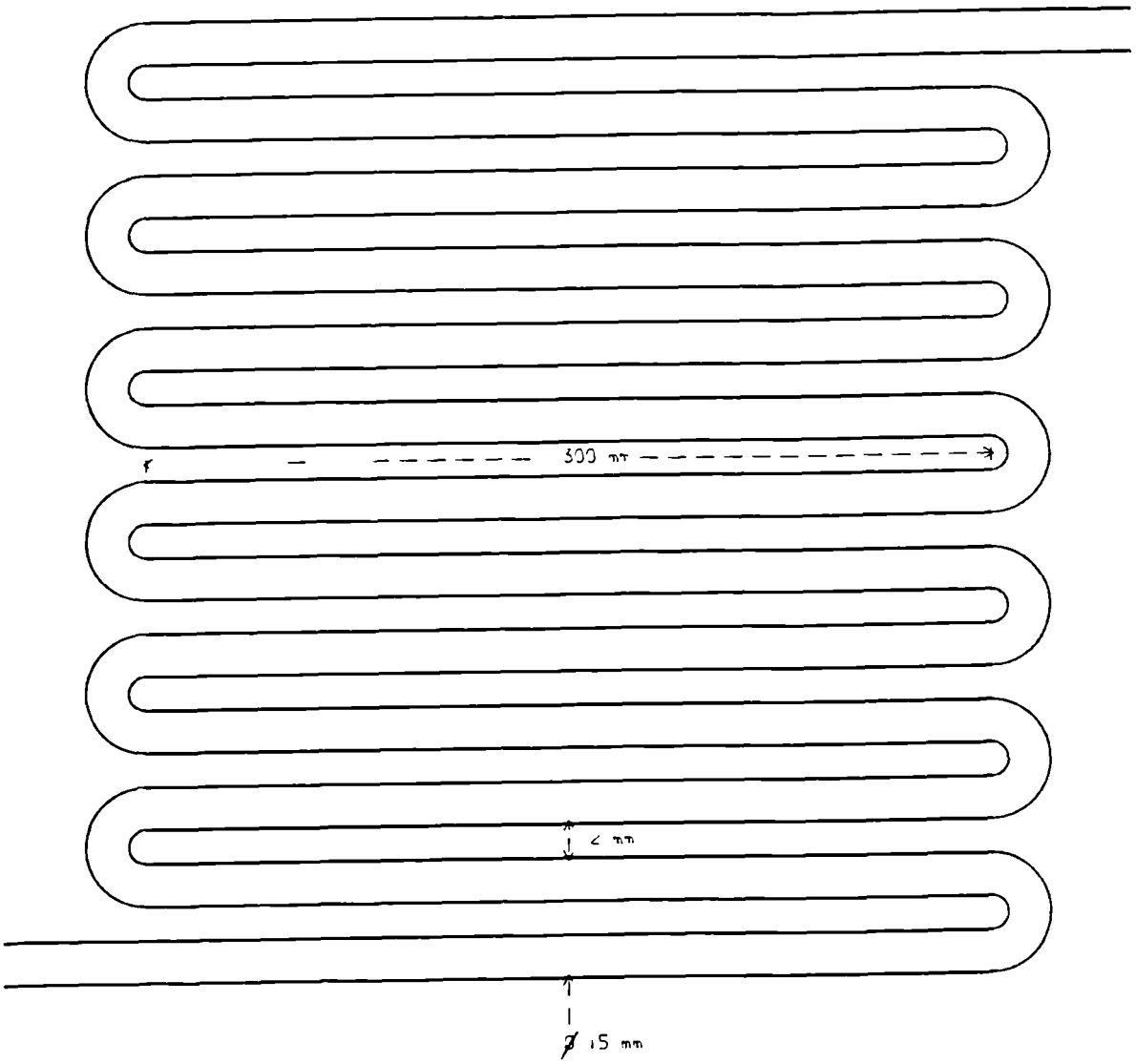

Fig.5.4 Generator coil

In summary, the generator specifications are :

(i) Type : shell and coil, spray or falling film. Strong solution flows over tubes and hot water inside tubes.

(ii) Specifications of coil tubes :

Material : copper half hard temper BS2871

Nominal diameter : 15 mm

Outside diameter: 14.965 mm

Inside diameter : 13.565 mm

Thickness : 0.7 mm

Length of tubes : 0.30 m

Number of tubes : 13

Arrangement : vertical coil

Space between tubes : 12 mm

5.4 Design of Condenser

A shell and coil condenser is used where water vapour is condensing in the shell and cooling water inside the coil tubes.

The design data are :

1. $\dot{Q}_C$−1.0462 kW, t_C 28°C , $\dot{m}_W$=1.499 kg/h
2. $t_{CW,i}$ 24°C, $t_{CW,e}$ 26°C , $\bar{t}_{CW}$=25°C
3. The properties of cooling water at 25°C are [53]

ρ_W 977.06 kg/m^3, μ_W=0.870x10^{-3} kg/m-s

k_W−0.611 W/m-°C, $C_{P,W}$=4.184 kJ/kg-°C

$P_{r,W}$ 6.13

4. The properties of saturated water refrigerant at 28°C are [53]

$\rho_{W,r}$=996.31 kg/m^3, $\rho_{vapour,r}$=0.0272 kg/m^3

$k_{W,r}$=0.615 W/m-°C , $\mu_{W,r}$=0.81x10^{-3}kg/m-s

latent heat of vaporization h_{fg}=2435.2 kJ/kg

The tubes are copper tubes of 15 mm nominal diameter.

The mass flow rate of cooling water is

$$\dot{m}_{CW} = \frac{\dot{Q}_C}{C_{P,W}\Delta t_{CW}} = \frac{1046.2}{4184x2} = 0.125\ kg/s$$

The cooling water velocity in tubes is

$$V_{CW} = \frac{\dot{m}_{CW}}{\rho_W \frac{\pi}{4}(D_i)^2} = 0.87\ m/s$$

Then the Reynolds number is

$$R_e - \rho_W \frac{V_{CW} D_i}{\mu_W} = 13525.12$$

For turbulent flow, Nusselt number is

$$N_u = 0.023\ R_e^{0.8} P_r^{0.4}$$

$$= 95.85$$

Inside heat transfer coefficient is

$$h_i - \frac{95.85x0.611}{13.565x10^{-3}} = 4317.3\ W/m^2 -^o C$$

Outside heat transfer coefficient is the condensing coefficient for film condensation [58] :

$$h_o = 0.725\left[\frac{g\rho_l(\rho_l - \rho_v)h_{fg}k^3}{\mu\ \Delta t\ N\ D_i}\right] \qquad (5.11)$$

Where

N=number of tubes in a vertical row

Δt=temperature difference between vapour and tube wall

ρ_l=density of liquid refrigerant

ρ_v=density of vapour refrigerant

h_o must be found assuming values of the outside wall temperature t_{wall}. A trial and error procedure is then necessary. A wall temperature is assumed and overall heat transfer coefficient determined until satisfactory check of t_{wall} is obtained from the following equation [55] :

$$h_o(t_{saturated} - t_{wall}) = U_o(t_{\substack{saturated \\ vapour}} - t_{\substack{mean \\ water}}) \tag{5.12}$$

Assuming a wall temperature of 27°C and 6 tubes in a vertical row,

$$\Delta t = t_{\substack{saturated \\ vapour}} - t_{wall} = 1^oC$$

and

$$h_o = 12326.52\ W/m^2 -^o C$$

From equation(5.8) with a fouling factor of $176\text{x}10^{-6}$, the overall heat transfer coefficient is

$$U_o = 1877.21\ W/m^2 -^o C$$

Using equation (5.12) the wall temperature is

$$t_{wall} = 28 - \frac{1877.21}{12326.52}(28 - 25)$$
$$= 27.6^oC$$

A new wall temperature of 27.6^oC is assumed. As a result,

$$h_o = 15499.85\ W/m^2 -^o C$$

$$U_o = 1937.6\ W/m^2 -^o C$$

A check of wall temperature gives t_{wall}=27.6°C which is the assumed value.

The logarithmic mean temperature difference is

$$LMTD = \frac{(t_C - t_{CW,e}) - (t_C - T_{CW,i})}{\ln \frac{t_C - t_{CW,e}}{t_C - t_{CW,i}}} \tag{5.13}$$

$$LMTD = 2.9°C$$

As for the calculation of $LMTD$ in the generator, the refrigerant saturation temperature has been used in the above expression. The vapour coming from the generator is usually superheated so that the temperature difference is higher. But the convection coefficient, in the section where the vapour is cooled to saturation temperature, is lower than the condensing coefficient.
Application of equation (5.13) produces reasonably accurate results [13].
Therefore, the required wetted area is

$$A - \frac{\dot{Q}_C}{F\ U_o\ LMTD} = \frac{1046.2}{1x1937.6x2.9} = 0.1862\ m^2$$

The total length tube is

$$L = \frac{A}{\pi D_o} = 3.96\ m$$

If there are two rows of 6 tubes each then the tube length is

$$L_{tube} - \frac{L}{12} = 0.33\ m$$

A space of 27 mm between tubes has been chosen. This value is more convenient for the construction of the coil as it is equal to the diameter of a return bend made from two 90° elbows.

The pressure drop of the cooling water is calculated using the total length tube and the equivalent length in straight tubes of the 11 return bends.
For R_e=13525.12, the friction factor is f=0.029.
Then

$$\Delta P = 13.75\ kpa$$

which is less than the allowable pressure drop.
The pressure drop of refrigerant vapour in the condenser shell is also assumed negligible.
The condenser coil is represented in figures 5.5 (a) and (b).

The specifications of the condenser are :

(i) Type : shell and coil. Water vapour is condensing in the shell and cooling water flowing inside coil tubes.

(ii) Specifications of coil tubes :
Material : copper BS2871
Nominal diameter : 13.565 mm
Inside diameter : 13.565 mm
Outside diameter : 14.965 mm
Thickness : 0.7 mm
Length : 0.33 m
Number of tubes : 12
Arrangement : 2 vertical rows
Space between tubes : 27 mm

5.5 Design of Evaporator

A shell and coil evaporator of the falling-film type is used where water is chilled inside tubes and water liquid refrigerant evaporated outside tubes.

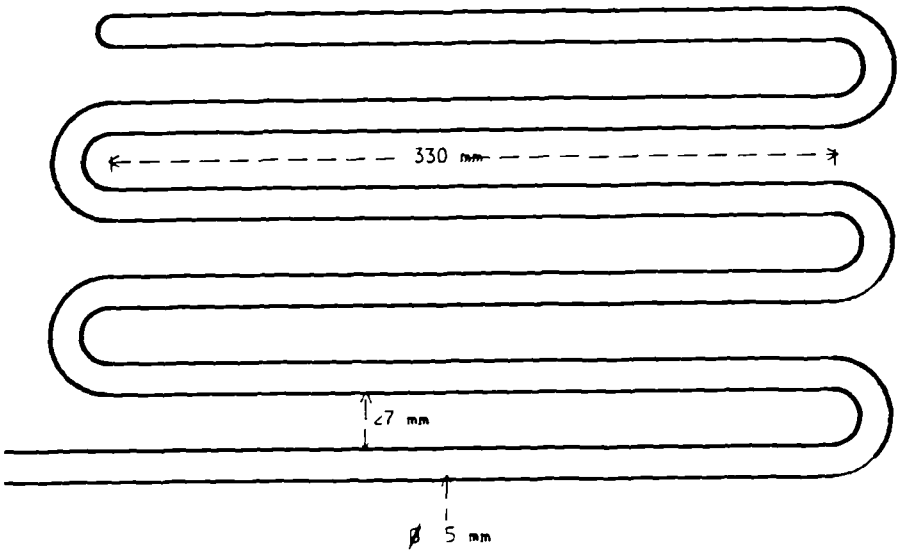

(a) Side view of condenser coil

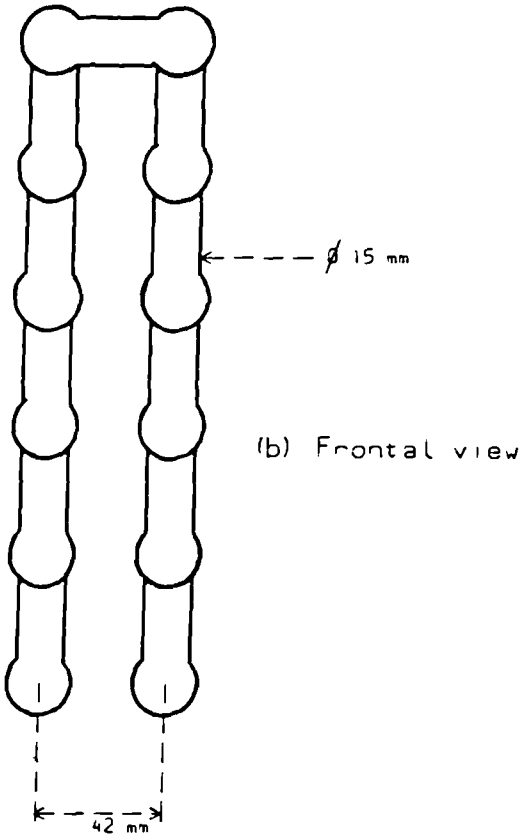

(b) Frontal view

Fig.5.5 (a),(b) Condenser coil

the design data are :

1. $\dot{Q}_E$–1.0 kW, t_E=10°C , $\dot{m}_W$=1.499 kg/h
2. $t_{CHW,i}$=15°C , $t_{CHW,e}$=12°C , $\bar{t}_{CHW}$=13.5°C
3. The chilled water properties at 13.5°C are [53]

ρ=999.35 kg/m^3, μ=1.185x10^{-3} kg/m-s

k 0.592 W/m-°C , C_P=4.195 kJ/kg-°C

P_r 8.4

4. The water refrigerant properties at 10°C are [53]

$\rho_{r,liquid}$–999.6 kg/m^3, $\rho_{r,vapour}$=9.4x10^{-3} kg/m^3

k_r 0.587 W/m-°C , $C_{P,r}$=4.199 kJ/kg-°C

μ_r 1.28x10^{-3} kg/m-s

The evaporator tubes are copper tubes of 15 mm nominal diameter.
Results of studies on transient modelling of absorption chillers [33] have shown that the thicker the film in the evaporator, the more time it took to approach steady state.
The thickness of falling films is [16] :

$$\delta - \left[\frac{3\Gamma\mu_r}{g\rho_{r,l}(\rho_{r,l} - \rho_{r,v})\sin\phi}\right]^{\frac{1}{3}} \tag{5.14}$$

Where

ϕ is the angle with the horizontal

$\rho_{r,l}$ the density of liquid refrigerant

$\rho_{v,l}$ the density of vapour refrigerant

If each tube is 0.3 m in length then

$$\Gamma = \frac{\dot{m}_W}{2L_{tube}} = \frac{1.499}{3600\text{x}2\text{x}0.30} = 6.94\text{x}10^{-4}\ kg/m - s$$
$$\phi = 90^{\circ}$$

and

$$\delta = 6.5\text{x}10^{-5}\ m = 0.06\ mm$$

For this low liquid film thickness the time to reach steady state operation will normally be very short of the order of few minutes after dripping starts in the evaporator.

The mass flow rate of chilled water is

$$m = \frac{\dot{Q}_E}{C_P\text{x}\Delta t} = \frac{1000}{4195\text{x}3} = 0.08\ kg/s$$

The water velocity in the tubes is

$$V = \frac{\dot{m}}{\rho A_i} = 0.55\ m/s$$

Thus

$$R_e - 6336.7$$

and

$$N_u \quad 0.023(6336.7)^{0.8}(8.4)^{0.3} = 48.0$$

The inside heat transfer coefficient is

$$h_i - \frac{48.0\text{x}0.592}{13.565\text{x}10^{-3}} = 2094.80\ W/m^2 - {}^{o}C$$

The outside heat transfer coefficient h_o is calculated from equation (5.6). The procedure carried out in the calculation of the outside heat transfer coefficient in the generator will be repeated for the evaporator design.

Thermal diffusivity of refrigerant is

$$\alpha = \frac{k_r}{\rho_r C_{P,r}} = 1.39\text{x}10^{-7}\ m^2/s$$

and by equation (5.3)

$$L_d = 7.0\text{x}10^{-7}\ m$$

The point of transition from laminar to turbulent correlation of h_c is

$$(\frac{4\Gamma}{\mu_r})_{tr} = 5800(\frac{\mu_r}{\rho_r \alpha_r})^{-1.06} = 559.47$$

For this design

$$(\frac{4\Gamma}{\mu_r}) = \frac{4\text{x}6.94\text{x}10^{-4}}{1.28\text{x}10^{-3}} = 2.16$$

Application of laminar correlation given by equation (5.4) produces

$$h_c = 7372\ W/m^2 -^o C$$

Average heat transfer coefficient in thermal developing region is

$$h_d = \frac{3}{8} C_{P,r} \frac{\Gamma}{L_d} = 1561128.2$$

Thus

$$h_o = h_d \frac{L_d}{L} + h_c(1 - \frac{L_d}{L})$$

$$h_o = 3.642 + 7371.98 = 7375.62\ W/m^2 -^o C$$

Substituting numerical values into equation (5.8) gives

$$U_o \quad 1271.0\ W/m^2 -^o C$$

The $LMTD$ is

$$LMTD - \frac{(t_{CHW,e} - t_E) - (t_{CHW,i} - t_E)}{\ln \frac{t_{CHW,e} - t_E}{t_{CHW,i} - t_E}} = 3.3^o C$$

The required area is then

$$A \quad \frac{\dot{Q}_E}{F\ U_o\ LMTD} = \frac{1000}{1\text{x}1271.0\text{x}3.3} = 0.238\ m^2$$

The total length of tubes is

$$L \quad \frac{0.238}{\pi\text{x}14.965\text{x}10^{-3}} = 5.08$$

The number of straight tubes is

$$n - \frac{L}{0.3} = 16.9 \text{ or } n = 17.$$

Effects of entrainment and deflection of droplets by the vapour crossflow are

assumed negligible and a space between tubes of 12 mm is chosen such that the droplets falling from one tube impige upon the next lower tube.
The pressure drop in liquid refrigerant side is negligible as the flow is laminar and its rate very small.
The pressure drop in the chilled water side is

$$\Delta P = fL\frac{V^2}{2D_i}\rho$$

As before, L is the total length of tubes plus the equivalent length in straight tubes of the return bends.
or

$$L = (17\text{x}0.3) + (16\text{x}2\text{x}0.6) = 24.3\ m$$

For R_e 6336.7, f−0.030 and ΔP=8.1 kpa.

Figure 5.6 shows the evaporator coil. The evaporator specifications are :

(i) Type : Shell and coil. Chilled water in tubes, evaporating refrigerant in shell.

(ii) Specifications of coil tubes :
Material : copper BS2871
Nominal diameter : 15 mm
Outside diameter : 14.965 mm
Inside diameter : 13.565 mm
Thickness : 0.7 mm
Length : 0.30 m
Number of tubes : 17
Arrangement : vertical row
Space between tubes : 12 mm

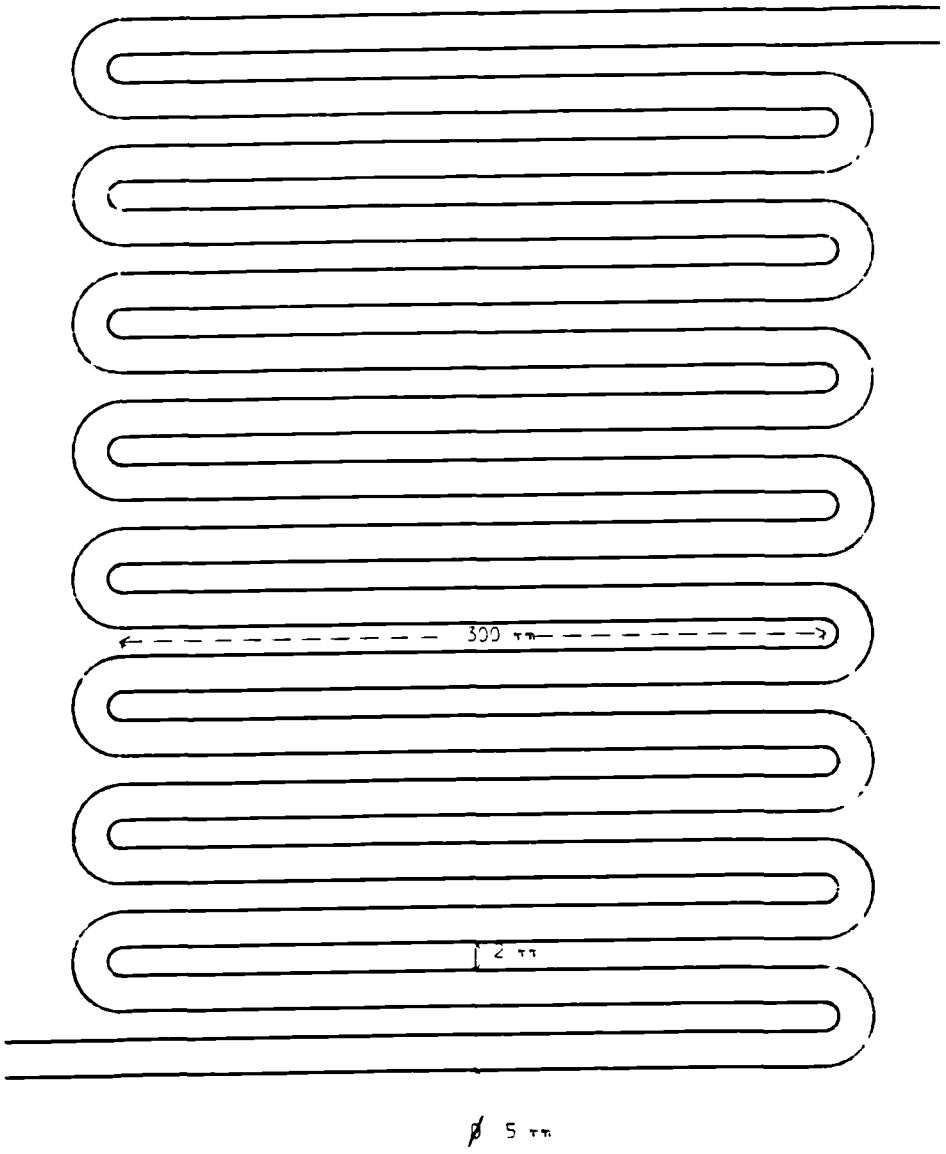

Fig.5.6 Evaporator coil

5.6 Design of Absorber

A shell and coil absorber of the falling film type is used in which the solution flows over the tubes and the cooling water inside tubes.

the design data are :

1. $\dot{Q}_A$−1.3034 kW, t_A=37°C
2. $\dot{m}_{SS}$−17.99 kg/h, t_{SS}=57.5°C , X_{SS}=58.5%
3. $\dot{m}_{WS}$ 19.49 kg/h, t_{WS}=37° , X_{WS}=54.0%
4. $t_{CW,i}$ 32°C , $t_{CW,e}$−35°C, $\bar{t}_{CW}$=33.5°C
5. The cooling water properties at 33.5°C are [53]

ρ_{CW} 994.43 kg/m^3, μ_{CW}=0.706x10^{-3} kg/m-s

k_{CW} 0.623 W/m-°C, $C_{P,CW}$=4.178 kJ/kg-°C

$P_{r,CW}$ 4.95

6. The solution properties at mean temperature of 47.25°C and mean concentration of 56.25% are:

ρ_S 1650 kg/m^3, μ_S−3.7x10^{-3} kg/m-s

$C_{P,S}$ 1.97 kJ/kg-°C

By extrapolation from [54] : k_S=0.426 W/m-°C

The tubes are copper of 15 mm nominal diameter and the length of each straight tube is assumed equal to 0.30 m.

The massflow rate of cooling water is

$$\dot{m}_{CW} = \frac{\dot{Q}_A}{C_{P,CW}\Delta t} - 0.156\ kg/s$$

The velocity of water in tubes is

$$V = 1.085\ m/s$$

Thus

$$R_e = 20730.94$$

and

$$N_u = 0.023(20730.94)^{0.8}(2.33)^{0.4} = 91.6$$

$$h_i = 4207\ W/m^2 - ^o\ C$$

The outside heat transfer coefficient is evaluated from the following conditions [16] :

For $\frac{4\Gamma}{\mu} < 2100$,

$$h_o = 0.50\left[\frac{k^2\rho^{\frac{4}{3}}C_p g^{\frac{2}{3}}}{\frac{\pi D_o}{2}\mu^{\frac{1}{3}}}\right]^{\frac{1}{3}}\left[\frac{\mu}{\mu_{wall}}\right]^{\frac{1}{4}}\left[\frac{4\Gamma}{\mu}\right]^{\frac{1}{9}} \tag{5.15}$$

with all properties evaluated at mean bulk temperature except μ_{wall} at the wall temperature

For $\frac{4\Gamma}{\mu} > 2100$

$$h_o - 0.01\left[\frac{k^3\rho^2 g}{\mu^2}\right]^{\frac{1}{3}}\left[\frac{\mu C_p}{k}\right]^{\frac{1}{3}}\left[\frac{4\Gamma}{\mu}\right]^{\frac{1}{3}} \tag{5.16}$$

In this design

$$\Gamma = \frac{\dot{m}_{SS}}{2L_{tube}} = \frac{17.99}{3600\text{x}2\text{x}0.3} = 8.32\ 10^{-3}\ kg/m - s$$

and

$$\frac{4\Gamma}{\mu_S} = 9 < 2100$$

Therefore equation (5.15) is used to calculate h_o.

Assume an average wall temperature of 36°C, then

$$\mu_{wall} = 4.5\ 10^{-3}\ kg/m - s$$

Substituting numerical values of $k_S, \rho_S, D_o, \mu_{wall}, \Gamma$ and g into equation (5.15)

gives h_o=1295.63 $W/m^2 -^o C$.

The overall heat transfer may now be calculated from equation (5.8) with a fouling factor of 176x10^{-6},

$$U_o = 844.9\ W/m^2 -^o C$$

To check the assumed wall temperature :

$$h_o(t_{\substack{mean \\ solution}} - t_{wall}) = U_o(t_{\substack{mean \\ solution}} - t_{\substack{mean \\ water}})$$

or t_{wall} 38.2°C .

The computed value of t_{wall} is sufficiently close to the assumed value of 36°C for estimation of μ_{wall}.

If the flow arrangement in the absorber is crossflow where cooling water enters the vertical coil from the bottom and leaves from the top, the $LMTD$ will be given by :

$$LMTD \quad \frac{(t_{WS,i} - t_{CW,e}) - (t_{WS,e} - t_{CW,i})}{\ln \frac{t_{WS,i} - t_{CW,e}}{t_{WS,e} - t_{CW,i}}} = \frac{(57.5 - 35) - (37 - 33)}{\ln \frac{22.5}{4}}$$

$$- 10.71^oC$$

The required area is

$$A \quad \frac{\dot{Q}_A}{F\ U_o\ LMTD}$$

The correction factor for crossflow falling film heat exchangers is found from charts [59], F 0.97.

And

$$A - 0.1485\ m^2$$

Because air and other non-absorbable gases can be present in the absorber, it is recommended to overdesign the heat transfer surface area by perhaps 20% [60].

So

$$A = 0.18\ m^2$$

The total tube length is

$$L = \frac{A}{\pi D_o} = 3.83\ m$$

The number of tubes will be

$$n = \frac{3.8}{0.3} = 12.7 \quad or \quad n = 13 \text{ tubes.}$$

Tabulated data are provided on mass transfer coefficients of aqueous solutions of L_iB_r for different sets of solution vapour pressure, massflow rates and cooling water temperature [22]. However, they are not representative of the conditions of this absorber such as solution massflow rate of only 1.499 kg/h and mean cooling water temperature of 34°C.

The pressure drop of the cooling water side is

$$\Delta P = f L \frac{V^2}{2D_i} \rho$$

For R_e 20730.94 f 0.027.

There are 12 return bends in the absorber coil, each made of two 90° elbows. Thus,

$$L = (13\text{x}0.3) + (12\text{x}2\text{x}0.6) = 18.3$$

and

$$\Delta P - 21.3\ kpa$$

The pressure drop of the solution side is negligible as the flow is laminar and the rate very small.

A space between tubes of 15 mm is chosen so that the droplets of solution can impige from one tube upon the next lower tube. Absorber coil is represented in figure 5.7.

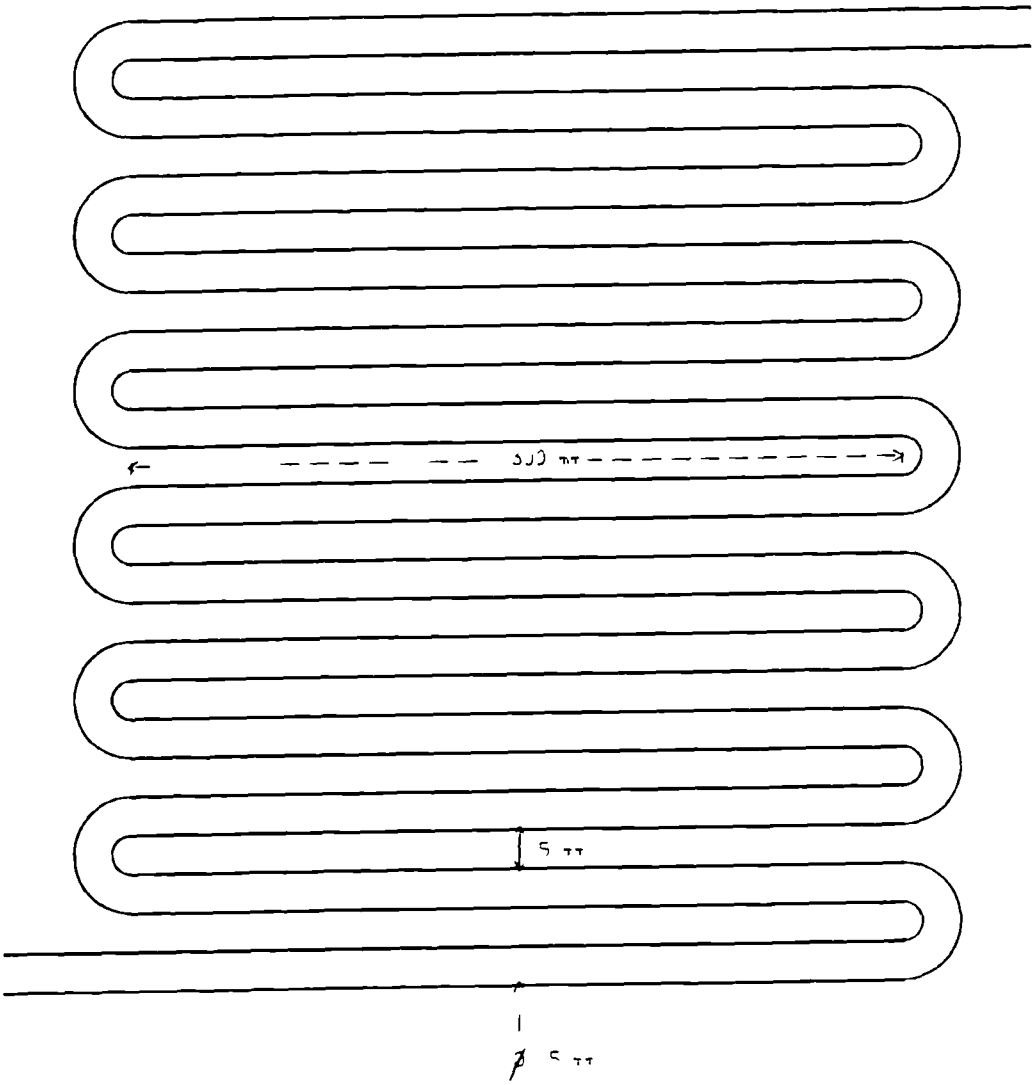

Fig.5.7 Absorber coil

The absorber specifications are :

(i) Type : Shell and coil. Cooling water in tubes, solution over tubes.

(ii) Specifications of coil tubes :

Material : copper BS2871

Nominal diameter : 15 mm

Outside diameter : 14.965 mm

Inside diameter : 13.565 mm

Thickness : 0.7 mm

Length : 0.3 m

Number of tubes : 13

Arrangement : vertical row

Space between tubes : 15 mm

5.7 Design of Solution Heat Exchanger

For small capacity lithium bromide-water refrigeration units, solution heat exchangers are usually formed of closely spaced steel plates to combine low pressure drop and good heat transfer .

Such a heat exchanger is designed in this section with hot strong solution in inner space and cold weak solution in outer space. Assume a cross sectional arrangement of heat exchanger as shown in figure 5.8.

The inner and outer spaces are rectangular shells with equal longitudinal length L which is the unknown dimension to be determined by design.

The design data are :

1. $\dot{Q}_E$−0.114 kW
2. $\dot{m}_{SS}$−17.99 kg/h; X_{SS}=58.5%; $t_{SS,i}$=69°C ; $t_{SS,e}$=57.5°C; t_{SS}=63.25°C
3. $\dot{m}_{WS}$ 19.49 kg/h; X_{WS}=54%; $t_{WS,i}$=37°C; $t_{WS,e}$=50.5°C; $\bar{t}_{WS}$=43.75°C

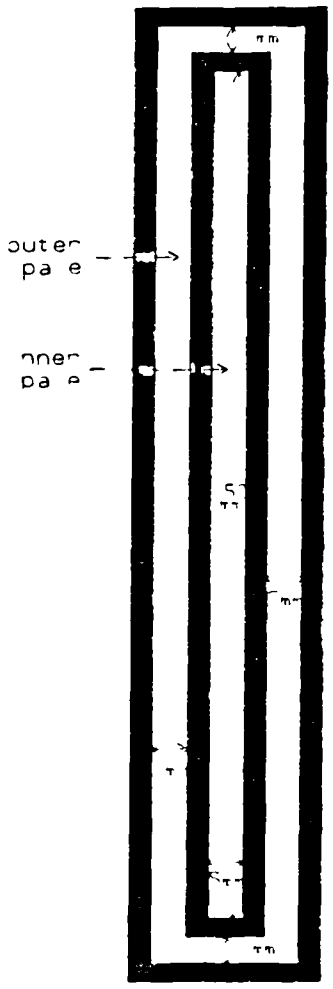

Fig.5.8 Cross sectional arrangement of solution heat exchanger

4. The properties of strong solution at 63.25°C are [11] :

ρ_{SS}=1670 kg/m^3, μ_{SS}=3.3x10^{-3} kg/m-s

$C_{p,SS}$=1905 j/kg-°C

By extrapolation from [54] : k_{WS}=0.427 W/m^2-°C

The inside and outside heat transfer coefficients are evaluated as follows.
If a fluid flows in a non circular channel, it is recommended that the heat transfer correlations be based on the equivalent diameter [58], defined by

$$D_e = \frac{4A_c}{P} \tag{5.17}$$

Where
A is the cross sectional area of the flow and P is the wetted area.
For strong solution in inner shell,

$$R_e = \frac{GD_e}{\mu_{SS}}$$

Where
G is the mass flow rate per unit cross sectional area.
P 2(0.15+0.005) 0.31 m; A_c–0.15x0.005=7.5x10^{-4} m^2
so

$$G - \dot{m}_{SS}/A_c = 6.66\ kg/m^2 - s,\quad D_e = 9.677\ 10^{-3}\ m$$

and

$$R_e - 19.53$$

The flow is laminar. The Nusselt number for laminar flow is [55]

$$N_u = 3.66 + \frac{0.0668(\frac{D}{L})R_e P_r}{1 + 0.04[(\frac{D}{L})R_e P_r]^{\frac{2}{3}}} \qquad (5.18)$$

Where all fluid properties are evaluated at the bulk temperature.

Since the length L must be known for the calculation of N_u, a trial and error procedure is necessary.

A first assumption is L=0.40 m.

$$P_{r,SS} = \frac{\mu_{SS} C_{P,S}}{k_{SS}} = 15.0$$

$$N_u = 4.07$$

then

$$h_i = N_u \frac{k_{SS}}{D_e} = 176.2\ W/m^2 - ^o C$$

For weak solution in outer space, the wetted perimeter for heat transfer is the outside perimeter of the inner space. If the plate thickness is 3 mm then

$$P' \quad 2(156 + 11) = 334\ mm = 0.334\ m$$

$$A'_C - (166\text{x}21) - (156\text{x}11) = 1770\ mm^2 = 1.77\ 10^{-3}\ m^2$$

and

$$D'_e - \frac{4A'_C}{P'} = 0.0212\ m$$

$$R_e \quad 19.1$$

The flow is laminar. Application of equation (5.18) with $P_{r,WS}$= 16.13 gives

$$N_u - 4.53$$

$$h_o \quad N_u \frac{k_{WS}}{D'_e} = 91.2\ W/m^2 - ^o C$$

The overall heat transfer coefficient is determined from the following expression

[11] :

$$U_o = \left[\frac{1}{h_o} + \frac{\delta_P}{k_P \frac{A_m}{A_o}} + \frac{1}{h_i \frac{A_i}{A_o}}\right]^{-1} \tag{5.19}$$

where δ_P is the plate thickness, k_P is the plate thermal conductivity and A_m the mean surface area of the inner space.

For steel plates k_P=69 W/m-°C.

The inside surface area of the inner space is A_i=0.124 m^2.

The outside surface area of the inner space is A_o=0.1336 m^2.

So A_m−0.1288 m^2 , thus U_o=58.4 W/m^2-°C .

If the heat exchanger is a counterflow exchanger then

$$LMTD = \frac{(t_{SS,i} - t_{WS,e}) - (t_{SS,e} - t_{WS,i})}{\ln \frac{t_{SS,i} - t_{WS,e}}{t_{SS,e} - t_{WS,i}}}$$
$$= 19.48\ ^oC$$

The required wetted area is

$$A = \frac{\dot{Q}_{HE}}{F\ LMTD\ U_o}$$

The correction factor F is 0.94 from charts [58], and A= 0.1066 m^2.

Since the wetted area A is the outside area of the inner space,

$$A \quad A_o - 2(L\text{x}0.011) + 2(L\text{x}0.156) = 0.1066$$

or

$$L \quad \frac{0.1066}{0.334} = 0.32\ m$$

The correspondence between the assumed and calculated values of L is not satisfactory. Therefore, the calculation is repeated for a new value of L.

Assume L 0.32 m.

For strong solution, the Nusselt number becomes N_u=4.17 and the inside heat transfer coefficient h_i 180.6 W/m^2-°C.

For weak solution, the Nusselt number will be N_u=4.71 and the outside heat

transfer coefficient h_o=94.9 W/m^2-°C.

So the overall heat transfer coefficient is

$$U_o = 60.43\ W/m^2 - ^o C$$

the required wetted area is

$$A = 0.1030\ m^2$$

and

$$L = 0.1030/0.334 = 31\ mm$$

This value of L is sufficiently close to the assumed value.

The pressure drop of the weak solution in the outer space is [59] :

$$\Delta P = \frac{4fG^2L}{2\rho D_e} \quad \text{in pascals} \tag{5.20}$$

where D_e is the equivalent diameter for pressure drop.

$$D_e = \frac{\text{4x flow area}}{\text{frictional wetted perimeter}}$$

The frictional wetted perimeter for the weak solution in the outer space is the sum of the perimeter of the outside surface of the inner space and the perimeter of the internal surface of the outer space.

So,

$$D_e \quad \frac{4\text{x}1.77\text{x}10^{-3}}{0.334 + 2(0.166 + 0.021)} = 0.01\ m$$

$$G \quad \frac{\dot{m}_{WS}}{A'_C} = 3.06\ kg\ m^2 - s$$

The friction factor for laminar flow is [13] :

$$f = \frac{64}{R_e.}$$

Since

$$R_e = \frac{GD_e}{\mu} = \frac{3.06\text{x}0.01}{3.4\text{x}10^{-3}} = 9 \qquad f = 7.11$$

and

$$\Delta P = 2.60\ pa = 1.5\text{x}10^{-3}\ mm\ Hg \qquad \text{which is negligible.}$$

Similarly, the pressure drop of the strong solution in the inner space will also be negligible.

The specifications of the solution heat exchanger are :

1. Type : counterflow exchanger with parallel plates. Strong solution in inner space and weak solution in outer space.

2. Specifications of plates :
   Material : steel
   Thickness : 3 mm

3. Arrangement : as shown in figure 5.8.

4. Dimensions :
   Inner rectangular shell : 150 x 5 x 310 mm
   Outer rectangular shell : 166 x 21 x 310 mm

5.8 Conclusion

In this chapter, the design of a thermodynamic L_iB_r-water absorption refrigeration system has been formulated. The operating conditions were selected using the results of chapter 4. The addition of a pregenerator to the basic cycle was studied.

Generator, evaporator and absorber heat exchangers of the falling film type were

designed. The tubes, in which the cycle external fluids flow, are arranged in vertical coils of one row each.

The condenser heat exchanger is of the shell and coil heat exchanger type with tubes arranged in a coil of two rows.

A counterflow solution heat exchanger was designed. The strong solution flows in the inner rectangular shell while the weak solution flows in the outer rectangular shell.

CHAPTER SIX

EXPERIMENTAL RIG DESIGN

6.1 Introduction

Following the thermodynamic design in chapter 5 of an absorption refrigeration system and of the generator, absorber, condenser, evaporator and solution heat exchanger components, the mechanical design and construction of an experimental absorption cooling rig are described in this chapter.
The rig is composed of an absorption refrigeration unit, a heater for energy supply to the generator, and of a water distribution system for providing water at different temperatures to the condenser, absorber and evaporator.
Figure 6.1 shows a schematic representation of the experimental rig. The absorption refrigeration unit consists of a solution heat exchanger, a circulating pump and two steel vessels, one comprising the generator and condenser coils and the other vessel the absorber and evaporator coils.
Figures 6.2 to 6.17 show detailed drawings of components.

6.2 Rig Design

6.2.1 Description of System

A schematic representation diagram of the experimental system is shown in figure 6.1.

The lithium bromide absorption chiller consists of two sealed steel vessels operating near vacuum conditions. Each vessel is composed of two heat exchangers separated by partitions and of internal piping through which flow the cycle working solution and refrigerant. External to the two vessels is a counterflow solution

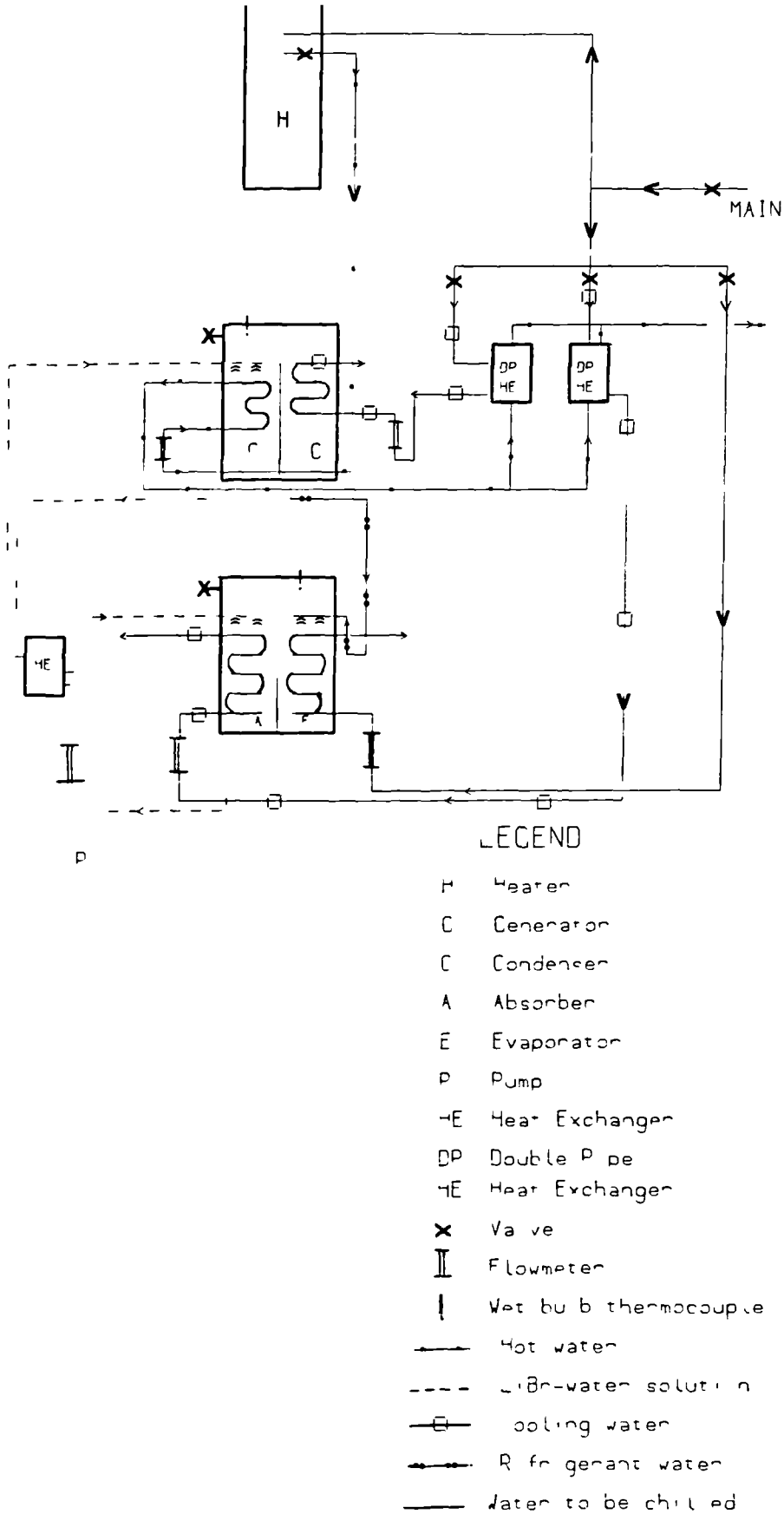

Fig.6.1 Shematic of absorption refrigeration rig

heat exchanger which heats the cool weak solution from the absorber and cools the strong solution returning from the generator to the absorber. The only moving part of the refrigeration unit is a circulating pump which is externally mounted.

The energy to the generator is supplied through hot water obtained from an insulated water heater of 30 gallons capacity.

Water to be chilled in the evaporator is delivered directly from the mains. Cooling water at different temperatures is supplied to condenser and absorber from the mains via double pipe heat exchangers where hot water out of the generator is used as the heat source.

The system instrumentation includes variable area flowmeters, thermocouples, vacuum gauge and valves.

6.2.2 Equipment Design

Specifications of generator, condenser, absorber and evaporator components of the absorption refrigeration cycle have been given in chapter 5. These components are usually arranged in a two-shell design but can also be assembled in a single shell divided by a diaphragm. It was however decided to use a two shell-design for simplicity and ease of fabrication.

The generator and condenser coils are combined inside the same vessel and so are the evaporator and absorber coils. The coils have been fabricated from straight copper tubes of 15 mm diameter soldered at their ends to 90° elbows that have been cut in height to give desired spacing between straight tubes.

Figure 6.2 shows a pictorial drawing of the generator-condenser box without coils and frontal plates. The box is 469 mm in height, 410 mm in length and 180 mm in width. An internal partition separating the generator from the condenser is attached to the bottom plate of the box. The partition is dimensioned (see figure 6.3) such that there is a space of 62 mm height at the top of the box for the vapour flow. The box bottom has been inclined upwards 3.5° so that refrigerant condensate and strong L_iB_r-water solution can drain.

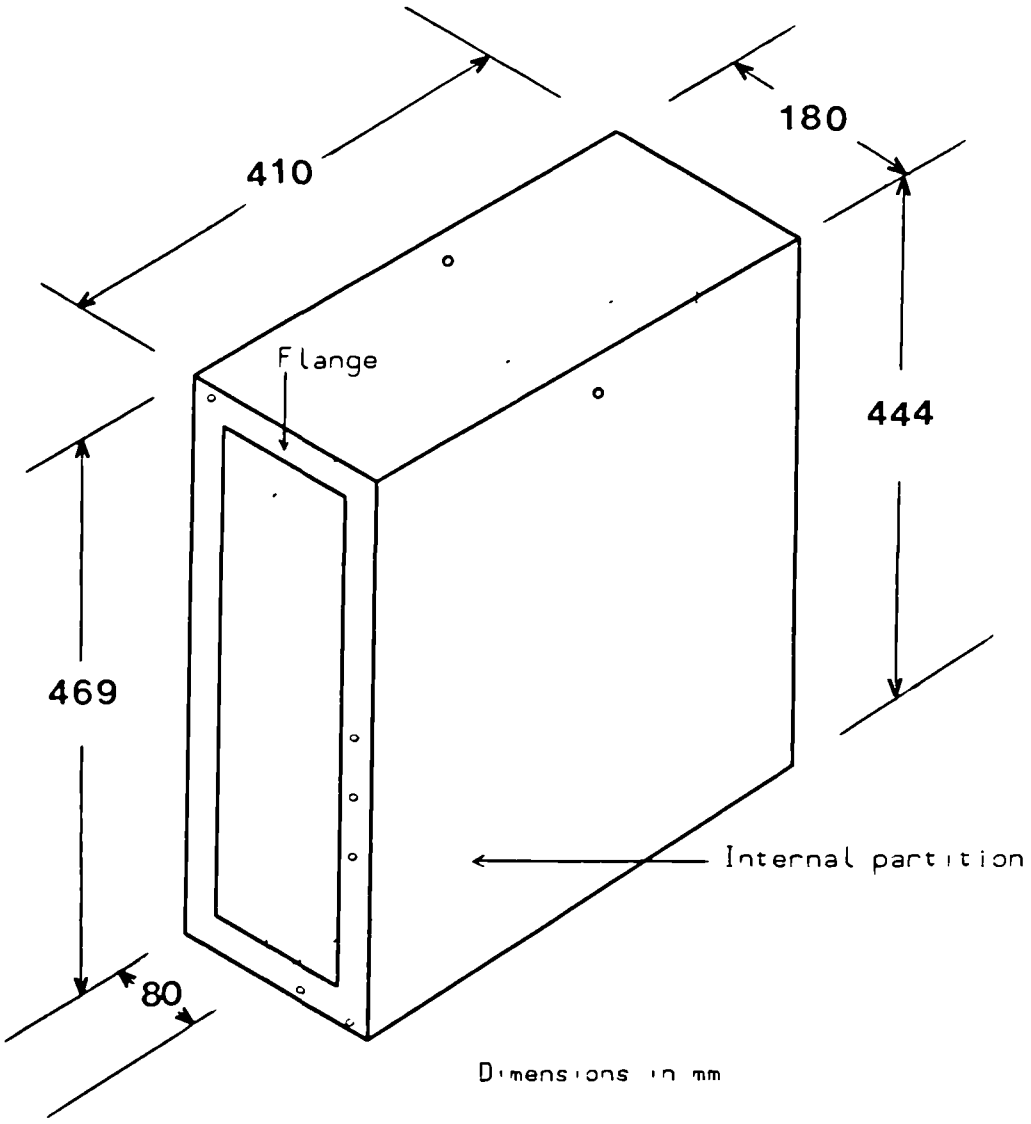

Fig.6.2 Generator-condenser box

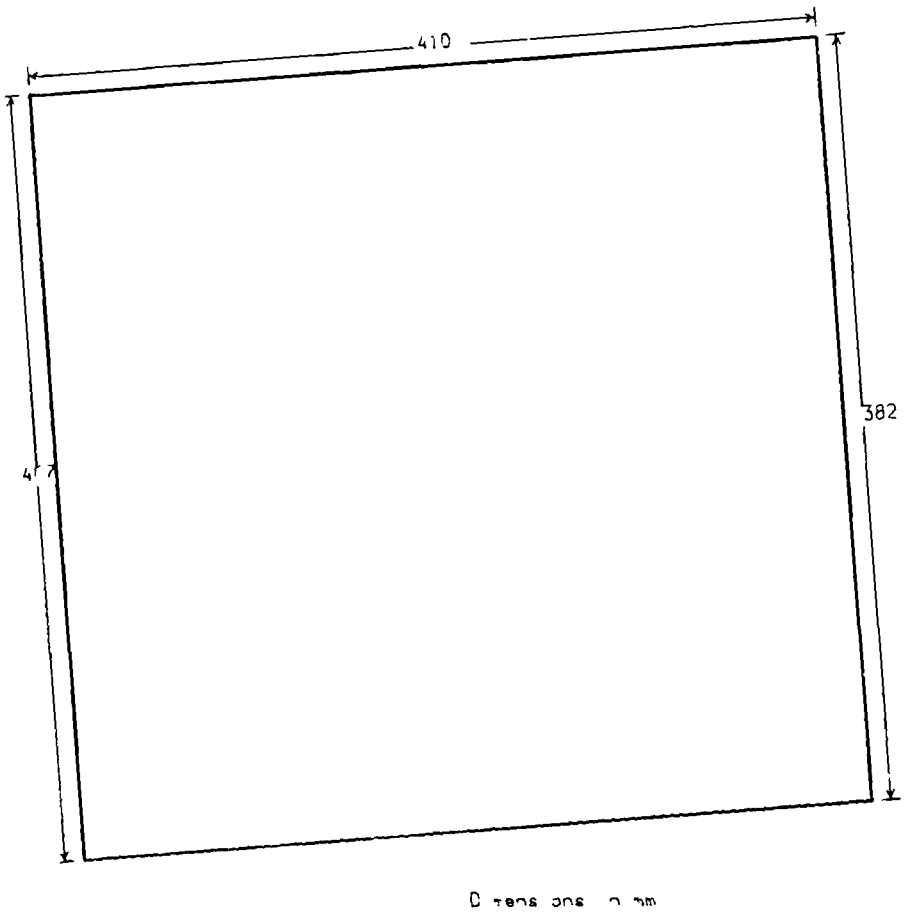

Fig.6.3 Internal partition of generator-condenser box

The box itself was fabricated from joined plates of steel of 4 mm thickness. As these parts will tend to deform inwards as a result of the difference between the outside atmospheric pressure and the inside vacuum pressure, the box was designed to withstand atmospheric pressure.

The maximum permissible pressure for a vessel is [61] :

$$P = \frac{KE}{n}(\frac{\delta}{D})^3 \tag{6.1}$$

Where

E is the modulus of elasticity of the material

K correction factor

n safety factor

δ thickness of vessel wall

D mean diameter of the vessel

Permissible values of (D/δ) are listed [61] of various materials when P 1 kg cm^2, n 4 and K–2.2 (for long vessels).

For steel E 20000 kg/mm^2, n=4, K=2.2 and P=1 kg/cm^2, the permissible $(D\ \delta)$ calculated from equation (6.1) is equal to 98.5.

In the design of the generator-condenser box of figure 6.2,

$$\frac{D}{\delta} = \frac{184}{4} = 46$$

which is well below the permissible value of 98.5 and the design is safe.

A six-view drawing of the generator-condenser vessel is shown in figure 6.4.

The drainage of strong solution and refrigerate condensate is achieved from the bottom of the box through 8 mm diameter piping. One hole ϕ $\frac{1}{4}$" in the top plate can take a bolt in which a thermocouple wire is placed as described in the

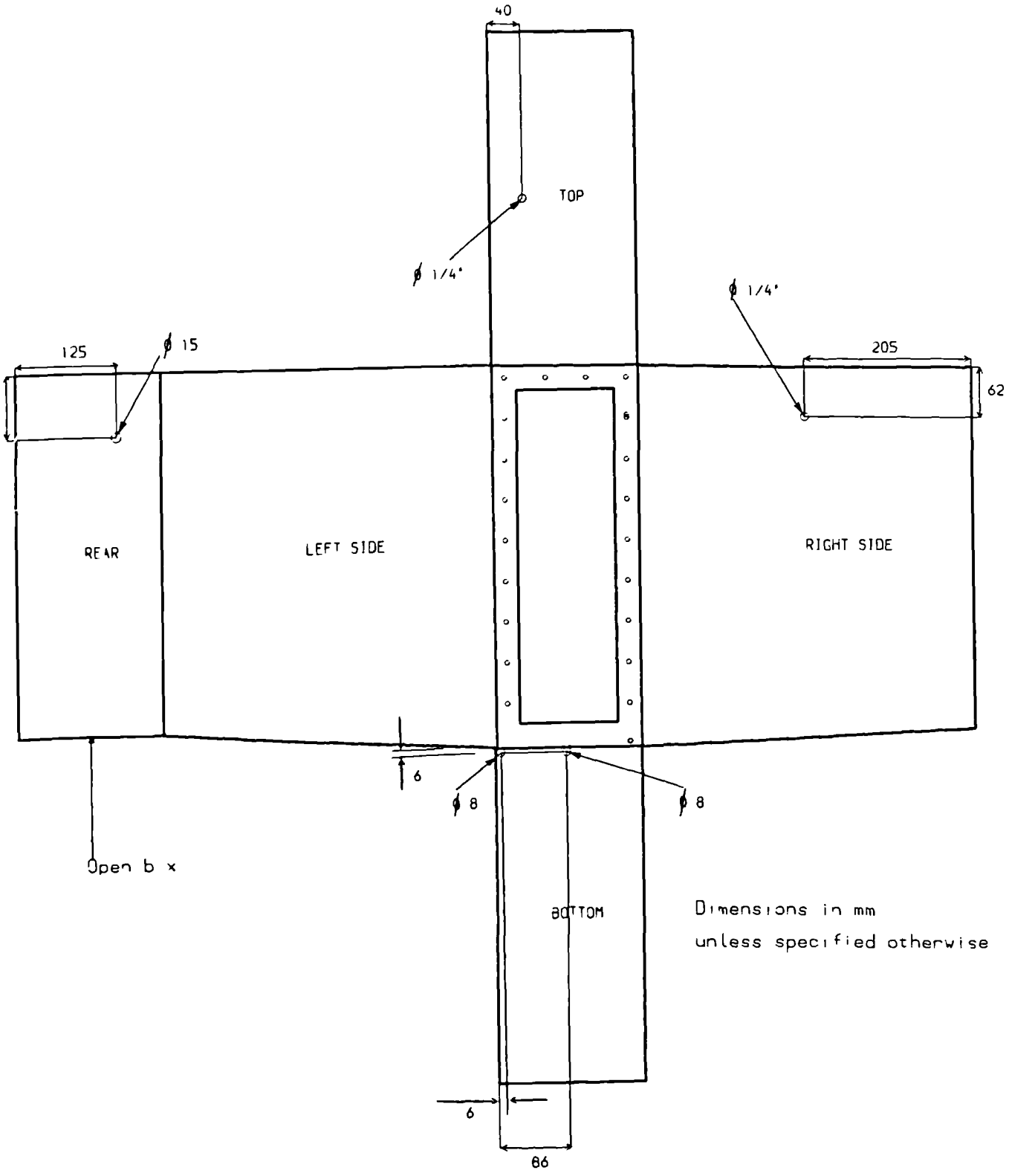

Fig.6.4 Six-view drawing of generator-condenser box

next section of this chapter. The remaining hole $\phi\ \frac{1}{4}$" can be used for evacuating and purging the vessel.

Figure 6.5 is a representation of the vessel frontal plate which is removable for maintenance or changes and fixed on the box flange by 24 equally-spaced bolts of 6 mm diameter.

A tight vacuum seal between the flange and the plate is required to reach and maintain the necessary vacuum pressure inside the vessel as well as to prevent external leaks. The back of the plate was covered by a rubber layer of 3 mm thickness and a rectangular cross section groove was made in the rubber along the plate periphery to receive a gasket seal.

To obtain a vacuum tight seal, a gasket must be compressed to a given ratio of its initial height. For rubber gaskets the compression ratio should be 20-40 percent depending on the hardness of the rubber [61].

Given the recommended dimensions of rectangular cross section grooves for various O-ring cross section diameters [61], a groove of design shown in figure 6.6 was constructed. An O-ring seal of 3 mm diameter was made from silicone rubber and placed in the groove on the frontal plate of the generator-condenser box.

For the distribution of solution over the tubes of the generator coil inside the vessel, a drip header (figure 6.7) was designed and fabricated using a 15 mm diameter copper tube.

15 mm diameter BSP unions for rubber tubing were used for fixing the coils and the drip header on the frontal plate and for connecting them to the external piping. One end of the coils and drip header tubes was soldered into the union. Rubber washers were used as vacuum seals between the BSP unions and the frontal plate.

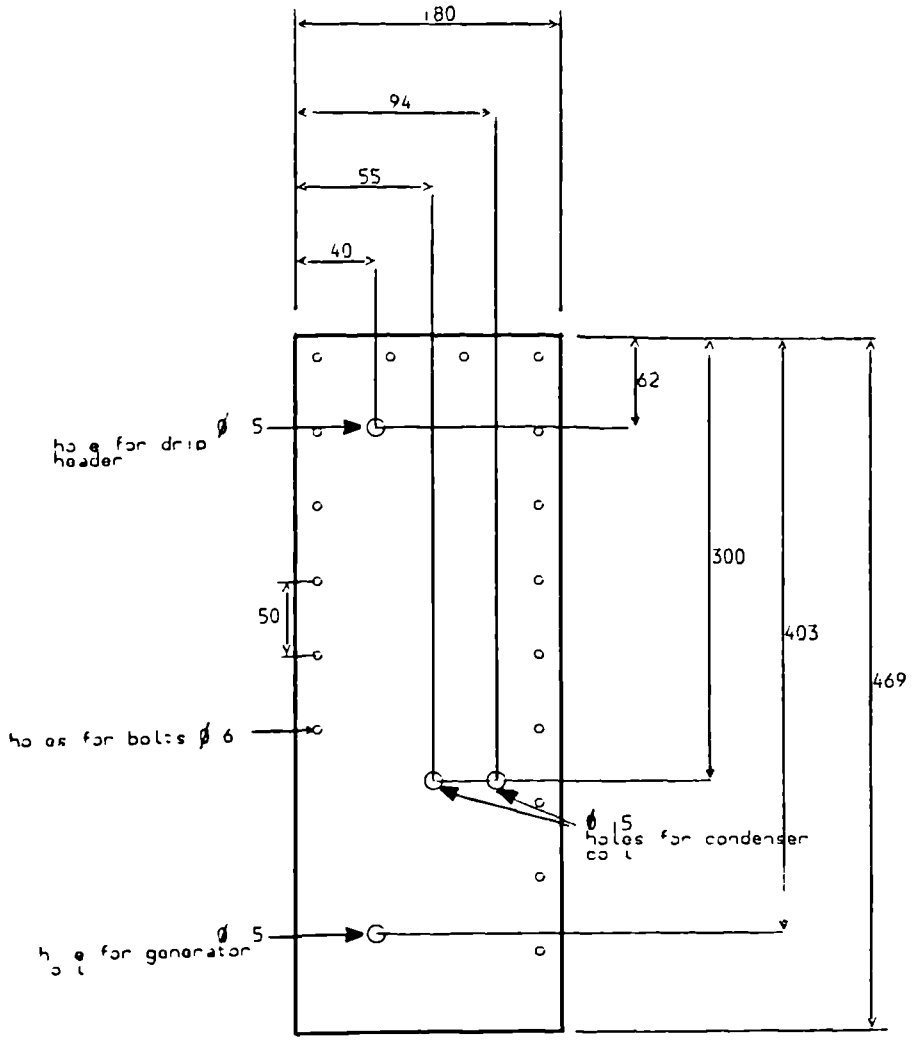

Fig.6.5 Frontal plate of generator-condenser box

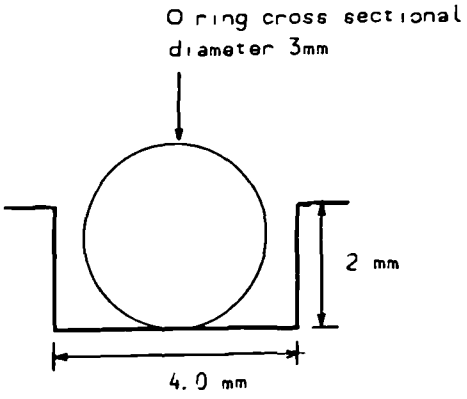

Fig.6.6 Dimensions of groove

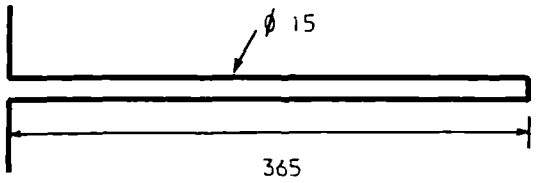

Side v ew

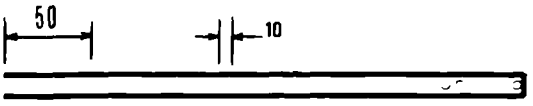

3 holes of d ameter 1 mm

Bottom v ew

Fig.6.7 Generator drip header

Figure 6.8 shows a drawing of the evaporator-absorber vessel without coils and frontal plate. The box is 609 mm in height, 410 mm in length and 180 mm in width. Design and fabrication of this box and the generator-condenser box are similar. All dimensions are given in figures 6.8 to 6.11.

Weak solution is taken out towards the bottom of the absorber through 8 mm piping. The ratio (D/δ) of the vessel mean diameter to the wall thickness is also equal to the safe value of 46 as for the generator-condenser vessel. The dismountable frontal plate of the box is fixed by 28 equally-spaced bolts of 6 mm diameter. A gasket seal made from silicone rubber was placed in a groove (figure 6.6) around the periphery of the frontal plate.

Two drip headers (figures 6.12 and 6.13) were designed and fabricated through which L_iB_r-water solution and refrigerant water are distributed over the evaporator and absorber tubes.

Saturated refrigerant water passing from condenser to evaporator can expand as its pressure is reduced and, as a result, vapour can form a wall to the liquid circulation. Therefore, a slot 350 mm x 5 mm is cut at the top of the evaporator drip header so that it acts also as a flash chamber.

Evaporator coil, absorber coil and drip headers were soldered on one end into BSP unions and attached to the frontal plates of the vessel.

A solution heat exchanger was fabricated from steel plates of 3 mm thickness. A box with an overall size 290 mm x 150 mm x 15 mm was made first (as represented in figures 6.14 and 6.15) and then attached by soldering to plates as suggested in the cross sectional arrangement of figure 5.8.

The heat exchanger external box was assembled by joining the remaining plates together (figures 6.16 and 6.17). The cool weak solution passes in the annulus of the external box and the hot strong solution in the annulus of the internal

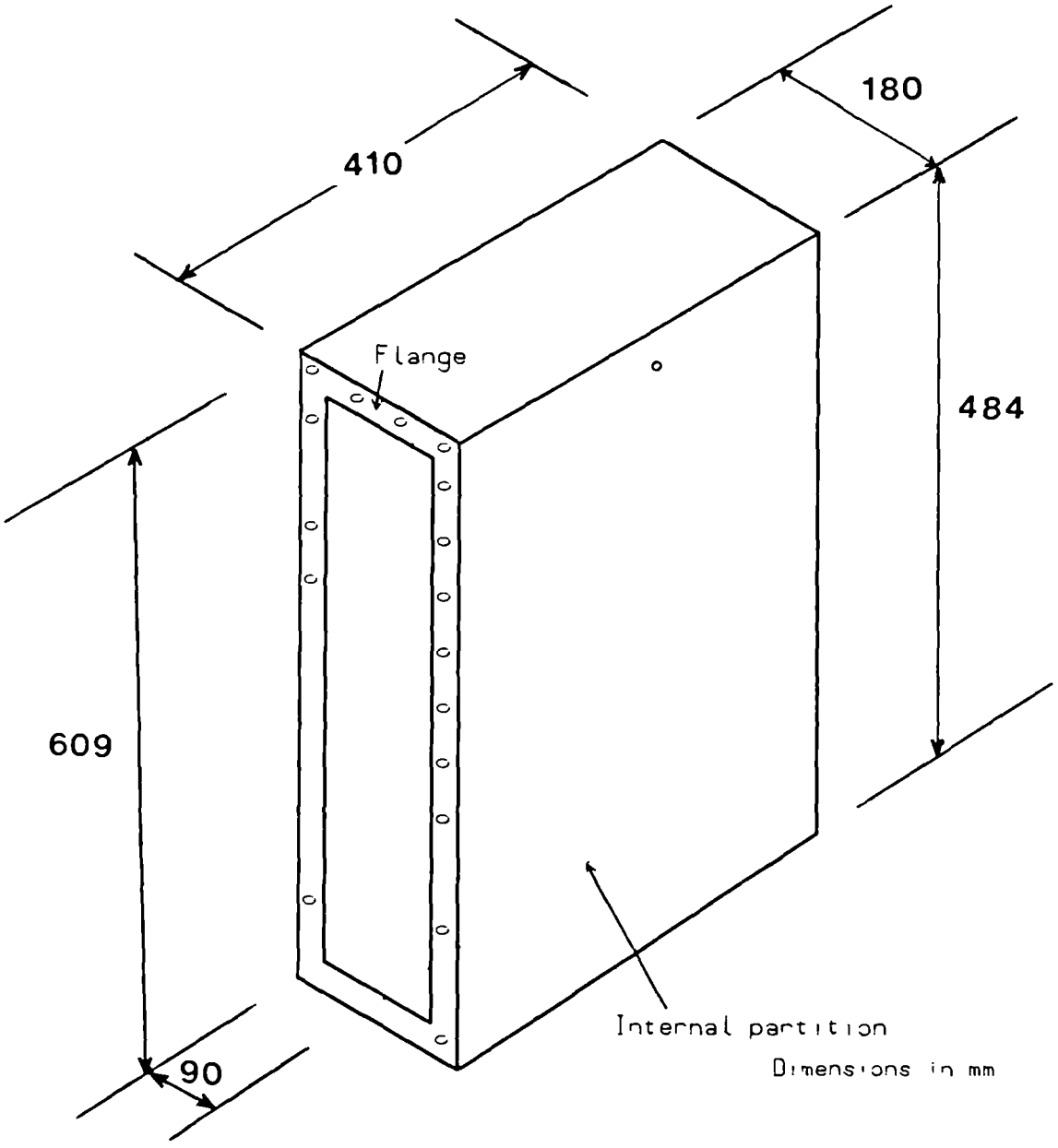

Fig.6.8 Evaporator-absorber box

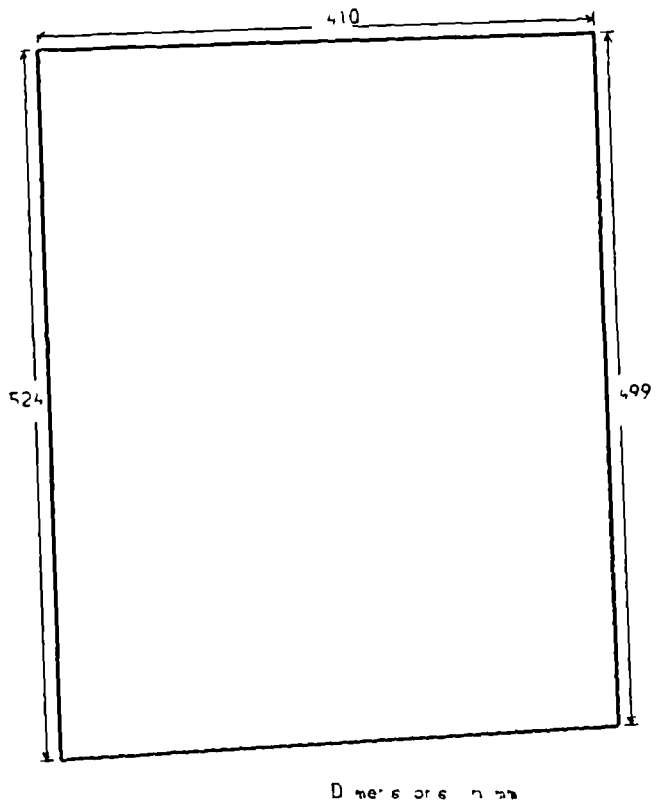

Fig.6.9 Internal partition of evaporator-absorber box

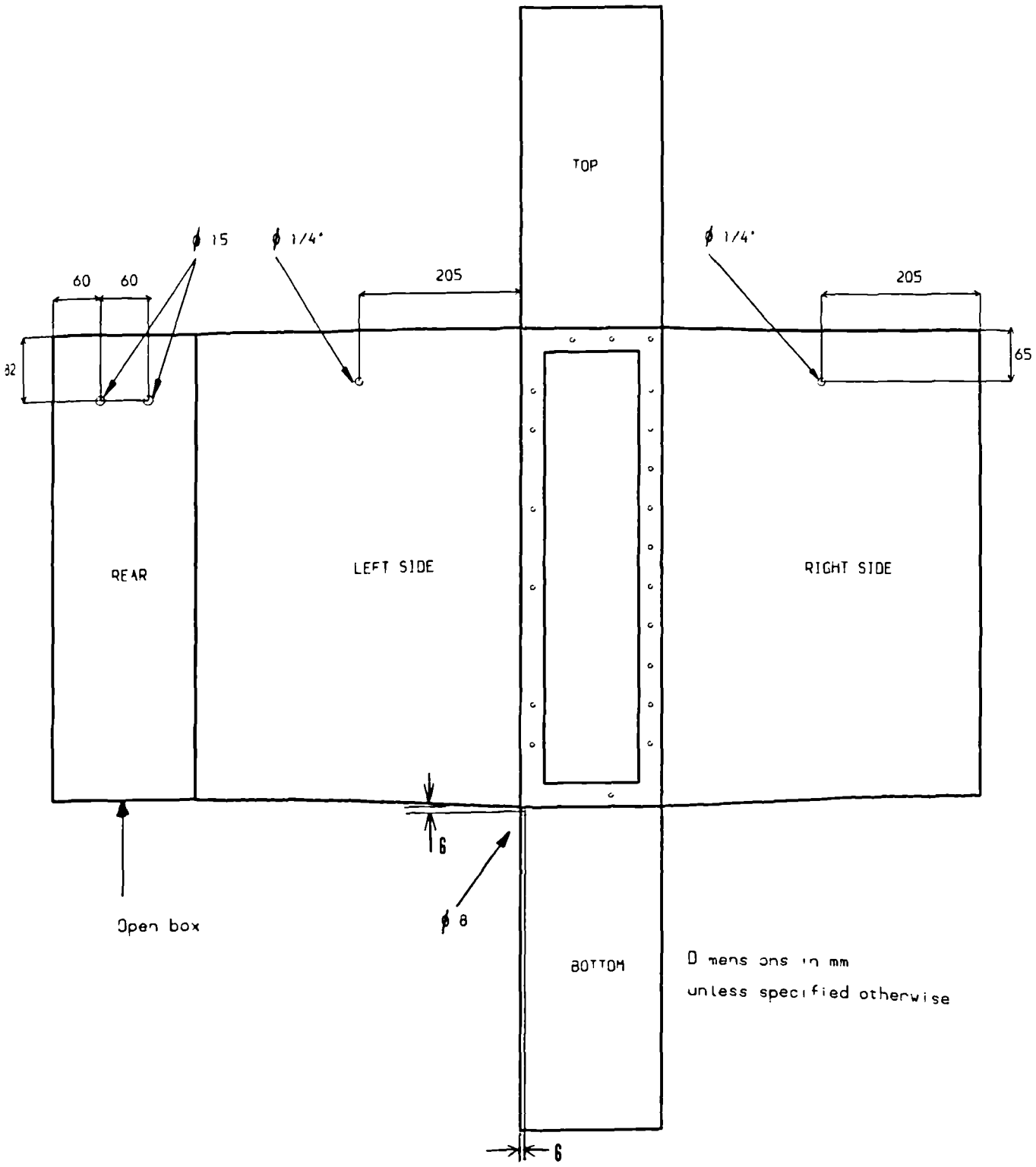

Fig.6.10 Six-view drawing of evaporator-absorber box

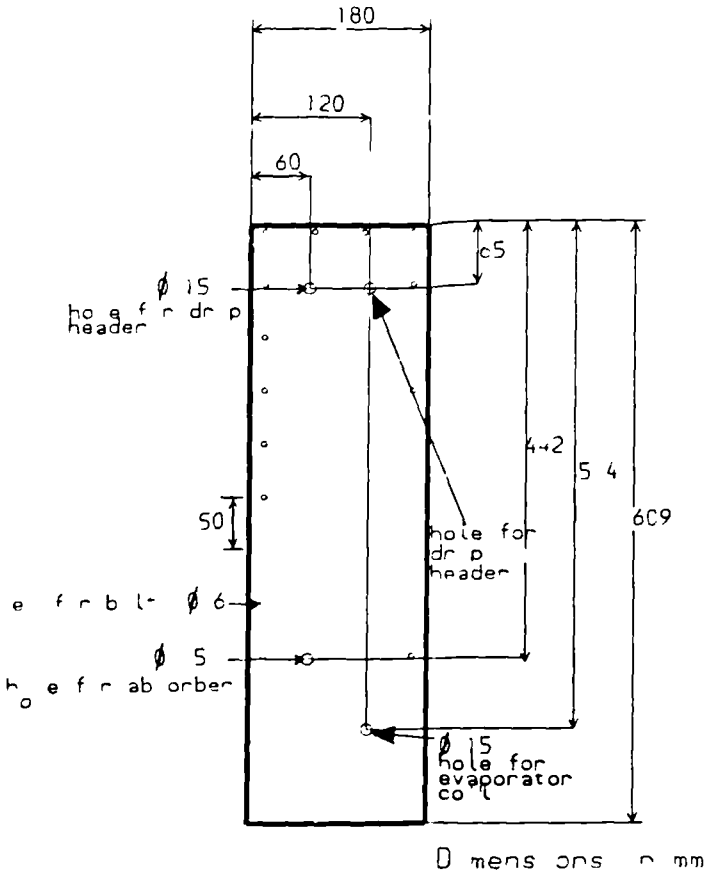

Fig.6.11 Frontal plate of evaporator-absorber box

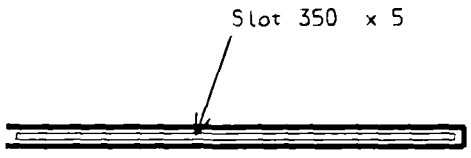

Top view

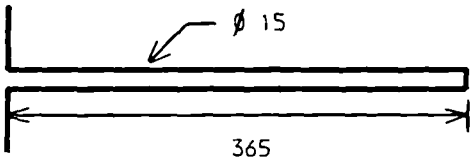

Side view

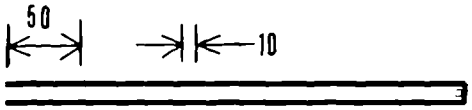

31 holes of diameter 1 mm

Bottom view

Dimensions in mm

Fig.6.12 Evaporator drip header

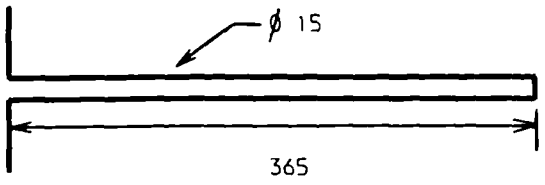

Side view

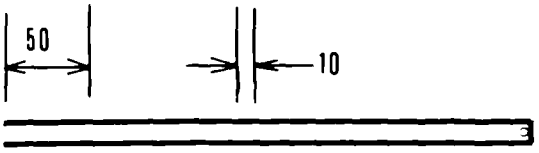

31 holes of d ameter 1 mm

Bottom view

Fig.6.13 Absorber drip header

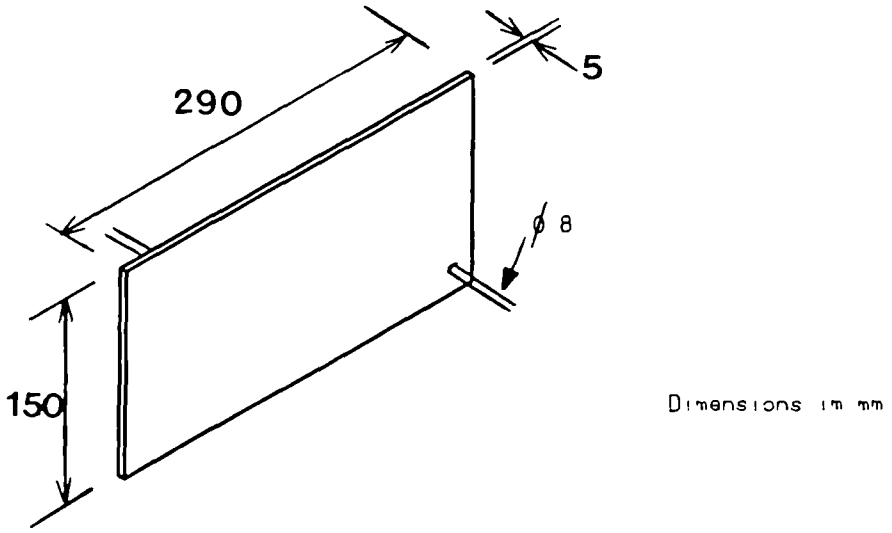

Fig.6.14 Internal box of solution heat exchanger

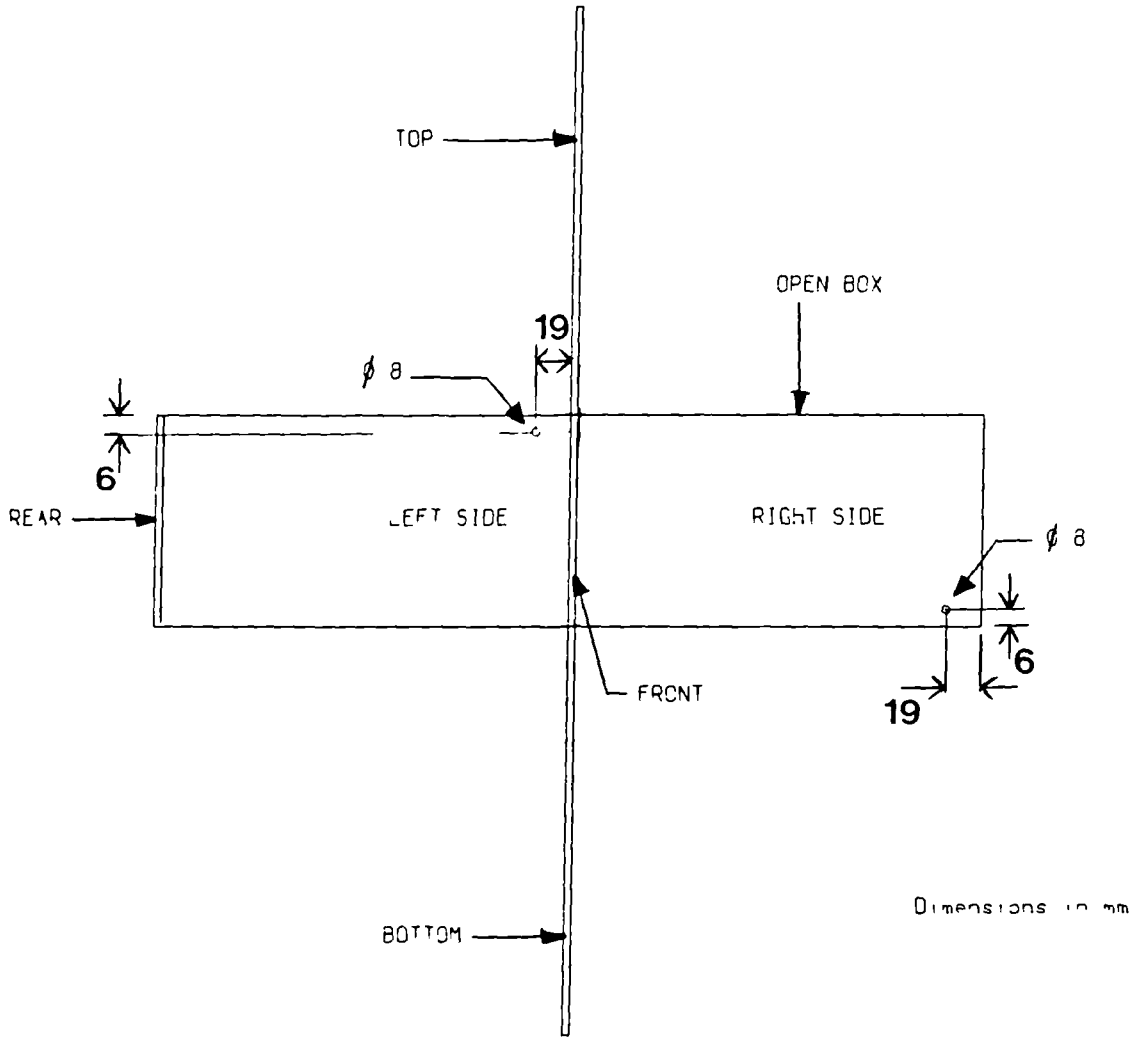

Fig.6.15 Six-view drawing of internal box of solution heat exchanger

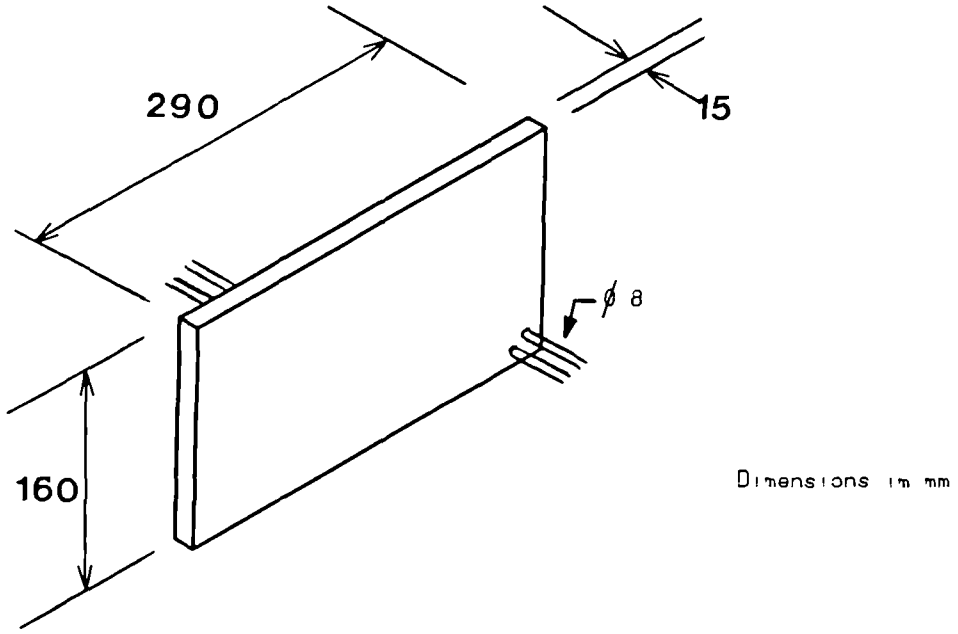

Fig.6.16 External box of solution heat exchanger

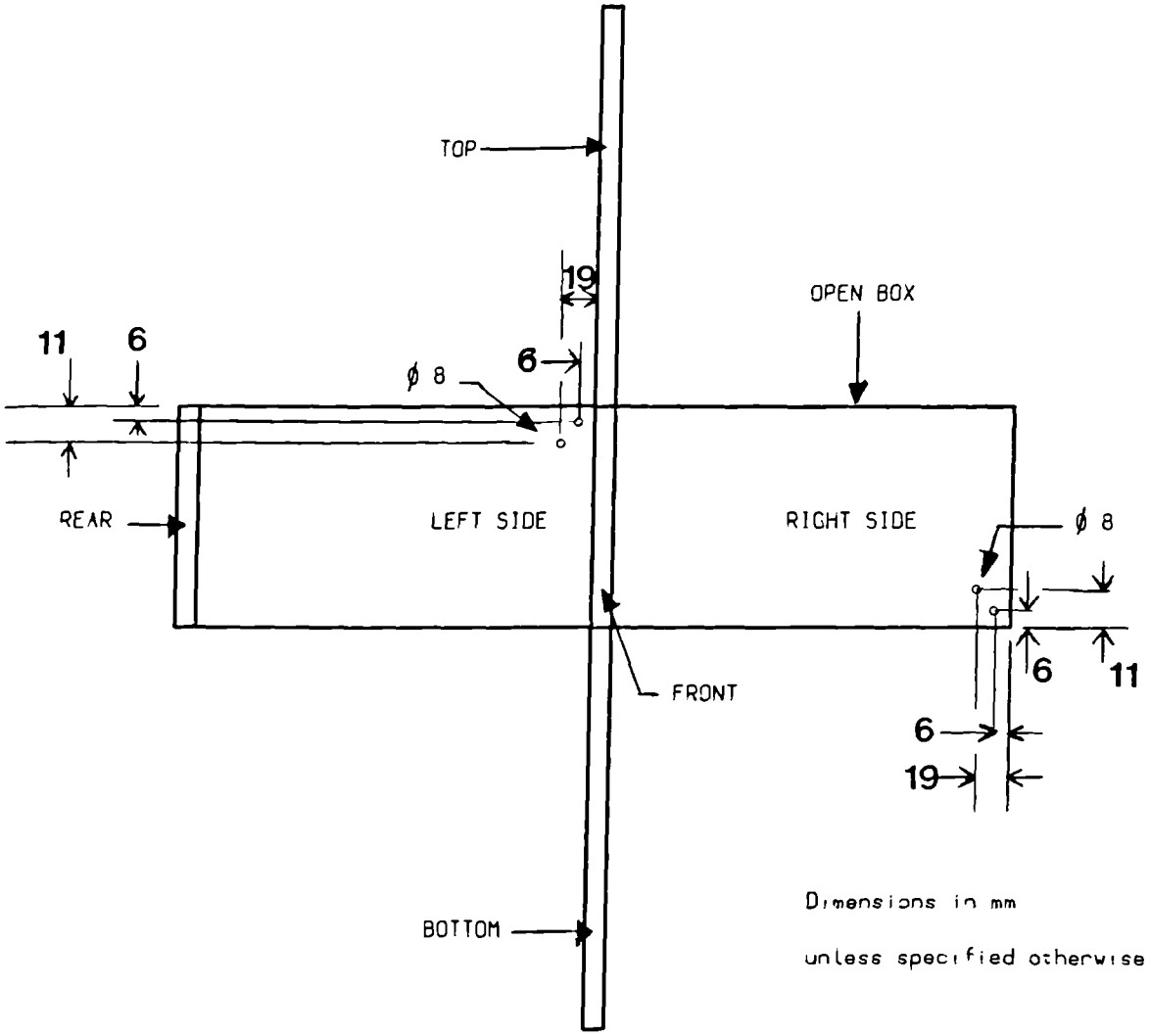

Fig.6.17 Six-view drawing of external box of solution heat exchanger

box through soldered 8 mm coupling tubes.

A small electric centrifugal pump was incorporated in the system for pumping the weak solution from the absorber to the generator.

Reinforced PVC hose of 8 mm bore was used to interconnect the generator, absorber, condenser, evaporator, pump and solution heat exchanger. All hoses were clamped to BSP unions and coupling nipples by means of worm drive hose clips.

The pressure difference between generator and condenser and between evaporator and absorber was maintained by use of U-tubes in which water condensate and strong solution undergo a pressure drop when flowing upwards. The height between the bottom of U-tubes and the drip headers was calculated as follows.

Between condenser and evaporator:

$$\Delta P = \rho_w g \Delta Z \tag{6.2}$$

Where

ΔP is the pressure difference between condenser and evaporator

ρ_w the density of saturated water at 28°C

ΔZ the height between U-tube and drip header

ΔP–19.16 mm Hg– 2.55 kpa and ρ_w=996.31 kg/m^3.

So ΔZ= 0.26 m= 26 cm.

Between generator and absorber:

$$\Delta P = \rho_s g \Delta Z \tag{6.3}$$

Where

ρ_s is the density of solution at 57.5°C and 58.5%

ΔP the pressure difference between generator and absorber.

ΔP=21.01 mm Hg= 2.8 kpa and ρ_s=1670 kg/m^3.

Then ΔZ= 0.17 m= 17 cm.

U-tubes were formed using 8 mm bore reinforced PVC hoses.

Hot water circulates by gravity from a heater and is fed to the generator coil through copper tubes and 15 mm bore reinforced PVC hoses. Hot water enters the coil from the frontal plate and leaves from the rear plate. The heater with incorporated thermostat was placed 1 metre above the generator. Cooling water was supplied to absorber and condenser coils from the mains via double pipe heat exchangers which consisted of straight copper tubes of 8 mm diameter within larger reinforced PVC hoses of 15 mm bore. Cooling water flows inside PVC hose in a counterflow arrangement.

Pictures of the experimental rig are given in figures 6.18 and 6.19.

6.2.3 Instrumentation

The system has been instrumented for the measurements of temperatures, pressures and flowrates at different sections.

Temperature of water liquid and L_iB_r-water solution is measured with thermocouples type K N_iC_r/N_iA_l SWG30 connected to a comark 6110 microprocessor thermometer (range-200°C to 1767°C) through a 24 junction thermocouple switch. Bare thermocouples were inserted into PVC hoses and sealed by an adhesive film of strong glue (cyanoacrylate adhesive).

In the vapour, wet bulb temperatures can be measured by using a wick to wet the thermocouple end with distilled water. The water temperature should attain wet bulb temperature before reaching the bulb but should not dry out before adequately wetting it. It is recommended that the wick should cover about one

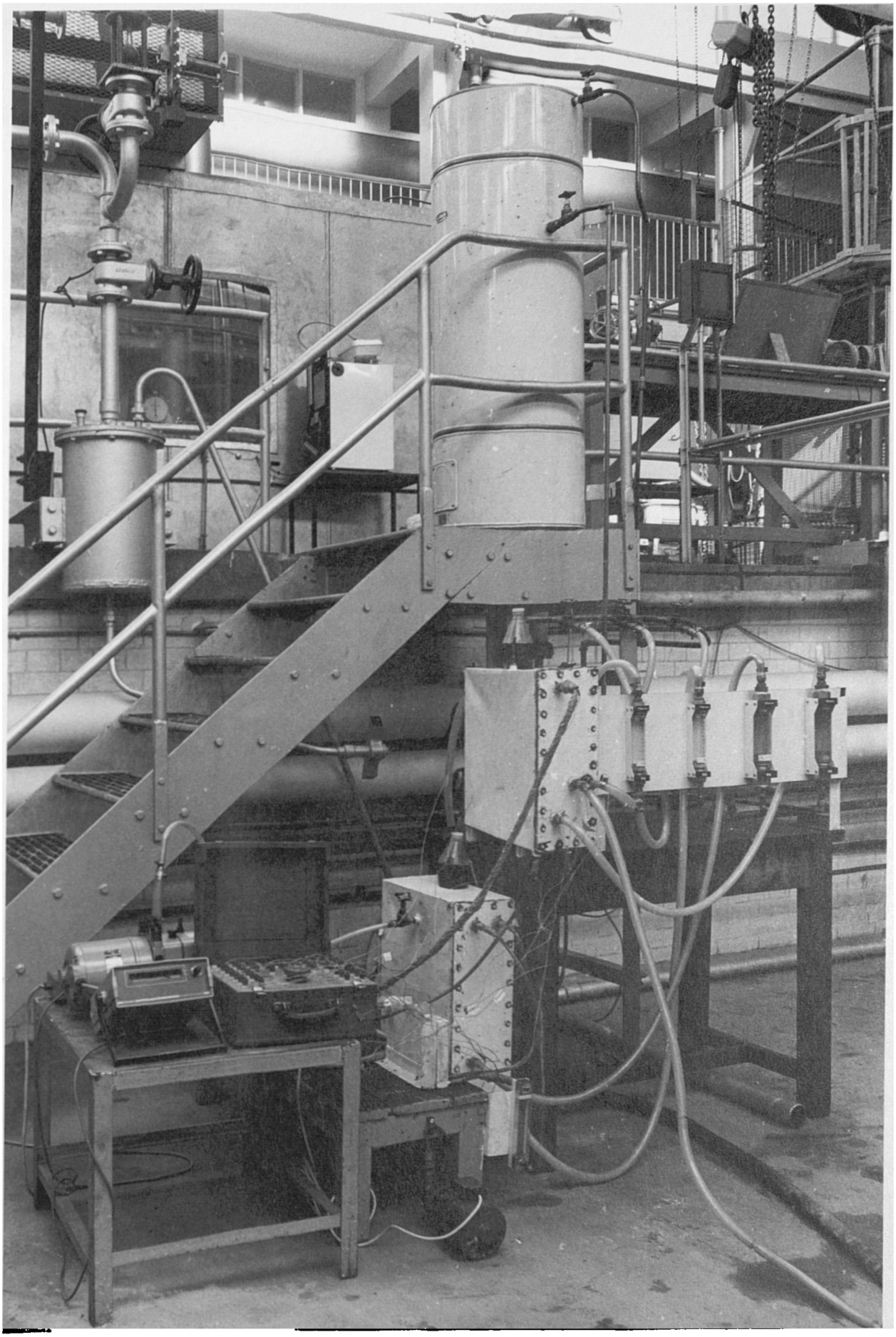

Fig 6.18 Photograph of the experimental rig

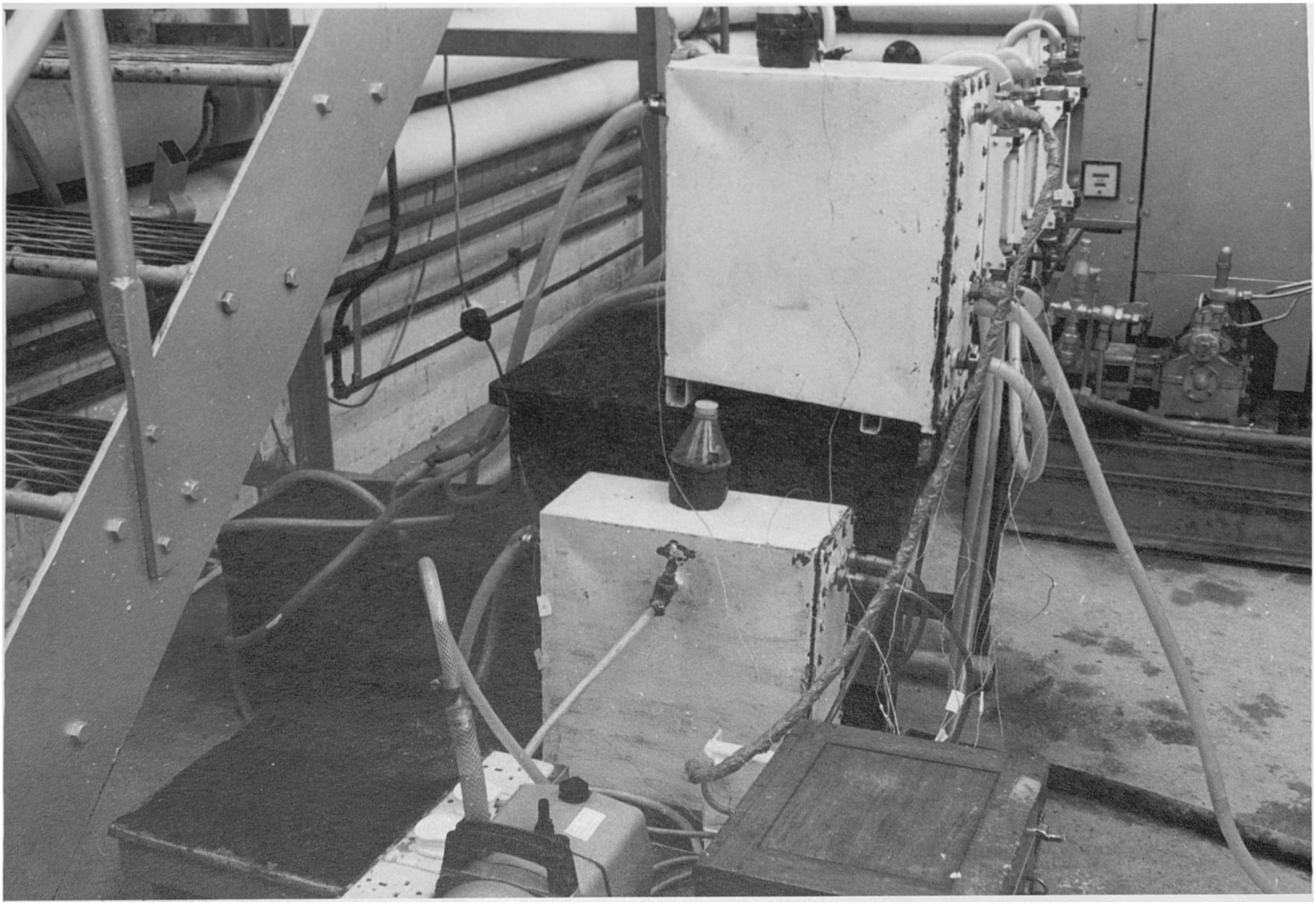

Fig 6.19 Photograph of the experimental rig

inch [62].

Therefore a cotton wick of 3 cm length inside the vessel was used to wet the thermocouple end with distilled water contained in a small recipient situated above the vessel. Thermocouple wires and cotton wick were placed in the head of bolts ϕ $\frac{1}{4}$" where a small hole of 1 mm diameter was made. The bolts are tightened into the vacuum vessels through one of the provided holes ϕ $\frac{1}{4}$" (see figures 6.4 and 6.10) and sealed by cyanoacrylate adhesive.

Saturation pressures can be obtained from measured saturation temperatures. Absolute pressure inside the boxes can also be measured using a MCLeod gauge connected to the vessels via gate valves $\frac{3}{4}$".

The flowrates of water and L_iB_r-water solution are measured by variable area flowmeters.

From chapter 5,the mass flowrates are :

Hot water at 74°C : 0.161 kg/s
Cooling water at 34°C : 0.156 kg/s
Cooling water at 25°C : 0.125 kg/s
Chilled water at 13.5°C : 0.0794 kg/s
L_iB_r- water solution at 37°C and 54% : 19.49 kg/h.

When converted to litres/minute these values of flowrates become :

Hot water : 9.91 l/min
Cooling water at 34°C : 9.4 l/min
Cooling water at 25°C : 7.6 l/min
Chilled water : 4.8 l/min
L_iB_r-water solution : 0.21 l/min.

Flowrates of hot water and cooling water at 34°C (to absorber) are measured with pannel mounted Platon flowmeters type PG/24FS/ASS unit scale (equivalent water flow 4-40 l/min). Flowrates of chilled water and cooling water at 25°C (to condenser) are measured with panel mounted Platon flowmeters type

PG/12FS/ASS unit scale (equivalent water flow 1-10 l/min) with an accuracy of 3%. Flowrate of L_iB_r-water solution is measured with a small valved flowmeter type Platon GTV $\frac{1}{4}$"B of $1\frac{1}{4}$% accuracy which was calibrated by the manufacturer for water at 20°C. Nevertheless, it can be used for L_iB_r-water solutions with values of scale graduations multiplied by a correction factor.
The density of water at 20°C is 998.3 kg/m^3 and the density of L_iB_r-water solution at 37°C and 54% is 1580 kg/m^3. If the aqueous solution is treated as water with density of 1580 kg/m^3 then the correction factor will be equal to 1580/998.3=1.58.

6.3 Conclusion

The design and fabrication of an experimental absorption refrigeration rig was presented. Conventional drilling,cutting and welding techniques were used to make most parts of it. The final assembly of rig consisted of mounting the generator-condenser and evaporator-absorber vessels on wooden frames together with the external solution heat exchanger, the small centrifugal pump and the external piping which is of PVC hose.
The generator-condenser vessel was placed at a height above the evaporator-absorber vessel for gravity circulation of solution from condenser to evaporator and from generator to absorber. A water heater of 30 gallons capacity was installed at a location above the generator-condenser box.

CHAPTER SEVEN

EXPERIMENTAL TESTS

7.1 Introduction

In this chapter the operating conditions of the absorption refrigeration rig designed in chapter 6 are investigated experimentally. Methods of leak detection used to test equipment prior to system operation are also described.
The practical operation of the absorption cooling cycle emphasizes the need of maintaining correctly a vacuum if acceptable performance is to be achieved. Therefore ways of improving sealing of vacuum vessels are discussed.
From the given preliminary data it is also found that improper flowrates to the components and low hot water supply temperatures may seriously degrade the operation of the system.
Measures to resolve practical problems of experimental rig and to improve system operation are reported in this chapter.

7.2 Experimental Procedure

Leak tightness is a major quality control element of absorption refrigeration units. Therefore, prior to system installation and operation, leaks had been tested in each hermetic component using one of the numerous leak detection methods reported in the literature [61,63].
In addition to system vessels, coils of generator, condenser, evaporator and absorber were also tested for leaks using the method of bubbles in liquid. The procedure is to pressurize the coils with compressed air and to find leaks which are indicated by bubbles appearing on the outside of the coils placed in a pool of water.
Using compressed air at 6 bars, small leaks were found in a soldered part of the

condenser coil and were subsequently repaired. Leaks were also detected in the solution heat exchanger by the method of bubbles in liquid.

The vessels containing the generator-condenser coils and the evaporator-absorber coils are relatively large in size and involve gasketed parts. Thus, tests were achieved using the method of wet outside surface. The inside of isolated vessels was filled with pressurized water and points were observed of wet outside surface. Several gross and small leaks were detected around the rubber seals and the compression bolts ϕ 6 mm of the removable frontal plates. Each leak was marked, repairs were made and reassembling of seals and frontal plates accomplished with proper care and attention.

The tightening of seals was done in 3 to 5 steps, beginning with one of the bolts and tightening it slightly, then tightening to the same degree the diametrically opposed bolt, continuing with one next to the first and then the one diametrically opposed to it, after the first cycle of tightening had been completed further tightening was repeated in the same sequence.

In order to seal all bolts ϕ 6 mm in the frontal plates of the vacuum vessels, small rubber washers were placed around the head of each bolt.

The vessels were isolated and evacuated to test for leaks. A minimum pressure of 5 torr was reached at a reasonable speed by means of a high vacuum pump connected through gate valves and 8 mm bore PVC hoses of short length. When no further improvement in the pressure was evident the pump was valved off from the component. Pressure rise with time was recorded using a vacuum gauge.

The leak rate Q_L of a tested volume is [61]

$$Q_L = \frac{V.\Delta P}{\Delta \tau} \tag{7.1}$$

Where

V—volume in litres

ΔP—pressure rise in microns

$\Delta\tau$=time period in sec.

and Q_L is expressed in lusec or micron litre per second.

For the generator-condenser box of 35 litres volume a pressure rise from 5 to 400 torr was recorded in 7 hours and 14 minutes.

Thus, by equation (7.1), Q_L=530.9 lusec.

It also means that the time required for a pressure rise of 10 mm Hg will be

$$\Delta\tau = \frac{35\ 10^4}{530.9} = 659 \text{ sec} \simeq 11\text{min}$$

For the evaporator-absorber box of 54 litres volume a pressure rise from 5 to 400 torr was recorded in 6 hours and 35 minutes.

Then, Q_L 900 lusec.

The time required for a pressure rise of 100 mm Hg will be equal to 10 minutes.

Clearly these measured rates of pressure rise are high and quite above the admissible leak rates for high vacuum systems that are manufactured to rigid standards of vacuum integrity.

However, commercial absorption units are manufactured to sustain leak-tightness throughout the life of the machine while laboratory absorption units can be designed mainly to perform experimental testing.

To reduce these leak rates and improve hermeticity, further repairing could be made. Better seals can be fabricated. Cleaning of parts and proper machining of surfaces of flanges may be considered. But this would take a considerable time to be done in the workshop and as this experimental work was already behind schedule, it was decided to operate the system with these conditions of leak rates.

The experimental rig was assembled and the vacuum system evacuated. The absorption refrigeration unit was flushed with a solution of L_iB_r-water prepared in a separate container. Circulation of solution, hot water and cooling water was carried out during a preliminary operation to check for system and equipment installation.

Before charging, a calculated quantity of L_iB_r-water solution with 0.54 concentration was prepared. For an uninterrupted flow of solution from absorber to generator at a rate of 0.21 l/min a minimum volume of 1.5 litre of L_iB_r-water solution is needed in the system to fill the inner and outer tanks of the solution heat exchanger as well as the 8 mm bore PVC hoses connecting the components of the refrigeration cycle. At absorber pressure and temperature the weak solution concentration is 0.54 and its density 1580 kg/m^3. Hence, mass of solution to be charged is 2.370 kg.
Therefore, required mass of anhydrous L_iB_r is 2.37 x 0.54 =1.280 kg and required mass of water is 1.090 kg.

In order to extract the maximum of information from the experiments the system has been intensely instrumented. In figure 7.1 temperature measuring points are indicated by numbers corresponding to :

1 Exit of strong solution in generator

2 Exit of strong solution in heat exchanger

3 Inlet of strong solution in absorber

4 Exit of weak solution in absorber

5 Inlet of weak solution in heat exchanger

6 Inlet of weak solution in generator or also exit of weak solution in heat exchanger

8 Exit of refrigerant water liquid in condenser or also entry of refrigerant water in evaporator.

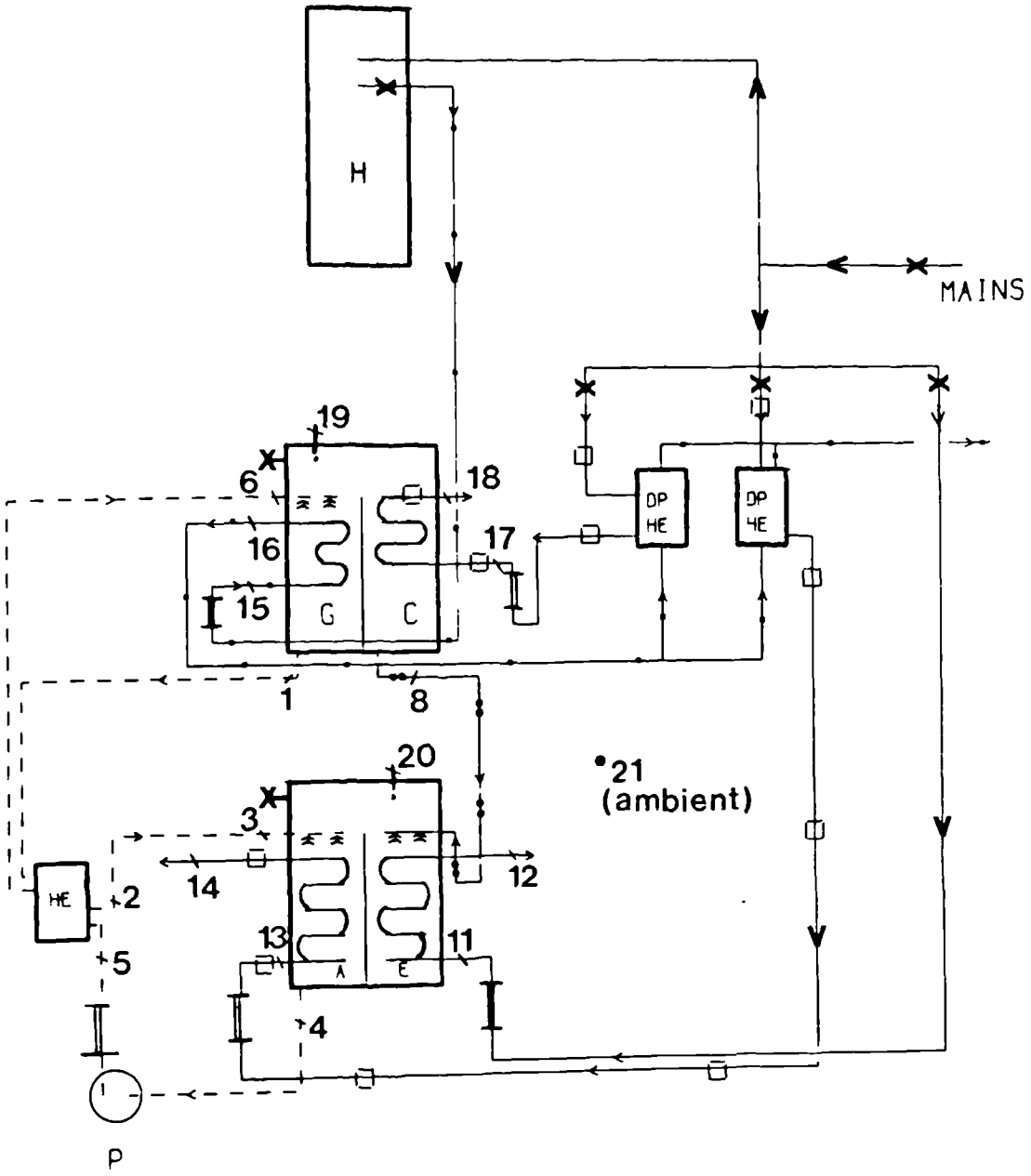

Fig.7.1 Schematic of absorption refrigeration rig with temperature measuring points

11 Inlet of water to be chilled in evaporator

12 Exit of chilled water in evaporator

13 Inlet of cooling water in absorber

14 Exit of cooling water in absorber

15 Inlet of hot water in generator

16 Exit of hot water in generator

17 Inlet of cooling water in condenser

18 Exit of cooling water in condenser

19 Refrigerant water vapour in generator-condenser vessel

20 Refrigerant water vapour in evaporator-absorber vessel

21 Ambient

A L_tB_r-water solution was prepared, mixed and well shaken to ensure complete solution of all salt. The required volume of 1.5 litre was then charged into the absorber.

For operation of the rig, first hot water at the desired flowrate is supplied from the heater to the generator. Cooling water at the required flowrate is circulated from the mains to the condenser and absorber via double pipe heat exchangers. Water to be refrigerated is delivered to the evaporator directly from the mains. The circulation pump is then operated to pump the weak solution to the generator with simultaneous adjustment of the flowrate of weak solution by controlling

the $L_i B_r$-water flowmeter.

Leaks into the system caused some problems. Stable conditions were difficult to obtain as the pressure rises in the system. To keep the pressure low the high vacuum pump was operated continuously. As a result, more stable conditions were reached after 10-15 minutes of operation but it seemed the flow was adversely affected by the continuous operation of the vacuum pump.

Other practical problems were observed. Although the heater thermostat was set at 82°C,the highest hot water temperature from the insulated heater was unexpectedely around 71°C which is less than the design temperature of 75°C at the inlet of the generator. This was due to heat losses from the heater itself and the connecting pipes.

Besides, when hot water was supplied at a flowrate of 9.9 l/min its temperature started to decrease quickly after about 10 minutes of operation. Thus lower flowrates of hot water were used to record readings.

Design temperatures of cooling water at design flowrates to condenser and absorber could not be attained in the counterflow double pipe heat exchangers. The causes of the trouble were the low inlet temperature of cooling water from the mains and the heat losses to the ambient. The system was tested over winter periods of time where the mains water was at approximately 8°C and the laboratory ambient temperature varying between 18°C and 23°C.

The system did not function properly because of the combining effects of :

1. Rise in system pressure

2. Lower delivery temperature of hot water

3. Drop in hot water inlet temperature after a short time of operation

4. Low inlet temperature of water to be chilled in evaporator

Modifications were made in the system by changing the concentration of the solution and the inlet temperature of water to be chilled.

The vapour pressure of a solution is a function of its temperature and concentration. It can be seen from equilibrium chart for aqueous lithium bromide solutions [18] that reducing the L_iB_r concentration of solutions at constant temperature would result in vapour being produced at higher pressures.

During the system initial operation the generator pressure was around 70 mm Hg and the average exit temperature of solution in generator was 60°C.At these levels of pressure and temperature, the solution will boil only if its L_iB_r concentration is below 44%.

Therefore a solution of 40% concentration was prepared, the system drained and evacuated, and a 1.5 litre volume of new weak solution charged into the absorber. The evaporator pressure was around 20 mm Hg which corresponds to a water saturation temperature of 22°C. Hence, water was delivered at higher temperatures to the evaporator via a double pipe heat exchanger while water from the mains at 8°C was used to cool the condenser.

Even with lower flowrates, the drop in inlet temperature of hot water reduced considerably the time period over which the rig was tested.

Some problems also occurred in the apparutuses of wet bulb thermocouples and in the small flowmeter for controlling the L_iB_r-water solution flow. Better sealing of thermocouples was needed to prevent leakage into the system.

7.3 Results of Experimentation

Many tests were conducted to investigate the operating conditions of the absorption refrigeration unit. However, data from only a few tests are presented as steady state conditions were difficult to reach. Numerous practical problems could not allow testing of absorption cooling system under a wide range of conditions. Tables 1, 2, 3 show the values of 10 sets of reading for three runs.

The arithmetical average of tested data and the standard deviation of the readings from their average have been reported.

Table 7.1 Measured temperatures (deg.C) for run 1.

t_1	t_2	t_4	t_5	t_6	t_8	t_{11}	t_{12}	t_{13}	t_{14}	t_{15}	t_{16}	t_{17}	t_{18}	t_{19}	t_{20}	t_{21}
63.0	43.6	31.6	31.6	30.3	37.5	25.9	20.5	21.1	25.3	71.8	63.4	10.0	14.9	41.6	20.7	19.5
63.7	44.9	32.1	33.0	34.2	35.5	25.7	20.7	20.7	24.7	71.7	64.7	9.2	14.1	41.0	20.8	19.8
64.0	45.2	32.3	33.5	35.8	33.1	25.4	19.9	20.4	24.4	71.8	64.5	8.7	13.6	43.6	21.8	20.5
64.0	45.3	32.8	33.5	37.3	31.6	25.5	21.4	19.2	24.0	71.8	64.8	8.5	13.3	43.5	22.2	20.4
64.1	45.1	32.0	33.4	37.2	30.8	25.4	21.4	19.2	23.9	71.8	64.9	8.3	13.2	44.1	23.3	20.4
63.7	44.9	32.3	33.5	38.9	28.8	25.6	21.4	19.2	23.9	71.7	65.4	8.2	13.1	43.4	23.4	20.4
63.5	44.7	31.7	33.4	39.5	25.3	25.5	21.4	19.1	23.8	71.7	65.8	8.1	13.0	44.5	24.2	19.8
63.4	44.6	31.3	33.2	39.3	25.5	25.5	21.2	19.1	23.7	71.7	66.0	8.0	13.1	43.8	24.0	20.6
63.4	43.7	31.0	32.8	39.2	26.6	25.4	21.2	18.9	23.4	71.7	65.8	8.0	12.9	43.2	24.2	20.4
63.4	43.2	30.8	32.7	38.8	27.6	25.3	21.2	19.0	23.3	71.6	65.6	7.9	12.9	42.6	23.0	20.4
63.6	44.5	31.8	33.0	37.0	30.2	25.5	21.3	19.3	24.0	71.7	65.1	8.5	13.4	43.1	22.7	20.2
0.3	0.7	0.6	0.6	2.8	3.9	0.2	0.2	0.3	0.6	0.1	0.7	0.6	0.6	1.0	1.1	0.3

$\bar{t}$

Standard deviation

Table 7.2 Measured temperatures (deg.C) for run 2.

t_1	t_2	t_4	t_5	t_6	t_8	t_{11}	t_{12}	t_{13}	t_{14}	t_{15}	t_{16}	t_{17}	t_{18}	t_{19}	t_{20}	t_{21}
60.0	35.2	21.9	21.7	32.3	30.2	26.0	24.6	24.2	24.4	71.1	67.3	10.8	12.3	51.9	19.4	21.8
62.6	40.8	24.5	23.8	34.8	34.9	26.0	24.8	23.5	31.0	71.2	67.5	10.5	12.0	40.8	20.3	21.8
62.7	38.8	25.6	26.2	35.9	30.8	25.5	24.6	23.2	29.7	71.2	67.1	10.1	11.7	48.0	20.6	22.7
60.5	34.1	25.0	26.6	34.6	30.2	24.9	24.0	22.9	27.0	71.2	66.7	9.6	11.5	49.8	21.2	21.6
61.6	33.6	25.8	25.9	33.6	39.0	24.3	23.9	22.8	25.2	71.2	68.6	9.2	11.4	51.1	21.5	22.1
59.8	33.6	26.1	25.8	36.5	36.3	24.8	23.9	22.9	23.8	71.1	69.4	8.9	10.8	49.1	21.7	21.6
58.0	34.2	25.7	26.7	38.2	33.6	24.7	23.9	22.7	22.9	71.1	69.5	8.7	10.6	47.5	21.9	22.4
55.5	34.8	25.4	28.1	37.9	26.8	24.5	23.4	22.5	22.2	71.1	69.6	8.7	10.2	46.2	22.1	22.3
53.6	35.9	25.6	29.2	37.7	26.5	24.3	23.6	22.2	21.6	71.1	69.3	8.7	10.3	47.6	22.2	22.2
52.1	35.5	25.3	29.8	37.4	27.0	24.2	23.4	22.0	21.0	70.8	69.2	8.6	10.0	46.7	22.4	21.9
$\bar{t}$ 58.6	35.7	25.1	26.4	35.9	31.6	24.9	24.0	22.9	24.9	71.1	68.4	9.4	11.1	47.9	21.3	22.0
Standard deviation 3.5	2.2	1.1	2.2	1.0	4.0	0.6	1.0	0.6	3.2	0.1	1.0	0.7	0.7	2.9	0.9	0.3

Table 7.3 Measured temperatures (deg.C) for run 3.

t_1	t_2	t_4	t_5	t_6	t_8	t_{11}	t_{12}	t_{13}	t_{14}	t_{15}	t_{16}	t_{17}	t_{18}	t_{19}	t_{20}	t_{21}
54.4	33.8	28.0	27.2	33.1	30.6	32.3	29.7	24.6	29.0	70.4	66.2	12.0	15.1	48.9	21.5	21.4
54.9	33.2	26.8	26.2	33.2	31.5	31.1	29.9	24.7	39.2	70.4	66.3	11.8	14.5	48.5	22.0	21.3
54.2	33.2	28.9	27.5	34.0	33.6	30.0	29.4	25.8	39.6	70.6	66.6	11.9	14.2	49.0	23.3	21.7
55.2	34.7	28.0	26.4	33.6	31.0	33.3	29.5	26.1	31.3	70.7	66.4	12.0	14.1	48.3	23.1	22.2
54.9	37.8	33.0	31.0	36.1	27.9	32.9	29.2	26.4	32.0	70.5	66.2	11.7	13.4	44.0	25.8	22.4
55.2	38.1	31.8	30.3	36.0	27.7	33.6	28.4	23.9	31.8	68.8	65.0	11.2	13.0	44.7	25.4	22.5
58.1	40.8	36.8	35.4	39.9	36.9	33.4	28.8	24.8	29.4	68.6	65.1	11.1	12.9	45.7	25.6	22.5
56.0	40.4	34.7	34.1	39.8	38.9	32.9	29.9	26.0	28.8	68.5	65.0	10.9	12.7	45.4	25.7	22.6
58.2	41.2	34.4	33.2	39.2	34.4	31.3	29.6	25.8	27.8	68.4	65.1	10.8	12.4	43.3	25.8	22.5
58.3	42.0	34.0	33.3	39.1	34.5	29.3	27.6	23.5	28.1	68.0	65.2	10.7	12.1	40.8	25.3	22.6
$\bar{t}$ 55.9	37.5	31.6	30.5	36.4	32.7	31.7	29.2	25.2	29.9	69.5	65.7	11.4	13.4	45.9	24.4	22.2
Standard deviation 1.5	3.3	3.3	3.2	2.7	3.5	1.5	0.4	0.9	1.4	1.0	0.6	0.5	0.9	2.6	1.6	0.5

The flowrates for runs 1, 2, and 3 were approximately as follows.

Hot water : 8, 7, 7 l/min.

Cooling water to absorber : 8, 6, 6 l/min.

Cooling water to condenser : 6, 6, 6 l/min.

Water to be chilled : 5, 5, 3 l/min.

L_iB_r-water solution : 0.21, 0.21, 0.21 l/min.

Due to the practical problems encountered during the rig operation in general and to the pressure rise in the evaporator in particular, acceptable levels could not be obtained of temperatures of water to be chilled. duration of runs was limited to 20-30 minutes due to drops of supply temperatures of hot water. There has been a temperature drop of about 2.7 to 6.6°C between the inlet and outlet of hot water in generator as compared with the design value of 2°C for a higher flowrate. Temperature difference between hot water at the outlet and solution in the generator was 4.8°C in run 1 and around 11°C in runs 2 and 3. Drop in cooling water temperature varied between 2 and 4.7°C from the inlet to the exit of absorber and between 1.7 and 4.9°C from the inlet to the exit of condenser. The temperature approach in the cold-end of the heat exchanger, expressed by $t_2 - t_5$, was 7°C, 9.3°C or 11.5°C for tests 3, 2, 1 respectively. Although the objective of water chilling at desired levels was not achieved and the reliability of the presented data is doubtful, the experimental measurements have been used to calculate heat transfer rates in the components, system COP and second law efficiency.

Using the inlet and outlet conditions of the external fluids in the generator, evaporator, condenser and absorber components of the absorption cooling cycle, the calculated quantities were :

For run 1

$$\dot{Q}_G = (\dot{m}C_p)_{HW}(t_{15} - t_{16}) = 3.60\ kW$$

$$\dot{Q}_E = (\dot{m}C_p)_{CHW}(t_{11} - t_{12}) = 1.46\ kW$$

$$\dot{Q}_A = (\dot{m}C_p)_{CW,2}(t_{13} - t_{14}) = -2.62\ kW$$

$$\dot{Q}_C = (\dot{m}C_p)_{CW,1}(t_{17} - t_{18}) = -2.05\ kW$$

Then

$$COP = \frac{\dot{Q}_E}{\dot{Q}_G} = 0.40$$

The second law efficiency of the absorption cycle is calculated from equation (3.17) with the following quantities :

$$\bar{T}_H = \frac{T_{15} + T_{16}}{2} = 341.5\ ^oK, \quad \bar{T}_{CHW} = \frac{T_{11} + T_{12}}{2} = 296.6\ ^oK$$

$$\bar{T}_{CW,1} - \frac{T_{17} + T_{18}}{2} = 284.1\ ^oK, \quad \bar{T}_{CW,2} = \frac{T_{13} + T_{14}}{2} = 294.8\ ^oK$$

$$T_o = T_{21} - 293.36^oK$$

Hence

$$\eta = 2.8\%.$$

For run 2

$$\dot{Q}_G = +1.333\ kW, \quad \dot{Q}_E = +0.314\ kW,$$

$$\dot{Q}_A = -0.846\ kW, \quad \dot{Q}_C = -0.712\ kW,$$

$$COP - 0.23$$

$$\eta = 1.2\%.$$

For run 3

$$\dot{Q}_G = +1.900\ kW, \quad \dot{Q}_E = +0.377\ kW,$$

$$\dot{Q}_A = -1.300\ kW, \quad \dot{Q}_C = +0.840\ kW,$$

$$COP = 0.19 \text{ and } \eta = 3.8\%.$$

Values of heat transfer rates to the absorption cycle internal fluids and heat losses to the surroundings have not been calculated. Hence,heat transfer coefficients in the subunits of the cooling machine have not been determined. Only

reliable experimental data accumulated over a time period of successful continuous operation can be used to assess the performance of the refrigeration unit and subunits.

The low values of COP and second law efficiency of the absorption cycle, calculated for runs 1, 2, 3 are due to inadequacy of operation and large departure from design conditions.

Unfortunately improper pressures in the generator and evaporator could not allow satisfactory system operation and degraded the performance of the machine.

A number of other factors also contributed towards inadequate operation of the system. These include improper temperatures of hot water to generator and off-design flowrates of external fluids. Merely preliminary results were obtained.

As the major problem was a pressure rise in the generator-condenser and evaporator-absorber vessels, it is believed that it can be reduced or eliminated only by design and fabrication of vessels to better standards of vacuum integrity.

Reliable seals should be used and grooves to receive the gaskets should be machined and designed to meet the requirements of ensuring a compression ratio for vacuum hermeticity.

Bolts closing holes in the wall of vacuum chambers should be sealed by placing an O-ring in a groove provided in the head of the bolts.

Internal cleanness is an important aspect of absorption machine operation and therefore suitable cleaning methods may be considered to remove contaminants introduced during fabricating processes.

Recommended techniques [61] should be observed of design and construction of welded joints for vacuum vessels.

Commercial leak detectors such as electronic halide detectors and helium mass spectrometers should be used to verify hermeticity and to ensure the leak-tightness of absorption refrigeration systems prior to operation.

Improvement in mechanical design of experimental rig will enhance the reliability of the absorption refrigeration unit.

The entire circuits of solution and refrigerant being hermetically sealed, it would be preferable to make external measurements only.

Large capacity heaters with adequate insulation are required to provide hot wa-

ter and to enable the system to operate a longer time with stable generator temperatures.

7.4 Conclusion

Using the test rig described in chapter 6, an experimental investigation of the operating conditions of an absorption refrigeration system has been conducted. The results show that it is necessary to maintain correctly the system vacuum to achieve an acceptable chiller performance.

Poor measurements were obtained with system working in off-design conditions. This is caused by a pressure rise in the generator-condenser and evaporator-absorber components which affected the temperature levels at which the system was designed to operate. Desired flowrates of hot water were not attained.

Operation and performance of system can be improved primarly by maintaining a correct vacuum inside the vessels which requires better design of seals and fabrication of equipment.

Testing for external leaks should be undertaken with sensitive leak detectors as the described methods used in the laboratory to verify rig hermeticity were unsatisfactory.

Heat transfer rates, cycle COP and second law efficiency have been calculated from values of flowrates and averaged temperatures of external fluids for three tests.

Preliminary measurements are given in tables 1, 2, 3. The presented calculations indicate poor performance levels.No reliable analysis of absorption cycle can however be pursued using these preliminary measurements. A discussion has been considered of practical problems encountered in rig operation and ways to eliminate the failure modes.

CHAPTER EIGHT

MODELLING AND DESIGN OF SOLAR THERMAL SYSTEMS

8.1 Introduction

In the last few years research into the design and sizing of solar energy systems has been developed considerably. Consequently, design procedures have been available which essentially yield estimates of long-term performance of solar-supplemented absorption refrigeration systems.

In this chapter a classification and description of various solar thermal systems is included as well as the modelling of system components.

The one-repetitive-day simulation procedure and the phibar-f chart method are presented.

A computer programme of the phibar-f chart method is developed to determine the yearly solar fraction of absorption refrigeration units operated by solar energy.

8.2 Description and modelling of solar thermal systems

8.2.1 Description of solar systems

Solar energy systems can be classified into the following classes :

(i) Stand-alone or solar-supplemented.

In stand-alone systems, solar energy is the only source of energy input. Such systems are usually designed for applications where electricity and other forms of energy are either scarce or not available.

In solar-supplemented systems, solar energy supplies part of the required thermal load, the rest being met by an auxiliary source of heat input. These systems have been widely used for several heat applications including air-conditioning and hot water processes.

(ii) Passive or active systems.

Passive systems collect or use solar energy without resorting to any source of conventional power.

In active systems, mechanical devices that require power input are used to collect solar energy.

(iii) Domestic and industrial systems.

In domestic systems, heat is withdrawn from the storage to supply the required thermal load at times when solar radiation is no longer available while in industrial or commercial applications, the solar thermal system is combined with a conventional system to assure the required thermal load at all desired times.

(iv) Liquid and air systems.

Solar air systems are those which supply hot air to meet the thermal load requirements. In these systems, air supplying energy to a thermal load can be heated by liquid-based or air-based collectors, the major difference between solar air collectors and solar liquid collectors being the choice of the heat transfer fluid.

In solar liquid systems, hot water is delivered to satisfy the required heat load and the fluid through the collectors is either water or an antifreeze solution.

(v) Daily and seasonal storage.

In seasonal storage, solar energy is stored during the summer for use in winter in domestic applications of space heating.

Systems with daily storage have storage capacities to at most a few days of heating loads. Heat may be stored in the form of the sensible heat of a liquid or solid medium, as latent heat of fusion, or by means of a reversible chemical reaction of two or more substances.

Active solar energy systems can be further classified as closed loop or

open loop depending on the system configuration. One of the several possible configurations of open loop systems is given in figure 8.1.

Open loop systems are normally defined as systems in which the solar collector performance is independent of the storage temperature.

Figure 8.2 shows a schematic of one possible closed loop system. The performance of the solar colector is directly dependent on the storage temperature.
A complete system is composed of three interconnected basic subsystems : the collector system, the storage system and the final terminal system or load system. The subsystems are interconnected by piping and pumps.
Use of solar energy to produce cooling for air-conditioning and other applications has always been an attractive idea since in many cases the maximum cooling demand coincides with the maximum solar radiation. Even when solar energy availability is not in phase with cooling demands, a properly designed solar system can compensate for the variations between solar input and load demand.
Several different methods to convert solar energy into cooling effect have been investigated. These are absorption cooling with liquid absorbents such as L_iB_r-H_2O, H_2O-NH_3, L_iC_l-H_2O; absorption cooling with solid absorbents; cooling by solar-mechanical systems. Most of these methods are being developed however the only systems which have reached the stage where they are commercially available incorporate hot water fired chillers using absorption of refrigerant in liquid absorbents.
Operation of absorption refrigerators with energy from flat-plate collectors and storage system is the most common approach for solar cooling.
Solar-operated absorption cooling units are normally solar-supplemented, solar liquid, active, domestic and industrial systems with daily storage. There are also other alternatives such as use of continuous or intermittent cycles, hot or cold energy storage, different types of solar collectors.
Solar thermal units for absorption cooling are closed-loop systems where the

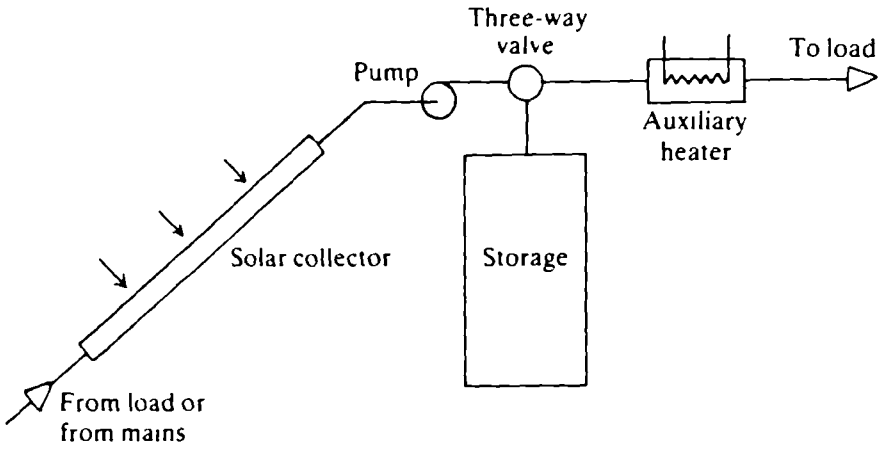

Fig.8.1 Schematic of an open-loop solar thermal system

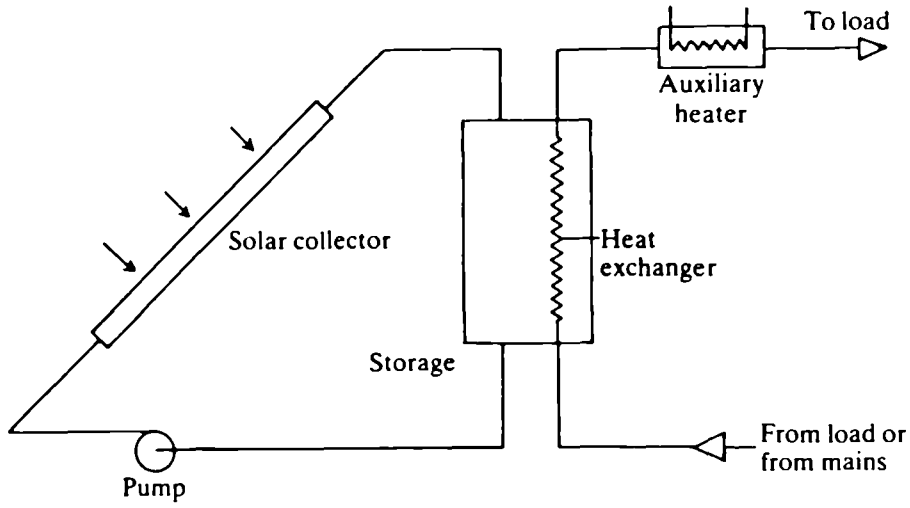

Fig.8.2 Schematic of a closed-loop solar thermal system

temperature drop in the load is low of the order of few degrees only.
Auxiliary heaters can be in series or in parallel with respect to the solar thermal unit. Auxiliary heaters in series (or also referred to as a topping-up type) supply just enough heat to raise the temperature of the load fluid to the required load temperature. However, auxiliary heaters in parallel (alternatively referred to as all-or-nothing type) either supply all the required heat load at any instant or nothing at all.
Solar thermal systems with the auxiliary heater in series are more efficient than those with the heater in parallel since the former supplies more solar energy.

8.2.2 Modelling of solar system components

A solar thermal system for cooling by absorption cycles consists of a solar collection subsystem, a storage subsystem and a load subsystem.
Mathematical modelling of each subsystem is considered separately below. Consider for example the solar system shown in figure 8.3.

(i) Solar collection subsystem.

The useful heat transfer rate delivered by a solar flat-plate collector, neglecting transient effects,can be expressed by the Hottel-Whillier-Bliss equation :

$$\dot{Q}_C = A_C F_R[I_T(\tau_r\alpha) - U_L(t_{fi} - t_o)]\delta_c \tag{8.1}$$

where
A_C is the collector area
F_R the collector heat removal factor
I_T the radiation intensity on the collector plane
$(\tau_r\alpha)$ the optical efficiency or product of the transmittance and absorptance of the collector cover
U_L the overall heat loss coefficient of the collector
t_{fi} the inlet temperature of the fluid in the collector

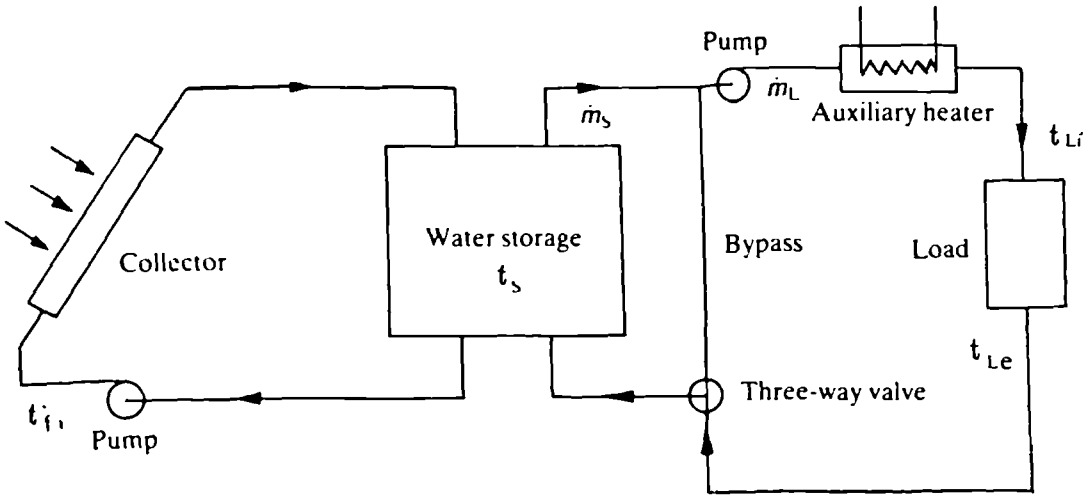

Fig. 8.3 Schematic of a closed-loop solar system for absorption cooling cycles

t_o the ambient temperature

δ_c is a control function whose value is either 0 or 1 depending on wether the collector is operating or not.

The instantaneous collector efficiency under normal solar incidence is

$$\eta_c \equiv \frac{\dot{Q}_C}{A_C I_T} \tag{8.2}$$

The collector parameters $F_R U_L$ and $F_R(\tau,\alpha)$ of a flat-plate collector can be calculated from basic heat transfer analysis or determined from experimental tests.

(ii) Storage subsystem

The thermal losses from the storage tank are given by

$$\dot{Q}_W = (UA)_S(t_S - t_o) \tag{8.3}$$

where $(UA)_S$ is the storage overall heat loss per unit temperature difference, t_S the storage temperature and t_o the ambient temperature.

The instantaneous energy balance equation for a fully-mixed storage tank is

$$(MC_P)_S \frac{dt_S}{d\tau} = \dot{Q}_C - \dot{Q}_W - \dot{Q}_U \tag{8.4}$$

where

τ is the time

$(MC_P)_S$ is the storage heat capacitance

$\dot{Q}_U$ the useful heat transfer rate to the load working fluid or rate of heat withdrawn from the storage.

In the case of stratified storage, the storage tank can be assumed as made up of N isothermal segments of equal volume.

(iii) Load subsystem

In solar systems for absorption cooling where there is an auxiliary source of energy,

$$\dot{Q}_L = \dot{m}_L C_{PL}(t_{Li} - t_{Le}) \tag{8.5}$$

where

$\dot{m}_L$ is the flowrate of the heating fluid

t_{Li} the inlet temperature of the fluid in the subsytem

t_{Le} the exit temperature of the fluid in the subsystem

A solar-supplemented system supplies part of the required thermal load and the index of contribution of the solar system is expressed by the solar fraction. The most used solar fractions are the monthly solar fraction f_M and the annual solar fraction f_Y.

$$f_M = \frac{Q_{UM}}{Q_{LM}} \tag{8.6}$$

$$f_Y = \frac{\sum Q_{UM}}{\sum Q_{LM}} \tag{8.7}$$

where

Q_{UM} is the monthly thermal energy supplied by the solar system and Q_{LM} the monthly total load.

A solar thermal system can be simulated using the appropriate component modelling equations subjected to certain constraints and conditions.

$$\dot{Q}_U = (\dot{m}C_P)_S(t_S - t_{Le})\delta_L \tag{8.8}$$

where

δ_L is a control function whose value is either 0 or 1 depending on wether there

is a heat load or not.

The amount of energy supplied by the auxiliary heater is given by

$$\dot{Q}_{AUX} = \dot{Q}_L - \dot{Q}_U \tag{8.9}$$

Neglecting thermal stratification in the storage tank, the rate of internal energy change of the tank is given by equation (8.4)

$$\begin{aligned}(MC_P)_S \frac{dt_S}{d\tau} = {} & A_C F_R[I_T(\tau_r\alpha) - U_L(t_S - t_o)]\delta_C \\ & - (\dot{m}C_P)_S(t_S - t_{Le})\delta_L - (UA)_S(t_S - t_o)\end{aligned} \tag{8.10}$$

If equation (8.10) is expressed in finite difference form using a Taylor's expansion for $t_S(\tau)$, an approximate solution will be

$$\begin{aligned}t_{Sf} = t_{Sb} + \frac{\Delta\tau}{(MC_P)_S}\Big(& A_C F_R[I_T(\tau_r\alpha) - U_L(t_{Sb} - t_o)]\delta_C \\ & - (U_A)_S(t_{Sb} - t_o) - (\dot{m}C_P)_S(t_{Sb} - t_{Le})\delta_L\Big)\end{aligned} \tag{8.11}$$

Where t_{Sb} and t_{Sf} are the storage temperatures at the beginning and end of the time step $\Delta\tau$.

8.3 Aqueous Lithium Bromide Cooling Systems

L_iB_r-water absorption machines are suitable for solar cooling and have advantages of good performance at the temperatures available from flat-plate collectors (60 to 90°C). The energy supplied to the generator is from a solar collector-storage-auxiliary heater combination. The auxiliary heater can be placed in series or in parallel with respect to the storage subsystem.

L_iB_r-water machines with water-cooled absorber and condenser have been used in many solar cooling applications. These units are usually classified as active, continuous, solar-supplemented, solar liquid, domestic and industrial systems

with daily storage.

Other alternatives have also been considered including firing the generator of the absorption chiller directly from the solar collector, cold storage in place of hot storage or a combination of the two, the addition of an auxiliary generator to solve the problem of back up required in solar-powered systems, the use of evacuated tube collectors instead of conventional flat plate collectors.

L_iB_r-water absorption units using solar energy have been modelled with both theoretical and empirical methods.

Mathematical modelling of solar-operated L_iB_r-water units can be approached from the analysis of section 2.2 of this chapter for solar collector and storage subsystems and from the analysis of chapter 4 for the absorption chiller subsystem.

Empirical representation of L_iB_r-water coolers can be derived from operating experience with the machine under consideration and on estimates of the effects of changing operating conditions.

8.4 Design Methods

Conventional energy systems are normally sized with a single design -point calculation while solar energy systems have to be sized with the consideration of time-dependent functions for solar radiation, ambient temperature, and load.

In order to design solar thermal systems, it is necessary to predict long-term system performances.

Unlike conventional absorption coolers which are usually designed with a single index of performance (COP), solar operated absorption units are sized with considerations involving two additional factors, the temperature level required in the solar collector and the ratio of cooling produced to solar energy incident on the collector (system COP). The solar collector thermal performance is of course dependent on the solar radiation, ambient temperature and the inlet temperature of the heat transfer fluid entering the collector (usually the storage temperature).

With properly formulated mathematical models for various system components,computer simulation on the dynamic performance of the system can be used as a design tool. Detailed simulation procedures need to be repeated every hour of a year and in some cases over several years in order to obtain mean yearly system performance. It is thus obvious that such simulation approaches are not suitable for routine design and sizing of solar systems due to the enormous computing time associated with it.

Design methods requiring less computing time have been developed to predict mean yearly performance of solar systems and determine the appropriate size of the collector array. Although these methods do not give information on system performance as accurate or as detailed as that provided by detailed computer simulations, they should yield all the necessary annual performance data.

Several design methods are available in the solar energy literature which are usually applicable for specific thermal system configurations and restrictive in the allowable range of variation of the different parameters.

Simplified design procedures that can be used for solar-supplemented active absorption cooling systems are :

(i) The one-repetitive-day simulation methods

(ii) The phibar-f chart empirical correlation method.

Both approaches yield estimates of long-term system performance for a given system configuration and size. Therefore the procedure of system size optimization relies on a search mode.

The one-repetitive-day methods are simplified methods of numerical simulation using fixed increment steps. The closed loop solar system performance is dependent on the collector fluid inlet temperature which is in turn assumed to be equal to the storage temperature. Due to radiation variations from day to day, the storage temperature will vary at any time of the day. However after a transition period of initial transient system operation the storage temperature t_S at a given time of the day will reach a mean level during quasi-steady state

operation. This mean storage temperature will show a repetitive diurnal cyclic variation.

The one-repetitive-day methods attempt to determine the diurnal cycle by an iterative procedure. An initial arbitrary storage temperature is assumed and the solar energy system is then simulated over the day. The following condition is verified :

$$||[t_S(\tau) - t_S(\tau + 24\text{h})]|| \leq \epsilon \tag{8.12}$$

Where ϵ is an error tolerance of recommended magnitude in the range of 0.1-0.5°C for non-stratified storage and in the range of 0.3-1.0°C for storage stratified up to 5 isothermal segments.

If condition (8.11) is not satisfied, the value of t_S at $(\tau + 24\text{h})$ is assumed as the initial value at time τ and the simulation procedure is repeated over another typical day until the condition is satisfied. The reduction in computing time using one-repetitive-day methods is significant as compared to detailed simulations because convergence occurs normally within a few days only.

In conclusion the one-repetitive-day simulation methods involve calculations over representative or specially constructed days and it is necessary to construct a diurnal solar radiation pattern that contains all the statistical information concerning long-term radiation variations. Finally, the system is simulated over repetitive or consecutive days having the same diurnal radiation pattern. An hour-by-hour numerical system simulation procedure is normally recommended. Different ways of construction of the diurnal radiation distribution have been used in solar system simulation using the simplified one-repetitive-day methods. These methods are also versatile design methods which can be applied not only to absorption cooling by solar- supplemented active systems but to any preheat application for any solar thermal system configuration wether closed loop or open loop.

Another type of method which can be used as a simple design tool for solar absorption refrigeration systems is the phibar-f chart method. The monthly average performance of every month of the year is estimated for one specified

combination of system parameters (basically the size of various components).
The phibar-f chart method is similar to the one-repetitive-day simulation procedure in the way of obtaining the optimal system size by a search mode, however it does not involve preparing an appropriate system simulation programme.Comparison with detailed computer programmes have shown that the prediction accuracy of the phibar-f chart method on an annual basis is very good.
The method was developed for closed loop solar thermal system configuration with finite storage and auxiliary heater in parallel (see figure 8.4) which is typical of absorption air-conditioning systems.

Nevertheless, the method was also applied for systems with auxiliary heater in series by use of a modified correlation. Despite some limitations in the range of parameters for which it has been developed, the phibar-f chart design method has been extensively used.
In this investigation of solar absorption cooling systems, the phibar-f chart design method has been chosen to calculate the yearly solar fraction of a standard closed loop solar system because it is a convenient, simple and fairly accurate procedure of predicting solar system thermal performances.
The phibar-f chart method can be described as an empirical correlation approach deduced from combination of the f-chart method and the utilizability concept.
The f-chart method was developed to predict the long term performance of solar space and/or domestic hot water heating systems with daily storage. It consists of a set of three algebraic correlations obtained from several hundreds of detailed hour-by-hour computer simulation runs for several solar system configurations covering a wide range of system parameters.
The f-chart predictions have been checked using the experimental data of several solar heating systems. The f-chart method is applicable only for the design of systems that require a minimum temperature at the load of 20°C (such as space heating loads) and for the design of domestic hot water systems provided the inlet water temperature is between 5 and 20°C and the upper hot water limit is

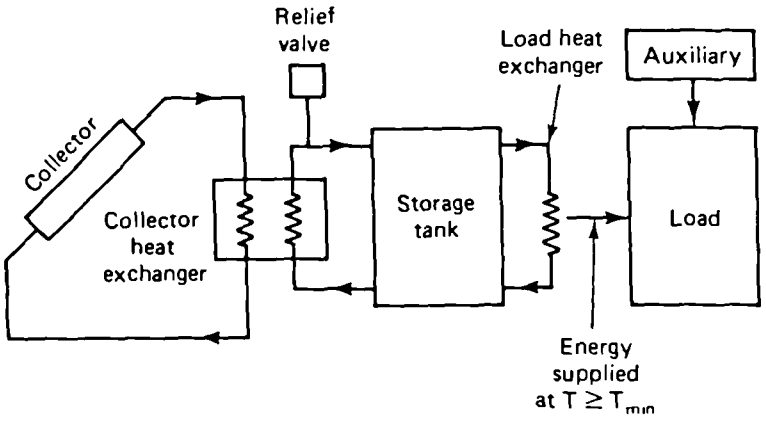

Fig. 8.4 Closed-loop solar energy system

between 50 and 70°C. Obviously the f-chart method cannot be applied to solar absorption cooling systems.

The phibar-f chart method is a generalization of the f-chart method in the sense that there are no restrictions on the temperature limits of hot water in the solar system.

However,the phibar-f chart method is valid only when the following conditions are satisfied :

(i) The thermal load must be constant and uniform over each day and for at least a month

(ii) The energy supply to the load must be above a minimum useful temperature

(iii) There is no conversion efficiency at the load (fluid used for direct thermal application) or alternatively the conversion efficiency is constant

(iv) Energy dumping through the relief valve is negligible and therefore the storage tank is assumed to be pressurized or filled with a liquid having a high boiling point.

A typical application of the phibar-f chart method is for absorption cooling systems where the energy supplied to the load at the generator is constant and maintained above a minimum temperature level for good performance of the absorption chiller.

The basic empirical correlation of the phibar-f chart method for systems with auxiliary heater in parallel is [64] :

$$f_M = Y\bar{\Phi}_K - a[\exp(bf_M) - 1][1 - \exp(cX)] \tag{8.13}$$

Where

f_M is the monthly solar fraction

X, Y are dimensionless variables

$\bar{\Phi}_K$ is the daily utilizability fraction

a, b, c are constants.

The dimensionless variables X and Y are given by

$$X = \frac{A_C F_R U_L \Delta\tau(100^oC)}{Q_{LM}} \tag{8.14}$$

$$Y = \frac{A_C F_R(\overline{\tau_r \alpha})\overline{H_T} N}{Q_{LM}} \tag{8.15}$$

where

A_C collector area (m^2)

F_R collector heat removal factor

U_L collector overall loss coefficient ($W/m^2 -^o C$)

$\Delta\tau$ total number of seconds in the month=3600 x 24 x N

Q_{LM}=monthly total heat load (J)

$\overline{\tau_r \alpha}$–monthly average collector optical efficiency

$\overline{H_T}$ monthly average daily radiation incident on the collector surface per unit area (J/m^2)

N–days in the month

Utilizability is defined as the fraction of the incident solar radiation that can be converted to useful heat by an ideal collector having no optical losses ($\bar{\tau}_r$=1,$\bar{\alpha}$=1) and a perfect heat removal circuit (F_R=1).

The daily utilizability fraction is found from

$$\bar{\Phi}_K = \exp\left([A + B(\frac{\bar{r}_{Tnoon}}{\bar{R}_T})][\bar{X}_{CK} + C\bar{X}_{CK}^2]\right) \tag{8.16}$$

Where

$$A = +7.476 - 20.0\bar{K} + 11.188\bar{K}^2 \tag{8.17a}$$

$$B = -8.562 + 18.679\bar{K} - 9,948\bar{K}^2 \qquad (8.17b)$$

$$C = -0.722 + 2.426\bar{K} + 0.439\bar{K}^2 \qquad (8.17c)$$

and

K is the monthly average clearness index of the atmosphere,

$\bar{X}_{CK}$ the dimensionless critical radiation ratio,

r_{Tnoon} the ratio of radiation at noon on the tilted surface of the collector to that on horizontal surface for the average day of the month,

$\bar{R}_T$ the ratio of the monthly average global radiation on the tilted surface of the collector to that on horizontal surface.

Expressions of $\bar{K}$, $\bar{X}_{CK}$, $\bar{r}_{Tnoon}$, $\bar{R}_T$ and other solar radiation relationships useful in calculations of this chapter are presented in appendix B1.

The empirical correlation of the phibar-f chart method given by equation (8.13) is valid for $0 < X < 20$ and $0 < Y < 1.6$.

The values of the constants a, b, c are given by the following conditions subjected to the time of load operation :

a) For a load operating between 6 a.m. and 6 p.m. every day of the month (7 days per week operation) :

$$a = 0.015[\frac{(MC_P)_S}{A_C \;\; 350\ kj/(m^2 - ^o C)}]^{-0.76} \quad \text{for}$$

$$175 \leq (MC_P)_S/A_C \leq 1400\ kJ/(m^2 - ^o C),$$

$$b = 3.85$$

$$c = -0.15$$

b) For a load operating 24 hours per day over the whole month (7 days per week operation) :

$$a = 0.043 \text{ only for } (MC_P)_S/A_C = 350\ kJ/m^2 - ^o C$$

c) For a load operating 12 hours per day (6 a.m. to 6 p.m.), 5 days per week :

$$a = 0.035 \text{ only for } (MC_P)_S/A_C = 350\ kJ/m^2 - ^oC$$

$$b = 3.18$$

$$c = -0.21$$

For solar systems with auxiliary heater in series the original phibar-f chart correlation (equation 8.13) is modified by introducing a corrective term:

$$f_M = Y\bar{\Phi}_K - a[\exp(bf_M) - 1][1 - \exp(cX)]\exp(-1.959Z) \qquad (8.18)$$

Where

$$Z = Q_{LM}/(M_L C_{PL} \text{ x } 100^oC) \qquad (8.19)$$

and

Q_{LM} is the monthly total heat demanded by the load

M_L the monthly total mass of water used.

8.5 Proposed Solar Thermal System

Figure 8.5 shows schematically a solar-supplemented active absorption refrigeration system with daily storage. The refrigeration cycle itself is the same as that described in chapters 3 and 4.

Flat-plate liquid-based solar collectors are used to absorb and convert solar radiation into useful heat delivered to a transport liquid. Water or an antifreeze solution is used as the heat transfer fluid in the closed collector loop. In freezing climates the collector fluid is kept separate from the storage tank liquid

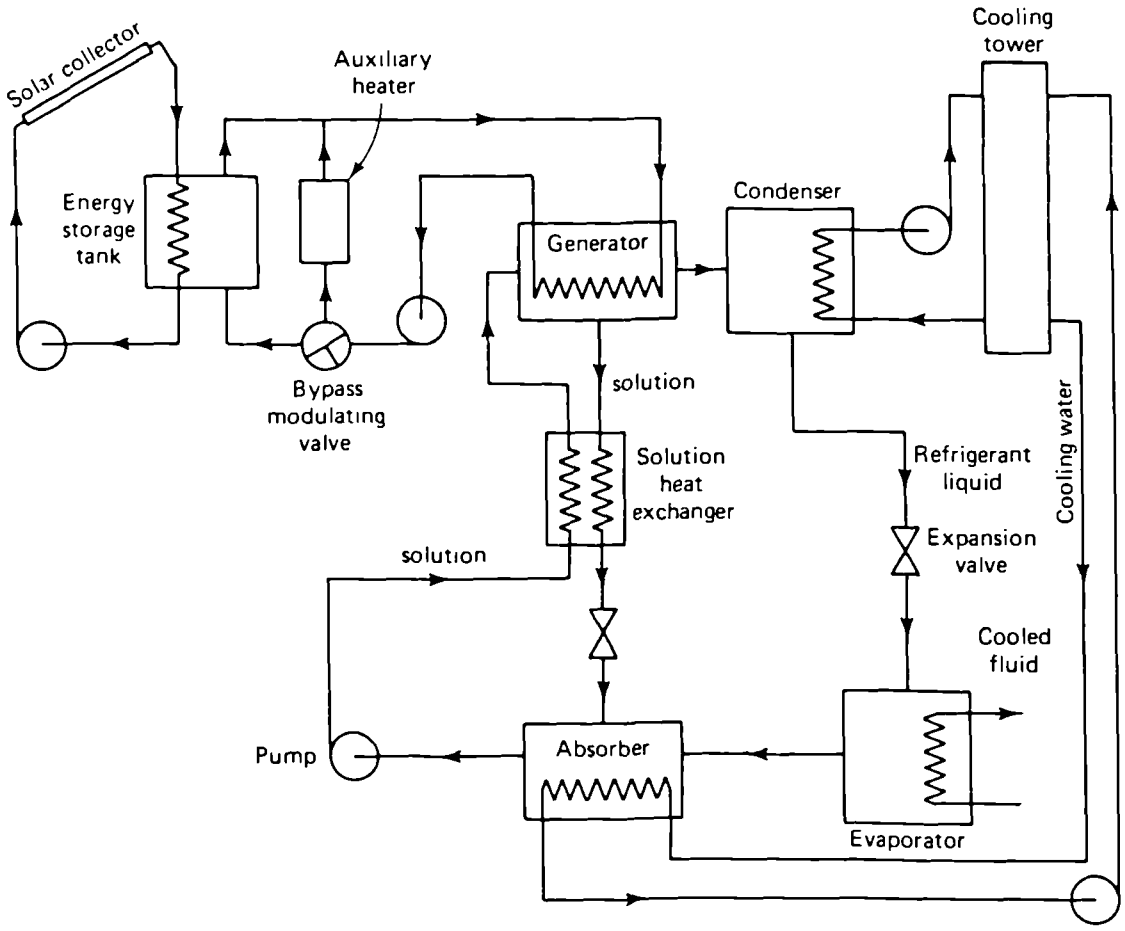

Fig. 8.5 Schematic diagram of a solar-operated absorption refrigeration system with auxiliary heater in parallel

and heat is therefore delivered to the storage through a heat exchanger.
The energy stored in a tank is then supplied to the generator to boil the strong solution. Heat is withdrawn from the storage tank at the top and reinjected at the bottom for reasons of stratification in the storage tank. A bypass valve is incorporated to modulate the flow of the fluid leaving the load when :

(a) the storage temperature is less than the fluid temperature entering the storage tank

(b) the storage temperature is such that the temperature entering the generator is greater than that required by the load.

The auxiliary heater is arranged in parallel with the storage tank. Although solar systems with an all-or-nothing type of auxiliary heater are less efficient than those with auxiliary heater in series (topping-up type), it is noted that in refrigeration loads where the temperature difference $(t_{Li} - t_{Le})$ is of the order of few degrees only, using a system with auxiliary heater in series leads to little benefit in thermal performance over a system with the auxiliary heater in parallel.
In the design of solar energy systems,the principal parameters are :

(a) collector type (specified by its performance factors)
(b) collector area
(c) storage volume per unit collector area.

the secondary design parameters are :

(a) collector array configuration
(b) storage tank configuration
(c) collector heat exchanger size
(e) fluid flowrate through collectors
(f) insulation of storage tank and piping.

Some design recommendations of variable system parameters are :

(1) collector type and performance such that collector efficiency is at least 0.5

(2) collector flowrate is between 30-60 kg/(h-m^2) of collector area

(3) collector slope is equal to latitude $\pm 10°$ and collector is equator-orientated but $\pm 15°$ is admissible

(4) storage capacity is between 0-200 kg/m^2 of collector area

(5) storage tank configuration is cylindrical with ratio of length by diameter $\frac{L}{D}$ from 1.0 to 2.0

(6) collector heat exchanger effectiveness (ratio of actual heat transfer rate by maximum possible heat transfer rate) is 0.85 to 0.95

(7) insulation of thermal conductance between 0.25 and 0.5 W/m^2-°C for the storage tank and equal to 0.5 W/m^2-°C for piping.

The principal aim of this study is to use the phibar-f chart method for the design of solar absorption refrigeration units such as the one shown schematically in figure 8.5. The long-term performance of the solar system is estimated for different collector areas and times of load operation. The determination of the optimal size of the solar system is usually decided on economic analysis.
a computer programme of the phibar-f chart method is prepared to calculate the yearly solar fraction of a solar thermal sytem with auxiliary heater in parallel. The programme is based on the following computational steps adapted from the procedure presented in the literature [64].
0. Input data.

(a) Location specific parameters (for a particular month) :

(i) latitude (L);

(ii) monthly mean daily global horizontal radiation $\bar{H}_T$,

(iii) monthly mean ambient temperature $\bar{t}_o$

(iv) ground surface albedo ρ.

(b) Thermal load parameters (for a particular month) :

(i) time of load operation;

(ii) thermal power P_L required by load;

(iii) minimum temperature level t_{min};

(iv) environment temperature t_{env} (temperature of air surrounding the storage tank to which heat losses will occur).

(c) Solar thermal system specific parameters:

(i) collector surface area A_C;

(ii)collector performance parameters $F_R U_L$ and $F_R\overline{\tau_r\alpha}$;

(iii) monthly mean collector incidence angle modifier $\bar{K}_n$;

(iv) collector surface tilt angle β,

(v) heat capacitance of storage per unit collector area $(MC_P)_S/A_C$;

(vi) storage overall heat loss coefficient $(UA)_S$;

1. Calculate the monthly total heat load Q_{LM}
2. Calculate $\bar{H}_T$ from expression in appendix B1
3. Calculate X from equation (8.14)
4. Calculate Y from equation (8.15)
5. Assume $\bar{t}_{S1} = t_{min}$ where $\bar{t}_{S1}$=monthly mean storage temperature
6. Assume $\bar{t}_{Ci} = \bar{t}_{S1}$ where $\bar{t}_{Ci}$=monthly mean fluid temperature inlet to the solar collector
7. Calculate $\bar{X}_{CK}$ from equation in appendix B1
8. Calculate $\bar{\Phi}$ from equation (8.16)
9. Compute the monthly solar fraction f_{M1} from equation (8.13) using any appropriate iterative procedure

10. Recalculate the utilizability fraction from

$$\bar{\Phi}_K = f_{M1}/Y$$

11. Calculate the new monthly mean storage temperature $\bar{t}_{S2}$ from

$$\bar{t}_{S2} = \bar{t}_{S1} + g[\exp(4.702\ f_{M1}) - 1][\exp(-4.002Z)] \tag{8.20}$$

where

$$g = 0.2136\left[\frac{(MC_P)_S}{A_C\ 350\ kj/(m^2 - ^\circ C)}\right]^{-0.704} \tag{8.20}$$

and Z is given by equation (8.19).

12. Calculate the monthly total heat losses from the storage tank

$$Q_{WM} = (UA)_S(\bar{t}_{S2} - t_{env})\Delta\tau \tag{8.22}$$

13. Proceed to next month.

In the developed computer programme, two successive loop iterations are used to calculate the solar fraction for the twelve months of the year and for different collector areas. An iterative solution is required for the solar fraction f_M in equation (8.13). Therefore, a procedure using the PICARD method [65] was included in the computer programme to solve equation (8.13) for f_M.

An arbitrary initial value of f_M of 0.01 was chosen as required by the iterative method and calculation performed until convergent solutions are obtained.

Numerical results have been obtained for the performance of a solar thermal system supplying hot water to an absorption refrigeration unit operating 24 hours per day (7 days per week) and requiring a thermal power of 6.2 kW at a minimum temperature of 80°C.A generator heat input of 6.2 kW results in a refrigeration capacity of approximately 4 kW in residential-size absorption chillers for solar cooling.

The values assigned to the flat plate collector performance parameters were such that $F_R U_L$=4.52 W/(m^2−°C) and $F_R(\overline{\tau_r \alpha})_n$=0.72.

The collector is assumed to be equator-facing and tilted at an angle equal to latitude.

The hot water storage capacity per unit collector area has been taken as 350 kJ/(m^2−°C). Heat losses from the storage tank have been accounted for and an overall heat loss coefficient of 2.0 W/°C has been assumed.

The yearly solar fraction was calculated from equation (8.7) where Q_{UM} is found from

$$Q_{UM} = f_M \times Q_{LM}$$

The solar radiation and air temperature data were estimated for the location of Constantine (Algeria) as follows.

The monthly mean daily global radiation $\bar{H}$ on a horizontal surface was determined from maps of solar radiation [66].

The sunset hour angle W_S was calculated for each month from equation B.1.14 in appendix B1.

Values of day of year n (from appendix B1) and number of days N in each month were assigned.

The monthly average temperature was obtained from values of monthly maximum and monthly minimum temperatures [67].

The input data for running performance tests are summarized in tables 8.1 and 8.2.

The computer programme is listed in appendix B2.

table 8.3 gives the month-by-month results of simulating the solar thermal system specified in figure 8.5 over the year using the phibar-f chart method.

The monthly solar fraction varies drastically from summer to winter for all solar collectors areas. This variation can be attributed to the large fluctuations of the

Table 8.1 Solar radiation and meteorological input data for Constantine(Algeria)

Month	$\bar{H}$ (Mj/sq.m-d)	n	N	$\bar{to}$ (deg.C)	Ws (deg.)
Jan.	08.36	17	31	08.00	73.66
Feb.	12.54	47	28	09.10	80.26
Mar.	16.72	75	31	12.00	88.22
Apr.	18.81	105	30	14.90	97.00
May	25.08	135	31	18.20	104.50
Jun.	25.08	162	30	22.80	108.30
Jul.	27.17	198	31	25.70	106.50
Aug.	25.08	228	31	25.80	100.00
Sep.	20.90	258	30	22.80	91.60
Oct.	12.54	288	31	17.25	82.85
Nov.	10.45	318	30	12.60	75.40
Dec.	08.36	344	31	08.90	71.75

Table 8.2 Input parameters for solar cooling system

Flat-plate collector	FR = 0.95
	$(\tau\alpha)n$ = 0.76
	Ul = 4.75 W/sq.m-C
	Slope β = 36.3
	tci = 80 deg.C
Storage tank	(MCp)/Ac = 350 Kj/sqm-C
	UA = 2.0 W/C
	tmin = 80 deg.C
Load	Qgen = 6.2 Kw
	tmin = 80 deg.C

Table 8.3 results of computer simulation of a closed-loop solar thermal system for absorption cooling.

FOR END-USE LOAD WORKING 24 HRS PER DAY (7 DAYS PER WEEK OPERATION)

£ For Ac (collector area) equal to 12.00 square meters

H (Mj/sqm day)	To (deg.C)	K	Qlm (Mj/month)	Qsolarm (Mj/month)	FM	NewFM
8.36	8.00	0.479	16632.86	-317.26	0.0041	-0.0191
12.54	9.10	0.555	15023.23	190.84	0.0355	0.0127
16.72	12.00	0.576	16632.86	529.38	0.0537	0.0318
18.81	14.90	0.529	16096.32	368.18	0.0439	0.0229
25.08	18.20	0.628	16632.86	1034.63	0.0821	0.0622
25.08	22.80	0.602	16096.32	944.24	0.0771	0.0587
27.17	25.70	0.668	16632.86	1635.44	0.1159	0.0983
25.08	25.80	0.675	16632.86	1864.63	0.1296	0.1121
20.90	22.80	0.667	16096.32	1635.19	0.1201	0.1016
12.54	17.25	0.513	16632.86	238.38	0.0346	0.0143
10.45	12.60	0.561	16096.32	186.11	0.0333	0.0116
8.36	8.90	0.522	16632.86	-197.23	0.0110	-0.0119

Yearly solar fraction = 4.14%

£ For Ac (collector area) equal to 18.00 square meters

H (Mj/sqm day)	to (deg.C)	K	Qlm (Mj/month)	Qsolarm (Mj/month)	FM	NewFM
8.36	8.00	0.479	16632.86	58.86	0.0267	0.0035
12.54	9.10	0.555	15023.23	762.18	0.0736	0.0507
16.72	12.00	0.576	16632.86	1310.20	0.1007	0.0788
18.81	14.90	0.529	16096.32	1045.84	0.0860	0.0650
25.08	18.20	0.628	16632.86	2046.55	0.1430	0.1230
25.08	22.80	0.602	16096.32	1883.94	0.1355	0.1170
27.17	25.70	0.668	16632.86	2921.37	0.1932	0.1756
25.08	25.80	0.675	16632.86	3262.18	0.2137	0.1961
20.90	22.80	0.667	16096.32	2912.63	0.1995	0.1809
12.54	17.25	0.513	16632.86	862.81	0.0721	0.0519
10.45	12.60	0.561	16096.32	780.36	0.0702	0.0485
8.36	8.90	0.522	16632.86	235.45	0.0371	0.0142

Yearly solar fraction = 9.23%

Table 8.3 Continued.

£ For Ac (collector area) equal to 24.00 square meters

H (Mj/sqm day)	to (deg.C)	K	Qlm (Mj/month)	Qsolarm (Mj/month)	FM	NewFM
8.36	8.00	0.479	16632.86	427.21	0.0489	0.0257
12.54	9.10	0.555	15023.23	1324.10	0.1110	0.0881
16.72	12.00	0.576	16632.86	2096.37	0.1480	0.1260
18.81	14.90	0.529	16096.32	1729.12	0.1284	0.1074
25.08	18.20	0.628	16632.86	3062.16	0.2041	0.1841
25.08	22.80	0.602	16096.32	2827.53	0.1942	0.1757
27.17	25.70	0.668	16632.86	4208.52	0.2707	0.2530
25.08	25.80	0.675	16632.86	4659.74	0.2978	0.2802
20.90	22.80	0.667	16096.32	4190.89	0.2790	0.2604
12.54	17.25	0.513	16632.86	1476.91	0.1090	0.0888
10.45	12.60	0.561	16096.32	1364.72	0.1065	0.0848
8.36	8.90	0.522	16632.86	659.82	0.0626	0.0397

Yearly solar fraction = 14.31%

£ For Ac (collector area) equal to 30.00 square meters

H (Mj/sqm day)	to (deg.C)	K	Qlm (Mj/month)	Qsolarm (Mj/month)	FM	NewFM
8.36	8.00	0.479	16632.86	806.40	0.0717	0.0485
12.54	9.10	0.555	15023.23	1895.94	0.1491	0.1262
16.72	12.00	0.576	16632.86	2858.23	0.1938	0.1718
18.81	14.90	0.529	16096.32	2390.01	0.1695	0.1485
25.08	18.20	0.628	16632.86	4049.66	0.2635	0.2435
25.08	22.80	0.602	16096.32	3744.63	0.2512	0.2326
27.17	25.70	0.668	16632.86	5461.92	0.3461	0.3284
25.08	25.80	0.675	16632.86	6020.88	0.3798	0.3620
20.90	22.80	0.667	16096.32	5435.73	0.3564	0.3377
12.54	17.25	0.513	16632.86	2101.98	0.1467	0.1264
10.45	12.60	0.561	16096.32	1959.71	0.1435	0.1217
8.36	8.90	0.522	16632.86	1095.10	0.0888	0.0658

Yearly solar fraction = 19.31%

Table 8.3 Continued.

£ For Ac (collector area) equal to 36.00 square meters

H (Mj/sqm day)	to (deg.C)	K	Qlm (Mj/month)	Qsolarm (Mj/month)	FM	NewFM
8.36	8.00	0.479	16632.86	1164.96	0.0933	0.070(
12.54	9.10	0.555	15023.23	2445.78	0.1857	0.162{
16.72	12.00	0.576	16632.86	3610.61	0.2391	0.2171
18.81	14.90	0.529	16096.32	3042.68	0.2101	0.1890
25.08	18.20	0.628	16632.86	5024.10	0.3222	0.3021
25.08	22.80	0.602	16096.32	4649.78	0.3075	0.2889
27.17	25.70	0.668	16632.86	6696.49	0.4205	0.4026
25.08	25.80	0.675	16632.86	7360.27	0.4605	0.4425
20.90	22.80	0.667	16096.32	6661.52	0.4327	0.4139
12.54	17.25	0.513	16632.86	2702.85	0.1828	0.1625
10.45	12.60	0.561	16096.32	2531.44	0.1791	0.1573
8.36	8.90	0.522	16632.86	1509.02	0.1137	0.0907

Yearly solar fraction = 24.20%

£ For Ac (collector area) equal to 42.00 square meters

H (Mj/sqm day)	to (deg.C)	K	Qlm (Mj/month)	Qsolarm (Mj/month)	FM	NewFM
8.36	8.00	0.479	16632.86	1518.82	0.1146	0.091:
12.54	9.10	0.555	15023.23	2989.31	0.2219	0.199(
16.72	12.00	0.576	16632.86	4354.02	0.2839	0.261{
18.81	14.90	0.529	16096.32	3687.77	0.2502	0.2291
25.08	18.20	0.628	16632.86	5985.39	0.3801	0.359:
25.08	22.80	0.602	16096.32	5543.02	0.3631	0.344{
27.17	25.70	0.668	16632.86	7910.75	0.4937	0.475(
25.08	25.80	0.675	16632.86	8675.59	0.5398	0.521(
20.90	22.80	0.667	16096.32	7866.60	0.5078	0.488:
12.54	17.25	0.513	16632.86	3296.81	0.2185	0.198:
10.45	12.60	0.561	16096.32	3096.60	0.2142	0.192{
8.36	8.90	0.522	16632.86	1917.84	0.1383	0.115:

Yearly solar fraction = 29.03%

Table 8.3 Continued.

£ For Ac (collector area) equal to 48.00 square meters

H (Mj/sqm day)	to (deg.C)	K	Qlm (Mj/month)	Qsolarm (Mj/month)	FM	NewFM
8.36	8.00	0.479	16632.86	1868.61	0.1356	0.1123
12.54	9.10	0.555	15023.23	3526.92	0.2578	0.2348
16.72	12.00	0.576	16632.86	5088.65	0.3281	0.3059
18.81	14.90	0.529	16096.32	4325.62	0.2899	0.2687
25.08	18.20	0.628	16632.86	6932.95	0.4372	0.4168
25.08	22.80	0.602	16096.32	6423.97	0.4179	0.3991
27.17	25.70	0.668	16632.86	9102.48	0.5656	0.5473
25.08	25.80	0.675	16632.86	9963.68	0.6177	0.5990
20.90	22.80	0.667	16096.32	9048.56	0.5816	0.5622
12.54	17.25	0.513	16632.86	3884.33	0.2539	0.2335
10.45	12.60	0.561	16096.32	3655.65	0.2490	0.2271
8.36	8.90	0.522	16632.86	2322.19	0.1626	0.1396

Yearly solar fraction = 33.77%

monthly radiation ($\bar{H}_T$) for the location of Constantine (L=36°22'N) and to the variation of the ambient temperature.

Nevertheless the solar system can supply as much as 33.8% of the yearly thermal load if a collector area of 48 m^2 is used.

In table 8.3 Q_{solarm} is the monthly energy delivered to the load by the solar system, FM is the solar fraction when there are no heat losses from the storage tank,and newFM is the monthly solar fraction when heat losses from the storage are accounted for.

For collectors areas above 48 m^2, the dimensionless variable Y is outside its allowable range and therefore the correlation cannot be used to predict accurately the system performance. The phibar-f chart method is however a very useful procedure of computing the solar fraction of absorption refrigeration systems operated by solar energy for the location of Constantine (Algeria).

It has not been intended to make a parameteric study on the system by varying the storage size, the load operating conditions and the solar collector performance parameters $F_R U_L$ and $F_R(\tau_r\alpha)_n$. The constructed technique to simulate the system was checked and the results show that the phibar-f chart method is indeed a convenient and simple way of predicting the thermal performance of active solar cooling systems. The determination of the optimal size of such solar thermal units remains dictated by economic considerations.

8.6 Conclusion

In this chapter, detailed classification of solar thermal systems has been presented. Solar-operated absorption refrigeration systems have been described and system components have been mathematically modelled. A description of solar L_iB_r-water absorption cooling units has been considered.

Two simplified design methodologies of solar-supplemented active absorption cooling systems have been discussed. The first method involves simulating the solar system over certain representative or specially constructed days from which the long-term system performance could be predicted. The second method uses

the phibar-f chart procedure to determine the yearly fraction of the total energy required by the load which is supplied by the solar system.

A computer programme of the phibar-f chart method is prepared which prints out the annual solar fraction of a solar system with storage for supplying heat to an absorption cooling unit requiring year-round thermal energy . Results of simulating a solar thermal system for operation in the location of Constantine (Algeria) are given.

CHAPTER NINE

CONCLUSIONS

An absorption refrigeration cycle employing a lithium bromide-water solution as the working fluid has been investigated in this work. Solar thermal systems providing a low temperature heat source for absorption cooling units have been also examined.

At first, theoretical absorption refrigeration systems were described and fully analysed using both the first law and the second law of thermodynamics. An aqueous L_iB_r absorption cooling cycle, with hot water as a heat source and cooling water as a heat sink, was then modelled and optimized. The optimisation study of the cycle was made made in relation to the parameter of solution heat exchanger effectiveness, and operating temperatures of the generator, condenser, absorber and evaporator as well as to the temperatures of the environment and the external fluids (hot water, cooling water and chilled water). To accomplish this objective, two computer programmes were developed to calculate a cycle thermodynamic efficiency based on the lost work concept.

The results of this study were then used to fix a practical thermodynamic cycle of operation. This, in conjunction with mass and energy balances, enabled the calculation of the heat transfer areas in the cycle components from appropriate heat transfer coefficients available in the literature.As a result the generator, condenser, evaporator, absorber and solution heat exchanger cycle components have been designed.

The mechanical design of an experimental absorption refrigeration rig was then carried out and the fabrication of system heat exchangers and vessels was described.

The steady-state operation of the experimental rig has been investigated to verify the mathematical model.

Finally, a review of solar thermal systems for absorption cooling has been presented and recent design methodologies have been discussed. The phibar-f chart

procedure was used to prepare a computer programme relevant to simulation and sizing studies of solar thermal systems for application with absorption refrigeration units. Numerical results have been obtained for the performance of a solar energy system supplying heat to an absorption refrigeration unit operating 24 hours per day, 7 days per week in the location of Constantine (Algeria).

Based on the results of the investigations performed in this study, the concluding remarks are as follows. Absorption refrigeration cycles can be analysed and modelled by using the second law of thermodynamics. The thermodynamic efficiency based on the lost work concept,as used in this research , is a simple way of evaluating the energy usage of absorption cooling cycles. It indicates how much heat can be removed from the cooling load by an actual absorption refrigeration process compared to the quantity of heat that would be removed by a totally reversible absorption cycle accepting heating and cooling inputs at the same temperature levels.

Computer calculations of such a thermodynamic efficiency are easily made and the results of its parameteric variation for a L_iB_r-water cooling cycle show that there are many ways at hand for designing an improved and more efficient cycle. The different modifications which can be made to reduce the system lost work and increase the second law efficiency have been discused in chapter 4.

The findings of the theoretical evaluation of L_iB_r-water absorption refrigeration cycles have been used to define a practical thermodynamic cycle operation. Design of an improved laboratory refrigeration system was made using conventional heat exchangers design methods.

After fabrication of the experimental rig with traditional drilling, cutting and welding techniques it was found that hermeticity of L_iB_r-water absorption units is difficult to achieve in the laboratory unless special care is taken in the design of static seals and in the machining of grooves which receive the seals. Mechanical design of L_iB_r-water absorption cooling units remains a formidable and important task to fulfill if desired system operation and performance are to be attained.

In consequence of this major problem of hermeticity and other minor difficul-

ties highlighted in chapter 7, no reliable and final experimental results were obtained to verify the relevance of the theoretical model. The elimination of these failure modes must be undertaken in order to fully establish the feasibility of the proposed design method of absorption refrigeration cycles. Based on the theoretical investigation of solar thermal systems for absorption cooling, the following conclusions are drawn :

(a) design and optimization of solar cooling systems can be made using simplified procedures of predicting the total annual solar fraction.

(b) The phibar-f chart method of design of solar thermal systems for absorption cooling applications requires less computational effort, is very simple to use and yields estimates of long-term system performance.

(c) Versatile computer programmes of the phibar-f chart method can be prepared which print out the annual performance of a solar system with storage supplying heat to an absorption refrigeration unit.

(d) Numerical performance tests were carried out for a solar absorption cooling system operating in Constantine (Algeria) and the results showed that the solar system can contribute effectively to the supply of heat to the refrigeration load.

CHAPTER TEN

RECOMMENDATIONS

The recommendations for the improvement of rig apparatus and for future research work are as follows.

(1) During operation of the experimental rig, the pressure rise in the vessels containing the heat exchangers coils was a limitation to reach stable conditions. This was due to external leaks into the system through the gasketed parts and the instrumentation used to make internal measurements.
The gaskets sealing the removable frontal plates of the vessels were made from silicone rubber and placed in grooves cut in the rubber back cover of the frontal plates. Perhaps the most necessary modifications are to be achieved in this area by using more reliable seals and machining the flanged surfaces.
The modifications required to eliminate the problem of leaks have been discussed in chapter 7. The entire L_iB_r-water solution and water refrigerant circuits being hermetically sealed, it would be preferable to make external measurements only. Efforts are to be made for the supply of proper flowrates (at the desired temperatures) of hot water and cooling water to the absorption unit.

(2) Further work is required in order to verify the results of the theoretical analysis and optimisation of a L_iB_r-water absorption refrigeration system. It would be necessary to carry out tests with the experimental rig after it has been modified for elimination of external leaks and other known failure modes. Experimental data need to be accumulated and used to calculate system capacity, COP, second law efficiency, heat fluxes and heat transfer coefficients in the various components.

(3) Research needs to be done to try to reduce the temperature differences between the internal and external fluids in the absorption cycle without considerable increase in heat transfer areas and/or in mass flowrates.

Cycle efficiency will be greatly improved as shown by the results of the optimisation study.

(4) Consideration should be given to the application of analysis and optimisation through lost work not only to the absorption refrigeration cycle but also to the streams of external fluids (hot water, cooling water and possibly chilled water). These are not free sources and sinks and therefore should be utilized with an improved and efficient operation.

(5) Further theoretical and practical research is necessary to develop new absorption refrigeration units with high efficiencies. Innovative heat transfer configurations should be conceived and proven. Description of basic design rules which allow to achieve high efficiencies should be included. Reduction in size of heat exchangers is to be examined.

(6) Solar thermal systems for absorption refrgeration can be designed by the phibar-f chart method, the one-repetitive-day simulation approach, or by one of the several solar simulation programmes that have been developed for the design and analysis of cooling systems. These latter are however very sophisticated programmes, expensive to operate and need extensive input data. Therefore simplified procedures such as the phibar-f chart correlation method are much needed for developing simple simulation programmes.
The phibar-f chart method offers a convenient, simple and fairly accurate mean of predicting the long-term performance of solar thermal systems. It is nevertheless restrictive in system configuration and in the allowable range of variation of the different parameters. Hence, additional empirical correlations are needed.

(7) Analysis of solar thermal systems can also be based on the second law of thermodynamics. This is an area where further research is being carried out by scientists. It would be beneficial to examine the operation of solar cooling systems with regard to the second law in general and to the lost work approach in particular.

REFERENCES

1. K P Tyagi : "Ammonia-salts vapour absorption refrigeration systems", *J Heat Recovery Syst*, vol 4 n 6 1984 p 427-431.

2. K P Tyagi and K S Rao : "Choice of absorbent-refrigerant mixtures", *Int J Energy Res*, vol 8 n 4 Oct-Dec 1984 p 361-368.

3. C A Infante-Ferreira : "Thermodynamic and physical property data equations for ammonia-lithium nitrate and ammonia-sodium thiocyanate solutions", *Sol Energy*, vol 32 n 2 1984 p 231-236.

4. K P Tyagi : "Comparison of binary mixtures for vapour absorption refrigeration systems", *J Heat Recovery Syst*, vol 3 n 5 1983 p 421-429.

5. G A Mansoori and V Patel : "Thermodynamic basis for the choice of working fluids for solar absorption cooling systems", *Sol Energy*, vol 22 n 6 1979, , p 483-491.

6. C F Kettleborough : "Solar-assisted comfort conditioning", *Mech Eng*, vol 105 n 12 Dec 1983 p 48-55.

7. W C Dickinson and P N Cheremisinoff, editors : "Solar energy technology handbook", part B Applications, Systems Design, and Economics Marcel Dekker, Inc. 1980 ch 30, 42

8. P Krusi and R Schmid : "A critical review of solar absorption air conditioning", *Australian Refrigeration, air conditioning and heating*, vol 35 part 3 March 1981 p 12-19.

9. G Grossman, J R Bourne, J Ben-Dror, Y Kimchi, I Vardi : "Design improvements in lithium bromide absorption chillers for solar applications",

J Sol Energy Eng., vol 103 Feb 1981 p 56-61.

10. R Lazzarin, E Rizzon, M Sourano, B Boldrin, G Scalabrin : "Performance predictions of a lithium bromide utilizing solar energy", *Sun, proceedings of the international solar energy congress*, New Delhi, India, January 1978. Vol 3, p 1572-1580 Pergamon.

11. ASHRAE handbook and product directory, "1977 Fundamentals volume".

12. W B Gosney : "Principles of refrigeration", Cambridge University Press, 1982 ch 6.

13. W F Stoecker and J W Jones : "Refrigeration and air conditioning ", 2nd edition, Mc Graw-Hill Book company 1982, ch 7, 12, 17.

14. J L Threlkeld : "Thermal environmental engineering, 2nd edition Prentice-Hall, Inc., 1970, p 103-115.

15. D Van Hatten and P Actis Dato : "Description and performance of an active solar cooling system using a lithium bromide-water absorption machine" , *Energy and Buildings*, vol 3 1981 p 169-196.

16. R H Perry and CH Chilton : "Chemical engineer's Handbook", 5th edition, Mc Graw-Hill Book cie, 1973, ch 12.

17. L M Rozenfeld and M S Karnaukh : "Analysis of actual processes in a lithium bromide absorption machine", *Proceedings of the 11th International Congress of Refrigeration* , Munich.P 653-657.

18. L A McNeely : "Thermodynamic properties of aqueous solutions of lithium bromide", *ASHRAE Transactions*, part 1, 1979, p 413-434.

19. N G Schmuilov and L M Rozenfeld : "Typical features of the design and optimization of L_iB_r absorption refrigerating machines", *Chem Pet Eng* vol 19 n 11-12 Nov-Dec 1983 p 514-519 Plenum Publishing corporation, 1984 p 514-518.

20. S B Gosh and G P Gupta : "Design of a solar energy operated L_iB_r-water absorption refrigeration system for refrigeration storage", *Sun, proceedings of the international solar energy congress*, New Delhi, India. Vol 3 January 1978 p 1997-2000.

21. V Y Nakoryakov and N I Girgor'yeva : "Combined heat and mass transfer in film absorption", *Heat Transfer-Soviet Research*, vol 12 n 3 1980 p 111-117.

22. V Y Nakoryakov, N S Bufetov, N I Grigor'yeva : "Heat and mass transfer in film absorption", *Fluid Mechanics-Soviet Research*, vol 11 n 3 May-June 1982 p 97-115.

23. R Chang, J A Duffie and G O G LOF : "A study of a solar air conditioner", *Mech Eng* , n 85 1963 p 31.

24. N R Sheridan : "Performance of the Brisbane solar house", it Solar energy, n 12 1952 p 395.

25. J C V Chinnappa : "Utilization of solar energy for space cooling : a review", *Int solar building Technology conference*, Royal Institute of British Architects, 25th-29th July, 1977, London.

26. S A Klein, P I Cooper, T L Freeman, D M Beeckman, W A Beckman, J A Duffie : "TRNSYS : A transient simulation program", *Solar energy*, vol 17 1975 p 29.

27. C B Winn, G R Johnson, T E Corder : "SIMSHAC : A Simulation programme for solar heating and cooling of buildings", *Journal of simulation*, n 165 1976.

28. Holmstead "Solsem and Martine Marietta Interactive thermal analysis system-user manual", Engin. Dept technical manual, Martin Marietta corp., Denver, 1976.

29. "An introduction to SOLCOST", ERDA, division of solar energy technology transfer, washington DC, june 1977.

30. S A K lein and W A Beckman : "A general design method for closed-loop solar energy systems", *Sol energy* vol 22 1979 p 269-282.

31. J A Duffie and W A Beckman : "Solar engineering of thermal processes", Wiley interscience, 1980.

32. M M El Sayed, I S Taha, M A Darwish : "Computer simulation of solar cooling", *Fundamentals and application of solar energy, AIChE Symposium series*, part 2 n 210 vol 77 1981 p 86-96. ch 2.33. D C Anand , R W Allen, B Kumar : "Transient simulation of absorption machines", *J sol energy engin*, vol 104 August 1982 p197-203.

34. H Perez-Blanco and R Radeemacher : "Absorption : an update", *ASHRAE J*, Nov 1986 p 25-26.

35. R W Haywood : "A critical review of the theorems of thermodynamic availability, with concise formulations Part 1 Availability", *J Mech Engin science*, vol 16 n 3 1974 p 160-173.

36. J E Ahern : "The exergy method of energy systems analysis", Aerojet Electrosystem cie, John-Wiley and sons 1980.

37. A Bejan : "Second law analysis in heat transfer and thermal design", *Advances in heat transfer*, vol 15, Academic Press Inc 1982.

38. W F Kenney : "Energy conservation in the process industries", Academic Press Inc 1984 ch 2.

39. F Bosnyakovic and P L Blackshear jr : "Technical thermodynamics ", 3rd edition Holt, Rinehart and Winston 1965.

40. C S Peng and J R Howell : "Analysis and design of hybrid double-absorption cooling systems for low grade thermal energy applications", *J sol energy engin*, vol 103 Nov 1981 p 331-338.

41. N De Nevers and J Seader : "Lost work : A measure of thermodynamic efficiency", *Energy*, Pergamon Press Ltd vol 5 1980 p 757-768.

42. S W Briggs : "Second law analysis of absorption refrigeration", *Proc AGA and IST conference on natural gas research and technology*, Chicago 1971 paper V 4.

43. Y El Sayed : "Minimum and optimum lost work in solar cooling systems", *Meeting on second law and irreversibility considerations in solar cooling*, Washington DC May 9-10 1983.

44. L London : "Identifying irreversibilities in solar absorption systems", *Meeting on second law and irreversibility considerations in solar cooling*, Washington DC May 9-10 1983.

45. M Wahlig : "Analysis and experiments on advanced absorption cycles", *Meeting on second law and irreversibility considerations in solar cooling*, Washington Dc May 9-10 1983.

46. D K Anand et al. : "Second law analysis of solar powered absorption cooling cycles and systems", *J sol energy engin* , vol 106 August 1984 p 291-298.

47. G J Van Wylen and R E Sonntag : "Fundamentals of classical thermodynamics", SI version, 2nd revised printing, John Wiley and sons Inc 1976 ch 7.

48. R L Akan and R J Schoenhals : "The second law efficiency of a heat pump system", *Energy*, Pergamon Press Ltd, vol 5 1980 p 583-663.

49. J F Kreider : "Medium and high temperature solar processes", Academic Press Inc, 1979 p 66.

50. M L Warren and M Wahlig : "Cost and performance goals for commercial active solar absorption cooling systems", *J sol energy engin*, vol 107 May 1985 p 136-140.

51. J L Lando et al. : "Solar powered environment control criteria and realization", *Proc Int sol energy conf*, Atlanta, GA, vol 1 May 1979 p 720-724.

52. W Bessler and C N Shen : "Study on parameter variations for solar powered lithium bromide absorption cooling", *IECEC 75 Record* p 178-185.

53. F Mc Quiston and J D Parker : "Heating, ventilating, and air conditioning : analysis and design", Wiley 1977.

54. R Planck : "Handbuch der Kaltetechnik", Springler-Verlag, Berlin, vol 7 1959 p 145.

55. A J Chapman : "Heat transfer", 3rd edition, Mc Millan publishing co, Inc 1974 ch 8, 12.

56. J J Lorenz and D Yung : "A note on combined boiling and evaporation of liquid films on horizontal tubes", *J heat transfer*, vol 101 Feb 1979 p 178-180.

57. D Yung et al. : "Vapor/liquid interaction and entrainment in falling film evaporators", *J heat transfer*, vol 102 Feb 1980 p 20-24.

58. J P Holman : "Heat transfer", 6th edition, Mc Graw hill book cie 1986 ch 6, 9, 10.

59. D Q Kern : "Process heat transfer", 23rd printing, Mc Graw hill Intern book cie 1986 ch 6, 20.

60. N P Chopey editor, T G Hicks series editor : "Handbook of chemical engineering calculations", Mc Graw hill book cie 1984 ch 7 p 64.

61. A Roth : "Vacuum sealing techniques", Pergamon Press 1966 ch 1 , 2, 3.

62. ASHRAE standard 41-66 part 1 : "Standard measurements guide : section on temperature measurements", p 8-10.

63. A Guthrie : "Vacuum technology", John Wiley and sons, Inc 1963 ch 9, 15.

64. T A Reddy : "The design and sizing of active solar thermal systems", Clarendon Press, Oxford 1987 ch 7.

65. G B Thomas jr and R L Finney : "Calculus and analytical geometry", 6th edition, Addison-welsey Publishing cie, 1984 p 171.

66. B De Jong : "Net radiation received by a horizontal surface at the earth", Delft University press 1973, Rotterdam, the Netherlands maps 14-25.

67. "Tables of temperature, relative humidity, precipitation and sunshine for the world", part 4 Africa, the atlantic ocean south of 35°N and the indian ocean. Meteorological office, 1983 p 3.

APPENDIX A1

COMPUTER PROGRAMME FOR CALCULATION OF EFFICIENCY AS A FUNCTION OF CYCLE INTERNAL PARAMETERS

```
**************************************************************
* PROGRAM calcul (input, output);
(*This program calculates the thermodynamic efficiency of a
  LiBr-water absorption refrigeration cycle as a function of
  the generator, absorber, condenser, evaporator, temperatures
  and the solution heat exchanger effectiveness for
  ambient temperatures of 25 and 30 deg.C.*)
**************************************************************
*
*
* CONST
*
*   A = - 2.00755;  B = 0.16976; C = - 3.13336E-3;
*   D = 1.97668E-5; E = 124.937; F = - 7.7165;
*   G = 0.152286;   H = -7.9509E-4; S = 2;  vv = 64.90;
*
* VAR
*
*   v : ARRAY [0..2,0..3] of real;
*
*   i ,j ,l , r , u , n ,k : integer;
*
*  QE , TG , XSS , hl, m , p , mss, mws, h7 :real;
   hl0, TC , h8 , XWS , TA , h4 , TGminim , T0 , TE :real;
   mw,  QG , QA , QC , HX , T2 , h2 , eff , effper, h6 :real;
*
* BEGIN
      P :=0;QG :=0;QA :=0;QC :=0;eff :=0;effper :=0;hl :=0;
      TG :=0;TGminim :=0;XSS :=0;TE :=0;T2 :=0,h6 :=0;
      m :=0;i:=0; j:=0;mss :=0;mws :=0;h7 :=0;n :=0;
```

```
      mw :=0;h8 :=0;TC :=0;XWS :=0;TA :=0;u :=2;h4 :=0;
      h2 :=0;HX :=0;k :=0;T0 :=0;1 :=0,r :=0;QE :=0,h10 :=0;
*
*     FOR i:=0 TO 2 DO
*
*     FOR j:=0 TO 3 DO
*
*     READ( v[i,j]);
*
*     FOR k :=0 TO 1 DO
*     BEGIN
*     T0 :=25 + (5*k) + 273.16;
*     FOR u :=0 TO 2 DO
*     BEGIN
*     HX :=v[u,3];
*     FOR i:=0 to 2 DO
*     BEGIN
*     TE :=4 +(i*3);
*
*     h10:=2501 +(1.88*TE);
*
*     FOR j :=0 TO 2 DO
*
*     BEGIN
*     TA :=-(j*10)+40;
*
*     h4 :=2.326*(-1015.07+(79.5387*v[i,j])-(2.358016*v[i,j]*
           v[i,j])+(0.03031583*v[i,j]*v[i,j]*v[i,j])-
           (1.40026E-4*v[i,j]*v[i,j]*v[i,j]*v[i,j])+
           ((4.68108-(3.037766E-1*v[i,j])+(8.44845E-3)*v[i,j]*
           v[i,j])-(1.047721E-4)*sqr(v[i,j])*v[i,j]+
          (4.80097E-7)*sqr(v[i,j])*sqr(v[i,j]))-
           (1.8*TA +32))+ ((-4.910E-3+(3.83184E-4*v[i,j])-
           (1.078963E-5*sqr(v[i,j]))+(1.3152E-7*v[i,j]*
           sqr(v[i,j]))-(5.897E-10*sqr(v[i,j])*sqr(v[i,j])))*
           (1.8*TA +32)*(1.8*TA +32));
*
```

```
*     FOR l:=0 TO S DO
*
*     BEGIN
*       n := 0;
*       TC :=(l*10) + 20;
*       TGminim :=((A+(B*v[i,j])+(C*sqr(v[i,j]))+(D*sqr(v[i,j])*
        v[i,j]))*TC)+(E+(F*v[i,j])+(G*sqr(v[i,j]))+
        (H*sqr(v[i,j])*v[i,j]));
*
*     WRITELN (0.00:l:2,'  ',TGminim:l:2);
*
*     REPEAT
*     n := n + l;
*     XSS :=(0.l*n)+v[i,j];
*     m := v[i,j] / (XSS - v[i,j]);
*     p := XSS / (XSS - v[i,j]);
*     h8 := 4.19*TC;
*     mw := l/(hl0 - h8);
*     mss := m * mw;
*     mws := p * mw;
*     TG := ((A+(B*XSS)+(C*XSS*XSS)+(D*XSS*XSS*XSS))*TC)+
            (E+(F*XSS)+(G*XSS*XSS)+(H*XSS*XSS*XSS));
*     T2 := (HX *TA)+((l-HX)*TG);
*     h7 := (l.88*TG) +250l;
*     hl := 2.326 * (- 1015.07+(79.5387*XSS)-(2.358016*XSS*XSS)+
        (0.03031583*XSS*XSS*XSS)-(l.400261E-4*XSS*XSS*XSS*XSS)+
        ((4.68108-(3.037766E-l)*XSS+(8.44845E-3)*XSS*XSS)-
        (l.047721E-4)*XSS*XSS*XSS +(4.80097E-7)*XSS*XSS*XSS*
        XSS)*(1.8*TG+32))+((-4.910E-3+(3.83184E-4*XSS)-
        (l.078963E-5 *XSS*XSS)+(l.3152E-7*XSS*XSS*XSS)-
        (5.897E-l0*XSS*XSS*XSS*XSS))*(1.8*TG+32)*(1.8*TG+32));
```

```
*
*    h2 := 2.326 * (-1015.07+(79.5387*XSS)-(2.358016*XSS*XSS)+
       (0.03031583*XSS*XSS*XSS)-(1.400261E-4*XSS*XSS*XSS*XSS)+
       ((4.68108-(3.037766E-1)*XSS+(8.44845E-3)*XSS*XSS)-
       (1.047721E-4)*XSS*XSS*XSS+(4.80097E-7)*XSS*XSS*XSS*XSS)*
       (1.8*T2 +32))+((-4.910E-3 + (3.83184E-4*XSS)-
       (1.078963E-5*XSS*XSS)+(1.3152E-7*XSS*XSS*XSS)-
       (5.897E-10*XSS*XSS*XSS*XSS))*(1.8*T2 +32)*(1.8*T2 +32));
*
*    h6 :=((mss/mws)*(h1-h2))+h4;
*    QE := mw*(h10 - h8);
*    QG := (mss*h1) + (mw*h7) - (mws*h6);
*    QA := (mss*h2) + (mw*h10)- (mws*h4);
*    QC := mw*(h7 - h8);
* eff :=(-QE*(1-(T0/(TE+281.16))))/((QG*(1-(T0/(TG+280.66))))-
          (QA*(1-(T0/(TA+268.66))))-(QC*(1-(T0/(TC+269.66)))));
* effper := 100*eff;
*
* Writeln (effper:1:2, ' ',TG:1:2);
*
* UNTIL XSS > vv;
* END
* END
* END
* END
* END
* END.
*****************************************************************'
INPUT DATA (CONCENTRATIONS AND HEAT EXCHANGER EFFECTIVENESS):
v[i,j]
58.0    52.5    46.5    0.00
```

```
56.5    50.6    44.0    0.75

55.5    48.0    40.0    0.95
**********************************************************************
```

APPENDIX A2

PLOTTING PROGRAMME OF EFFICIENCY VARIATION

```
**********************************************************************
*This Programme plots the second law efficiency variation curves
 for different sets of cycle internal operating parameters
 and one set of external parameters. The input Data are the
 numerical results obtained from running the programme of
 efficiency  calculation (Appendix A1)*
**********************************************************************

      REAL X(26000), Y(26000)
      READ(5,*) (Y(I),X(I),I=1,24264)
      CALL PAPER(1)
      CALL CTRMAG(10)
      CALL MAP(30.0,100.0,0.0,70.0)
      CALL PSPACE(0.05, 0.45, 0.55, 0.95)
      CALL AXORIG (30.0,0.0)
      CALL AXESSI(1.0,1.0)
      CALL CURVEO(X, Y, 1, 71)
      CALL CURVEO(X, Y, 72, 142)
      CALL CURVEO(X, Y, 143, 213)
      CALL BROKEN(5,5,5,5)
      CALL CURVEO(X, Y, 214, 339)
      CALL CURVEO(X, Y, 340, 465)
      CALL CURVEO(X, Y, 466, 591)
      CALL BROKEN(20,5,20,5)
      CALL CURVEO(X, Y, 592, 782)
      CALL CURVEO(X, Y, 783, 973)
      CALL CURVEO(X, Y, 974, 1164)
      CALL FULL
      CALL CTRMAG(10)
      CALL PLOTCS(70.0, -8.0, 'TGenerator(C)---->')
      CALL CTRORI(90.0)
      CALL PLOTCS(22.5, 20.0, 'Efficiency % ---->')
      CALL CTRORI(0.0)
      CALL PLOTCS(41.0,55.0,'TE=4C,h.exchanger effectiv.=0.00')
      CALL PLOTCS(41.0, 50.0, 'Tambient=25C')
      CALL PLOTCS(102.0, 30.0, 'Fig.6(a).')
      CALL PLOTCS(67.0, 24.5, '1')
      CALL PLOTCS(83.0, 21.5, '2')
      CALL PLOTCS(85.0, 10.0, '3')
      CALL PLOTCS(55.0, 25.0, '4')
```

```
CALL PLOTCS(61.0, 17.0, '5')
CALL PLOTCS(73.5, 11.0, '6')
CALL PLOTCS(39.0, 24.0, '7')
CALL PLOTCS(49.5, 9.0, '8')
CALL PLOTCS(61.5, 9.0, '9')
CALL BORDER
CALL PSPACE(0.05, 0.45, 0.08, 0.48)
CALL AXORIG (30.0,0.0)
CALL CTRMAG(10)
CALL AXESSI(1.0,1.0)
CALL FULL
CALL CURVEO(X, Y, 1165, 1250)
CALL CURVEO(X, Y, 1251, 1336)
CALL CURVEO(X, Y, 1337, 1422)
CALL BROKEN(5,5,5,5)
CALL CURVEO(X, Y, 1423, 1567)
CALL CURVEO(X, Y, 1568, 1712)
CALL CURVEO(X, Y, 1713, 1857)
CALL BROKEN(20,5,20,5)
CALL CURVEO(X, Y, 1858, 2068)
CALL CURVEO(X, Y, 2069, 2279)
CALL CURVEO(X, Y, 2280, 2490)
CALL FULL
CALL CTRMAG(10)
CALL PLOTCS(70.0, -8.0, 'TGenerator(C)---->')
CALL CTRORI(90.0)
CALL PLOTCS(22.0, 20.0, 'Efficiency % ---->')
CALL CTRORI(0.0)
CALL PLOTCS(41.0,55.0,'TE=7C,h.exchanger effectiv.=0.00')
CALL PLOTCS(41.0, 50.0, 'Tambient=25C')
CALL PLOTCS(102.0, 30.0, 'Fig.6(b).')
CALL PLOTCS(64.0, 21.0, '1')
CALL PLOTCS(79.0, 18.0, '2')
CALL PLOTCS(81.2, 8.0, '3')
CALL PLOTCS(54.0, 21.2, '4')
CALL PLOTCS(57.5, 14.0, '5')
CALL PLOTCS(69.4, 6.0, '6')
CALL PLOTCS(44.0, 21.5, '7')
CALL PLOTCS(47.0, 10.0, '8')
CALL PLOTCS(58.5, 8.0, '9')
CALL BORDER
CALL FRAME
CALL PSPACE(0.10, 0.50, 0.50, 0.90)
CALL AXORIG (30.0,0.0)
CALL CTRMAG(10)
CALL AXESSI(1.0,1.0)
CALL CURVEO(X, Y, 2491, 2586)
CALL CURVEO(X, Y, 2587, 2682)
CALL CURVEO(X, Y, 2683, 2778)
CALL BROKEN(5,5,5,5)
CALL CURVEO(X, Y, 2779, 2949)
CALL CURVEO(X, Y, 2950, 3120)
CALL CURVEO(X, Y, 3121, 3291)
CALL BROKEN(20,5,20,5)
CALL CURVEO(X, Y, 3292, 3542)
```

```
CALL CURVEO(X, Y, 3543, 3793)
CALL CURVEO(X, Y, 3794, 4044)
CALL FULL
CALL CTRMAG(10)
CALL PLOTCS(70.0, -8.0, 'TGenerator(C)---->')
CALL CTRORI(90.0)
CALL PLOTCS(22.5, 20.0, 'Efficiency % ---->')
CALL CTRORI(0.0)
CALL PLOTCS(41.0,55.0,'TE=10C,h.exchanger effectiv.=0.00')
CALL PLOTCS(41.0, 50.0, 'Tambient=25C')
CALL PLOTCS(59.0, 16.0, '1')
CALL PLOTCS(76.0, 13.5, '2')
CALL PLOTCS(79.5, 6.0, '3')
CALL PLOTCS(45.0, 18.0, '4')
CALL PLOTCS(52.0, 11.0, '5')
CALL PLOTCS(63.0, 5.0, '6')
CALL PLOTCS(38.0, 18.0, '7')
CALL PLOTCS(42.5, 10.0, '8')
CALL PLOTCS(95.0, 7.9, '9')
CALL PLOTCS(45.0, -15.0, 'Legend:(TA,TC)')
CALL PLOTCS(45.0, -20.0, '1:(40C,20C); 2:(40C,30C);
                          3:(40C,40C)')
CALL PLOTCS(45.0, -25.0, '4:(30C,20C); 5:(30C,30C);
                          6:(30C,40C)')
CALL PLOTCS(45.0, -30.0, '7:(20C,20C); 8:(20C,30C);
                           9:(20C,40C)')
CALL PLOTCS(102.0, 30.0, 'Fig.6(c).')
CALL PLOTCS(29.0,-40.0, 'Fig.6(a),(b),(c).Variation of')
CALL PLOTCS(75.0,-40.0,'efficiency with cycle parameters')
CALL BORDER
CALL FRAME
CALL CTRMAG(10)
CALL PSPACE(0.05, 0.45, 0.55, 0.95)
CALL AXORIG (30.0,0.0)
CALL AXESSI (1.0,1.0)
CALL CURVEO(X, Y, 4045, 4115)
CALL CURVEO(X, Y, 4116, 4186)
CALL CURVEO(X, Y, 4187, 4257)
CALL BROKEN(5,5,5,5)
CALL CURVEO(X, Y, 4258, 4383)
CALL CURVEO(X, Y,24384, 4509)
CALL CURVEO(X, Y, 4510, 4635)
CALL BROKEN(20,5,20,5)
CALL CURVEO(X, Y, 4636, 4826)
CALL CURVEO(X, Y, 4827, 5017)
CALL CURVEO(X, Y, 5018, 5208)
CALL FULL
CALL CTRMAG(10)
CALL PLOTCS(70.0, -8.0, 'TGenerator(C)---->')
CALL CTRORI(90.0)
CALL PLOTCS(22.5, 20.0, 'Efficiency % ---->')
CALL CTRORI(0.0)
CALL PLOTCS(41.0,55.0,'TE=4C,h.exchanger effectiv.=0.75')
CALL PLOTCS(41.0, 50.0, 'Tambient=25C')
CALL PLOTCS(62.0, 30.0, '1')
```

```
CALL PLOTCS(79.0, 27.0, '2')
CALL PLOTCS(83.0, 10.0, '3')
CALL PLOTCS(52.0, 30.0, '4')
CALL PLOTCS(59.5, 19.5, '5')
CALL PLOTCS(97.0, 20.7, '6')
CALL PLOTCS(37.5, 28.5, '7')
CALL PLOTCS(49.5, 10.0, '8')
CALL PLOTCS(60.5, 8.0, '9')
CALL PLOTCS(102.0, 30.0, 'Fig.7(a).')
CALL BORDER
CALL CTRMAG(10)
CALL PSPACE(0.05, 0.45, 0.08, 0.48)
CALL AXORIG (30.0,0.0)
CALL AXESSI (1.0,1.0)
CALL FULL
CALL CURVEO(X, Y, 5209, 5294)
CALL CURVEO(X, Y, 5295, 5380)
CALL CURVEO(X, Y, 5381, 5466)
CALL BROKEN(5,5,5,5)
CALL CURVEO(X, Y, 5467, 5611)
CALL CURVEO(X, Y, 5612, 5756)
CALL CURVEO(X, Y, 5757, 5901)
CALL BROKEN(20,5,20,5)
CALL CURVEO(X, Y, 5902, 6112)
CALL CURVEO(X, Y, 6113, 6323)
CALL CURVEO(X, Y, 6324, 6534)
CALL FULL
CALL CTRMAG(10)
CALL PLOTCS(70.0, -8.0, 'TGenerator(C)---->')
CALL CTRORI(90.0)
CALL PLOTCS(22.5, 20.0, 'Efficiency % ---->')
CALL CTRORI(0.0)
CALL PLOTCS(41.0,55.0,'TE=7C,h.exchanger effectiv.=0.75')
CALL PLOTCS(41.0, 50.0, 'Tambient=25C')
CALL PLOTCS(58.0, 25.5, '1')
CALL PLOTCS(72.0, 23.0, '2')
CALL PLOTCS(79.5, 8.0, '3')
CALL PLOTCS(44.5, 25.0, '4')
CALL PLOTCS(56.0, 10.0, '5')
CALL PLOTCS(97.0, 16.0, '6')
CALL PLOTCS(34.5, 22.0, '7')
CALL PLOTCS(46.5, 10.0, '8')
CALL PLOTCS(57.5, 8.0, '9')
CALL PLOTCS(102.0, 30.0, 'Fig.7(b).')
CALL BORDER
CALL FRAME
CALL CTRMAG(10)
CALL PSPACE(0.10, 0.50, 0.50, 0.90)
CALL AXORIG (30.0,0.0)
CALL AXESSI (1.0,1.0)
CALL CURVEO(X, Y, 6535, 6630)
CALL CURVEO(X, Y, 6631, 6726)
CALL CURVEO(X, Y, 6727, 6822)
CALL BROKEN(5,5,5,5)
CALL CURVEO(X, Y, 6823, 6993)
```

```
CALL CURVEO(X, Y, 6994, 7164)
CALL CURVEO(X, Y, 7165, 7335)
CALL BROKEN(20,5,20,5)
CALL CURVEO(X, Y, 7336, 7586)
CALL CURVEO(X, Y, 7587, 7837)
CALL CURVEO(X, Y, 7838, 8088)
CALL FULL
CALL CTRMAG(10)
CALL PLOTCS(70.0, -8.0, 'TGenerator(C)---->')
CALL CTRORI(90.0)
CALL PLOTCS(22.5, 20.0, 'Efficiency % ---->')
CALL CTRORI(0.0)
CALL PLOTCS(41.0,55.0,'TE=10C,h.exchanger effectiv.=0.75')
CALL PLOTCS(41.0, 50.0, 'Tambient=25C')
CALL PLOTCS(54.0, 10.0, '1')
CALL PLOTCS(65.5, 8.0, '2')
CALL PLOTCS(78.0, 8.0, '3')
CALL PLOTCS(41.0, 21.0, '4')
CALL PLOTCS(52.5, 19.0, '5')
CALL PLOTCS(62.0, 6.0, '6')
CALL PLOTCS(35.0, 20.0, '7')
CALL PLOTCS(41.5, 08.0, '8')
CALL PLOTCS(95.0, 8.5, '9')
CALL PLOTCS(45.0, -15.0, 'Legend:(TA,TC)')
CALL PLOTCS(45.0, -20.0, '1:(40C,20C); 2:(40C,30C);
                          3:(40C,40C)')
CALL PLOTCS(45.0, -25.0, '4:(30C,20C); 5:(30C,30C);
                          6:(30C,40C)')
CALL PLOTCS(45.0, -30.0, '7:(20C,20C); 8:(20C,30C);
                          9:(20C,40C)')
CALL PLOTCS(102.0, 30.0, 'Fig.7(c).')
CALL PLOTCS(30.0,-40.0,'Fig.7(a),(b),(c).Variation of ')
CALL PLOTCS(75.0,-40.0,'efficiency with cycle parameters')
CALL BORDER
CALL FRAME
CALL CTRMAG(10)
CALL PSPACE(0.05, 0.45, 0.55, 0.95)
CALL AXORIG (30.0,0.0)
CALL AXESSI(1.0,1.0)
CALL CURVEO(X, Y, 8089, 8159)
CALL CURVEO(X, Y, 8160, 8230)
CALL CURVEO(X, Y, 8231, 8301)
CALL BROKEN(5,5,5,5)
CALL CURVEO(X, Y, 8302, 8427)
CALL CURVEO(X, Y, 8428, 8553)
CALL CURVEO(X, Y, 8554, 8679)
CALL BROKEN(20,5,20,5)
CALL CURVEO(X, Y, 8680, 8870)
CALL CURVEO(X, Y, 8871, 9061)
CALL CURVEO(X, Y, 9062, 9252)
CALL FULL
CALL CTRMAG(10)
CALL PLOTCS(70.0, -8.0, 'TGenerator(C)---->')
CALL CTRORI(90.0)
CALL PLOTCS(22.5, 20.0, 'Efficiency % ---->')
```

```
CALL CTRORI(0.0)
CALL PLOTCS(41.0,55.0,'TE=4C,h.exchanger effectiv.=0.95')
CALL PLOTCS(41.0, 50.0, 'Tambient=25C')
CALL PLOTCS(59.0, 32.5, '1')
CALL PLOTCS(71.0, 31.5, '2')
CALL PLOTCS(82.5, 10.0, '3')
CALL PLOTCS(47.5, 33.5, '4')
CALL PLOTCS(59.0, 10.0, '5')
CALL PLOTCS(97.0, 21.0, '6')
CALL PLOTCS(37.0, 28.0, '7')
CALL PLOTCS(49.0, 10.0, '8')
CALL PLOTCS(60.0, 7.0, '9')
CALL PLOTCS(102.0, 30.0, 'Fig.8(a).')
CALL BORDER
CALL CTRMAG(10)
CALL PSPACE(0.05, 0.45, 0.08, 0.48)
CALL AXORIG (30.0,0.0)
CALL AXESSI(1.0,1.0)
CALL FULL
CALL CURVEO(X, Y, 9253, 9338)
CALL CURVEO(X, Y, 9339, 9424)
CALL CURVEO(X, Y, 9425, 9510)
CALL BROKEN(5,5,5,5)
CALL CURVEO(X, Y, 9511, 9655)
CALL CURVEO(X, Y, 9656, 9800)
CALL CURVEO(X, Y, 9801, 9945)
CALL BROKEN(20,5,20,5)
CALL CURVEO(X, Y, 9946, 10156)
CALL CURVEO(X, Y, 10157, 10367)
CALL CURVEO(X, Y, 10368, 10578)
CALL FULL
CALL CTRMAG(10)
CALL PLOTCS(70.0, -8.0, 'TGenerator(C)---->')
CALL CTRORI(90.0)
CALL PLOTCS(22.5, 20.0, 'Efficiency % ---->')
CALL CTRORI(0.0)
CALL PLOTCS(41.0,55.0,'TE=7C,h.exchanger effectiv.=0.95')
CALL PLOTCS(41.0, 50.0, 'Tambient=30C')
CALL PLOTCS(57.0, 27.5, '1')
CALL PLOTCS(67.0, 26.0, '2')
CALL PLOTCS(80.0, 24.0, '3')
CALL PLOTCS(45.0, 28.0, '4')
CALL PLOTCS(55.8, 10.0, '5')
CALL PLOTCS(68.0, 12.0, '6')
CALL PLOTCS(34.0, 22.0, '7')
CALL PLOTCS(46.5, 10.0, '8')
CALL PLOTCS(57.5, 7.0, '9')
CALL PLOTCS(102.0, 30.0, 'Fig.8(b).')
CALL BORDER
CALL FRAME
CALL CTRMAG(10)
CALL PSPACE(0.10, 0.50, 0.50, 0.90)
CALL AXORIG (30.0,0.0)
CALL AXESSI(1.0,1.0)
CALL CURVEO(X. Y. 10579, 10674)
```

```
CALL CURVEO(X, Y, 10675, 10710)
CALL CURVEO(X, Y, 10771, 10866)
CALL BROKEN(5,5,5,5)
CALL CURVEO(X, Y, 10867, 11037)
CALL CURVEO(X, Y, 11038, 11208)
CALL CURVEO(X, Y, 11209, 11379)
CALL BROKEN(20,5,20,5)
CALL CURVEO(X, Y, 11380, 11630)
CALL CURVEO(X, Y, 11631, 11881)
CALL CURVEO(X, Y, 11882, 12132)
CALL FULL
CALL CTRMAG(10)
CALL PLOTCS(70.0, -8.0, 'TGenerator(C)---->')
CALL CTRORI(90.0)
CALL PLOTCS(22.5, 20.0, 'Efficiency % ---->')
CALL CTRORI(0.0)
CALL PLOTCS(41.0,55.0,'TE=10C,h.exchanger effectiv.=0.95')
CALL PLOTCS(41.0, 50.0, 'Tambient=25C')
CALL PLOTCS(54.0, 10.0, '1')
CALL PLOTCS(65.5, 9.0, '2')
CALL PLOTCS(77.5, 6.0, '3')
CALL PLOTCS(39.5, 22.0, '4')
CALL PLOTCS(52.0, 22.0, '5')
CALL PLOTCS(97.0, 11.7, '6')
CALL PLOTCS(35.0, 21.0, '7')
CALL PLOTCS(41.5, 08.0, '8')
CALL PLOTCS(90.0, 10.7, '9')
CALL PLOTCS(45.0, -15.0, 'Legend:(TA,TC)')
CALL PLOTCS(45.0, -20.0, '1:(40C,20C); 2:(40C,30C);
                          3:(40C,40C)')
CALL PLOTCS(45.0, -25.0, '4:(30C,20C); 5:(30C,30C);
                          6:(30C,40C)')
CALL PLOTCS(45.0, -30.0, '7:(20C,20C); 8:(20C,30C);
                          9:(20C,40C)')
CALL PLOTCS(102.0,30.0,'Fig.8(c).')
CALL PLOTCS(30.0,-40.0,'Fig.8(a),(b),(c).Variation of ')
CALL PLOTCS(75.0,-40.0,'efficiency with cycle parameters')
CALL BORDER
CALL FRAME
CALL CURVEO(X, Y, 12133,12203)
CALL CURVEO(X, Y, 12204,12274)
CALL CURVEO(X, Y, 12275,12345)
CALL BROKEN(5,5,5,5)
CALL CURVEO(X, Y, 12346,12471)
CALL CURVEO(X, Y, 12472,12597)
CALL CURVEO(X, Y, 12598,12723)
CALL BROKEN(20,5,20,5)
CALL CURVEO(X, Y, 12724,12914)
CALL CURVEO(X, Y, 12915,13105)
CALL CURVEO(X, Y,13106,13296)
CALL FULL
CALL CTRMAG(10)
CALL PLOTCS(70.0, -8.0, 'TGenerator(C)---->')
CALL CTRORI(90.0)
CALL PLOTCS(22.5, 20.0, 'Efficiency % ---->')
```

```
CALL CTRORI(0.0)
CALL PLOTCS(41.0,55.0,'TE=4C,h.exchanger effectiv.=0.00')
CALL PLOTCS(41.0, 50.0, 'Tambient=30C')
CALL PLOTCS(102.0, 30.0, 'Fig.9(a).')
CALL PLOTCS(67.0, 31.0, '1')
CALL PLOTCS(83.0, 27.0, '2')
CALL PLOTCS(84.0, 10.0, '3')
CALL PLOTCS(55.0, 32.0, '4')
CALL PLOTCS(61.0, 22.5, '5')
CALL PLOTCS(75.0, 18.0, '6')
CALL PLOTCS(38.0, 30.0, '7')
CALL PLOTCS(50.0, 10.0, '8')
CALL PLOTCS(61.0, 9.0, '9')
CALL BORDER
CALL PSPACE(0.05, 0.45, 0.08, 0.48)
CALL AXORIG (30.0,0.0)
CALL CTRMAG(10)
CALL AXESSI(1.0,1.0)
CALL FULL
CALL CURVEO(X, Y, 13297,13382)
CALL CURVEO(X, Y, 13383,13468)
CALL CURVEO(X, Y, 13469,13554)
CALL BROKEN(5,5,5,5)
CALL CURVEO(X, Y, 13555,13699)
CALL CURVEO(X, Y, 13700,13844)
CALL CURVEO(X, Y, 13845,13989)
CALL BROKEN(20,5,20,5)
CALL CURVEO(X, Y, 13990,14200)
CALL CURVEO(X, Y, 14201,14411)
CALL CURVEO(X, Y, 14412,14622)
CALL FULL
CALL CTRMAG(10)
CALL PLOTCS(70.0, -8.0, 'TGenerator(C)---->')
CALL CTRORI(90.0)
CALL PLOTCS(22.0, 20.0, 'Efficiency % ---->')
CALL CTRORI(0.0)
CALL PLOTCS(41.0,55.0,'TE=7C,h.exchanger effectiv.=0.00')
CALL PLOTCS(41.0, 50.0, 'Tambient=30C')
CALL PLOTCS(102.0, 30.0, 'Fig.9(b).')
CALL PLOTCS(64.0, 28.0, '1')
CALL PLOTCS(54.0, 28.0, '4')
CALL PLOTCS(44.0, 28.3, '7')
CALL PLOTCS(79.0, 24.7, '2')
CALL PLOTCS(57.5, 18.3, '5')
CALL PLOTCS(47.0, 10.0, '8')
CALL PLOTCS(80.2, 8.0, '3')
CALL PLOTCS(68.4, 6.0, '6')
CALL PLOTCS(58.0, 8.0, '9')
CALL BORDER
CALL FRAME
CALL PSPACE(0.10, 0.50, 0.50, 0.90)
CALL AXORIG (30.0,0.0)
CALL CTRMAG(10)
CALL AXESSI(1.0,1.0)
CALL CURVEO(X, Y, 15623,14718)
```

```
CALL CURVEO(X, Y, 14719,14814)
CALL CURVEO(X, Y, 14815,14910)
CALL BROKEN(5,5,5,5)
CALL CURVEO(X, Y, 14911,15081)
CALL CURVEO(X, Y, 15082,15252)
CALL CURVEO(X, Y, 15253,15423)
CALL BROKEN(20,5,20,5)
CALL CURVEO(X, Y, 15424,15674)
CALL CURVEO(X, Y, 15675,15925)
CALL CURVEO(X, Y, 15926,16176)
CALL FULL
CALL CTRMAG(10)
CALL PLOTCS(70.0, -8.0, 'TGenerator(C)---->')
CALL CTRORI(90.0)
CALL PLOTCS(22.5, 20.0, 'Efficiency % ---->')
CALL CTRORI(0.0)
CALL PLOTCS(41.0,55.0,'TE=10C,h.exchanger effectiv.=0.00')
CALL PLOTCS(41.0, 50.0, 'Tambient=30C')
CALL PLOTCS(59.0, 24.2, '1')
CALL PLOTCS(76.0, 20.5, '2')
CALL PLOTCS(78.0, 6.0, '3')
CALL PLOTCS(45.0, 27.8, '4')
CALL PLOTCS(52.5, 17.5, '5')
CALL PLOTCS(62.0, 5.0, '6')
CALL PLOTCS(38.0, 27.3, '7')
CALL PLOTCS(42.0, 10.0, '8')
CALL PLOTCS(56.5, 19.5, '9')
CALL PLOTCS(45.0, -15.0, 'Legend:(TA,TC)')
CALL PLOTCS(45.0, -20.0, '1:(40C,20C); 2:(40C,30C);
                          3:(40C,40C)')
CALL PLOTCS(45.0, -25.0, '4:(30C,20C); 5:(30C,30C);
                          6:(30C,40C)')
CALL PLOTCS(45.0, -30.0, '7:(20C,20C); 8:(20C,30C);
                          9:(20C,40C)')
CALL PLOTCS(102.0, 30.0, 'Fig.9(c).')
CALL PLOTCS(30.0,-40.0,'Fig. 9(a),(b),(c).Variation of')
CALL PLOTCS(75.0,-40.0,'efficiency with cycle parameters')
CALL BORDER
CALL FRAME
CALL CTRMAG(10)
CALL PSPACE(0.05, 0.45, 0.55, 0.95)
CALL AXORIG (30.0,0.0)
CALL AXESSI (1.0,1.0)
CALL CURVEO(X, Y, 16177,16247)
CALL CURVEO(X, Y, 16248,16318)
CALL CURVEO(X, Y, 16319,16389)
CALL BROKEN(5,5,5,5)
CALL CURVEO(X, Y, 16390,16515)
CALL CURVEO(X, Y, 16516,16641)
CALL CURVEO(X, Y, 16642,16767)
CALL BROKEN(20,5,20,5)
CALL CURVEO(X, Y, 16768,16958)
CALL CURVEO(X, Y, 16959,17149)
CALL CURVEO(X, Y, 17150,17340)
CALL FULL
```

```
CALL CTRMAG(10)
CALL PLOTCS(70.0, -8.0, 'TGenerator(C)---->')
CALL CTRORI(90.0)
CALL PLOTCS(22.5, 20.0, 'Efficiency % ---->')
CALL CTRORI(0.0)
CALL PLOTCS(41.0,55.0,'TE=4C,h.exchanger effectiv.=0.75')
CALL PLOTCS(41.0, 50.0, 'Tambient=30C')
CALL PLOTCS(65.0, 36.0, '1')
CALL PLOTCS(79.0, 33.0, '2')
CALL PLOTCS(81.0, 10.0, '3')
CALL PLOTCS(52.0, 37.0, '4')
CALL PLOTCS(59.0, 20.5, '5')
CALL PLOTCS(97.0, 26.0, '6')
CALL PLOTCS(36.0, 28.5, '7')
CALL PLOTCS(49.5, 10.0, '8')
CALL PLOTCS(60.5, 8.0, '9')
CALL PLOTCS(102.0, 30.0, 'Fig.10(a).')
CALL BORDER
CALL CTRMAG(10)
CALL PSPACE(0.05, 0.45, 0.08, 0.48)
CALL AXORIG (30.0,0.0)
CALL AXESSI (1.0,1.0)
CALL FULL
CALL CURVEO(X, Y, 17341,17426)
CALL CURVEO(X, Y, 17427,17512)
CALL CURVEO(X, Y, 17513,17598)
CALL BROKEN(5,5,5,5)
CALL CURVEO(X, Y, 17599,17743)
CALL CURVEO(X, Y, 17744,17888)
CALL CURVEO(X, Y, 17889,18033)
CALL BROKEN(20,5,20,5)
CALL CURVEO(X, Y, 18034,18244)
CALL CURVEO(X, Y, 18245,18455)
CALL CURVEO(X, Y, 18456,18666)
CALL FULL
CALL CTRMAG(10)
CALL PLOTCS(70.0, -8.0, 'TGenerator(C)---->')
CALL CTRORI(90.0)
CALL PLOTCS(22.5, 20.0, 'Efficiency % ---->')
CALL CTRORI(0.0)
CALL PLOTCS(41.0,55.0,'TE=7C,h.exchanger effectiv.=0.75')
CALL PLOTCS(41.0, 50.0, 'Tambient=30C')
CALL PLOTCS(58.0, 33.0, '1')
CALL PLOTCS(72.0, 30.5, '2')
CALL PLOTCS(79.5, 8.0, '3')
CALL PLOTCS(43.5, 23.0, '4')
CALL PLOTCS(56.0, 10.0, '5')
CALL PLOTCS(97.0, 21.0, '6')
CALL PLOTCS(34.0, 22.0, '7')
CALL PLOTCS(46.5, 10.0, '8')
CALL PLOTCS(57.5, 8.0, '9')
CALL PLOTCS(102.0, 30.0, 'Fig.10(b).')
CALL BORDER
CALL FRAME
CALL CTRMAG(10)
```

```
CALL PSPACE(0.10, 0.50, 0.50, 0.90)
CALL AXORIG (30.0,0.0)
CALL AXESSI (1.0,1.0)
CALL CURVEO(X, Y, 18666,18762)
CALL CURVEO(X, Y, 18763,18858)
CALL CURVEO(X, Y, 18859,18954)
CALL BROKEN(5,5,5,5)
CALL CURVEO(X, Y, 18955,19125)
CALL CURVEO(X, Y, 19126,19296)
CALL CURVEO(X, Y, 19297,19467)
CALL BROKEN(20,5,20,5)
CALL CURVEO(X, Y, 19468,19718)
CALL CURVEO(X, Y, 19719,19969)
CALL CURVEO(X, Y, 19970,20220)
CALL FULL
CALL CTRMAG(10)
CALL PLOTCS(70.0, -8.0, 'TGenerator(C)---->')
CALL CTRORI(90.0)
CALL PLOTCS(22.5, 20.0, 'Efficiency % ---->')
CALL CTRORI(0.0)
CALL PLOTCS(41.0,55.0,'TE=10C,h.exchanger effectiv.=0.75')
CALL PLOTCS(41.0, 50.0, 'Tambient=30C')
CALL PLOTCS(54.0, 17.0, '1')
CALL PLOTCS(66.0, 15.0, '2')
CALL PLOTCS(77.5, 10.0, '3')
CALL PLOTCS(41.0, 31.5, '4')
CALL PLOTCS(52.5, 28.5, '5')
CALL PLOTCS(62.0, 11.0, '6')
CALL PLOTCS(35.0, 30.0, '7')
CALL PLOTCS(41.5, 08.0, '8')
CALL PLOTCS(51.0, 5.0, '9')
CALL PLOTCS(45.0, -15.0, 'Legend:(TA,TC)')
CALL PLOTCS(45.0, -20.0, '1:(40C,20C); 2:(40C,30C);
                          3:(40C,40C)')
CALL PLOTCS(45.0, -25.0, '4:(30C,20C); 5:(30C,30C);
                          6:(30C,40C)')
CALL PLOTCS(45.0, -30.0, '7:(20C,20C); 8:(20C,30C);
                          9:(20C,40C)')
CALL PLOTCS(102.0, 30.0, 'Fig.10(c).')
CALL PLOTCS(30.0,-40.0,'Fig.10(a),(b),(c).Variation of ')
CALL PLOTCS(75.0,-40.0,'efficiency with cycle parameters')
CALL BORDER
CALL FRAME
CALL CTRMAG(10)
CALL PSPACE(0.05, 0.45, 0.55, 0.95)
CALL AXORIG (30.0,0.0)
CALL AXESSI(1.0,1.0)
CALL CURVEO(X, Y, 20221,20291)
CALL CURVEO(X, Y, 20292,20362)
CALL CURVEO(X, Y, 20363,20433)
CALL BROKEN(5,5,5,5)
CALL CURVEO(X, Y, 20434,20559)
CALL CURVEO(X, Y, 20560,20685)
CALL CURVEO(X, Y, 20686,20811)
CALL BROKEN(20,5,20,5)
```

```
CALL CURVEO(X, Y, 20812,21002)
CALL CURVEO(X, Y, 21003,21193)
CALL CURVEO(X, Y, 21194,21384)
CALL FULL
CALL CTRMAG(10)
CALL PLOTCS(70.0, -8.0, 'TGenerator(C)---->')
CALL CTRORI(90.0)
CALL PLOTCS(22.5, 20.0, 'Efficiency % ---->')
CALL CTRORI(0.0)
CALL PLOTCS(41.0,55.0,'TE=4C,h.exchanger effectiv.=0.95')
CALL PLOTCS(41.0, 50.0, 'Tambient=30C')
CALL PLOTCS(59.0, 39.0, '1')
CALL PLOTCS(71.0, 38.5, '2')
CALL PLOTCS(82.0, 10.0, '3')
CALL PLOTCS(47.5, 28.0, '4')
CALL PLOTCS(59.0, 10.0, '5')
CALL PLOTCS(97.0, 27.0, '6')
CALL PLOTCS(37.0, 28.0, '7')
CALL PLOTCS(48.5, 10.0, '8')
CALL PLOTCS(60.0, 7.0, '9')
CALL PLOTCS(102.0, 30.0, 'Fig.11(a).')
CALL BORDER
CALL CTRMAG(10)
CALL PSPACE(0.05, 0.45, 0.08, 0.48)
CALL AXORIG (30.0,0.0)
CALL AXESSI(1.0,1.0)
CALL FULL
CALL CURVEO(X, Y, 21385,21470)
CALL CURVEO(X, Y, 21471,21556)
CALL CURVEO(X, Y, 21557,21642)
CALL BROKEN(5,5,5,5)
CALL CURVEO(X, Y, 21643,21787)
CALL CURVEO(X, Y, 21788,21932)
CALL CURVEO(X, Y, 21933,22077)
CALL BROKEN(20,5,20,5)
CALL CURVEO(X, Y, 22078,22288)
CALL CURVEO(X, Y, 22289,22499)
CALL CURVEO(X, Y, 22500,22710)
CALL FULL
CALL CTRMAG(10)
CALL PLOTCS(70.0, -8.0, 'TGenerator(C)---->')
CALL CTRORI(90.0)
CALL PLOTCS(22.5, 20.0, 'Efficiency % ---->')
CALL CTRORI(0.0)
CALL PLOTCS(41.0,55.0,'TE=7C,h.exchanger effectiv.=0.95')
CALL PLOTCS(41.0, 50.0, 'Tambient=30C')
CALL PLOTCS(57.0, 36.0, '1')
CALL PLOTCS(67.0, 34.0, '2')
CALL PLOTCS(80.0, 32.5, '3')
CALL PLOTCS(45.0, 37.0, '4')
CALL PLOTCS(55.5, 10.0, '5')
CALL PLOTCS(68.0, 15.0, '6')
CALL PLOTCS(34.0, 22.0, '7')
CALL PLOTCS(46.5, 10.0, '8')
CALL PLOTCS(57.5, 7.0, '9')
```

```
CALL PLOTCS(102.0, 30.0, 'Fig.11(b).')
CALL BORDER
CALL FRAME
CALL CTRMAG(10)
CALL PSPACE(0.10, 0.50, 0.50, 0.90)
CALL AXORIG (30.0,0.0)
CALL AXESSI(1.0,1.0)
CALL CURVEO(X, Y, 22711,22806)
CALL CURVEO(X, Y, 22807,22842)
CALL CURVEO(X, Y, 22843,22998)
CALL BROKEN(5,5,5,5)
CALL CURVEO(X, Y, 22999,23169)
CALL CURVEO(X, Y, 23170,23340)
CALL CURVEO(X, Y, 23341,23511)
CALL BROKEN(20,5,20,5)
CALL CURVEO(X, Y, 23512,23762)
CALL CURVEO(X, Y, 23763,24013)
CALL CURVEO(X, Y, 24014,24264)
CALL FULL
CALL CTRMAG(10)
CALL PLOTCS(70.0, -8.0, 'TGenerator(C)---->')
CALL CTRORI(90.0)
CALL PLOTCS(22.5, 20.0, 'Efficiency % ---->')
CALL CTRORI(0.0)
CALL PLOTCS(41.0,55.0,'TE=10C,h.exchanger effectiv.=0.95')
CALL PLOTCS(41.0, 50.0, 'Tambient=30C')
CALL PLOTCS(53.5, 15.0, '1')
CALL PLOTCS(65.5, 15.0, '2')
CALL PLOTCS(77.5, 6.0, '3')
CALL PLOTCS(39.5, 18.0, '4')
CALL PLOTCS(52.0, 32.0, '5')
CALL PLOTCS(97.0, 18.0, '6')
CALL PLOTCS(35.0, 30.0, '7')
CALL PLOTCS(41.5, 08.0, '8')
CALL PLOTCS(50.5, 5.0, '9')
CALL PLOTCS(45.0, -15.0, 'Legend:(TA,TC)')
CALL PLOTCS(45.0, -20.0, '1:(40C,20C); 2:(40C,30C);
                          3:(40C,40C)')
CALL PLOTCS(45.0, -25.0, '4:(30C,20C); 5:(30C,30C);
                          6:(30C,40C)')
CALL PLOTCS(45.0, -30.0, '7:(20C,20C); 8:(20C,30C);
                          9:(20C,40C)')
CALL PLOTCS(102.0, 30.0, 'Fig.11(c).')
CALL PLOTCS(30.0,-40.0,'Fig.11(a),(b),(c).Variation of ')
CALL PLOTCS(75.0,-40.0,'efficiency with cycle parameters')
CALL BORDER
CALL FRAME
CALL GREND
STOP
END
```

APPENDIX A3

COMPUTER PROGRAMME FOR CALCULATION OF EFFICIENCY AS A FUNCTION OF CYCLE EXTERNAL PARAMETERS

```
*****************************************************************
*PROGRAM calcul (input, l);
     (*calculate the second law efficiency of a LiBr-Water
       absorption refrigeration cycle as a function of the
       temperature differences between the internal and the
       external fluids for an ambient temperature of 25 and
       30 deg.C.*)
*****************************************************************
*CONST
 A = - 2.00755;     B = 0.16976;    C = - 3.13336E-3;
 E = 124.937;       F = - 7.7165;   G = 0.152286;
 TA = 40;           TC = 20;        HX = 0.75;
 D = 1.97668E-5;    H = - 7.9509E-4;  TG = 65;    XSS =61.5;
*VAR
 l , u , n ,i , j , k ,jj : integer;
 QE ,hl,m,p,mss,mws,h7,QG,QA,QC,effl,effperl :real;
 hl0,h8,h4,mw,eff2,eff3,effper2,effper3,TE :real;
 eff4,effper4,T2,XWS,h2,h6,T0 :real;
*BEGIN
 l :=0; jj :=0; T0 :=0;  QG :=0;  QA :=0;  QC :=0;
 effl :=0; effperl :=0;  eff2 :=0; effper2 :=0; TE :=0;
 effper3 :=0; eff3 :=0;  eff4 :=0; effper4 :=0; hl :=0;
 XWS :=0; mws :=0; n :=0;  h7 :=0; mw :=0; h8 :=0;
```

```
  i :=0; j:=0; k :=0; h4 :=0; QE :=0; hl0 :=0;
  T2 :=0; h6 :=0; h2 :=0;  m :=0; p :=0;
 *FOR jj :=0 TO 1 DO
 *    BEGIN
 *    T0 :=25+(5*JJ)+273.16;
 *    FOR i :=0 TO 1 DO
 *    BEGIN
 *    TE :=(i*3)+4;
 *    XWS :=58.7 -(i*1.8);
 *    hl0 :=2501 +(1.88*TE);
 *
 *    h4 :=2.326*(-1015.07+(79.5387*XWS)-(2.358016*XWS*XWS)+
       (0.03031583*XWS*XWS*XWS)-(1.40026E-4*XWS*XWS*XWS*XWS)+
       ((4.68108-(3.037766E-1*XWS)+(8.44845E-3)*XWS*XWS)-
       (1.047721E-4)*XWS*XWS*XWS+(4.80097E-7)*XWS*XWS*XWS
       XWS)*(1.8*TA +32))+((-4.910E-3+(3.83184E-4*XWS)-
       (1.078963E-5*XWS*XWS)+(1.3152E-7*XWS*XWS*XWS)-
       (5.897E-10*XWS*XWS*XWS*XWS))*(1.8*TA +32)*(1.8*TA +32));
 *
 *    m := XWS / (XSS - XWS);
 *    p := XSS / (XSS - XWS);
 *    h8 := 4.19*TC;
 *    mw := 1/(hl0 - h8);
 *    mss := m * mw;
 *    mws := p * mw;
 *    T2 := (HX *TA)+((1-HX)*TG);
 *    h7 := (1.88*TG) +2501;
 *    hl := 2.326*(-1015.07+(79.5387*XSS)-(2.358016*XSS*XSS)+
       (0.03031583*XSS*XSS*XSS)-(1.400261E-4*XSS*XSS*XSS*XSS)+
       ((4.68108-(3.037766E-1)*XSS+(8.44845E-3)*XSS*XSS)-
```

```
      (1.04772lE-4)*XSS*XSS*XSS+(4.80097E-7)*XSS*XSS*XSS*XSS)*
      (1.8*TG+32))+((-4.910E-3+(3.83184E-4*XSS)-(1.078963E-5*
      XSS*XSS)+(1.3152E-7*XSS*XSS*XSS)-(5.897E-10*XSS*XSS*XSS*
      XSS))*(1.8*TG+32)*(1.8*TG+32 ));
*     h2 := 2.326*(-1015.07+(79.5387*XSS)-(2.358016*XSS*XSS)+
      (0.03031583*XSS*XSS*XSS)-(1.400261E-4*XSS*XSS*XSS*XSS)+
      ((4.68108-(3.037766E-1)*XSS+(8.44845E-3)*XSS*XSS)-
      (1.04772lE-4)*XSS*XSS*XSS+(4.80097E-7)*XSS*XSS*XSS*XSS)*
      (1.8*T2+32))+((-4.910E-3+(3.83184E-4*XSS)-(1.078963E-5*
      XSS*XSS)+(1.3152E-7*XSS*XSS*XSS)-(5.897E-10*XSS*XSS*XSS*
      XSS))*(1.8*T2+32)*(1.8*T2+32 ));
*     h6 :=((mss/mws)*(hl-h2))+h4;
*     QE := mw*(h10-h8);
*     QG := (mss*hl)+(mw*h7)-(mws*h6);
*     QA := (mss*h2)+(mw*hl0)-(mws*h4);
*     QC := mw*(h7-h8);
*     FOR l:=0 TO 20 DO
*     BEGIN
*   effl :=-QE*(1-(T0/(TE+281.16)))/((QG*(1-(T0/(TG+280.66))))-
    (QA*(1-(T0/(TA+268.66))))-(QC*(1-(T0/(TC+269.66)))));
*   effperl := 100*effl;
*   Writeln (effperl:1:2, '  ', l:l);
*   END;
*   FOR j:=0 to 20 DO
*   BEGIN
*eff2 :=-QE*(1-(T0/(TE+281.16)))/((QG*(1-(T0/(TG+j+273.16))))-
 (QA*(1-(T0/(TA+268.66))))-(QC*(1-(T0/(TC+269.66)))));
```

```
*   effper2 := 100*eff2;
*   writeln (effper2:1:2,'  ', j:1);
*   END;
*   FOR k:=0 TO 20 DO
*   BEGIN
*   eff3 :=-QE*(1-(T0/(TE+281.16)))/((QG*(1-(T0/(TG+280.66))))-
    (QA*(1-(T0/(TA+273.16-k))))-(QC*(1-(T0/(TC+269.66)))));
*   effper3 := 100*eff3;
*   writeln (effper3:1:2,'  ', k:1);
*   END;
*   FOR n:=0 TO 20 DO
*   BEGIN
* eff4 :=-QE*(1-(T0/(TE+281.16)))/((QG*(1-(T0/(TG+280.66))))
  -(QA*(1-(T0/(TA+268.66))))-(QC*(1-(T0/(TC+273.16- n)))));
* effper4 := 100*eff4;
* writeln (effper4:1:2,'  ', n:1);
* END;
* END;
* END
* END.
```

APPENDIX A4

PLOTTING PROGRAMME OF EFFICIENCY VARIATION with Cycle external parameters

```
**************************************************************
*This programme plots the variation of absorption cycle
 efficiency with the temperature differences between the
internal and external operating parameters for an ambient
temperature of 25 and 30 deg.C. The input data for this
 programme are obtained from running the efficiency
calculation programme listed in appendix A3.*
**************************************************************

      REAL X(600), Y(600)
      READ(5,*) (Y(I),X(I),I=1,336)
      CALL PAPER(1)
      CALL MAP(0.0,50.0,0.0,50.0)
      CALL PSPACE(0.30, 0.70, 0.55, 0.95)
      CALL AXESSI(1.0,1.0)
      CALL CTRMAG(16)
      CALL CURVEO(X, Y, 1, 21)
      CALL BROKEN(5,5,5,5)
      CALL CURVEO(X, Y, 22, 42)
      CALL BROKEN(20,5,20,5)
      CALL CURVEO(X, Y, 43, 63)
      CALL BROKEN(40,5,40,5)
      CALL CURVEO(X, Y, 64, 84)
      CALL FULL
      CALL BORDER
      CALL CTRMAG(10)
      CALL PLOTCS(15.0, -5.5, 'Temperature difference--->')
      CALL CTRORI(90.0)
      CALL PLOTCS(-8.0, 25.0, 'Efficiency % --->')
      CALL CTRORI(0.0)
      CALL PLOTCS(10.0,45.0,'TE=4C,h.exchanger effectiv.=0.75')
      CALL PLOTCS(10.0,42.0,'Tambient=25C,TG=65C,TA=40C,TC=20C')
      CALL PLOTCS(3.5, 40.0, '1')
      CALL PLOTCS(20.0, 22.0, '2')
      CALL PLOTCS(2.0, 29.0, '3')
      CALL PLOTCS(2.0, 26.0, '4')
      CALL PLOTCS(55.0, 40.0, '1:Evaporator')
      CALL PLOTCS(55.0, 37.0, '2:Generator')
      CALL PLOTCS(55.0, 34.0, '3:Absorber')
      CALL PLOTCS(55.0, 31.0, '4:Condenser')
      CALL BORDER
```

```
CALL PSPACE(0.30, 0.70, 0.09,0.49)
CALL AXESSI(1.0,1.0)
CALL CTRMAG(16)
CALL FULL
CALL CURVEO(X, Y, 85, 105)
CALL BROKEN(5,5,5,5)
CALL CURVEO(X, Y, 106, 126)
CALL BROKEN(20,5,20,5)
CALL CURVEO(X, Y, 127, 147)
CALL BROKEN(40,5,40,5)
CALL CURVEO(X, Y, 148, 168)
CALL FULL
CALL CTRMAG(10)
CALL PLOTCS(15.0, -8.0, 'Temperature difference--->')
CALL CTRORI(90.0)
CALL PLOTCS(-8.0, 25.0, 'Efficiency % --->')
CALL CTRORI(0.0)
CALL PLOTCS(10.0,45.0,'TE=7C,h.exchanger effectiv.=0.75')
CALL PLOTCS(10.0,42.0,'Tambient=25C,TG=65C,TA=40C,TC=20C')
CALL PLOTCS(2.0, 37.0, '1')
CALL PLOTCS(20.0, 18.0, '2')
CALL PLOTCS(2.0, 23.0, '3')
CALL PLOTCS(3.0, 20.0, '4')
CALL BORDER
CALL GREND
CALL PAPER(1)
CALL MAP(0.0,50.0,0.0,50.0)
CALL PSPACE(0.30, 0.70, 0.55, 0.95)
CALL AXESSI(1.0,1.0)
CALL CTRMAG(16)
CALL CURVEO(X, Y, 169,189)
CALL BROKEN(5,5,5,5)
CALL CURVEO(X, Y,190,210)
CALL BROKEN(20,5,20,5)
CALL CURVEO(X, Y,211,231)
CALL BROKEN(40,5,40,5)
CALL CURVEO(X, Y,232,252)
CALL FULL
CALL BORDER
CALL CTRMAG(10)
CALL PLOTCS(15.0, -5.5, 'Temperature difference--->')
CALL CTRORI(90.0)
CALL PLOTCS(-8.0, 25.0, 'Efficiency % --->')
CALL CTRORI(0.0)
CALL PLOTCS(10.0,45.0,'TE=4C,h.exchanger effectiv.=0.75')
CALL PLOTCS(10.0,42.0,'Tambient=30C,TG=65C,TA=40C,TC=20C')
CALL PLOTCS(4.0, 45.0, '1')
CALL PLOTCS(20.0, 28.0, '2')
CALL PLOTCS(2.0, 36.0, '3')
CALL PLOTCS(2.0, 33.0, '4')
CALL PLOTCS(55.0, 34.0, '1:Evaporator')
CALL PLOTCS(55.0, 31.0, '2:Generator')
CALL PLOTCS(55.0, 28.0, '3:Absorber')
CALL PLOTCS(55.0, 25.0, '4:Condenser')
CALL BORDER
```

```
CALL PSPACE(0.30, 0.70, 0.09,0.49)
CALL AXESSI(1.0,1.0)
CALL CTRMAG(16)
CALL FULL
CALL CURVEO(X, Y,253, 273)
CALL BROKEN(5,5,5,5)
CALL CURVEO(X, Y, 274, 294)
CALL BROKEN(20,5,20,5)
CALL CURVEO(X, Y, 295, 315)
CALL BROKEN(40,5,40,5)
CALL CURVEO(X, Y, 316, 336)
CALL FULL
CALL CTRMAG(10)
CALL PLOTCS(15.0, -8.0, 'Temperature difference--->')
CALL CTRORI(90.0)
CALL PLOTCS(-8.0, 25.0, 'Efficiency % --->')
CALL CTRORI(0.0)
CALL PLOTCS(10.0,45.0,'TE=7C,h.exchanger effectiv.=0.75')
CALL PLOTCS(10.0,42.0,'Tambient=30C,TG=65C,TA=40C,TC=20C')
CALL PLOTCS(5.0, 37.0, '1')
CALL PLOTCS(20.0, 24.0, '2')
CALL PLOTCS(2.0, 31.0, '3')
CALL PLOTCS(2.0, 28.5, '4')
CALL BORDER
CALL GREND
STOP
END
```

Appendix B1

SUN-EARTH GEOMETRIC RELATIONS AND CONCEPTS

Several parameters have been mentioned in the text of chapter 8 and used in the solar computer programme of appendix B2 without the necessary equations being given to calculate them.These are given below.

1) The sun's monthly mean declination *decl* is

$$decl = 23.45 \sin [360(\frac{284 + n}{365})] \qquad \text{B1.1}$$

Where

n is the recommended day of the year counted from 1st january.

The recommended average day for each month and corresponding day of the year are :

Month	Date	n
January	17	17
February	16	47
March	16	75
April	15	105
May	15	135
June	11	162
July	17	198
August	16	228
September	15	258
October	15	288
November	14	318
December	10	314

2) The normal extraterrestrial solar flux over a specified day is

$$I_{Sn} = 1367(1 + 0.033 \cos \frac{360n}{365}) \quad W/m^2 \qquad \text{B1.2}$$

3) The daily total extraterrestrial solar radiation H_o on a horizontal surface is

$$H_o = \frac{24\text{x}3.6}{1000\pi} I_{Sn}[\cos L \cos(decl) \sin W_S + \frac{\pi}{180} W_S \sin L \sin(decl)] \qquad \text{B1.3}$$

Where

H_o is in $MJ/(m^2 d)$ and I_{Sn} in W/m^2,

L is the latitude

W_S the sunset hour angle on a horizontal surface defined by

$$W_S = \arccos[-\tan(decl) \tan L] \qquad \text{B1.4}$$

4) The monthly average daily clearness index $\overline{K}$ is

$$\overline{K} = \frac{\overline{H}}{\overline{H}_o} \qquad \text{B1.5}$$

Where

$\overline{H}_o$ is the monthly mean value of H_o found from equation B1.3 with *decl* and W_S computed for the mean day of the month n,

and $\overline{H}$ is the monthly average daily global radiation on a horizontal surface.

5) The sunset hour angle W_{SS} on equator-facing surfaces can be found from

$$W_{SS} = \min\Big(W_S, \arccos[-\tan(L-\beta)\tan(decl)]\Big) \qquad \text{B1.6}$$

Where

β is the slope of the collector.

6) The ratio $\overline{H}_d/\overline{H}$ of the monthly average daily horizontal diffuse radiation by the monthly average daily global radiation on horizontal surface is given by the following correlation valid for the range $0.3 \leq \overline{K} \leq 0.8$:

$$\overline{H}_d/\overline{H} = \begin{cases} 1.391 - 3.560\overline{K} + 4.189\overline{K}^2 - 2.137\overline{K}^3 & \text{for } W_S \leq 81.4^o \\ 1.311 - 3.022\overline{K} + 3.427\overline{K}^2 - 1.821\overline{K}^3 & \text{for } W_S > 81.4^o \end{cases} \qquad \text{B1.7}$$

7) The ratio R_{bT} of the daily beam radiation on the tilted surface to that on horizontal surface is

$$R_{bT} = \frac{\cos(L-\beta)\cos(decl)\sin(W_{SS}) + (\pi/180)W_{SS}\sin(L-\beta)\sin(decl)}{\cos L\cos(decl)\sin W_S + (\pi/180)W_S \sin L\sin(decl)} \quad \text{B1.8}$$

Monthly mean values of R_{bT} are obtained by selecting values of decl, W_S and W_{SS} to correspond to the mean day of the month.

8) The ratio R_T of the mean daily global radiation on the tilted surface to that on horizontal surface is

$$R_T \quad (1-(\overline{H}_d/\overline{H}))R_{bT} + (\overline{H}_d/\overline{H})(\frac{1+\cos\beta}{2}) + \rho(\frac{1-\cos\beta}{2}) \quad \text{B1.9}$$

Where mean values of R_{bT} are used.

9) The monthly mean daily global radiation $\overline{H}_T$ on the plane of the collector is

$$\overline{H}_T = R_T\overline{H} \quad \text{B1.10}$$

10) The solar angle of incidence θ_i on the collector plane is

$$\cos\theta_i - \cos(L-\beta)\cos(decl)\cos W + \sin(decl)\sin(L-\beta) \quad \text{B1.11}$$

Where W is the hour angle (west positive).

The hour angle at a particular location expresses the time of day with respect to solar noon. One hour of time is represented by (360/24)° or 15° of hour angle.

11) The monthly mean collector incidence angle modifier $\overline{K}_n$ is

$$\overline{K}_n \quad \overline{R}_{bT}\frac{(H \quad H_d)}{\overline{H}_T}[1+b_o(\frac{1}{\cos\theta_i}-1)] + \frac{\overline{H}_d(1+\cos\beta)+\overline{H}\rho(1-\cos\beta)}{2H_T}(1+b_o) \quad \text{B1.12}$$

Where b_o is the incidence angle modifier coefficient equal to -0.10 and -0.17 for

one-glass and two-glass collector covers respectively, ρ is the ground albedo (0.2 for plain earth) and the solar angle of incidence on the collector plane is assumed to be corresponding to that at 14.30 h (solar time).

12) The monthly mean collector optical efficiency is

$$\overline{\tau\alpha} = \overline{K}_n(\tau\alpha)_n \qquad \text{B1.13}$$

With $(\tau\alpha)$ is the collector optical efficiency at normal solar incidence and is usually known for a particular collector.

13) The ratio r of the monthly mean hourly global radiation to the monthly mean daily global radiation on a horizontal surface is

$$r(W) \quad \pi/24(d + e\cos W)\left[\frac{(\cos W - \cos W_S)}{(\sin W_S - (\pi/180)W_S \cos W_S)}\right] \qquad \text{B1.14}$$

Where

$$d = 0.409 + 0.5016\sin(W_S - 60) \qquad \text{B1.15}(a)$$

$$e - 0.6609 - 0.4767\sin(W_S - 60) \qquad \text{B1.15}(b)$$

r_{noon} is found from equation B1.14 with W=0.

14) The ratio r_d of the monthly mean hourly diffuse radiation to the monthly mean daily diffuse radiation on a horizontal surface is

$$r_d(W) = \frac{\pi}{24}\left[\frac{(\cos W - \cos W_S)}{(\sin W_S - (\pi/180)\cos W_S)}\right] \qquad \text{B1.16}$$

r_{dnoon} is found from equation B1.16 with W=0.

15) The ratio r_{bT} of the hourly beam radiation on the tilted surface to that on a horizontal surface is

$$r_{bT} = \cos\theta_i/\cos\theta_Z \qquad \text{B1.17}$$

Where $\cos\theta_i$ is given by equation B1.11 and

$$\cos\theta_Z = \cos(decl)\cos W\cos L + \sin(decl)\sin L \qquad \text{B1.18}$$

For monthly mean hourly ratios $\bar{r}_{bT}$, equation B1.17 is used with θ_i and θ_Z calculated for the particular hour at the mean day of the month.

17) The ratio r_T of hourly global radiation on the tilted surface to that on a horizontal surface is

$$r_T = \left[1 - (\frac{r_d\ H_d}{r\ H})\right] r_{bT} + (\frac{1+\cos\beta}{2})(\frac{r_d\ H_d}{r\ H}) + (\frac{1-\cos\beta}{2})\rho \qquad \text{B1.19}$$

This equation is also valid for monthly mean ratios $\bar{r}_T$ if (H_d/H) is replaced by $(\overline{H}_d/\overline{H})$ and calculation is made for the mean day of the month.

r_{bTnoon} and r_{Tnoon} are computed for W=0.

18) The critical radiation intensity I_C of the solar collector (at above which useful energy is delivered) is given by

$$I_C - U_L(T_{Ci} - \overline{T}_o)/(\tau\alpha)_n \qquad \text{B1.20}$$

19) The mean hourly global radiation $\overline{I}_{Tnoon}$ on the plane of the tilted collector is

$$\overline{I}_{Tnoon} = \bar{r}_{noon}\bar{r}_{Tnoon}\overline{H} \qquad \text{B1.21}$$

20) The dimensionless critical radiation level $\overline{X}_{CK}$ is

$$\overline{X}_{CK} = I_C/I_{Tnoon} \qquad \text{B1.22}$$

APPENDIX B2

COMPUTER PROGRAMME FOR SOLAR FRACTION CALCULATION

```
*****************************************************************
*PROGRAM Solarfra(input, output);
 (*This program uses the phibar f-chart method to calculate the
   solar fraction for a solar-powered absorption refrigeration
   system working 24 h per day (7 days per week) in Constantine
   (Algeria)*)
*****************************************************************
*CONST
*    L =36.36; BETA= 36.36; bo = -0.10; TrAbn = 0.76;
*    a = 0.043; b = 2.81; c = -0.18; Tsl = 80; Tci = 80;
*    Qgen = 6.21; pi =3.14159; ca =pi/180; UAs =2.0;
*    FR = 0.951; UL = 4.75; gc =0.2136;
*VAR
* v : ARRAY [0..11,0..4] of real;
* m,i, j : integer;
* ask4 : text;
* Ac,decl,RbT,RT,HT,Qlm,costeta :real;
* K,Isn,Wsp,Ho,HdH,Wss:real;
* costetaz,costetap,Kn,X,Y,d,e,rnoon,rdnoon,rbTnoon : real;
* rTnoon,Ic,ITnoon,Xck,AA,BB,CC,FI,FM,SF : real;
* diff,Z,Ts2,Qwm,newFM,TrAb,R  :real;
* Qsolarm,Qsolary,Qlmtotal,YearlySF :real;
*BEGIN
  decl := 0;RbT :=0;RT:=0;HT:=0;Qlm:=0;costeta:=0;
```

```
  costetaz:=0;costetap:=0;Kn:=0;X:=0;Y:=0;d:=0;e:=0;rnoon:=0;
  rbTnoon:=0;rdnoon:=0;rTnoon:=0;Ic:=0;ITnoon:=0;Xck:=0;
  AA:=0;BB:=0;CC:=0;FI:=0;FM:=0;SF:=0;TrAb:=0;R:=0;
  K:=0;Isn:=0;Wsp:=0;Ho:=0;HdH:=0;Wss:=0;Z:=0;Ts2:=0;Qwm:=0;
 newFM:=0; YearlySF:=0;Qsolarm:=0;Qsolary:=0;Qlmtotal:=0;
*FOR i:=0 TO 11 DO
*FOR j:=0 TO 4 DO
*   read( v[i,j]);
*Writeln('FOR END-USE LOAD WORKING 24 HRS PER DAY (7 DAYS PER
          WEEK OPERATION)');

*Writeln('  ');
* FOR m:=2 TO 9 DO
* BEGIN
*   Qsolarm :=0;Qsolary :=0;Qlmtotal :=0;
*   Ac := 6*m;
*   Writeln ('  ');
*   Writeln ('  ');
*Writeln ('£ For Ac (collector area) equal to ',Ac:4:2,'
            square meters');
*Writeln ('  ');
*Writeln ('  H            To        K       Qlm        Qsolarm
               FM    NewFM');
*Writeln ('(Mj/sqm day)  (deg.C)    (Mj/month)   (Mj/month)');
*Writeln ('  ');
*   FOR i:=0 TO 11 DO
*   BEGIN
*   FM := 0.010;
```

```
*    Qlm :=(Qgen*24*3600*v[i,2])/1000;
*    decl := 23.45*sin(ca*360*(284+v[i,1])/365);
*    Isn :=1367*(1+(0.033*cos(360*v[i,1]*ca/365)));
*    Ho :=(24*3.6/pi)*Isn*(cos(L*ca)*cos(decl*ca)*sin(v[i,4]*
       ca)+ca*v[i,4]*sin(L*ca)*sin(decl*ca))/1000;
*    K :=v[i,0]/Ho;
*    IF v[i,4] <= 81.4 THEN
*    HdH :=1.391-(3.560*K)+(4.189*K*K)-(2.137*K*K*K)
*    ELSE
*    HdH :=1.311-(3.022*K)+(3.427*K*K)-(1.821*K*K*K);
*    Wsp :=90;
*    IF Wsp > v[i,4] THEN
*    Wss := v[i,4]
*    ELSE
*      Wss := Wsp;
*    RbT :=(cos(ca*decl)*sin(ca*Wss))/(cos(ca*L)*cos(ca*decl)*
     sin(ca*v[i,4])+(ca*v[i,4]*sin(ca*L)*sin(ca*decl)));
*    RT := (1-HdH)*RbT+(HdH)*((1+cos(ca*BETA))/2)+0.2*
     ((1-cos(ca*BETA))/2);
*    HT := RT*v[i,0];
*    X := (Ac*FR*UL*100*24*3600*v[i,2])/(Qlm*1E06);
*    IF X >= 20 THEN
*    WRITELN(' X IS OUTSIDE THE RANGE OF CORRELATION')
*    ELSE
*    costeta := cos(ca*37.5)*cos(ca*decl);
*    Kn := RbT*(1-(HdH))*(1+bo*((1/costeta)-1))/(HT/v[i,0])+
*    HdH*(1+cos(BETA*ca))*(1+bo)/(2*(HT/v[i,0]))+
*    0.2*(1-cos(BETA*ca))*(1+bo)/(2*(HT/v[i,0]));
```

```
*    TrAb := (Kn*TrAbn);
*    Y := (Ac*FR*TrAb*HT*v[i,2])/Qlm;
*    IF Y >=1.6 THEN
*    WRITELN(' Y IS OUTSIDE THE RANGE OF CORRELATION')
*    ELSE
*    d := 0.409+(0.5016*sin(ca*(v[i,4]-60)));
*    e := 0.6609-(0.4767*sin(ca*(v[i,4]-60)));
*    rnoon := (pi/24)*(d+e)*(1-cos(ca*v[i,4]))/(sin(ca*v[i,4])-
*    (ca*v[i,4]*cos(ca*v[i,4])));
*    rdnoon := (pi/24)*(1-cos(ca*v[i,4]))/(sin(ca*v[i,4])-
*    (ca*v[i,4]*cos(ca*v[i,4])));
*   costetaz :=cos(ca*L)*cos(ca*decl)+(sin(ca*L)*sin(ca*decl));
*    costetap := cos(ca*decl);
*    rbTnoon := costetap/costetaz;
*    rTnoon := (1-(rdnoon*(HdH)/rnoon))*rbTnoon +
*    (((1+cos(ca*36.36))/2)*(rdnoon/rnoon)*(HdH)+
     ((1-cos(ca*36.36))/2)*0.2);
*    IC :=((UL*(Tci-v[i,3]))/(TrAb))*3600E-06;
*    ITnoon := rnoon*rTnoon*v[i,0];
*    Xck := IC/ITnoon;
*    AA := 7.476-(20.0*K)+(11.188*K*K);
*    BB := -8.562+(18.679*K)-(9.948*K*K);
*    CC := -0.722+(2.426*K)+(0.439*K*K);
*    FI := exp((AA+BB*(rTnoon/RT))*(Xck+CC*(Xck*Xck)));
*    SF := (Y*FI)-a*((exp(b*FM))-1)*(1-exp(c*X));
*    REPEAT
*          FM := SF;
```

```
*          SF := (Y*FI)-a*exp(((b*FM)-1)*(1-exp(c*X)));
*          diff :=FM - SF;
*    UNTIL abs(diff) <0.001;
*          Z:=(Qlm*1000)/(4.199*5.34*100*3600*24*v[i,2]);
*          Ts2 := Ts1+gc*(exp(4.702*SF)-1)*(exp(-4.002*Z));
*          Qwm :=UAs*(Ts2-v[i,3])*24*3600*v[i,2]/1000000;
*          newFM :=FM-(Qwm/Qlm);
*          Qsolarm :=newFM*Qlm;
*          Qsolary :=Qsolary +Qsolarm;
*          Qlmtotal :=Qlmtotal+Qlm;
* Writeln(' ',v[i,0]:4:2,'        ',v[i,3]:4:2,'     ',K:5:3,
    '   ',Qlm:7:2,'   ', Qsolarm:4:2,'     ',FM:5:4,'  ',
  newFM:5:4);
*END;
* YearlySF :=(Qsolary/Qlmtotal)*100;
* Writeln('                          Yearly solar fraction = ',
  YearlySF:4:2,'%');
*Writeln ('  ');
*END;
*END.
```